AD-A218 436

USAAVSCOM TR 89-D-22C

US ARMY AVIATION SYSTEMS COMMAND

AIRCRAFT CRASH SURVIVAL DESIGN GUIDE

VOLUME III - AIRCRAFT STRUCTURAL CRASH RESISTANCE

SIMULA INC.
10016 SOUTH 51st STREET
PHOENIX, ARIZONA 85044

DECEMBER 1989

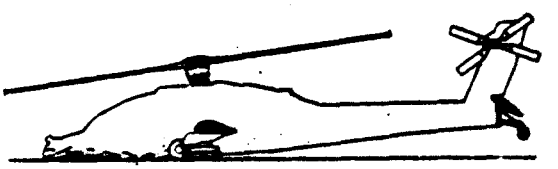

FINAL REPORT

Approved for public release; distribution is unlimited.

Prepared for

AVIATION APPLIED TECHNOLOGY DIRECTORATE
US ARMY AVIATION RESEARCH AND TECHNOLOGY ACTIVITY (AVSCOM)
FORT EUSTIS, VA 23604-5577

AVIATION APPLIED TECHNOLOGY DIRECTORATE POSITION STATEMENT

This revised edition of the Aircraft Crash Survival Design Guide (ACSDG) was prepared to assist those design engineers responsible for the incorporation of crashworthiness into the design of helicopters, light fixed-wing aircraft, and tilt rotor aircraft. Also, this guide may be used in the evaluation of the level of crashworthiness design available in the various types of aircraft.

This report documents the components and principles of crashworthiness and suggests specific design criteria. In general, a systems approach is presented for providing a reasonable level of aircrew and aircraft protection in a crash, which is considered the preferred approach. The original Crash Survival Design Guide was published in 1967 as USAAVLABS TR 67-22 and subsequent revisions published as USAAVLABS TR 70-22, USAAMRDL TR 71-22, and USARTL-TR-79-22A thru E. This edition consists of a consolidation of up-to-date design criteria, concepts, and analytical techniques developed through research programs sponsored by this Directorate and others over the past 27 years.

This document has been coordinated with other Government agencies and helicopter airframe manufacturers active in aircraft crashworthiness research and development, and is considered to offer sound design criteria and approaches to design for crashworthiness.

The technical monitors for this program were Messrs. LeRoy Burrows, Harold Holland, and Kent Smith of the Safety and Survivability Technical Area, Aeronautical Systems Division, Aviation Applied Technology Directorate.

NOTE: All previous editions of the Aircraft Crash Survival Design Guide are obsolete and should be destroyed.

REPORT DOCUMENTATION PAGE

Form Approved
OMB No. 0704-0188

1. AGENCY USE ONLY (Leave blank)	2. REPORT DATE	3. REPORT TYPE AND DATES COVERED
	December 1989	Final FROM 9/86 TO 8/89

4. TITLE AND SUBTITLE

Aircraft Crash Survival Design Guide
Volume III - Aircraft Structural Crash Resistance

5. FUNDING NUMBERS

DAAJ02-86-C-0028

6. AUTHOR(S)

Richard E. Zimmermann, James C. Warrick, Alan D. Lane,
Norman A. Merritt, Akif O. Bolukbasi

7. PERFORMING ORGANIZATION NAME(S) AND ADDRESS(ES)

Simula Inc.
Phoenix, Arizona 85044-5299

8. PERFORMING ORGANIZATION REPORT NUMBER

9. SPONSORING/MONITORING AGENCY NAME(S) AND ADDRESS(ES)

Aviation Applied Technology Directorate
U.S. Army Aviation Research & Technology Activity (AVSCOM)
Fort Eustis, VA 23604-5577

10. SPONSORING/MONITORING AGENCY REPORT NUMBER

USAAVSCOM TR 89-D-22C

11. SUPPLEMENTARY NOTES

Volume III of five-volume report

12a. DISTRIBUTION/AVAILABILITY STATEMENT

Approved for public release; distribution unlimited

12b. DISTRIBUTION CODE

13. ABSTRACT *(Maximum 200 words)*

This five-volume publication has been compiled to assist design engineers in understanding the design considerations associated with the development of crash-resistant U.S. Army aircraft. A collection of available information and data pertinent to aircraft crash resistance is presented, along with suggested design conditions and criteria. The five volumes of the Aircraft Crash Survival Design Guide cover the following topics: Volume I - Design Criteria and Checklists; Volume II - Aircraft Design Crash Impact Conditions and Human Tolerance; Volume III - Aircraft Structural Crash Resistance; Volume IV - Aircraft Seats, Restraints, Litters and Cockpit/Cabin Delethalization; and Volume V - Aircraft Postcrash Survival. This volume (Volume III) contains information on the design of aircraft structures and structural elements for improved crash survivability. Current requirements for structural design of U.S. Army aircraft pertaining to crash resistance are discussed. Principles for crash-resistant design are presented in detail for the landing gear and fuselage subject to a range of crash conditions, including impacts that are primarily longitudinal, vertical, or lateral in nature and those that involve more complicated dynamic conditions, such as rollover. Analytical methods for evaluating structural crash resistance are described.

14. SUBJECT TERMS		15. NUMBER OF PAGES
Aircraft Design Guide	Design Data	250
Aircraft Structures	Structural Crash Resistance	16. PRICE CODE
Crash Resistance		

17. SECURITY CLASSIFICATION OF REPORT	18. SECURITY CLASSIFICATION OF THIS PAGE	19. SECURITY CLASSIFICATION OF ABSTRACT	20. LIMITATION OF ABSTRACT
UNCLASSIFIED	UNCLASSIFIED	UNCLASSIFIED	

PREFACE

This report was prepared for the Safety and Survivability Technical Area of the Aviation Applied Technology Directorate, U.S. Army Aviation Research and Technology Activity (AVSCOM), Fort Eustis, Virginia, by Simula Inc. under Contract DAAJ02-86-C-0028, initiated in September 1986. This guide is a revision of USARTL Technical Report 79-22, Aircraft Crash Survival Design Guide, published in 1980.

A major portion of the data contained herein was taken from U.S. Army-sponsored research in aircraft crash resistance conducted from 1960 to 1987. Acknowledgment is extended to the U.S. Air Force, the Federal Aviation Administration, NASA, and the U.S. Navy for their research in crash survival. Appreciation is extended to the following organizations for providing accident case histories leading to the establishment of the impact conditions in aircraft accidents:

- U.S. Army Safety Center, Fort Rucker, Alabama.
- U.S. Naval Safety Center, Norfolk, Virginia.
- U.S. Air Force Inspection and Safety Center, Norton Air Force Base, California.

Information was also provided by the Civil Aeronautics Board, which is no longer in existence.

Additional credit is due the many authors, individual companies, and organizations listed in the bibliographies for their contributions to the field. The contributions of the following authors to previous editions of the Aircraft Crash Survival Design Guide are most noteworthy:

D. F. Carroll, R. L. Cook, S. P. Desjardins, J. K. Drummond, J. L. Haley, Jr., A. D. Harper, H. G. C. Henneberger, N. B. Johnson, G. Kourouklis, D. H. Laananen, W. H. Reed, S. H. Robertson, J. Shefrin, L. M. Shaw, G. T. Singley, III, A. E. Tanner, Dr. J. W. Turnbow, and L. W. T. Weinberg.

This volume was prepared by Richard E. Zimmermann, James C. Warrick, Alan D. Lane, and Norman A. Merritt of Simula Inc., and Akif O. Bolukbasi of McDonnell Douglas Helicopter Co. Technical review and comments were provided by S. P. Desjardins of Simula Inc.

TABLE OF CONTENTS

	Page
PREFACE	iii
LIST OF ILLUSTRATIONS	viii
LIST OF TABLES	xiv
INTRODUCTION	1
1. BACKGROUND DISCUSSION	4
2. DEFINITIONS	8
2.1 AIRCRAFT COORDINATE SYSTEMS AND ATTITUDE PARAMETERS	8
2.2 ACCELERATION-RELATED TERMS	10
2.3 VELOCITY-RELATED TERMS	10
2.4 FORCE TERMS	12
2.5 DYNAMICS TERMS	13
2.6 CRASH SURVIVABILITY TERMS	14
2.7 OCCUPANT-RELATED TERMS	14
2.8 STRUCTURAL TERMS	16
3. CRASH IMPACT CONDITIONS	18
3.1 INTRODUCTION	18
3.2 STRUCTURAL DAMAGE THAT FREQUENTLY RESULTS IN OCCUPANT INJURY	18
3.2.1 Longitudinal (Crushing) Loads on Cockpit Structure	19
3.2.2 Vertical (Crushing) Loads on Fuselage Shell	19
3.2.3 Lateral (Crushing) Loads on Fuselage Shell	19
3.2.4 Transverse (Bending) Loads on Fuselage Shell	20
3.2.5 Deformation (Buckling) of Floor Structure	20
3.2.6 Landing Gear Penetration of Fuselage Shell	20
3.2.7 Helicopter Lateral Rollover	20
3.2.8 Rupture of Flammable Fluid Containers	20
3.3 ENERGY CONTENT OF AIRCRAFT AT IMPACT	21
3.3.1 Translational Kinetic Energy	21
3.3.2 Rotational Kinetic Energy	21
3.3.3 Potential Energy	22
3.3.4 Strain Energy	22
3.4 POSTIMPACT ENERGY DISSIPATION	22
3.5 CRASH KINEMATICS	23
4. CRASH PERFORMANCE REQUIREMENTS	24
4.1 INTRODUCTION	24
4.2 GENERAL REQUIREMENTS	24

TABLE OF CONTENTS (CONTD)

		Page
4.3	DETAIL REQUIREMENTS	25
4.3.1	Airframe Crash Resistance	25
4.3.2	Ancillary Equipment Retention	33
4.3.3	Occupant Retention	35
4.3.4	Cargo Retention	35
5.	GENERAL DESIGN CONSIDERATIONS	37
5.1	INTRODUCTION	37
5.2	MISSION CONSTRAINTS	38
5.2.1	Combat Support Requirements	38
5.2.2	Helicopters	39
5.2.3	Fixed-Wing Aircraft	39
5.2.4	Tilt-Rotor Aircraft	39
5.3	GENERAL CONFIGURATION	39
5.3.1	Failure Modes	46
5.3.2	Impact Parameters	48
5.3.3	Initial Layout	50
5.3.4	Analysis and Simulation Iterations	51
5.3.5	Margins of Safety	54
5.3.6	Joint Concepts	56
5.3.7	Materials	56
6.	SUBSYSTEM DESIGN	64
6.1	INTRODUCTION	64
6.2	FUSELAGE	64
6.2.1	General	64
6.2.2	Load-Limiting Fuselage Structure	66
6.2.3	Fuselage Protective Shell	88
6.2.4	Engine Mounts	97
6.2.5	Fuel Tank Installation	98
6.2.6	Seat Installation	98
6.2.7	Cargo and Equipment Retention	101
6.3	LANDING GEAR	111
6.3.1	Landing Gear Loads	112
6.3.2	Selection of Landing Gear Stroke	115
6.3.3	Fuselage Velocity Change Controlled by Landing Gear	116
6.3.4	Wheel Versus Skid	116
6.3.5	Wheeled Gear	116
6.3.6	Weight of Landing Gear	118
6.3.7	Components and Load Paths	118
6.3.8	Skid Gear	121
6.3.9	Shock Strut	124
6.3.10	Shock Strut Oleo Total Load	127
6.3.11	Shock Strut Load Transients and Failure Conditions	128

TABLE OF CONTENTS (CONTD)

		Page
	6.3.12 Containment of Flammable Hydraulic Fluid	129
	6.3.13 Series Coupling of Shock Strut Energy-Absorbing Devices	130
	6.3.14 Transient Effects and Efficiency	131
6.4	SUBSYSTEMS EXTERNAL TO THE FUSELAGE OTHER THAN LANDING GEAR	132
	6.4.1 General	132
	6.4.2 Rotor Blade	132
	6.4.3 Wing, Empennage, Engine, End External Stores	134
	6.4.4 Special Tilt-Rotor Considerations	134
7.	ANALYTICAL METHODS	136
7.1	INTRODUCTION	136
7.2	DYNAMICS OF THE CRASH IMPACT CONDITIONS	136
	7.2.1 Kinematic Relationships	136
	7.2.2 Energy Absorption During Deceleration	140
	7.2.3 Stopping Distance	147
7.3	APPLICATION OF KINEMATIC RELATIONSHIPS AND ENERGY ABSORPTION PRINCIPLES TO PRELIMINARY DESIGN STUDIES	166
	7.3.1 Selection of Seat System Stroking Forces	166
	7.3.2 Selection of Landing Gear System Stroking Forces	168
	7.3.3 Fuselage Structure	172
7.4	LANDING GEAR ANALYSIS	188
7.5	SEMIEMPIRICAL ANALYSIS OF AIRFRAME STRUCTURAL CRASH RESISTANCE	191
	7.5.1 Analysis Procedure	191
	7.5.2 Substructure Test Results	192
	7.5.3 Correlation of Test and Analysis Results	193
	7.5.4 Example of Analysis for Vertical Impact	195
	7.5.5 Example of Analysis for Longitudinal Impact	203
	7.5.6 Lateral Impact	207
	7.5.7 Rollover	207
7.6	STRUCTURAL CRASH RESISTANCE SIMULATION COMPUTER PROGRAMS	208
	7.6.1 Program KRASH	210
	7.6.2 Program DYCAST	212
	7.6.3 PAM-KRASH	219
7.7	POTENTIAL SOURCES OF BASIC STRUCTURAL DATA FOR CRASH-RESISTANCE ANALYSIS	219
	7.7.1 Estimates	219
	7.7.2 Aircraft Accident Data	222
8.	TESTING	223
8.1	INTRODUCTION	223
8.2	STATIC STRUCTURAL TESTING	224
8.3	LANDING GEAR CRASH TESTING	224
8.4	CARGO RESTRAINT	224
8.5	SEAT AND RESTRAINT SYSTEM	225

TABLE OF CONTENTS (CONTD)

		Page
8.6	FUEL SYSTEM	225
8.7	ANCILLARY EQUIPMENT RETENTION	225
8.8	FULL-SCALE TESTING	225
8.9	SCALE MODEL TESTING	226
REFERENCES		233
BIBLIOGRAPHY		248

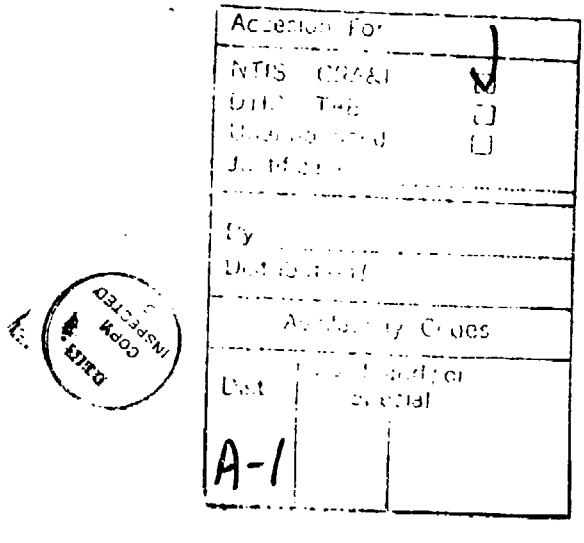

LIST OF ILLUSTRATIONS

Figure		Page
1	Energy management system	5
2	Procedure for evaluation of structural designs with respect to crash resistance	6
3	Aircraft coordinates and attitude directions	8
4	Typical aircraft floor acceleration pulse	11
5	Terminology for directions of forces on the body	15
6	Low-angle impact design conditions (simulated approach with antitorque loss under poor visibility)	28
7	Nose section design conditions	29
8	Rollover, roof impact design conditions	31
9	Rollover, side impact design conditions	32
10	Design features for crash survival	37
11	Side elevations of typical U.S. Army utility and cargo helicopters	40
12	Side elevations of typical U.S. Army observation and attack helicopter	41
13	Side elevation of typical U.S. Army training helicopter	42
14	Selected helicopter crash-resistant features	42
15	Side elevations of typical U.S. Army fixed-wing aircraft	43
16	Tilt-rotor aircraft	45
17	Wing/rotor/pylon crash failure modes	47
18	Compressive buckling at base of buttline beam structure on a medium cargo helicopter following vertical impact	48
19	Typical buckling collapse of vertical bulkhead and buttline beam on a medium cargo helicopter following vertical impact	49
20	Typical frame failure away from occupied space in the cockpit area of a medium cargo helicopter following vertical impact	50

LIST OF ILLUSTRATIONS (CONTD)

Figure		Page
21	Typical frame failure away from occupied space in the cabin area of a medium cargo helicopter following vertical impact	51
22	Failure modes resulting in jagged elements protruding into occupied space in the cabin area of a medium cargo helicopter following vertical impact	52
23	Rotational joint failure with compression and bending in a medium cargo helicopter following vertical impact	53
24	Failure of frame member and joint with fragmentation, compression, and bending in a medium cargo helicopter following vertical impact	53
25	Direction and attitude of impact	54
26	Structural layout for occupant protection during crash impact conditions	55
27	Energy-absorbing joint concept	57
28	Stress-strain relationship for aluminum alloy (7075) and 0-degrees graphite/epoxy composite	58
29	Specific energy absorption comparisons	59
30	NASA drop test of civil light twin-engine aircraft	65
31	Overall fuselage concepts	67
32	Typical vertical and longitudinal crash pulses	69
33	Fuselage structure with overhead large mass items (idealization)	69
34	Deceleration of overhead high-mass items by energy-absorbing material	70
35	Fuselage structure without overhead mass items (idealization)	71
36	Vertical impact crushing loads	72
37	Roll and pitch attitude envelopes	73
38	Energy absorption concepts - beams and bulkhead (vertical impact)	74

LIST OF ILLUSTRATIONS (CONTD)

Figure		Page
39	Underfloor beams designed with potential energy-absorbing capability	75
40	Energy-absorbing underfloor structure.	76
41	Development of composite energy-absorbing underfloor structure.	77
42	Composite cabin test section	78
43	Impulsive aircraft acceleration as a function of velocity and ratio of accelerated mass of earth to aircraft mass (based upon assumed time, t, for acceleration of earth mass).	82
44	Design criteria for plowing condition.	83
45	Methods of designing nose structure to reduce earth scooping	83
46	Features of helicopter nose section to prevent nose plowing.	84
47	Typical underfloor canted frame and longitudinal beam member to minimize nose plowing.	85
48	Longitudinal impact design criteria.	86
49	Observation helicopter - layout of crash resistant features	89
50	Longitudinal impact and blade strike protection in nose section. The figure delineates those members requiring careful design consideration	90
51	Longitudinal impact protection in cabin section.	90
52	Typical longitudinal beams adjacent to cockpit for longitudinal continuity of overhead structure.	92
53	Typical full-depth longitudinal beams for overhead support of large mass items and longitudinal continuity of structure.	92
54	Examples of closed box-beam frame sections	93
55	Overhead mass protection and rollover protection in cabin section.	94

LIST OF ILLUSTRATIONS (CONTD)

Figure		Page
56	Typical structural sections for nose section.	95
57	Typical cockpit overhead longitudinal beam member	96
58	Externally mounted blade strike deflectors.	97
59	Typical interior support structure for fuel cell.	99
60	Typical crash-resistant seat configurations	100
61	Load-displacement requirements for energy-absorbing cargo restraint systems (forward loading of rotary and fixed-wing aircraft).	103
62	Cargo lateral load-displacement requirements.	104
63	Results of integrated cargo restraint/crash simulation tests using energy absorbers and low-elongation tension members and forward longitudinal load-displacement requirements.	105
64	Cargo restraint load limiter.	106
65	Energy-absorbing restraint system designed to replace existing metallic cargo cage.	109
66	Crash-resistant barrier net	110
67	Load-limiting tiedown assembly.	110
68	Landing gear peak load selected to protect both human life and equipment.	113
69	Example of achievable landing gear performance.	114
70	Location and geometry of landing gear	117
71	Wheel landing gear concepts	119
72	Gear geometry selected layout to continue absorbing energy during crushing of fuselage floor.	120
73	Possible structural layout for attack helicopter with signature reduction	122
74	Helicopter skid gear and improved, pitch-interconnected concepts.	123
75	Air/oil oleo schematic.	124

LIST OF ILLUSTRATIONS (CONTD)

Figure		Page
76	Example of effects of different orifices on the velocity sensitivity of a hydraulic oleo.	126
77	Response of a simple oleo to two test conditions	129
78	Two-stage shock strut concepts	130
79	Frangible main rotor blade tip	133
80	Definition of position and displacement for crashing aircraft	137
81	Assumed relationship for illustration of crash kinematics.	138
82	Definition of work	141
83	Illustration of impact reducing aircraft kinetic energy. .	142
84	Illustration of deceleration by constant force	143
85	Force-displacement curve for honeycomb materials	144
86	Theoretical stopping distance as a function of velocity change and average deceleration level.	148
87	Deceleration, velocity, and distance as functions of time for five pulse shapes.	157
88	Comparison of stopping distance for various deceleration pulse shapes	158
89	Energy absorption sequence during vertical crash of a crash-resistant aircraft system.	167
90	Example crash geometry with 10-degree roll attitude at impact	170
91	Schematic of aircraft crash-resistant system using rigid fuselage sidewalls	173
92	Schematic of aircraft crash-resistant system using deformable fuselage sidewalls.	181
93	Lower fuselage bulkhead and stiffener arrangement.	192
94	Predicted versus test load-deflection curves for a representative specimen.	194
95	Comparison of test and analysis results for "like" specimens.	194

LIST OF ILLUSTRATIONS (CONTD)

Figure		Page
96	Load distributions on hard and soft surfaces	196
97	Typical load-displacement characteristics for airframe structure.	197
98	Simplified load-deflection characteristics for a statically loaded stringer-skin combination.	197
99	Typical frame section of side element of a medium cargo helicopter center fuselage	198
100	Crippling allowables for typical aluminum alloy extrusions	199
101	Crippling allowables for aluminum alloy formed sections other than simple zees and channels.	201
102	Effective area of skin for aluminum alloy stringer-skin combination.	202
103	Estimated dynamic energy absorption capability of typical fuselage structure	204
104	Example of longitudinal impact resistance analysis	205
105	Program KRASH model of the Sikorsky ACAP helicopter. . . .	213
106	Prediction of crash behavior with program KRASH.	215
107	Comparison of structure deformation for flat drop test . .	216
108	Bell ACAP KRASH versus test comparison	217
109	Program DYCAST model of composite helicopter structure . .	220
110	14 m/sec impact of a structure-fuel tank system (PAM EFHYD 3D)	221
111	NASA Langley impact dynamic facility	227
112	NASA Langley crash facility layout and fixed camera positions.	228
113	Full-scale crash test of a YAH-63 helicopter	229
114	Cost ratio (scale model test cost/full-scale test cost) versus scale factor for structures weighing less than 10,000 lb.	231
115	Stiffened panel specimen	232

LIST OF TABLES

Table		Page
1	Crash-resistance criteria for the preliminary design process	7
2	Crash impact design conditions with landing gear extended	25
3	Performance requirements under crash impact conditions per table 2	26
4	Other structural performance requirements	27
5	Aircraft cargo categories	36
6	Ultimate strength and elastic moduli for typical structural composites	60
7	Thermal coefficients of expansion for composite and metallic materials	61
8	Minimum conditions under which certain abraded metal particles will ignite	62
9	Cargo restraint loads and displacement requirements	107
10	Cargo net materials - relative characteristics	108
11	Uninstalled weights of equivalent crash-resistant landing gear	118
12	Comparison of capabilities of three versions of program KRASH	212
13	Experimental validation of program KRASH	214
14	Type of test possibilities	223

INTRODUCTION

For many years, emphasis in military aircraft accident investigation was placed on determining the cause of the accident. Very little effort was expended on the crash survival aspects of aviation safety. However, it became apparent through detailed studies of accident investigation reports that significant improvements in crash survival could be made if consideration were given in the initial aircraft design to the following factors that influence survivability:

1. Crash Resistance of Aircraft Structure - The ability of the aircraft structure to maintain living space for occupants throughout a crash.

2. Tiedown Strength - The strength of the linkage preventing occupant, cargo, or equipment from breaking free and becoming missiles during a crash sequence.

3. Occupant Acceleration During Crash Impact - The intensity and duration of accelerations experienced by occupants (with tiedown assumed intact) during a crash.

4. Occupant Crash Impact Hazards - Barriers, projections, and loose equipment in the immediate vicinity of the occupant that may cause contact injuries.

5. Postcrash Hazards - The threat to occupant survival posed by fire, drowning, entrapment, exposure, etc., following the impact sequence.

Early in 1960, the U.S. Army Transportation Research Command* initiated a long-range program to study all aspects of aircraft safety and survivabilty. Through a series of contracts with the Aviation Safety Engineering and Research (AvSER) Division of the Flight Safety Foundation, Inc., the problems associated with occupant survival in aircraft crashes were studied to determine specific relationships among crash forces, structural failures, crash fires, and injuries. A series of reports covering this effort was prepared and distributed by the U.S. Army, beginning in 1960. In October 1965, a special project initiated by the U.S. Army consolidated the design criteria presented in these reports into one technical document suitable for use as a designer's guide by aircraft design engineers and other interested personnel. The document was to be a summary of the current state of the art in crash survival design, using not only data generated under Army contracts but also information collected from other agencies and organizations. The Crash Survival Design Guide, TR 67-22, published in 1967, realized this goal.

Since its initial publication, the Design Guide has been revised and expanded four times to incorporate the results of continuing research in crash resistance technology. The third edition, published in 1971, was the basis for

---

*Now the Aviation Applied Technology Directorate, Aviation Research and Technology Activity of the U.S. Army Aviation Systems Command (AVSCOM).

the criteria contained in the original version of the Army's military standard MIL-STD-1290 (Reference 1). The fourth edition, published in 1980, entitled Aircraft Crash Survival Design Guide, expanded the document to five volumes, which have been updated by the current edition to include information and changes developed from 1980 to 1987.

This current edition, the fifth, contains the most comprehensive treatment of all aspects of aircraft crash survival now documented. It can be used as a general text to establish a basic understanding of crash impact conditions and the techniques that can be employed to improve chances for survival. It also contains design criteria and checklists on many aspects of crash survival and thus can be used as a source of design requirements.

The current edition of the Aircraft Crash Survival Design Guide is also published in five volumes. Volume titles and general subjects included in each volume are as follows:

Volume I - Design Criteria and Checklists

Pertinent criteria extracted from Volumes II through V, presented in the same order in which they appear in those volumes.

Volume II - Aircraft Design Crash Impact Conditions and Human Tolerance

Crash impact conditions, human tolerance to impact, military anthropometric data, occupant environment, test dummies, accident information retrieval.

Volume III - Aircraft Structural Crash Resistance

Crash load estimation, structural response, fuselage and landing gear requirements, rotor requirements, ancillary equipment, cargo restraints, structural modeling.

Volume IV - Aircraft Seats, Restraints, Litters, and Cockpit/Cabin Delethalization

Operational and crash impact conditions, energy absorption, seat design, litter requirements, restraint system design, occupant/restraint system/seat modeling, delethalization of cockpit and cabin interiors.

Volume V - Aircraft Postcrash Survival

Postcrash fire, ditching, emergency escape, crash locator beacons.

This volume (Volume III) contains information on aircraft structural crash resistance. Following a general discussion of aircraft crash resistance in Chapter 1, a number of terms commonly used in discussing crash impact conditions and aircraft structures are defined in Chapter 2. Although Volume II discusses crash impact conditions in detail, Chapter 3 summarizes crash impact information pertinent to aircraft structural design. Chapter 4 presents performance requirements for airframe crash resistance; retention of ancillary equipment, occupant, and cargo; and special tilt-rotor considerations. Mission constraints and general configuration design considerations are

discussed in Chapter 5. Design of the fuselage, landing gear, and other external subsystems is covered in Chapter 6. Analytical techniques for evaluating structural crash resistance are presented in Chapter 7, while Chapter 8 concludes this volume with a discussion of full-scale and scale-model testing.

The units of measurement shown in the Design Guide vary depending upon the units used in the referenced sources of information, but are mostly USA units. In some cases the corresponding metric units are shown in parentheses following the USA units. For the convenience of the reader a conversion table of some commonly used units follows:

USA Unit	Abbr. or Symbol	Metric Equivalent	Abbr. or Symbol
Weight			
Ounce	oz.	28.35 grams	g
Pound	lb or #	0.454 kilogram	kg
Capacity (U.S. liquid)			
Fluidounce	fl oz	29.57 milliliters	ml
Pint	pt	0.473 liter	l
Quart	qt	0.946 liter	l
Gallon	gal	3.785 liters	l
Length			
Inch	in.	2.54 centimeters	cm
Foot	ft	30.48 centimeters	cm
Yard	yd	0.9144 meter	m
Mile	mi	1.609 kilometers	km
Area			
Square Inch	sq in. or $in.^2$	6.452 square centimeters	sq cm or cm^2
Square Foot	sq ft or ft^2	0.093 square meter	sq m or m^2
Volume			
Cubic Inch	cu in. or $in.^3$	16.39 cubic centimeters	cu cm or cm^3
Cubic Foot	cu ft or ft^3	0.028 cubic meter	cu m or m^3
Force			
Pound	lb	4.448 newtons 4.448×10^5 dynes	N

1. BACKGROUND DISCUSSION

The overall objective of designing for crash resistance is to eliminate injuries and fatalities in relatively mild impacts and minimize them in severe but survivable mishaps. A crash-resistant aircraft will also reduce aircraft crash impact damage. By minimizing personnel and material losses due to crash impact, crash resistance conserves resources, is a positive morale factor, and improves the effectiveness of the fleet both in peacetime and in war. Results from analyses and research during the past several years have shown that the relatively small cost in dollars and weight of including crash resistance features is a wise investment (References 2 through 13). Consequently, new generation Army rotary-wing aircraft are being procured to stringent, yet practical, requirements for crash resistance.

It might seem sufficient to simply specify human tolerance requirements and an array of vehicle crash impact conditions and then develop the aircraft with the necessary crash-resistant features. However, available structural and human tolerance analytical techniques are not sufficient to support such an approach; neither is it practical to test complete aircraft sufficiently early in the development cycle to permit evaluation of system concepts. Therefore, specific performance criteria have been established to assure adequate system performance.

Current crash resistance criteria for U.S. Army light fixed- and rotary-wing aircraft are stated in MIL-STD-1290 (Reference 1). These criteria and their origins are described in Volume II. Testing requirements are based on ensuring compliance with the strength and deformation requirements of these criteria.

To provide as much occupant protection as possible, a systems approach to crash resistance must be followed. This means that the landing gear, aircraft structure, and occupant seats must all be designed to work together to absorb kinetic energy and slow the occupants to rest without injurious loading, as shown in Figure 1 (Reference 14). In addition, the occupants must be restrained in a protective structural shell. Weapon sights, controls, instrument panels, and other objects must be delethalized if they lie within the strike envelope of the occupant. Postcrash hazards, such as fire, drowning, entrapment, emergency egress, and rescue must also be considered in an effective crash-resistant design. In addition to a system requirement, minimum criteria are also specified for a number of crash-critical components. For example, minimum crash energy-absorption requirements for landing gear are specified.

The systems approach dictates that the designer consider probable crash conditions wherein some subsystems do not perform their desired functions. For example, the landing gear may not absorb its share of the impact energy because of aircraft attitude. The composition of the earth's surface being impacted must also be considered early in the design phase, when decisions concerning the relative energy-absorption of the landing gear, structure, and seats are made. When impacting on relatively hard surfaces, landing gear with high energy-absorbing capacity can protect the fuselage from damage during low-velocity impacts and help provide occupant protection during higher-velocity impacts. However, during impacts with soft surfaces, such as

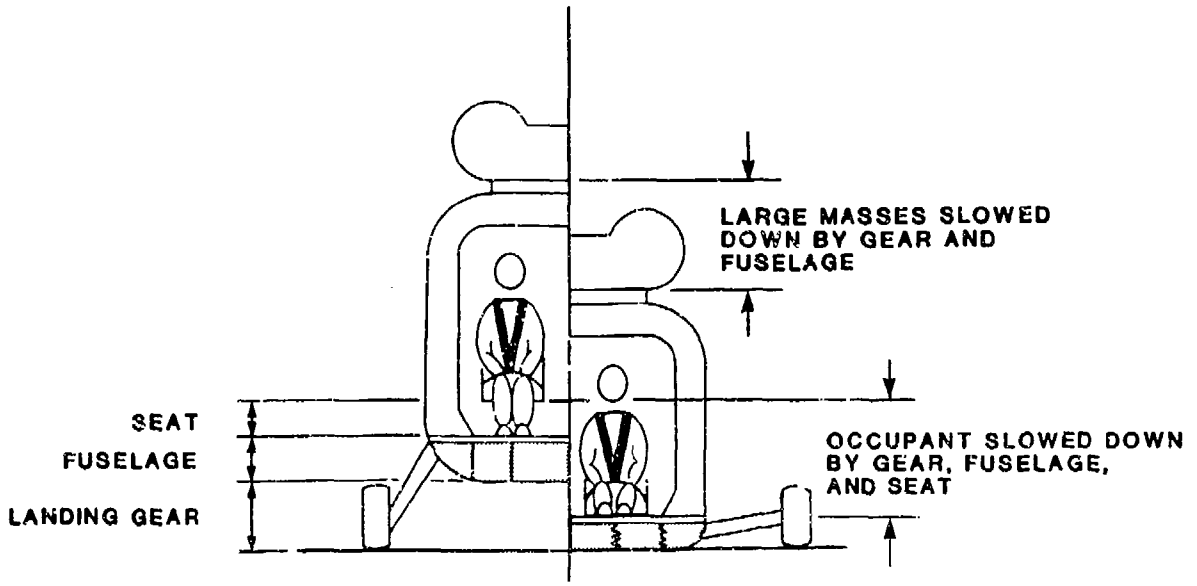

FIGURE 1. ENERGY MANAGEMENT SYSTEM. (FROM REFERENCE 14)

water or marshy ground, or uneven surfaces caused by rocks, trees, etc., the force acting on the landing gear may not be great enough to activate its energy-absorption function, and it will contribute little to occupant protection. Thus it is usually not practical to design a system that relies only on one or two of the three energy absorption features available (landing gear, structure, and seats).

Although more difficult to design, an energy-absorbing fuselage structure is as important as the other components in the system. In addition, the introduction of composite primary structure into modern aircraft presents special problems for the designer dealing with crash resistance. The brittle failure modes of many composites makes the design of energy-absorbing crushable structures more difficult, but not impossible.

Although crash resistance can be most efficiently achieved during the development of new aircraft, the crash resistance of existing aircraft may be significantly improved by retrofitting them with crash-resistant components. This may even be achieved while expanding the combat effectiveness of the aircraft. An example of this is the successful program to retrofit all U.S. Army helicopters with a crash-resistant fuel system that was also self-sealing (Reference 15).

While the definition of an adequate crash-resistant structure may appear relatively simple, many parameters must be considered for an optimum design. A complete systems approach (as summarized in Figure 2) should be employed to include all parameters influencing design, manufacture, performance, and cost. Trade-offs may be required in order to arrive at a final design that most closely meets specifications. Each type of aircraft may require a different emphasis in the parameter mix. Table 1 summarizes major crash-resistance criteria that should be considered during the preliminary design phase.

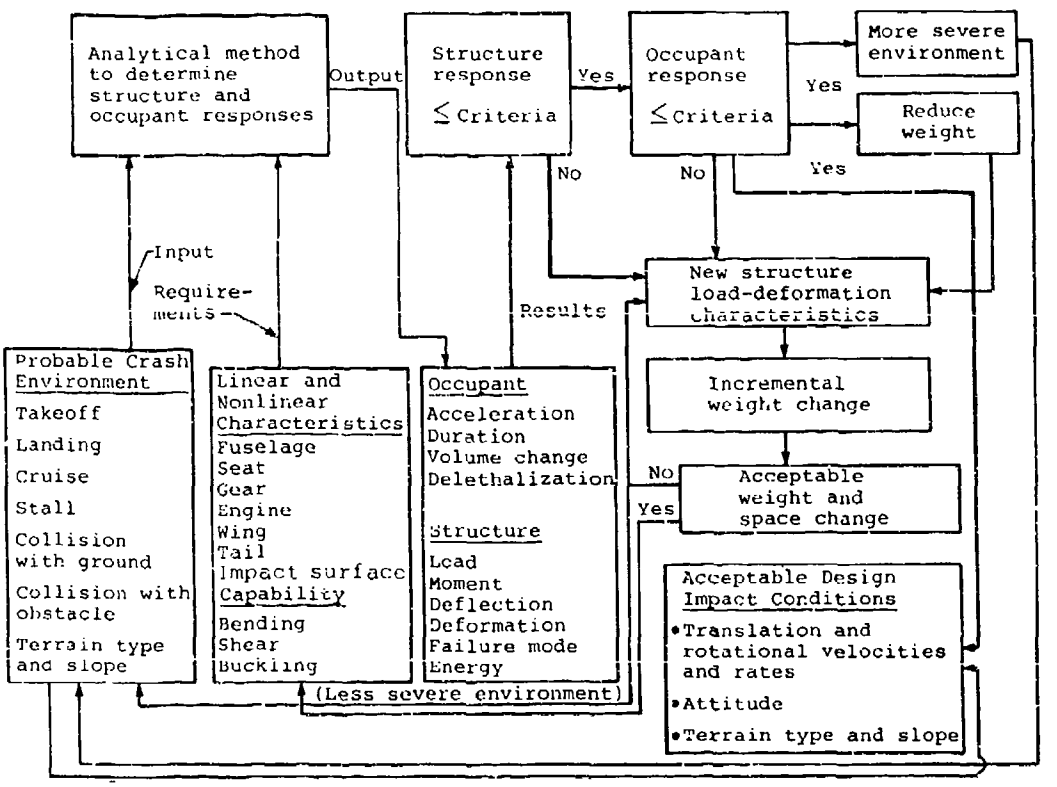

FIGURE 2. PROCEDURE FOR EVALUATION OF STRUCTURAL DESIGNS WITH RESPECT TO CRASH RESISTANCE.

TABLE 1. CRASH-RESISTANCE CRITERIA FOR THE PRELIMINARY DESIGN PROCESS

Crash Scenarios	Primary Structure	Energy Absorption	Postcrash Requirements
• MIL-STD-1290 defines predominant impact conditions • Single axis and combination of: - Vertical impact - Longitudinal impact - Lateral impact - Post impact Rollover Pitchover Nose plowing	• Support of large mass items • Support of systems • Occupant support and protection • Cargo containment and tiedown • Support of landing gear loads • Space consistent with occupant strike envelope • Emergency exit structure	• Landing gear • Controlled structural collapse • Crash-resistant energy-absorbing seats • Shedding of large mass items: - Engines - External stores - Tail boom (Shed items must not impact occupied areas) • Controlled displacement of: - Transmissions - Rotor heads • Impacted surface (soft ground etc.)	• Emergency egress - Occupant release from seats - Door/exit opening - Accessibility and illumination of exits • Minimization of postcrash fire hazards - Fuel containment - Oil and hydraulic fluid containment - Fuel modification - Ignition source control • Reduced material flammability, smoke and toxicity

2. DEFINITIONS

2.1 AIRCRAFT COORDINATE SYSTEMS AND ATTITUDE PARAMETERS

- Aircraft Coordinates

  Positive directions for velocity, acceleration, and force components and for pitch, roll, and yaw are illustrated in Figure 3. When referring to an aircraft in any flight attitude, it is standard practice to use a basic set of orthogonal axes as shown in Figure 3, with x, y, and z referring to the longitudinal, lateral, and vertical directions, respectively.

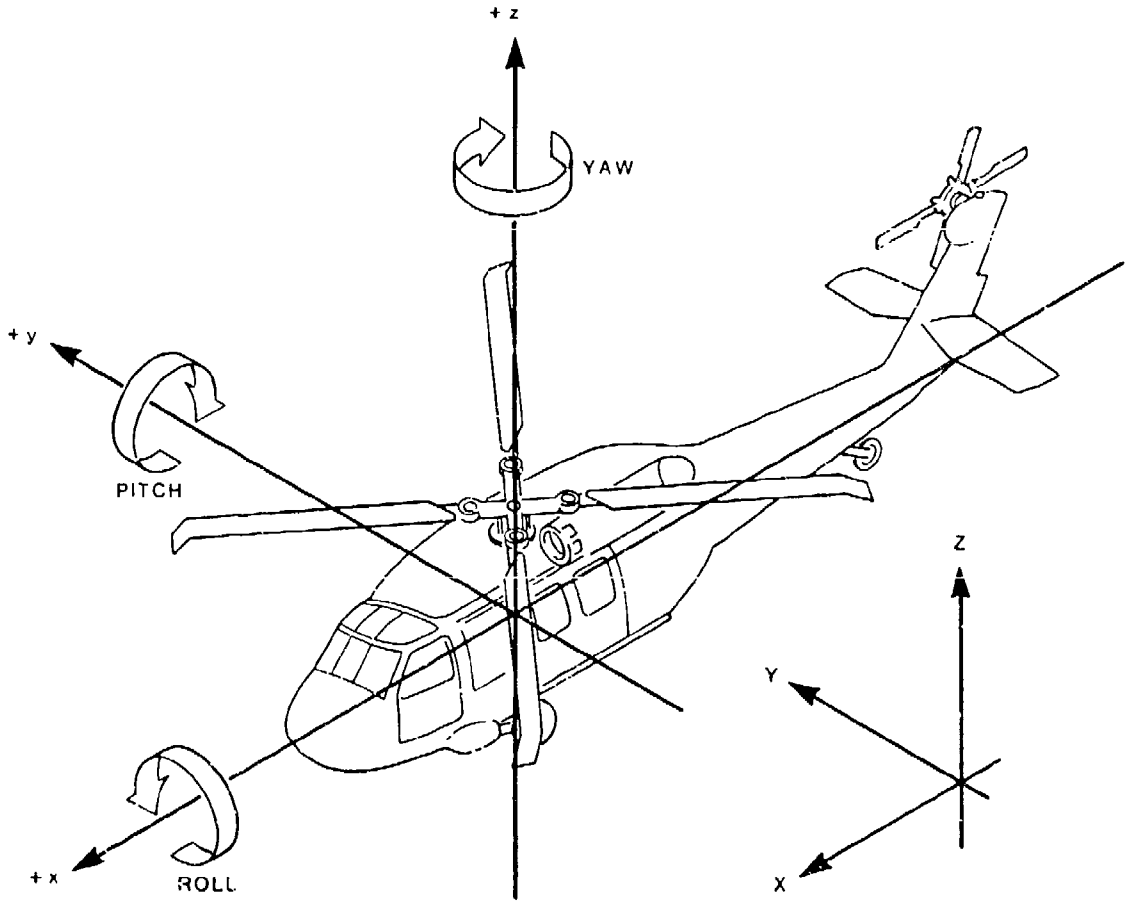

FIGURE 3. AIRCRAFT COORDINATES AND ATTITUDE DIRECTIONS.

However, care must be exercised when analyzing ground impact cases where structural failure occurs, aircraft geometry changes, and reaction loading at the ground plane takes place. In the simulation of such impacts, it is often necessary to use more than one set of reference axes, including the earth-fixed system shown in Figure 3 as X, Y, Z.

- Flight Path Angle

  The angle between the aircraft flight path and the horizontal at the moment of impact.

- Terrain Angle

  The angle between the impact surface and the horizontal, measured in a vertical plane. The algebraic sign of the Terrain Angle is positive when the direction of flight is uphill, and negative when the direction of flight is downhill.

- Impact Angle

  The angle between the flight path and the terrain, measured in a vertical plane. The impact angle is the algebraic sum of the flight path angle plus the terrain angle.

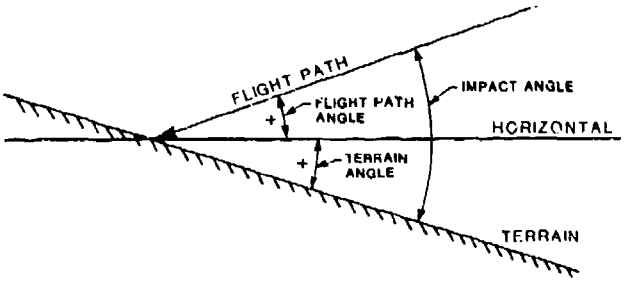

UPHILL FLIGHT

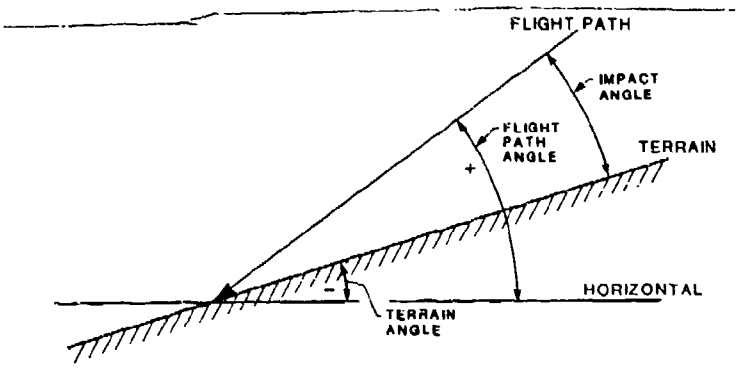

DOWNHILL FLIGHT

- Attitude at Impact

  The aircraft attitude with respect to the aircraft coordinate system, in degrees at the moment of initial impact. The attitude at impact is stated in degrees of pitch, yaw, and roll (see Figure 3).

2.2 ACCELERATION-RELATED TERMS

- Acceleration

  The rate of change of velocity. An acceleration is required to produce any velocity change, whether in magnitude or in direction. Acceleration may produce either an increase or a decrease in velocity. There are two basic types of acceleration: linear, which changes translational velocity, and angular (or rotational), which changes angular (or rotational) velocity. With respect to crash impact conditions, unless otherwise specified, all acceleration values are those at a point approximately at the center of the floor of the fuselage or at the center of gravity of the aircraft

- Deceleration

  Acceleration in a direction to cause a decrease in velocity.

- Abrupt Accelerations

  Accelerations of short duration primarily associated with crash impacts, ejection seat shocks, capsule impacts, etc. One second is generally accepted as the dividing point between abrupt and prolonged accelerations. Within the extremely short duration range of abrupt accelerations (0.2 sec and below), the effects on the human body are limited to mechanical overloading (skeletal and soft tissue stresses), there being insufficient time for functional disturbances due to fluid shifts.

- The Term G

  The ratio of a particular acceleration (a) to the acceleration (g) due to gravitational attraction at sea level (32.2 ft/sec^2 or 9.81 m/sec^2); $G = a/g$. In accordance with common practice, this report will refer to accelerations measured in G. To illustrate, it is customarily understood that 5 G represents an acceleration of 5×32.2, or 161 ft/sec^2.

2.3 VELOCITY-RELATED TERMS

- Velocity Change in Major Impact (Δv)

  The decrease in velocity of the airframe during the major impact, expressed in feet per second. The major impact is the one in which the highest forces are incurred, not necessarily the initial impact. For the acceleration pulse shown in Figure 4, the major impact should be considered ended at time t_2. Elastic recovery in the structure will tend to reverse the direction of the aircraft

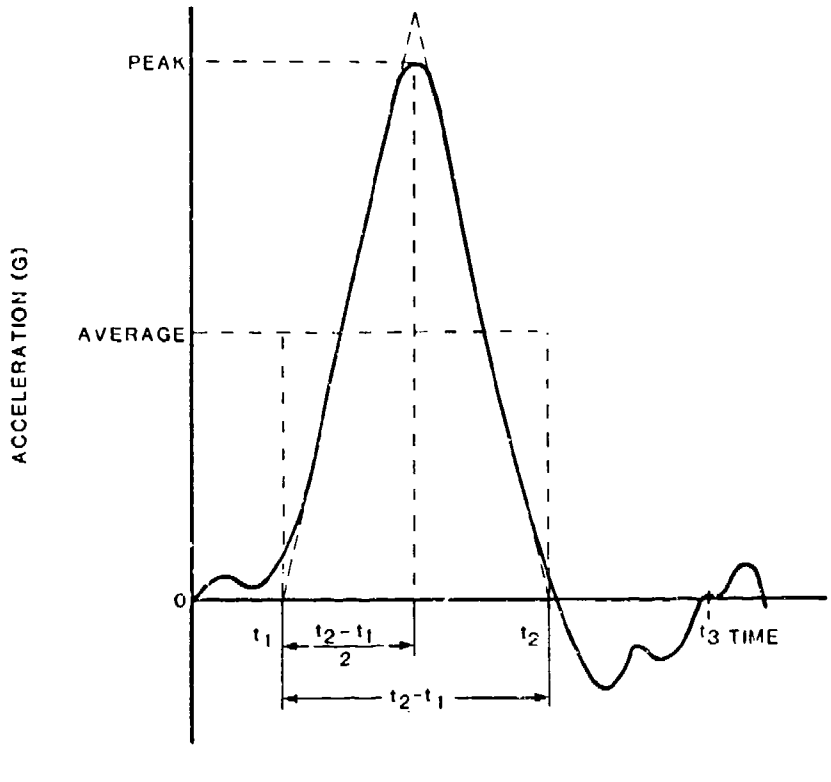

FIGURE 4. TYPICAL AIRCRAFT FLOOR ACCELERATION PULSE.

velocity prior to t_2. Should the velocity actually reverse, its direction must be considered in computing the velocity change. For example, an aircraft impacting downward with a vertical velocity component of 30 ft/sec and rebounding with an upward component of 5 ft/sec should be considered to experience a velocity change

$$\Delta v = 30 - (-5) = 35 \text{ ft/sec}$$

during the major impact. The velocity change during impact is further explained in Section 7.2.

- Longitudinal Velocity Change

The decrease in velocity during the major impact measured along the longitudinal (roll) axis of the aircraft. The velocity may or may not reach zero during the major impact. For example, an aircraft impacting the ground at a forward velocity of 100 ft/sec and slowing to 35 ft/sec would experience a longitudinal velocity change of 65 ft/sec during this impact.

- Vertical Velocity Change

  The decrease in velocity during the major impact measured along the vertical (yaw) axis of an aircraft. The vertical velocity generally reaches zero during the major impact and may reverse if rebound occurs.

- Lateral Velocity Change

  The decrease in velocity during the major impact measured along the lateral (pitch) axis of the aircraft.

2.4 FORCE TERMS

- Load Factor

  A crash force can be expressed as a multiple of the weight of an object being accelerated. A load factor, when multiplied by a weight, produces a force which can be used to establish static strength (see Static Strength). Load factor is expressed in units of G. Crash load factors are ultimate load factors.

- Forward Load

  Loading in a direction toward the nose of the aircraft, parallel to the aircraft longitudinal (roll) axis.

- Aftward Load

  Loading in a direction toward the tail of the aircraft, parallel to the aircraft longitudinal (roll) axis.

- Downward Load

  Loading in a downward direction parallel to the vertical (yaw) axis of the aircraft.

- Upward Load

  Loading in an upward direction parallel to the vertical (yaw) axis of the aircraft.

- Lateral Load

  Loading in a direction parallel to the lateral (pitch) axis of the aircraft.

- Combined Load

  Loading consisting of components in more than one of the directions described in Section 2.1.

- Crash Force Resultant

The geometric sum of horizontal and vertical crash forces: horizontal and vertical velocity components at impact, and horizontal and vertical stopping distances. The Crash Force Resultant is fully defined by determination of both its magnitude and its direction. The algebraic sign of the resultant crash force angle is positive when the line of action of the resultant is above the horizontal, and negative if the line of action is below the horizontal.

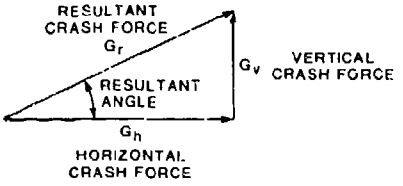

- Crash Force Angle

The angle between the resultant crash force and the longitudinal axis of the aircraft. For impacts with little lateral component of force, the crash force angle is the algebraic sum of the crash force resultant angle plus the aircraft pitch angle.

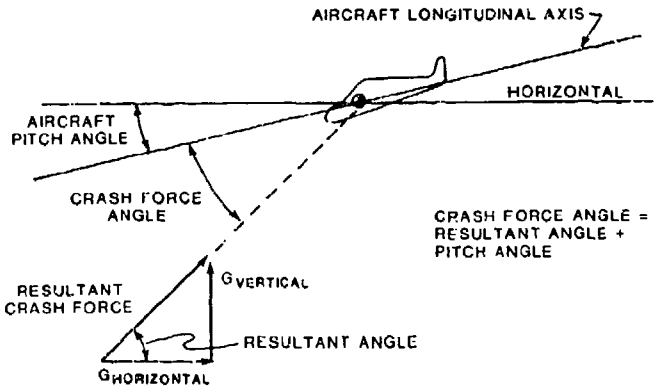

2.5 DYNAMICS TERMS

- Rebound

Rapid return toward the original position upon release or rapid reduction of the deforming load, usually associated with elastic deformation.

- Dynamic Overshoot

  The amplification of decelerative force on cargo or personnel above the floor input decelerative force (ratio of output to input). This amplification is a result of the dynamic response of the system.

- Transmissibility

  The amplification of a steady-state vibrational input amplitude (ratio of output to input). Transmissibilities maximize at resonant frequencies and may increase acceleration amplitude similar to dynamic overshoot.

2.6 CRASH SURVIVABILITY TERMS

- Survivable Accident

  An accident in which the forces transmitted to the occupant through the seat and restraint system do not exceed the limits of human tolerance to abrupt accelerations and in which the structure in the occupant's immediate environment remains substantially intact to the extent that a livable volume is provided for the occupants throughout the crash sequence.

- Survival Envelope

  The range of impact conditions, including magnitude and direction of pulses and duration of forces occurring in an aircraft accident, wherein the occupiable area of the aircraft remains substantially intact, both during and following the impact, and the forces transmitted to the occupants do not exceed the limits of human tolerance when current state-of-the-art restraint systems are used.

  It should be noted that, where the occupiable volume is altered appreciably through elastic deformation during the impact phase, survivable conditions may not have existed in an accident that (from postcrash inspection) outwardly appeared to be survivable.

2.7 OCCUPANT-RELATED TERMS

- Human Body Coordinates

  In order to minimize the confusion sometimes created by the terminology used to describe the directions of forces applied to the body, a group of NATO scientists compiled the accelerative terminology table of equivalents shown in Figure 5 (Reference 16). Terminology used throughout this guide is compatible with the NATO terms as illustrated.

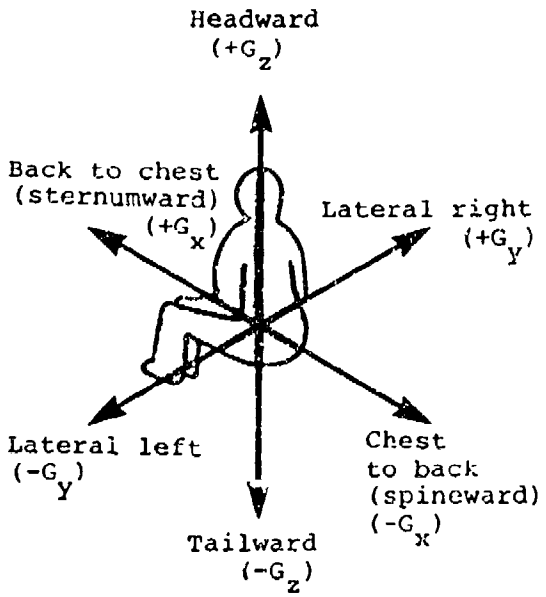

Direction of accelerative force

Vertical

Headward - Eyeballs-down
Tailward - Eyeballs-up

Transverse

Lateral right	- Eyeballs-left
Lateral left	- Eyeballs-right
Back to chest	- Eyeballs-in
Chest to back	- Eyeballs-out

Note:

The accelerative force on the body acts in the same direction as the arrows.

FIGURE 5. TERMINOLOGY FOR DIRECTIONS OF FORCES ON THE BODY.

- Anthropomorphic Dummy

A device designed and fabricated to represent not only the appearance of humans but also the mass distribution, joint locations, motions, geometrical similarities such as flesh thickness and load/deflection properties, and relevant skeletal configurations such as iliac crests, ischial tuberosities, rib cages, etc. Attempts are also made to simulate human response of major structural assemblages such as thorax, spinal column, neck, etc. The dummy is strapped into seats or litters and used to simulate a human occupant in dynamic tests.

- Human Tolerance

For the purposes of this document, human tolerance is defined as a selected array of parameters that describe a condition of decelerative loading for which it is believed there is a reasonable probability for survival without major injury. As used in this volume, designing for the limits of human tolerance refers to providing design features that will maintain these conditions at or below their tolerable levels to enable the occupant to survive the given crash impact conditions.

Obviously, the tolerance of the human body to crash impact conditions is a function of many variables including the unique characteristics of the individual person as well as the loading variables. The loads applied to the body include decelerative loads imposed by seats and restraint systems as well as localized forces due to impact with surrounding structures. Tolerable magnitudes of the decelerative loads depend on the direction of the load, the orientation of the body, and the means of applying the load. For example, the critical nature of loads parallel to the occupant's spine manifests itself in any of a number of spinal fractures, but typically the fracture is an anterior wedge, or compressive failure of the front part of a vertebra. Forces perpendicular to the occupant's spine can produce spinal fracture through shear failures or from hyperflexion resulting, for example, from jackknife bending over a lap-belt-only restraint. The lap belt might inflict injuries to the internal organs if it is not retained on the pelvic girdle but is allowed to exert its force above the iliac crests in the soft stomach region. Excessive rotational or linear acceleration of the head can produce concussion. Further, skull fracture can result from localized impact with surrounding structure. Therefore, tolerance is a function of the method of occupant restraint as well as the characteristics of the specific occupant. Refer to Chapter 5 of Volume II for a more detailed discussion of human tolerance.

2.8 STRUCTURAL TERMS

- Airframe Structural Crash Resistance

  The ability of an airframe structure to maintain a protective shell around occupants during a crash and to minimize accelerations applied to the occupiable portion of the aircraft during crash impacts.

- Structural Integrity

  The ability of a structure to sustain crash loads without collapse, failure, or deformation of sufficient magnitude to cause injury to personnel.

- Static Strength

  The maximum or ultimate static load that can be sustained without structural failure, often expressed in terms of ultimate static load factor.

- Strain

  The ratio of change in length to the original length of a loaded component.

- Collapse

  Deformation or fracture of structure to the point of loss of useful load-carrying ability or useful volume.

- Failure

  Loss of functional capability or collapse.

- Limit Load

  In a structure, limit load refers to the load the structure will carry before yielding. Similarly, in an energy-absorbing device, it represents the load at which the device deforms in performing its function.

- Ultimate Load

  The maximum load restrained by a structure progressively loaded until fracture or collapse occurs.

- Load Limiter, Load-Limiting Device, or Energy Absorber

  These are interchangeable names of devices used to limit the load in a structure to a preselected value. These devices absorb energy by providing a resistive force applied over a deformation distance without significant elastic rebound and without failure.

- Specific Energy Absorbed (SEA)

  The energy absorbed by an energy-absorbing device or structure divided by its weight.

- Bottoming

  With respect to energy-absorbing structure, bottoming is a condition in which the deforming structure or material becomes compacted and the load increases rapidly with little further deformation.

- Bulkhead

  A structural partition extending upward from the floor and dividing the aircraft into separate compartments. Seats can be mounted on bulkheads instead of the floor.

3. CRASH IMPACT CONDITIONS

3.1 INTRODUCTION

This section describes general impact conditions, failure modes of aircraft structure in a crash impact, and resulting injury mechanisms. It also describes the energy present at and after impact and possible ways that it may be dissipated.

Helicopters are often used in areas where fixed-wing aircraft cannot function and, of necessity, spend time maneuvering at low forward velocities. Under such conditions, power failure at low altitude results in a predominantly vertical impact. However, side or fuselage impact with ground obstacles, such as overhead wires, trees, or buildings, can generate aircraft rotation. Fixed-wing aircraft can impact with high vertical velocity if a stall occurs at low altitude.

Impacts with a predominantly longitudinal velocity vector occur when aircraft are flown into inclined surfaces, mountains, ground obstacles, or when ground impact occurs with the aircraft in an extreme nose-down diving attitude. When an impact occurs with an obstacle located near the ground, i.e., overhead wires, trees, or buildings, the subsequent rotational motions can result in ground impact occurring at almost any attitude.

Although the major impact generally produces the most severe hazard for occupants, additional hazards can be encountered during the remainder of the crash sequence. Items such as rotor blades, transmission assemblies, engines, and external stores may become detached from the aircraft and impact occupied sections or cause the release of flammable fluids. External objects such as trees and ground equipment may also penetrate occupied aircraft sections and present a hazard.

3.2 STRUCTURAL DAMAGE THAT FREQUENTLY RESULTS IN OCCUPANT INJURY

Although the distribution of accident types may vary considerably for fixed-wing conventional aircraft and vertical takeoff and landing aircraft, they tend to experience similar structural loading for similar impact conditions. Therefore, the structural damage that produces occupant injury is generally the same for both.

Usually, the structure that first contacts the impact surface is the first to deform. As decelerative forces increase, deformation continues and more structure becomes involved. Eventually, buckling may occur throughout the aircraft. The protective shell is then compressed between the impact surface and masses aft or above the protective shell. If parts of the aircraft, such as wings and tail sections of fixed-wing aircraft, break free from the cabin section during the impact, this may limit cabin deformation; however, it may also produce a higher acceleration level within the cabin.

The following subsections describe frequently occurring impact conditions and injury-causing events. The aircraft involved were not designed to be crash-resistant in accordance with current specifications.

3.2.1 Longitudinal (Crushing) Loads on Cockpit Structure

During an impact with high longitudinal velocity on soft earth, the aircraft nose structure is sometimes deformed so that it scoops earth as it slides along the ground. This produces high forces that may collapse the forward cockpit structure and cause entrapment of occupants and/or injury to their lower extremities. In addition, the high forces produce high aircraft accelerations, resulting in high loads on personnel and cargo restraint systems. A similar effect may be experienced on water.

A combination of nose structure crushing and friction between the structure and the terrain (particularly in "long-nose" aircraft) may cause the forward structure to be pulled beneath the rest of the aircraft. This type of damage causes rupture of the cockpit floor and higher longitudinal acceleration than would be experienced if a smooth "skid" were maintained under the nose.

Longitudinal crushing also occurs if a high angle of attack exists between the aircraft and the obstacle against which it crashes. This can result from a shallow-angle impact with terrain features such as a hillock or bank, from a steep-flight angle impact with respect to relatively flat terrain, or from a nose-on impact into vertical walls, such as revetments. The resulting crushing may be sufficient to destroy occupied areas of the cockpit or cabin and reduce chances for occupant survival.

3.2.2 Vertical (Crushing) Loads on Fuselage Shell

Collapse of the protective shell due to vertical loading often occurs in high-sink-rate accidents or rollover accidents. The collapse is often aggravated by the large masses above the fuselage structure such as engines, transmissions, and rotor mechanisms in rotary-wing aircraft and high wings in fixed-wing aircraft. This damage also results in loss of occupiable volume.

Also, if the underfloor structure collapses without absorbing sufficient energy, the energy-absorbing capacity of stroking seats may be exceeded in the impact. The seat will then bottom out, and high loads transmitted to the occupant may then cause spinal injury.

3.2.3 Lateral (Crushing) Loads on Fuselage Shell

Lateral impact of utility helicopters occurs frequently. A 1971 study showed that over half of severe utility helicopter crashes result in rollover or side impact (Reference 17). Eyewitnesses of side impact crashes in which landing or hovering helicopters caught rotor blades on trees or other obstacles report that the helicopters tend to flip on their sides and may rise to a height of approximately 15 ft before crashing.

If the sides of the fuselage are not designed for crash protection, severe injuries can result from relatively minor accidents. Occupants are placed close to the sides of the fuselage, and often their restraint systems, such as lap belts used alone or with gunner tethers, are not adequate to restrain the occupants laterally. On occasions, the doors have been removed previously or are lost during the crash. The occupant is then exposed to a variety of additional hazards.

3.2.4 Transverse (Bending) Loads on Fuselage Shell

Rupture or collapse of the protective shell often occurs due to the high bending loads during rapid pitch change associated with longitudinal crashes at moderate-to-high impact angles. Rupture of the protective shell exposes occupants to injury through direct contact with the impact surface, contact with jagged metal, and loss of restraint. Miscellaneous equipment also may strike occupants after breakup of the aircraft.

3.2.5 Deformation (Buckling) of Floor Structure

In most aircraft, occupant and cargo restraint depends heavily upon the integrity of the floor structure. When this structure fails, restraint is lost. Often floor failure is caused by crushing and warping of underfloor supporting structure. Localized damage is frequently caused when fuselage-mounted landing gear are driven into the floor structure.

3.2.6 Landing Gear Penetration of Fuselage Shell

Landing gear failures often result in personnel injuries, either directly (as mentioned above) or indirectly, through fire exposure caused by rupture of flammable fluid lines and tanks.

3.2.7 Helicopter Lateral Rollover

In helicopter accidents, rollover invariably causes the main rotor blades to strike the ground. This contact involves two potential hazards: displacement of the transmission and intrusion of blades into occupied areas.

Transmission displacement is controlled basically by the strength of the mounts. In aircraft with fully articulated main rotor hubs, the blades tend to destroy themselves without transferring excessively high loads to the transmission. For rotor craft with a high inertia main rotor, blade impact loads will be transferred to the transmission mounts. However, a high inertia main rotor may afford some additional margin during an autorotation, thereby reducing the frequency and severity of accidents.

The UH-60A Black Hawk mishap experience and that of other helicopters with similar transmission/rotor and engine retention strengths have shown that the high-mass-item retention strengths required by MIL-STD-1290 effectively prevent separation of the transmission.

3.2.8 Rupture of Flammable Fluid Containers

Rupture of structure surrounding flammable fluid containers or transfer lines is often an indirect cause of occupant injury as a result of postcrash fire.

3.3 ENERGY CONTENT OF AIRCRAFT AT IMPACT

The total energy which the complete aircraft system possesses immediately prior to impact is dissipated in the crash sequence. This energy includes the following:

- Translational kinetic energy, $(K.E.)_T$.
- Rotational kinetic energy, $(K.E.)_R$.
- Potential energy, P.E.
- Strain energy, S.E.

The total energy input during the crash sequence, T.E., is

$$T.E. = (K.E.)_T + (K.E.)_R + P.E. + S.E. \tag{1}$$

3.3.1 Translational Kinetic Energy, $(K.E.)_T$

This energy component is a direct function of the aircraft mass and the velocity of the mass center at impact.

If v_G = resultant velocity of mass center

$\dot{x}_G$ = longitudinal component of velocity

$\dot{y}_G$ = lateral component of velocity

$\dot{z}_G$ = vertical component of velocity

Then:

$$(K.E.)_T = \frac{1}{2} m v_G^2$$

$$= \frac{m}{2} (\dot{x}_G^2 + \dot{y}_G^2 + \dot{z}_G^2) \tag{2}$$

The total K.E. of the aircraft is the summation for all mass elements of the aircraft.

3.3.2 Rotational Kinetic Energy, $(K.E.)_R$

Rotational kinetic energy may be associated with the total aircraft and with aircraft elements such as engines or rotor systems. In a helicopter, major sources of rotational energy are the rotor head system and the rotating machinery elements, such as engines and transmissions. During a crash, the rotating element may impact external agents and/or the helicopter structure.

However, if, for example, gas turbine engines are not severely damaged, it is likely that there will be no appreciable change in the angular velocity of the rotational elements during the crash and no structural deformation.

Selective assessment of rotational kinetic energy contributions to the crash energy balance must be made.

Basically, $$(K.E.)_R = \frac{1}{2}I_\theta \dot{\theta}^2 + \frac{1}{2}I_\phi \dot{\phi}^2 + \frac{1}{2}I_\psi \dot{\psi}^2 \quad (3)$$

where $\dot{\theta}$ = angular velocity component in x-z plane (pitch)

$\dot{\phi}$ = angular velocity component in y-z plane (roll)

$\dot{\psi}$ = angular velocity component in x-y plane (yaw).

and I_θ, I_ϕ, I_ψ, are the mass moments of inertia of the vehicle with respect to pitch, roll, and yaw axes, respectively, at its mass center.

3.3.3 Potential Energy, (P.E.)

For the crash sequence, the total potential energy input into the system equals the summation of the vertical displacement, ΔZ, contribution of each mass from the time of impact until the time of completion.

$$P.E. = \sum(mg\Delta Z) \quad (4)$$

The large mass items, such as transmissions and engines, are major contributors to the energy balance.

3.3.4 Strain Energy, (S.E.)

Structural strain energy may exist due to in-flight loading. In addition, pressurized systems may have stored energy. However, such energy is usually insignificant.

3.4 POSTIMPACT ENERGY DISSIPATION

After initial impact, there are several ways of absorbing energy to bring the vehicle to a stop while providing survivable conditions for the occupants. Possible major contributors in the energy-absorption process are the following:

1. Energy-Absorbing Landing Gear - The landing gear may provide a high level of energy absorption, depending on design criteria for the aircraft and the impact surface.

2. Structural Deformation - Structural deformation can provide another major means of energy absorption. Compression, tension, bending, torsion, and shear from low levels up to ultimate conditions all contribute to energy absorption. Vertical loads may be limited by crushing and deformation of the structure, while the frame and bulkhead members still support large mass items. Longitudinal loads are likewise limited by structural crushing.

3. Breakaway of High-Mass Items - The breakaway of high-mass items causes an instantaneous mass change and a corresponding reduction in kinetic and potential energies to be absorbed by the remaining structure. A major problem involved is designing the vehicle to ensure clean breakaway characteristics with adequate clearance between each free item and the occupied area. If potential hazards from impacting occupied areas or generating fires can be identified, it is better to retain the large mass items.

4. Ground Friction and Nose Plowing - Longitudinal deceleration is provided by ground friction and/or nose plowing depending on the type of impacted surface. Impact with ground obstacles such as rocks, trees, stumps, and poles, could be included in this category of energy absorption. However, these types of obstacles usually absorb small amounts of energy because of their relatively small size.

5. Displacement of Soft Earth During Vertical Impact - Vertical deceleration may be limited by compacting and displacing soft earth (or loam, sand, mud, water, etc.). Forces are very high when a large flat portion of the fuselage contacts the earth all at once, and forces are more moderate when rounded corners of the fuselage penetrate the earth.

6. Energy-Absorbing Seats - The seat is the final link between an aircraft occupant and the ground. Because the human body has a relatively low tolerance to decelerations parallel to the spine, it is usually necessary that energy absorption be included in the seat design. Crash-resistant seat design is described in detail in Volume IV.

3.5 CRASH KINEMATICS

The motion of the c.g. of the aircraft is relatively easily characterized in terms of velocities and stopping distances if appropriate assumptions about the impact acceleration can be made. These calculations may not be used often by the aircraft designer, but they are useful in crash reconstructions and the development of performance criteria. A complete development of these kinematic relationships and numerous examples of stopping distance calculations for a variety of deceleration pulses are included in the chapter on analytical methods.

4. CRASH PERFORMANCE REQUIREMENTS

4.1 INTRODUCTION

A crash can involve a wide range of dynamic conditions, from a simple unidirectional impact to a complex combination of rotational and multidirectional impacts. Historically, accident data from severe survivable crashes were used to define velocity changes occurring in the major impact. In addition, estimates of accelerations experienced on the cabin floor were made for use in the design of seats and cargo restraints. The data were obtained from investigations of light fixed- and rotary-wing aircraft accidents from 1960 to 1965 and from 1971 to 1976. The aircraft did not contain crash-resistant structures, energy-absorbing seats, or crash-resistant landing gear. More recently, crash data have been utilized along with operational and cost constraints to arrive at an optimal set of design impact conditions for Army aircraft. The current crash design impact conditions for Army light fixed- and rotary-wing aircraft in accordance with MIL-STD-1290 are summarized in Table 2. Table 3 shows corresponding performance requirements under these impacts and Table 4 lists other design requirements specified by MIL-STD-1290.

4.2 GENERAL REQUIREMENTS

Aircraft should be designed to prevent fatalities and minimize the number and severity of injuries during crash impacts of the severity defined in Table 2. In a severe crash, the service life of the aircraft is usually ended, and the only structural requirement is to provide occupant protection. In order to accomplish this, structure must be allowed to crush and deform in a controlled, predictable manner so that forces and accelerations imposed upon occupants will be minimized while still maintaining the protective shell. This means that any analysis for crash resistance should consider the large deflections of structural members and joints as well as loading in the plastic range of stress. Excessively strong airframe structure is no more acceptable than understrength structure for crash resistance. Not only will unnecessary strength result in an unacceptable weight penalty but on impact high acceleration that degrades occupant survivability may be generated. In crashes of lesser energy content, which could be called hard landings, the intent is to avoid expensive damage to the aircraft and mission equipment. Energy-absorbing landing gear is the primary means of achieving this.

The probability of occupant survival will be increased if proper attention is given to the following features during initial design:

- Airframe protective shell around occupants
- Adequate tiedown strength for occupants, cargo, and equipment
- Noninjurious occupant acceleration environment
- Noninjurious occupant environment hazards
- Elimination of postcrash fire
- Adequate emergency escape and rescue provisions.

TABLE 2. CRASH IMPACT DESIGN CONDITIONS, WITH LANDING GEAR EXTENDED, MIL-STD-1290

Condition No.	Impact Direction (Aircraft Axes)	Object Impact	Velocity Change ΔV (ft/sec)
1	Longitudinal (cockpit)	Rigid vertical barriers	20
2	Longitudinal (cabin)		40
3	Vertical*	Rigid horizontal surface	42
4	Lateral, Type I**		25
5	Lateral, Type II***		30
6	Combined high angle*		
	Vertical		42
	Longitudinal		27
7	Combined low angle	Plowed Soil	
	Vertical		14
	Longitudinal		100

*For the case of retracted landing gear the seat and airframe combination shall have a vertical crash impact design velocity change capability of at least 26 ft/sec.

**Type I - Light fixed-wing aircraft.

***Type II - Rotary-wing, including tilt-prop/rotor aircraft.

Note: See Volume II for vehicle attitude.

4.3 DETAIL REQUIREMENTS

4.3.1 Airframe Crash Resistance

The aircraft structure should provide a protective shell and deform in a predictable manner so that forces imposed upon the occupants will be limited. In areas where large structural deformations are anticipated, joints and attachments should be designed to withstand large angular deflections and/or large linear displacements without failure. All structure likely to be in contact with the impact surface should be constructed of materials which resist abrasion-induced sparking.

Unless otherwise stated, the aircraft design gross weight (DGW) should be used for the vehicle weight in the analyses described below. Directions are assumed with respect to the aircraft (Figure 3) unless otherwise stated.

TABLE 3. PERFORMANCE REQUIREMENTS UNDER CRASH IMPACT CONDITIONS PER TABLE 2

Condition No.	Impact Direction	Percentage Volume Reduction	Other Requirements
1	Longitudinal (Cockpit)	No serious hazard to pilot/copilot	Does not impede postcrash egress. Engine transmission, rotor system remain intact and in place
2	Longitudinal (Cabin)	15 maximum length reduction for passenger/troop compartment	Inward buckling of side walls should not pose hazard to occupants or restrict their evacuation
3	Vertical	15 maximum height reduction in cockpit and passenger/troop compartment	G loads not injurious
4 & 5	Lateral	15 maximum width reduction	Lateral collapse of occupied areas not hazardous, no entrapment of limbs
6	Combined High Angle	No serious hazard to occupant due to cockpit/cabin reduction	
7	Combined Low Angle	No serious hazard to occupant	

4.3.1.1 Longitudinal Impact

4.3.1.1.1 Impact Conditions. The basic airframe should be capable of impacting longitudinally into a rigid abutment or wall at a contact velocity of 20 ft/sec without crushing the pilot and copilot stations to an extent which would either preclude pilot and copilot evacuation of the aircraft or otherwise be hazardous to the life of the aircraft occupants. For such an impact, the engine(s), transmission, and rotor system for helicopters should remain intact and in place in the aircraft except for damage to the rotor blades. The basic airframe of passenger-carrying helicopters should be capable of impacting longitudinally into a rigid abutment or wall at a contact velocity of 40 ft/sec without reducing the length of the passenger/troop compartment by more than 15 percent. Any consequent inward buckling of walls, floor, and/or roof should not be hazardous to the occupants and/or restrict their evacuation. The aircraft should also be designed to withstand impact following a low angle missed approach. This impact in plowed soil (Figure 6) can result in a rollover and side impacts which may crush and/or separate the

TABLE 4. OTHER STRUCTURAL PERFORMANCE REQUIREMENTS

Impact Direction	Impacted Surface	Velocity Differential (ft/sec)	Vehicle Attitude Limits	Percentage Volume Reduction	Other Requirements
Rollover	Earth	-	90^{o} sideward or 180^{o} inverted or any intermediate angle	Minimal (door hatches etc. assumed to be non-load carrying)	Forward fuselage buried to depth of 2 in. (inverted or on side). Load uniformly distributed over forward 25% of occupied fuselage length. Can sustain 4 G without injury to seated and restrained occupants. All loading directions between normal and parallel to skin to be considered.
Rollover (Post-impact)	Rigid		Two 360^{o} Rolls (maximum)	15 maximum volume reduction (5 percent desired)	
Earth Plowing & Scooping	Earth	-	-	-	Preclude plowing when forward 25% of fuselage has uniformly applied vertical load of 10 G and rearward load of 4 G or the ditching loads of MIL-A-008865, whichever is the greatest.
Landing Gear	Rigid	20	$\pm 10^{o}$ Roll $+15^{o}$ to -5^{o} Pitch	None. Plastic deformation of gear and mounting system allowable	Aircraft deceleration at normal G.W. for impact with no fuselage to ground contact. All other A/C structural parts, except blades, should be flightworthy following crash.
Landing Gear	Sod	100 long.[c]* 14 vertical	-5^{o} Pitch $\pm 10^{o}$ Roll $\pm 20^{o}$ Yaw	15 maximum volume reduction (5 percent desired)	No rollover, or if rollover occurs, two 360^{o} rolls without fuselage crushing.

* Velocity at impact, not differential.

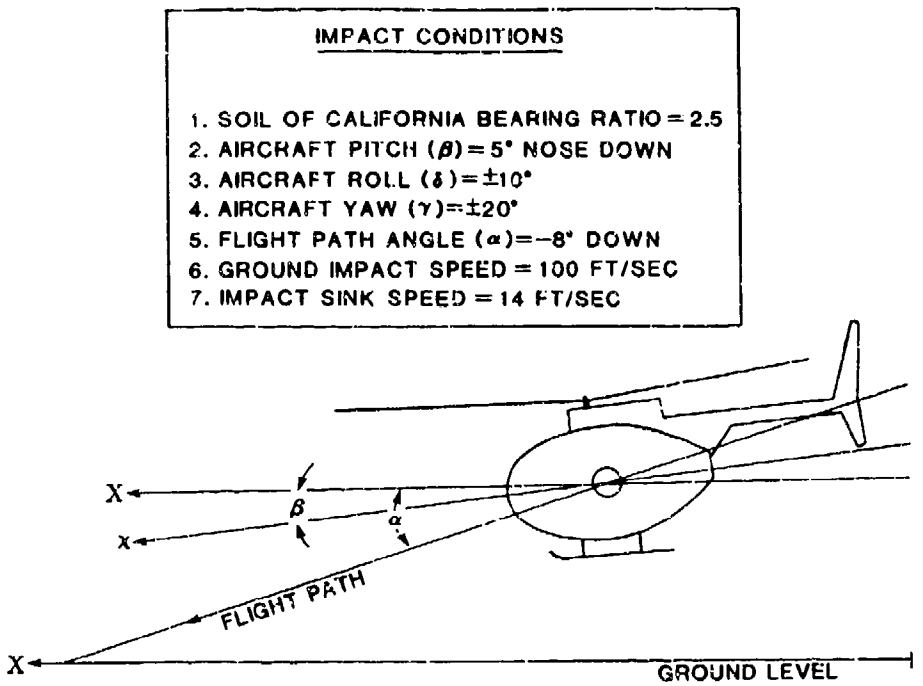

FIGURE 6. LOW-ANGLE IMPACT DESIGN CONDITIONS (SIMULATED APPROACH WITH ANTITORQUE LOSS UNDER POOR VISIBILITY).

fuselage. The volume of the cockpit or the occupied passenger/troop compartment should not be reduced by more than 15 percent (5 percent desired). Static loads for rollover analysis are described in Section 4.3.1.4.

4.3.1.1.2 Earth Scooping Effects. Earth scooping effects encountered in longitudinal impacts should be minimized as follows:

- A large, relatively flat surface should be provided in those areas which could gouge or plow, thereby increasing the aircraft's tendency to slide over the impacted terrain.
- Inward buckling of the fuselage nose or engine nacelle should be minimized to maintain skid surface integrity.
- The nose section should be designed to preclude any earth plowing and scooping tendency when the forward 25 percent of the fuselage has a uniformly applied local upward load of 10 G and an aft load of 4 G, as shown in Figure 7.

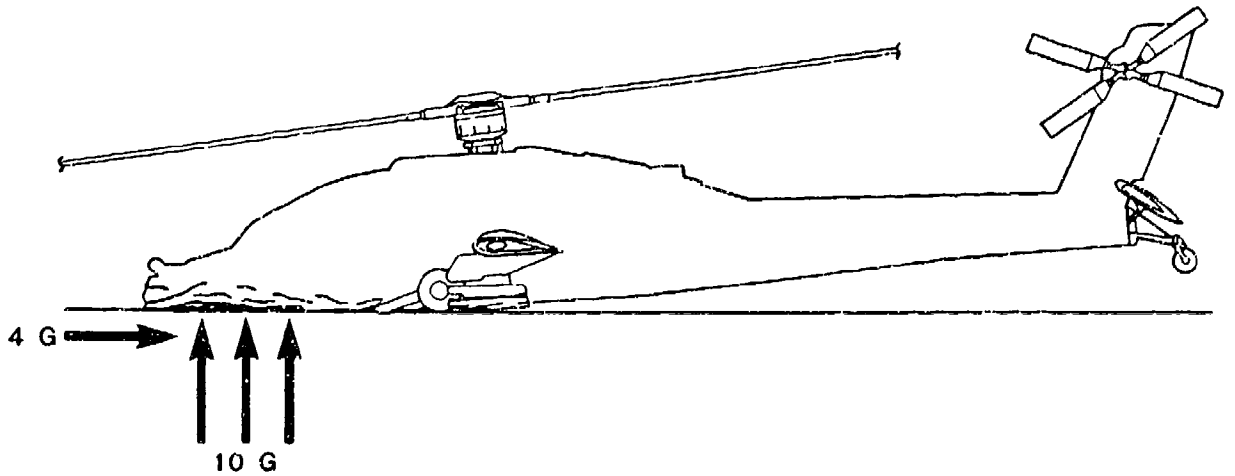

FIGURE 7. NOSE SECTION DESIGN CONDITIONS.

4.3.1.1.3 Buckling Effects. To minimize hazards created by buckling, the aircraft should be designed to:

- Provide sufficient structural strength in the protective shell around the occupants to prevent bending or buckling failure of the fuselage.
- Have the fuselage buckle outward rather than inward if it does collapse.
- Have the cargo restraints to be effective even when fuselage bending failure occurs.

4.3.1.1.4 Floor. The floor structure should possess sufficient strength and ductility to carry, without failure, loads applied by the occupants and cargo restraint systems even when deformation and substructure crushing occurs.

4.3.1.2 Vertical Impact.

4.3.1.2.1 Impact Conditions. With the landing gear extended and the rotor/wing lift equal to design gross weight (DGW), the aircraft should withstand a 42-ft/sec vertical impact, without reducing the height of the cockpit or cabin by more than 15 percent and/or causing the occupants to experience injurious accelerative loading. Support of all mass, including troop seats attached to overhead structure, must be provided. For this analysis, the aircraft attitude should be within +15/-5 degrees of pitch and ±10 degrees of roll, in accordance with MIL-STD-1290. Criteria for combinations of pitch and roll are defined by Figure 2 of MIL-STD-1290. For the case of retracted landing gear, the seat and airframe combination should have a vertical velocity change capability of at least 26 ft/sec.

4.3.1.2.2 **Design Application.** Design features for accomplishing the above goal may include the following:

- Locate high-mass items so that they will not intrude into occupied areas during the crash
- Provide sufficient vertical crushing strength to prevent more than 15-percent crush
- Provide load-limiting structure beneath the floor
- Provide load-limiting landing gear
- Provide load-limiting seating for all occupants.

4.3.1.3 Lateral Impact. Light fixed-wing and rotary-wing aircraft should withstand a lateral impact of 25 and 30 ft/sec, respectively, into a rigid barrier without reducing the width of occupied areas by more than 15 percent. The design of the vehicle should minimize the chance of the occupant being trapped between the structure and any impacting surface following failure of doors, canopies, or hatches.

4.3.1.4 Rollover Impact. The aircraft should be designed to resist an earth impact loading as occurs when the aircraft impacts the ground and rolls to a 90-degree (sideward) or 180-degree (inverted) attitude. A rollover should not cause structural failure or major intrusion into occupied areas. It should be assumed that the forward fuselage roof is buried to a depth of 2.0 in. in soil for the inverted attitude and that the load is uniformly distributed over the forward 25 percent of the occupied fuselage length. It should also be assumed that the forward fuselage side is buried to a depth of 2.0 in. in soil for the sideward attitude and that the load is uniformly distributed over the forward 25 percent of the occupied fuselage length. The fuselage should be capable of sustaining a 4-G (i.e., 4.0 x aircraft DGW) load applied over the area(s) described for either the inverted or sideward attitudes shown in Figures 8 and 9, respectively, without structural failure or more than 15-percent loss of living space. For both cases in Figures 8 and 9, the 4-G distributed load should be analyzed for any angle of load application ranging from perpendicular to the fuselage skin (i.e., compressive loading) to parallel to the fuselage skin (i.e., shear loading). When designing for this condition, it should be assumed that all doors, hatches, transparencies, and similar openings cannot carry any loading. However, the mast, wings (if applicable) and tail boom are assumed to be intact.

4.3.1.5 Wings and Empennage. For fixed-wing aircraft, wing design should possess frangible characteristics to allow wings to break free from the fuselage under high longitudinal inertia loads for distributed impact loads caused by striking a barrier such as an earth mound. Empennage structure may also be designed to collapse or break away during longitudinal crash impact.

For rotary-wing aircraft, wings used to support external stores prevent rollover of the helicopter in many accidents and should not be frangible, but should allow the stores to separate under high-G loads while maintaining the structural integrity of the wing. However, the wing should break off before the fuselage structure itself collapses.

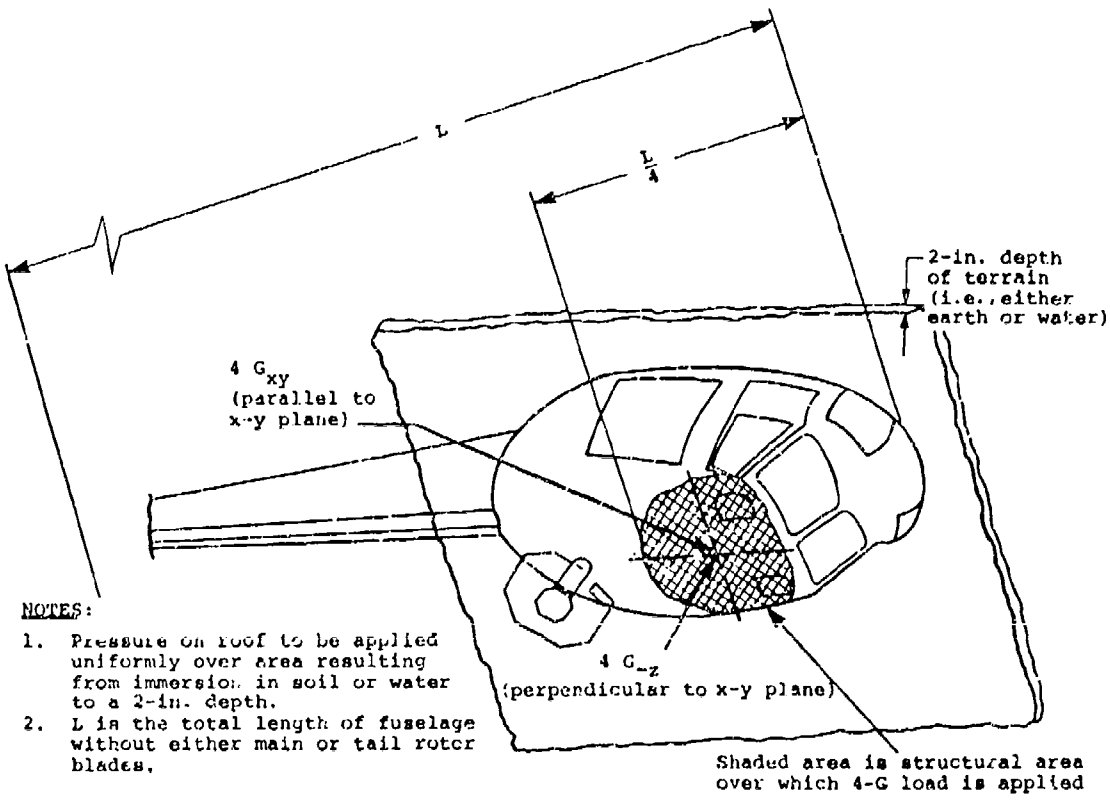

FIGURE 8. ROLLOVER, ROOF IMPACT DESIGN CONDITIONS.

4.3.1.6 Engine/Transmission Mounts. Engine mounts should be designed to keep the engine attached to the basic structure, even though large distortions of the engine mount and support structure occur.

On helicopters, the transmission, rotor mast, rotor hub, and rotor blades should not displace in a manner hazardous to the occupants during the following impact conditions:

- Rollover about the vehicle's roll or pitch axis on sod.
- Advancing and retreating blade obstacle strikes that occur within the outer 10 percent of blade span, assuming the obstacle to be an 8-in.-diameter rigid cylinder.

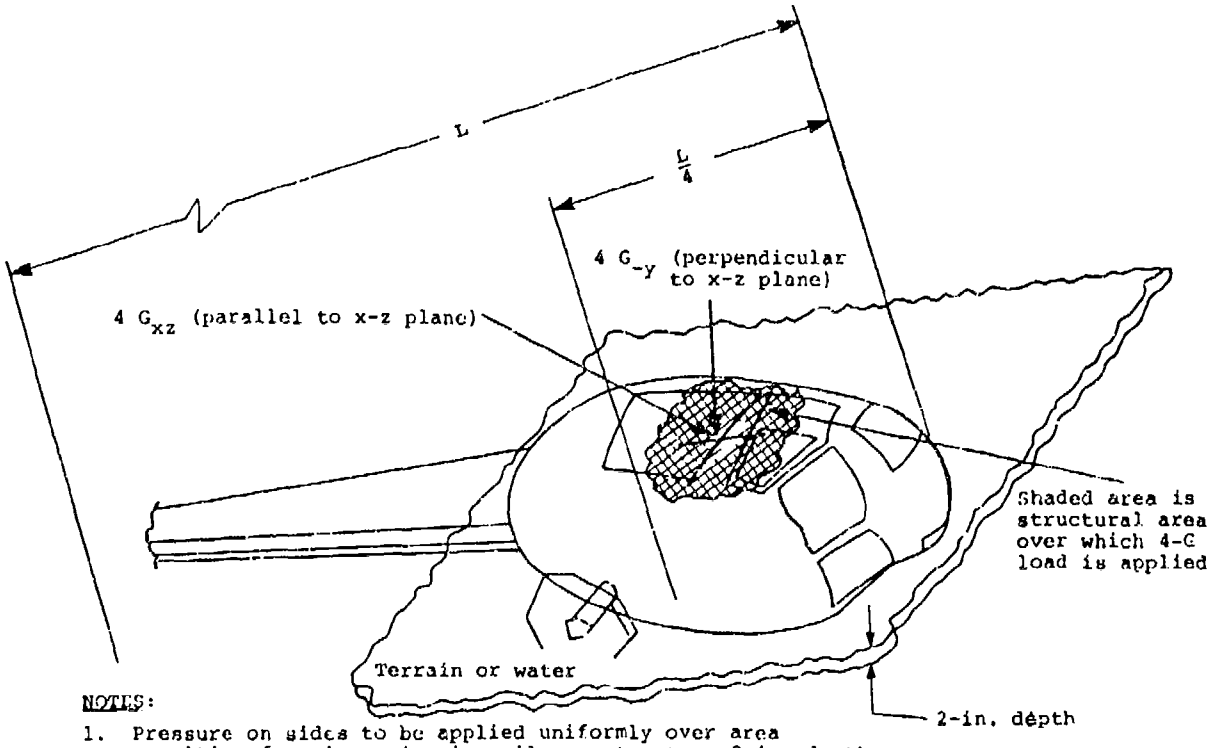

FIGURE 9. ROLLOVER, SIDE IMPACT DESIGN CONDITION.

Unless otherwise specified, all engines, transmissions, rotor masts, fuel tanks, armament systems, external stores, and rotor hubs that could be hazardous to the occupants should be designed to withstand the following ultimate load factors (G) in the directions that cause those hazards and remain restrained:

- Applied Separately

Longitudinal	±20
Vertical	+20/-10
Lateral	±18

- Applied Simultaneously

	Design Conditions		
	1	2	3
Longitudinal	±20	±10	±10
Vertical	+10/-5	+20/-10	+10/-5
Lateral	±9	±9	±18

4.3.1.7 Landing Gear. The landing gear should be capable of ground taxi, towing, ground handling, takeoff and landing roll, and landings including autorotative landings at design sink speeds in accordance with AMCP 706-201 (Reference 18). Unless otherwise specified, strength and rigidity requirements should be provided in accordance with MIL-S-8698 (Reference 19). An analytical casting factor of 1.25 should be applied for the design of all castings which will not be static tested to failure, or which are not procured to MIL-A-21180 (Reference 20). The yield factor of safety should be 1.0.

4.3.1.7.1 Landing Gear Location. The landing gear subsystem location should minimize the possibility that a part of the gear or support structure will be driven into an occupiable section of the aircraft, or into a region containing a flammable fluid tank or line. If this cannot be accomplished by location, the gear should be designed to break away under longitudinal impact conditions, with points of failure located so that damage to critical areas is minimized.

Failure of the landing gear should not result in a failure of any personnel seat/restraint system or seat/restraint system tiedown. Also, failure of the landing gear should not result in blockage of a door or other escape route or prevent the opening of any door or other escape route.

4.3.1.7.2 Vertical Crash Force Attenuation. Landing gear should be of the load-limiting type and should be capable of decelerating the aircraft at DGW from a vertical impact velocity of 20 ft/sec onto a level, rigid surface without allowing contact of the fuselage proper with the ground. Plastic deformation and damage of the gear and mounting system are acceptable in meeting this requirement. The aircraft should be capable of meeting this requirement in accidents with simultaneous roll and pitch of $\pm$10 degrees and +15 to -5 degrees respectively.

The landing gear should provide energy absorption at sink rates up to 42 ft/sec onto an impact surface with $\pm$10 degrees roll and +15 degrees to -5 degrees pitch. The gear should continue to absorb energy even after fuselage contact has been made to maximize the protection afforded by the gear.

4.3.2 Ancillary Equipment Retention

Ancillary equipment is all removable equipment carried inside the aircraft that could constitute a hazard if unrestrained during a crash.

Typical items are:

- Emergency Equipment

  Oxygen bottles
  Fire extinguishers
  First-aid kits
  Portable search lights
  Crash axes

- Aircraft Subcomponents

  Panel-type consoles containing control circuitry
  Radio and electronic equipment
  Auxiliary power units
  Batteries
  Special equipment

- Survival Equipment

  Survival kits
  Life rafts
  Life jackets
  Locator beacons
  Special clothing
  Food and water

- Miscellaneous Equipment

  Navigation kits
  Briefcases
  Log books
  Flashlights
  Luggage
  Toolboxes.

All ancillary equipment frequently carried aboard an aircraft should be provided with integrated restraint devices to ensure retention of the equipment during any survivable crash. Stowage space should be provided for nonrestrained items that are not regularly carried. This space should be located so that the items stored in it cannot become hazards in a survivable crash. Stowage under energy-attenuating seats is not acceptable.

4.3.2.1 Strength. Restraint devices and supporting structure for ancillary equipment should be designed for static loads of 50 G downward, 10 G upward, 35 G forward, 15 G aftward, and 25 G sideward. Load-limiting devices are recommended for restraint of heavier equipment. However, load-limiter stroking should not allow equipment to enter an occupant strike envelope.

4.3.2.2 Emergency and Survival Equipment Stowage Location. Equipment should be: (1) located close to the primary crew chief station, if applicable; (2) stowed in easy view of crew and passengers; and (3) easily and reliably accessible in an emergency. Equipment should not be placed in areas where cargo shifting or fuselage distortion will prevent or impair access to it. Extreme temperatures, abrasion, and contamination should be minimized.

4.3.2.3 Release of Emergency and Survival Equipment. Retention devices used to restrain emergency and survival equipment should be capable of quick release without the use of tools by one person using one hand. Release should be effected by a single motion actuating one device and should not require more than 5 sec from time of contact with the actuating device to the time when the equipment either falls free or is lifted free. If equipment is stowed in an enclosure, no more than 5 sec should be required for opening the enclosure and removing the equipment. Aircraft attitude should not adversely affect release device operation. It should be possible to see the latch

position (open or closed) of the release device. The release device actuating handle should be of a color that contrasts with the surrounding area and be easily discernible in poor light or smoky conditions.

4.3.3 Occupant Retention

Seating and litter systems should ensure that occupants are retained in their precrash positions within the aircraft. Seating and litter systems design should be coordinated and interfaced with the design of the other surrounding aircraft areas to achieve a completely integrated and efficient crash-resistant aircraft system design. Seat and litter design should provide the greatest practical amount of support and contact area for the occupants in the directions of the most severe and likely impacts. Seats should provide an integral means of crash force attenuation. Occupant comfort should not be compromised to the extent that flight safety and/or crew efficiency is adversely affected. Volume IV contains a detailed discussion of occupant retention.

4.3.4 Cargo Retention

Cargo restraint should:

- Be as light as possible.
- Require minimum storage space.
- Be easy to install and remove.
- Be easily and reliably adjustable for different sizes and shapes of cargo.
- Provide sufficient restraint of cargo in all directions to prevent injury to personnel in a survivable crash.

If the structure of the fuselage and floor is not strong enough to withstand the longitudinal loads, load limiters should be used. Cargo restraints should be capable of maintaining their integrity under longitudinal loads of 16 G peak with a longitudinal velocity change of 43 ft/sec. Lateral and forward strength-deformation characteristics are discussed in Section 6.2.7.4. If load-limiters are used, low-elongation restraining lines should be used to ensure the most efficient energy absorption.

Nets used to restrain small bulk cargo should be constructed of material with low-elongation characteristics in order to reduce dynamic overshoot to a minimum. Restraining lines without load limiters used for large cargo, as defined in Table 5, for longitudinal restraint should be so arranged that maximum load in all lines is reached simultaneously. Restraining lines having different elongation characteristics should not be used on the same piece of cargo.

TABLE 5. AIRCRAFT CARGO CATEGORIES

Small Bulk Cargo (Net Restraint)	Large Rigid Cargo (Line Restraint)
This class includes all boxes or unpacked cargo of approximately 3 ft^3 or less in size.	This class includes all rigid cargo of 3 ft^3 or more in size.
Examples:	Examples:
1. Ammunition boxes	1. Wheeled or tracked vehicles
2. Foodstuffs	2. Aircraft engines
3. Medical supplies	3. Fuel barrels
4. Clerical supplies	4. Artillery pieces
5. Vehicle maintenance components	5. Special weapons (priority cargo)

5. GENERAL DESIGN CONSIDERATIONS

5.1 INTRODUCTION

An aircraft design requires a number of distinct features for crash survival, some of which are indicated in Figure 10. First, and most important, the structure surrounding occupiable areas must remain reasonably intact, without reducing occupant living space to the point of creating a hazard. If occupants are injured because the protective shell collapses around them, then efforts to improve survivability through other methods are futile. An aircraft which does not provide the protective shell can never be considered crash-resistant. Second, the structure and the seats should be designed to attenuate occupant accelerations to survivable levels and to retain large mass items, interior equipment, seats, and cargo. In addition, cabin penetration should be minimized.

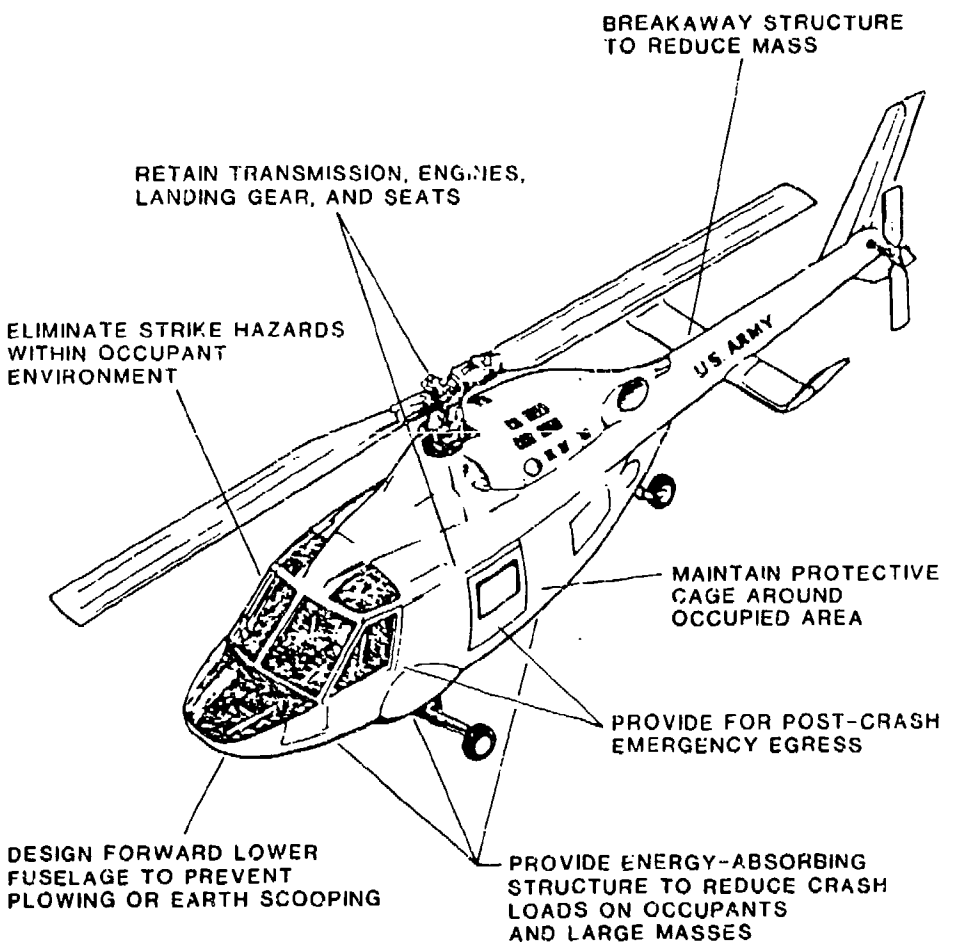

FIGURE 10. DESIGN FEATURES FOR CRASH SURVIVAL.

Survival is achieved by controlling acceleration magnitudes, durations, and rates of acceleration change actually experienced by the body, rather than by the aircraft impact velocity. Since deceleration loads are a function of the strength of the structure, a systems analysis should be performed to establish the distribution of energy-absorbing properties to the gear, fuselage, and seats. For new aircraft, the elements can then be designed to provide the required properties. For older aircraft undergoing retrofit, certain elements cannot be changed. Thus, those that can be changed should be modified as much as possible within practical limits to provide some compensation for those items that cannot be changed.

5.2 MISSION CONSTRAINTS

The type, mission and size of an aircraft can affect the degree of crash survival which can be achieved. Therefore, an understanding of mission constraints may be useful to the designer.

5.2.1 Combat Support Requirements

Army aviation supports the Army's ground combat function in both peace and war in the following areas:

- Command, Control, and Communications. Army aviation support includes courier and liaison missions, control of vehicular columns, message drop and pickup, command and control of airmobile operations, wire laying, and radio relay.

- Intelligence. Army aviation is an important means of gathering intelligence. It provides aerial "eyes" over the battlefield and conducts missions in support of aerial survey operations, aerial radiological survey, and target acquisition.

- Mobility. By airlifting troops and combat equipment, Army aviation provides an additional means of maneuver to the ground commander. Using Army aviation's airmobile capability, weapons may be emplaced rapidly and troops may be carried quickly over obstacles.

- Firepower. Army aviation, which provides aerial adjustment of indirect fire, is expanding the use of Army aircraft as weapon platforms to fill the gap between the support provided by conventional ground fire and fixed-wing aircraft.

- Training. This includes flight training of crews in both peactime and war.

- Combat Service Support. Army aviation supports logistical operations by providing delivery of troops and equipment and evacuation of casualties and damaged equipment within the Army combat zone.

To conduct the combat support mission, Army aviation utilizes a variety of aircraft with mission specific characteristics. Several types of aircraft, including helicopters, fixed-wing, and tilt-rotor are described in the following sections.

5.2.2 Helicopters

The U.S. Army inventory of helicopters can be divided into five types by mission:

- Observation (OH)
- Attack (AH)
- Utility (UH)
- Cargo (CH)
- Training (TH)

Figures 11, 12, and 13 show side elevations for typical helicopters to indicate comparative sizes and layouts. When considering a design for occupant protection, it becomes apparent that each type of helicopter poses different problems. The size, proximity of occupied areas to the ground impact plane, distribution of mass items and external stores, and the location of transparencies and cutouts for exits combine to provide the designer with major challenges in the efficient allocation of the primary structure.

Figure 14 shows a helicopter whose design considered the parameters listed above. Notations indicate several major design features necessary in a primary aircraft structure to satisfy the crash resistance requirements of MIL-STD-1290.

5.2.3 Fixed-Wing Aircraft

Side elevations of these aircraft types are shown in Figure 15. All except the OV-1 are military versions of commercial aircraft. The maximum capacity of any listed aircraft is a crew of two with 20 passengers.

5.2.4 Tilt-Rotor Aircraft

Tilt-rotor aircraft share operating characteristics with both helicopter and fixed-wing airplanes. A typical tilt-rotor configuration is shown in Figure 16. The tilt-rotor is a recent development, and there is no service experience available. Therefore, crash resistance features for them must be based on similarities with helicopter and fixed-wing aircraft coupled with analytical evaluation of potential hazards. Special considerations for tilt-rotor aircraft are presented in Section 6.4.4.

5.3 GENERAL CONFIGURATION

The design of an aircraft structure involves a series of compromises with respect to payload, performance, aerodynamics, strength, simplicity of fabrication, economics, etc. The additional requirement that crash resistance become an important structural consideration brings a need for further compromise and good judgment. As more attention is directed toward airframe crash resistance throughout the design stages, methods and techniques of construction will improve so that adequate crash resistance will be achieved with acceptable weight, cost, and performance penalties.

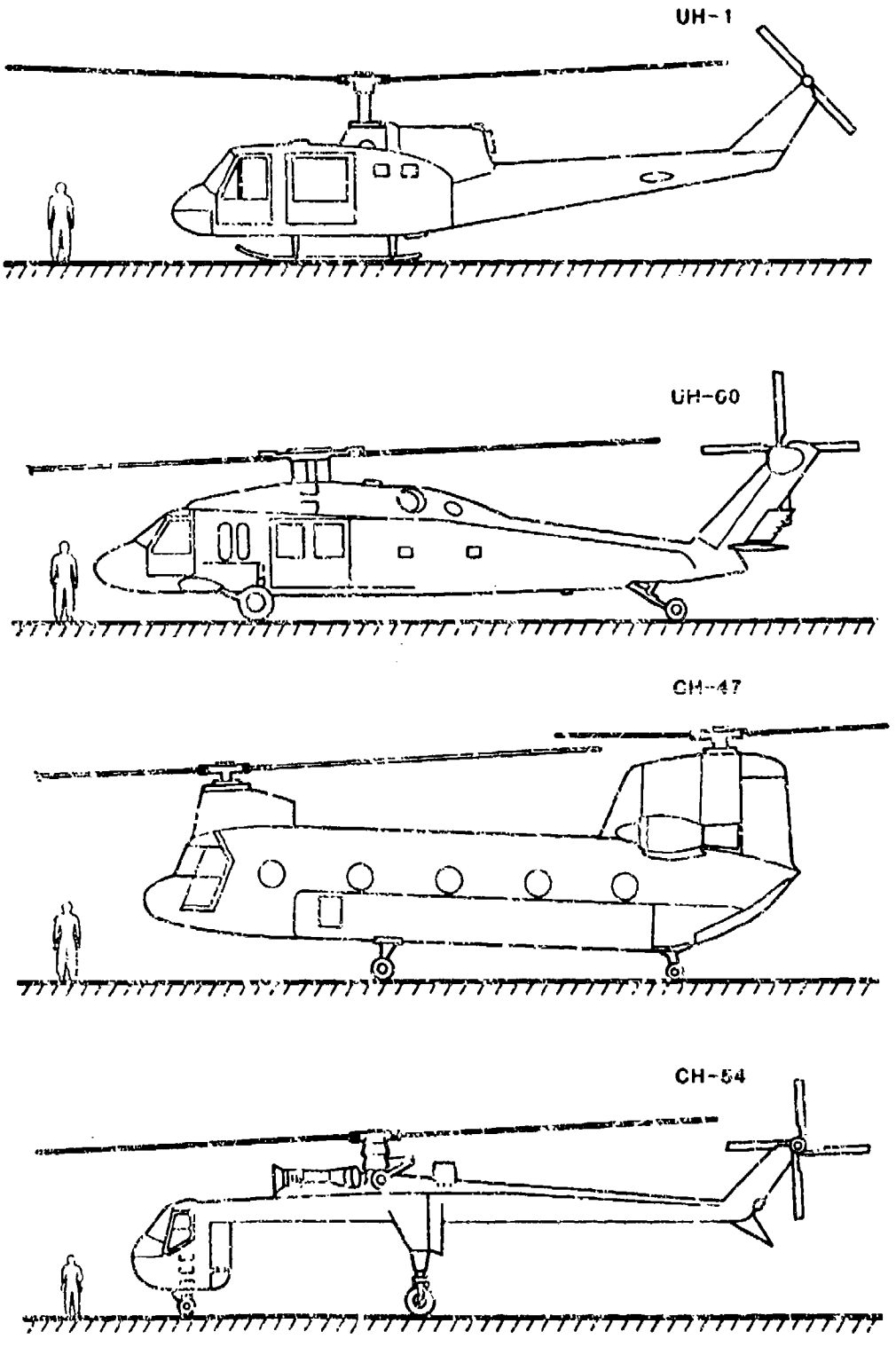

FIGURE 11. SIDE ELEVATIONS OF TYPICAL U.S. ARMY UTILITY AND CARGO HELICOPTERS.

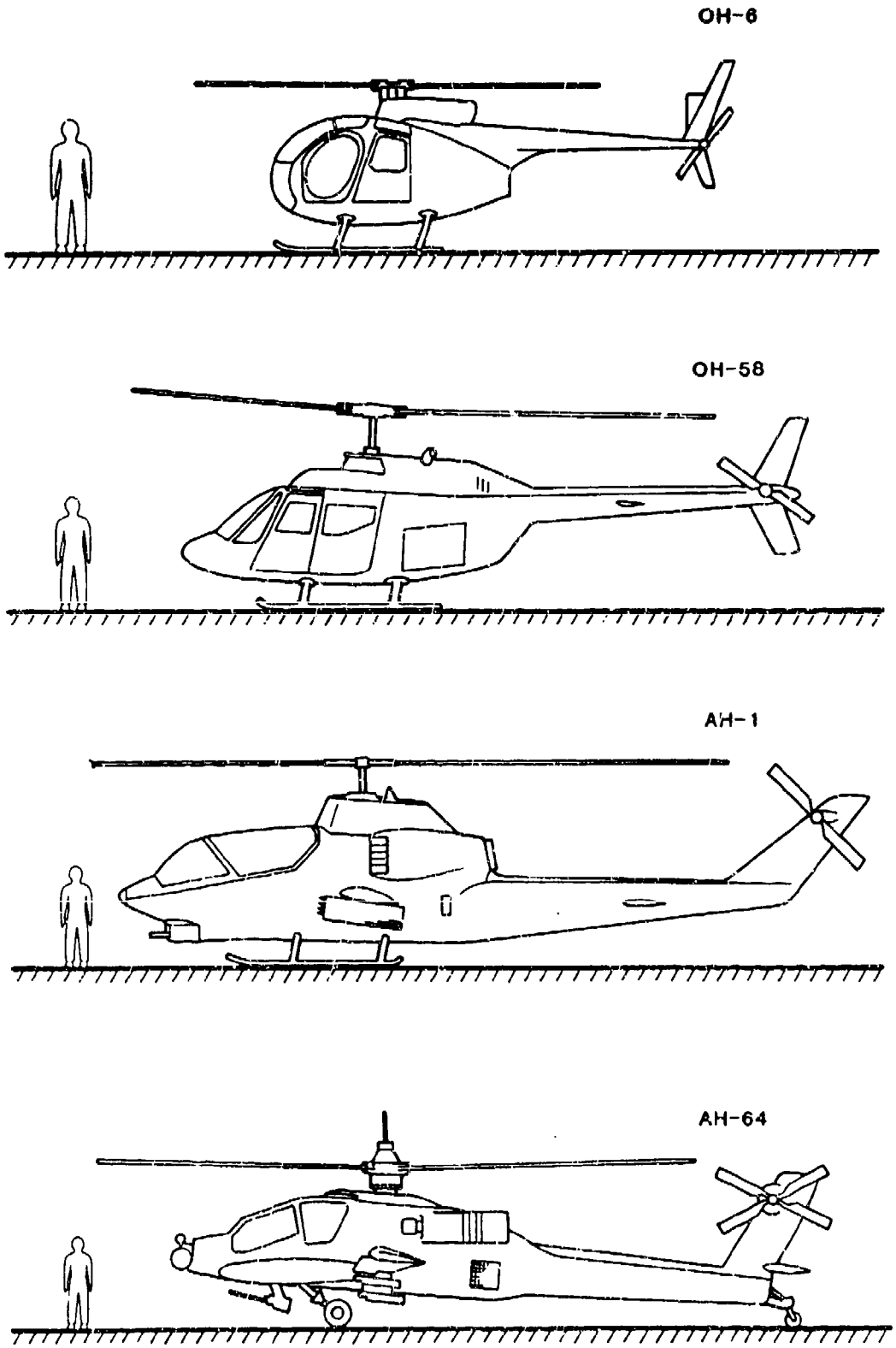

FIGURE 12. SIDE ELEVATIONS OF TYPICAL U.S. ARMY OBSERVATION AND ATTACK HELICOPTERS.

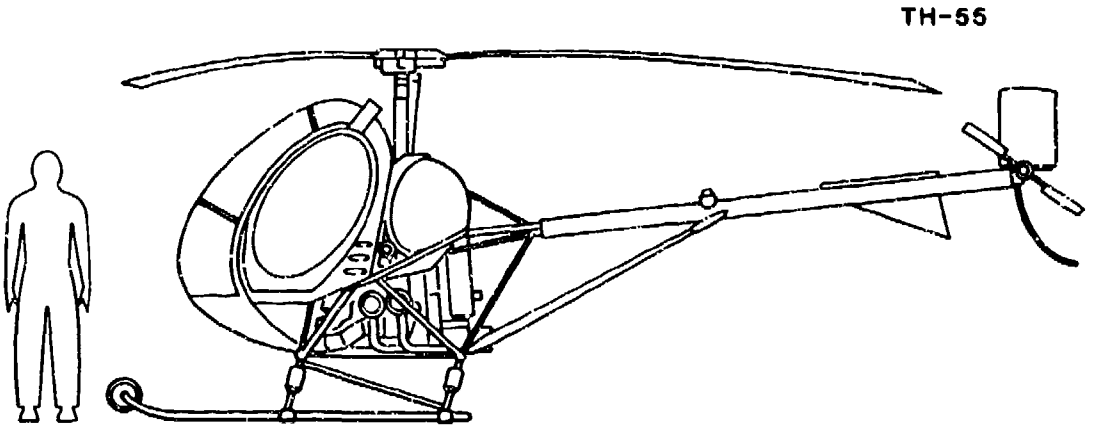

FIGURE 13. SIDE ELEVATION OF TYPICAL U.S. ARMY TRAINING HELICOPTER.

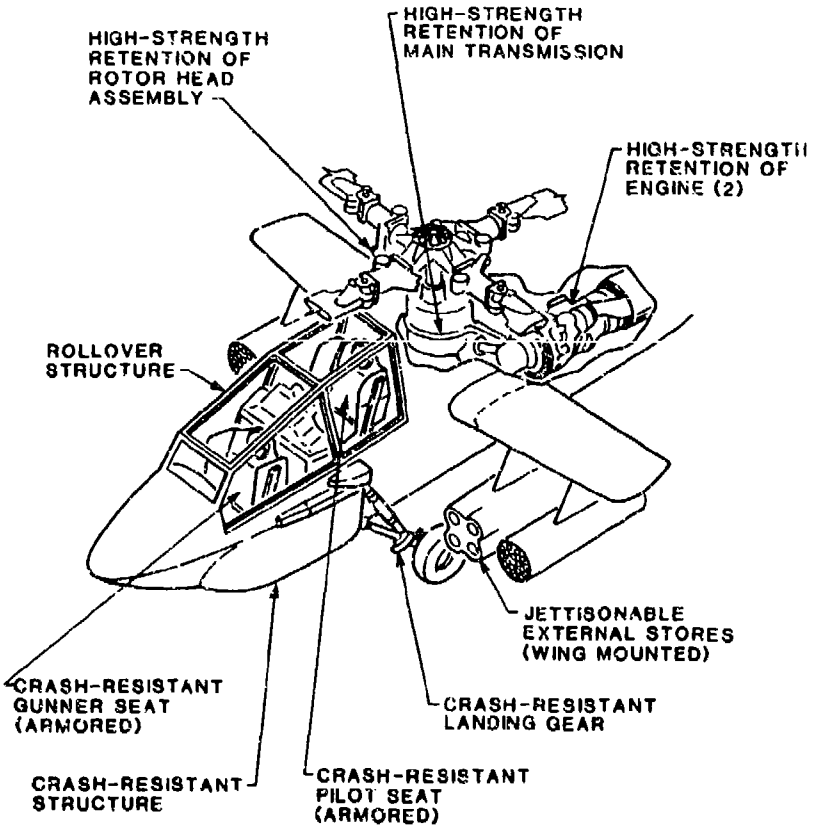

FIGURE 14. SELECTED HELICOPTER CRASH-RESISTANT FEATURES.

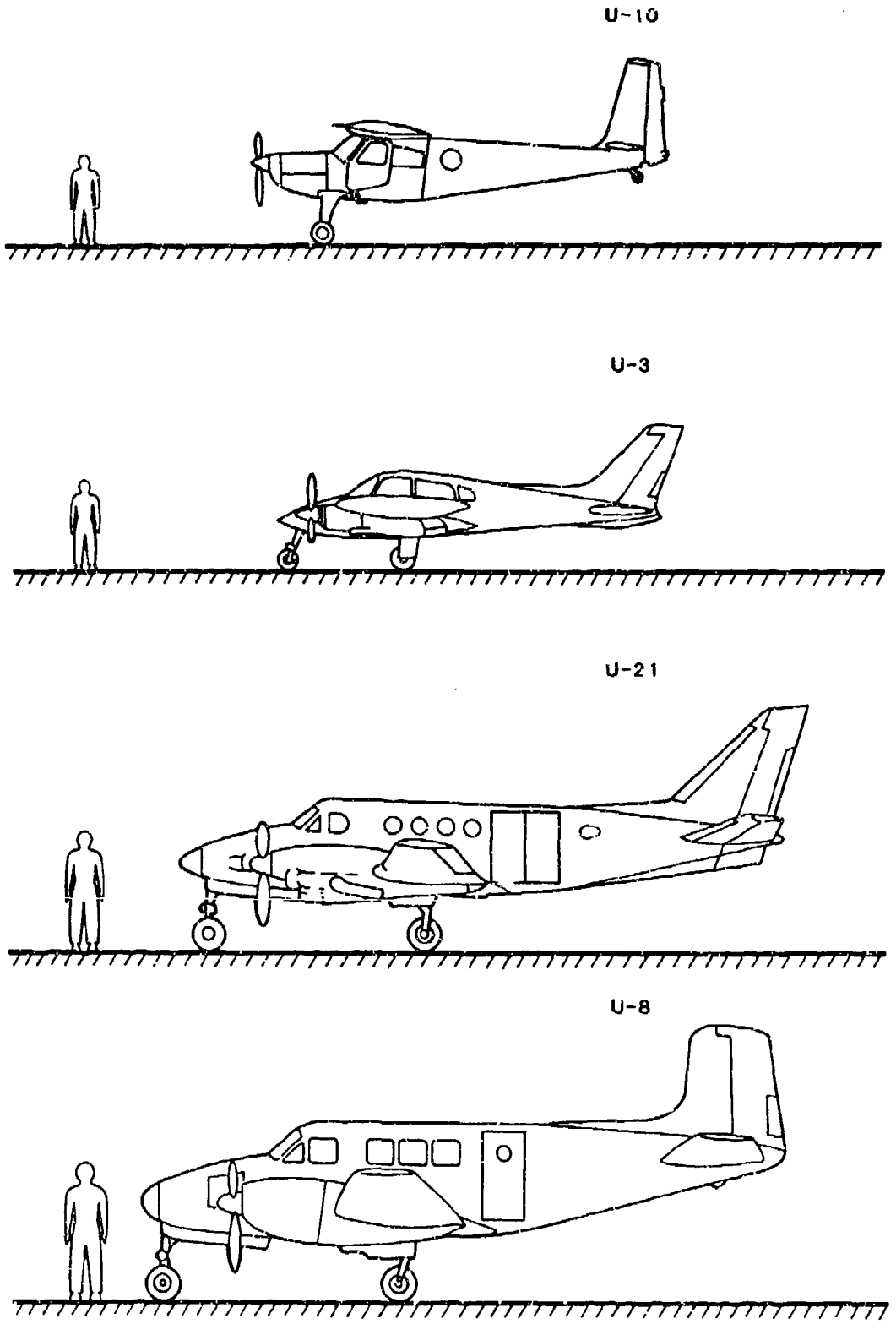

FIGURE 15. SIDE ELEVATIONS OF TYPICAL U.S. ARMY FIXED-WING AIRCRAFT.

C-12

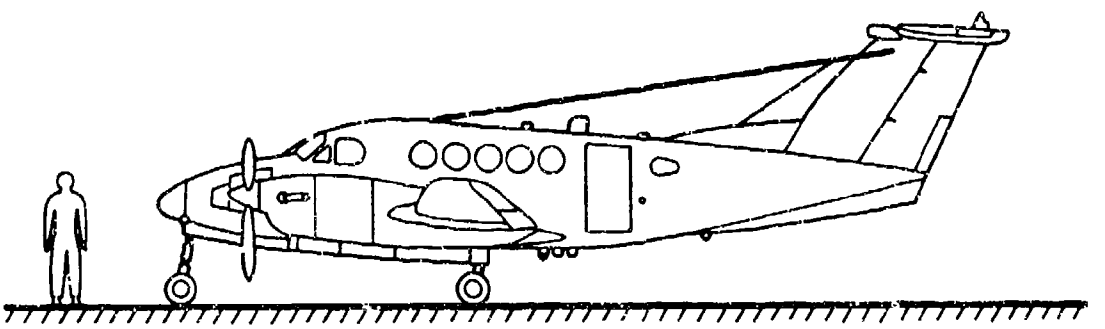

UV-18

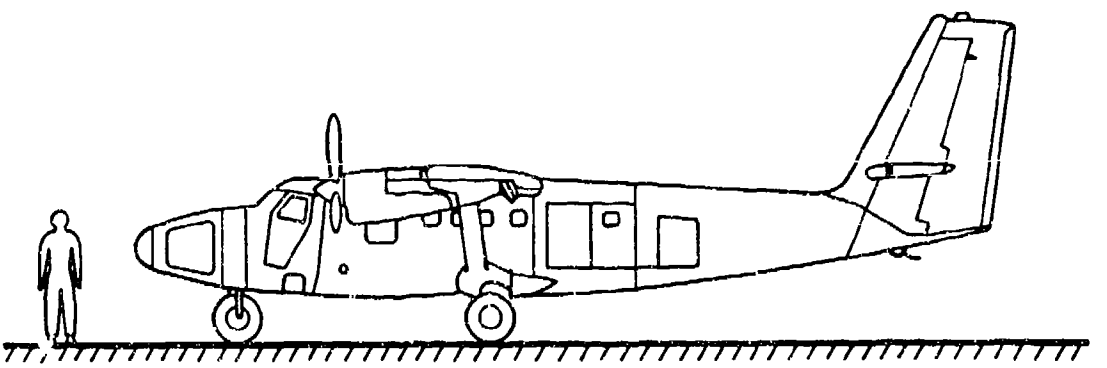

OV-1

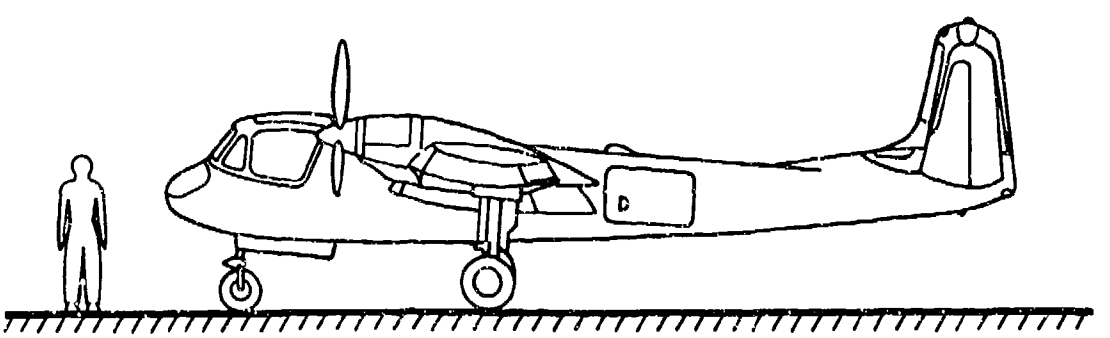

FIGURE 15 (CONTD). SIDE ELEVATIONS OF TYPICAL U.S. ARMY FIXED-WING AIRCRAFT.

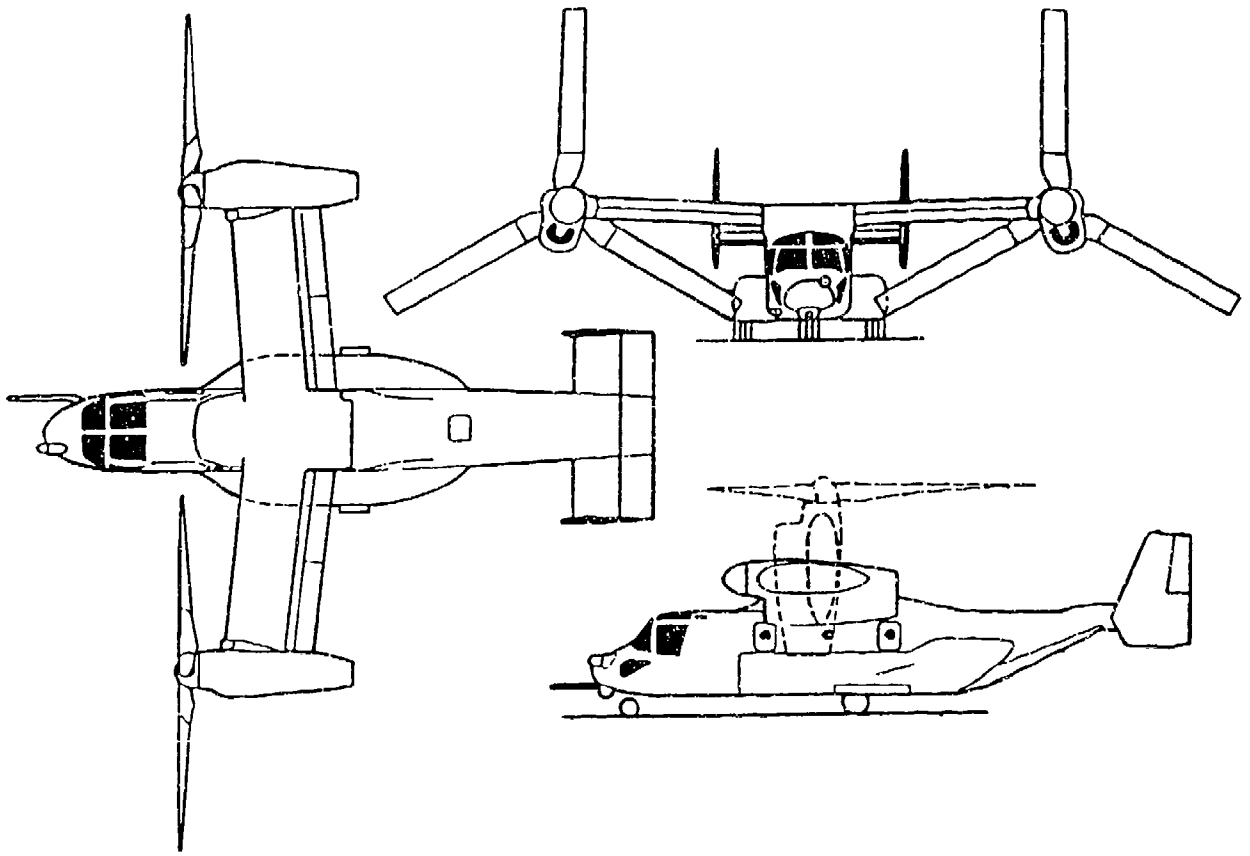

FIGURE 16. TILT-ROTOR AIRCRAFT.

Often, the upgrading of crash resistance will not result directly from an increase in strength. Consideration of the deformations which are likely to occur, and ensuring that several parallel load paths are available to keep the structure intact even though localized damage occurs, will also improve crash resistance. Failure mode control will require much more consideration when designing for crash resistance.

An excessively strong airframe structure is no more acceptable for crash resistance than an understrength structure. Not only will unnecessary strength impose a highly undesirable weight penalty but it may also develop high floor accelerations that reduce survivability. This is particularly true of underfloor structure, which must be designed not only to support normal flight and landing loads but to absorb energy when subjected to vertical crash loads.

Fabrication techniques and structural configurations, especially for areas where severe damage is probable, should be selected after consideration of the overall effects of structural failure on occupant protection. Wherever

possible, multiple structural members should be used instead of larger single structural members, so that localized impact damage will not result in complete loss of structural integrity. Multiple load paths also aid in maintaining uniform force transmission charcteristics throughout structural collapse.

When designing for the use of composites in the primary fuselage structure, it is desirable to conduct representative substructure crush tests as part of the design process to evaluate the energy-absorbing properties of proposed structural concepts.

The airframe structure should, of course, be designed for normal airloads, ground handling loads, and fatigue life, while considering the details of the aircraft specification with respect to size, range, performance, space envelopes, etc. After the basic structural layout has been defined, the effects of crash loads must be considered to determine where structural modifications are needed to improve crash resistance. Concurrent with this process, space allocations must be made for critical systems, such as landing gear, equipment racks, seats, cargo tiedowns, and emergency exits, to ensure an integrated approach to crash-resistance .

5.3.1 Failure Modes

The following failure modes should be avoided:

- Occupied area penetrations by failed structural elements.
- Inward buckling structures, such as sidewalls, bulkheads, and floors.
- Failures of members such as frames that result in jagged, failed ends protruding into occupied space or fuel tanks.
- Fastener failures that may produce structural discontinuities and projectiles.
- Brittle fractures that suddenly unload, causing impulse effects in adjacent structures with potential for progressive failures and generation of projectiles.
- Emergency exit surroundings that distort excessively and preclude the opening or removal of doors or windows.
- Flammable fluid container penetrations.

Also, predetermined failure points can be introduced into a design to help control structural response under dynamic loading conditions. These points may be plastic hinges that allow earlier plastic yielding and rotations in weaker sections. Alternatively, joints may be designed to fail progressively to allow rotation of structural elements with subsequent load redistribution. A final joint condition of effectively pin-ended members will quite often be more desirable than member breakaway.

Typical examples of failure modes discussed in this section are shown in Figures 17 through 24, demonstrating, in particular, the requirements for failure away from occupied areas and prevention of potentially damaging projectiles and structural elements. These photographs were taken after a vertical impact of a test vehicle onto a concrete ground plane at a velocity of more than 42 ft/sec. The structural failures, in general, did not result in unacceptable intrusions into occupied space. The resulting sharp-edged elements could have been eliminated by using materials with better fracture toughness properties and/or increased dimensions.

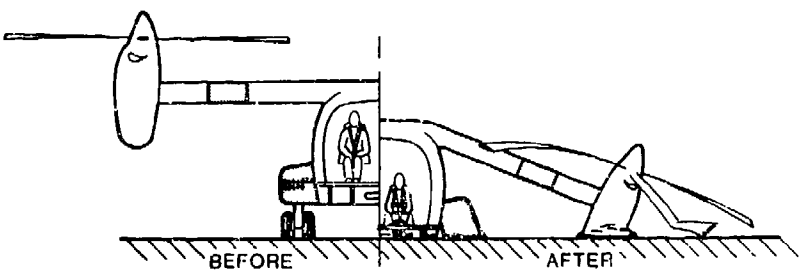

CONTROLLED WING FAILURE ALLOWS MASS RELIEF.
PREVENTS FUSELAGE COLLAPSE.

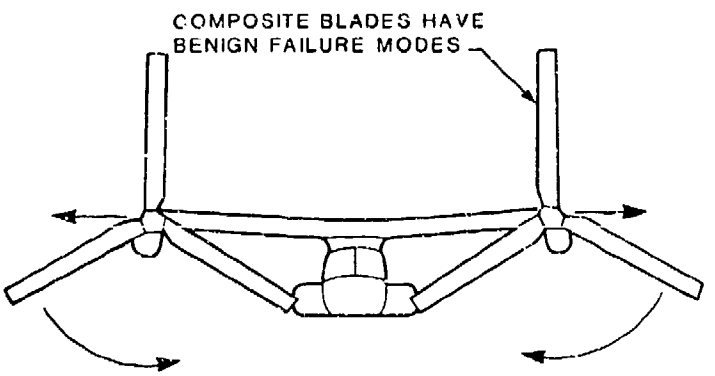

DIRECTION OF ROTATION CAUSES PYLONS/ROTORS
TO BE DRIVEN AWAY FROM FUSELAGE SHOULD
BLADE STRIKE OCCUR.

FIGURE 17. WING/ROTOR/PYLON CRASH FAILURE MODES.

FIGURE 18. COMPRESSIVE BUCKLING AT BASE OF BUTTLINE BEAM STRUCTURE ON A MEDIUM CARGO HELICOPTER FOLLOWING VERTICAL IMPACT.

Other structural factors that can influence human survival in a crash impact are presented in Table 1.

5.3.2 Impact Parameters

The design of a crash survivable aircraft is heavily dependent upon the impact parameters specified to be survivable. Impact velocity (speed and direction) and attitude as illustrated in Figure 25 are critical. Design criteria for these values are specified in MIL-STD-1290 and are discussed in Section 4 of this volume of the Design Guide. Attitude is especially critical, since energy-absorbing features, such as landing gear or underfloor structure, may be only partially effective if the aircraft is pitched or rolled at impact. As illustrated in Figure 25, only one gear may function during a major portion of the initial deceleration prior to fuselage impact in the case of a 10-degree roll.

FIGURE 19. TYPICAL BUCKLING COLLAPSE OF VERTICAL BULKHEAD AND BUTTLINE BEAM ON A MEDIUM CARGO HELICOPTER FOLLOWING VERTICAL IMPACT.

FIGURE 20. TYPICAL FRAME FAILURE AWAY FROM OCCUPIED SPACE IN THE COCKPIT AREA OF A MEDIUM CARGO HELICOPTER FOLLOWING VERTICAL IMPACT.

5.3.3 Initial Layout

Structurally, the aircraft should be capable of performing its mission of carrying the required payload. Initial layouts should consider the volume required to carry the requisite crew, passengers, and cargo after allocation of space for aircraft systems. The structure needed to carry and/or house the systems and occupants should be laid out to adequately support all systems and to provide basic structural protection during a crash.

Figure 26 shows a structure designed to protect the occupants in a crash. Adequate space for allowing the structure to stroke and/or collapse to absorb energy in the support of large mass items should be provided. At the same time, seated occupants and cargo should be restrained and G levels limited to provide a survivable crash impact condition. Crash-resistant seats should be supported by an integral part of the primary structure. Sufficient space should be provided around the seats to allow them to operate properly when under load and deformed. Proper seat stroking loads and sufficient stroking distance should be provided.

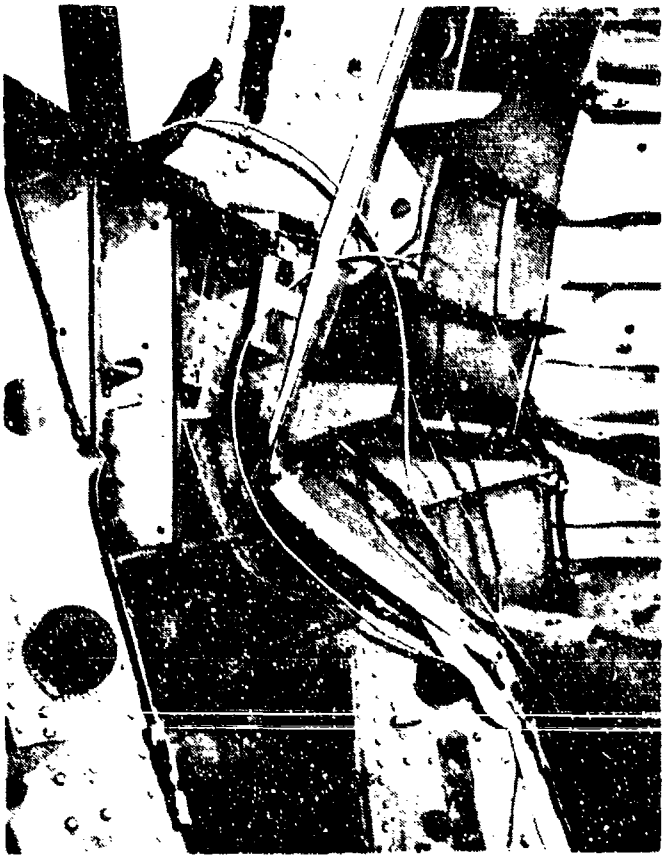

FIGURE 21. TYPICAL FRAME FAILURE AWAY FROM OCCUPIED SPACE IN THE CABIN AREA OF A MEDIUM CARGO HELICOPTER FOLLOWING VERTICAL IMPACT.

5.3.4 Analysis and Simulation Iterations

Once the preliminary design is established, computer simulations, such as described in Chapter 7, are used to model primary structure, large mass items, systems, occupants, and cargo. Then, potential impact conditions are simulated to investigate the aircraft's dynamic response, structural collapse, and acceleration.

An iterative process is used to optimize energy-absorption concepts, structural distributions, failure modes, mass retention concepts, landing gear locations, etc. This process, conducted concurrently with inputs from design, stress, and performance, ensures design optimization. Further modifications are made to control weight and weight distribution, producibility, maintainability, safety, and cost. Several cycles of iteration should be expected in the evolution of the optimum design, adequately satisfying the requirements of the basic helicopter specification.

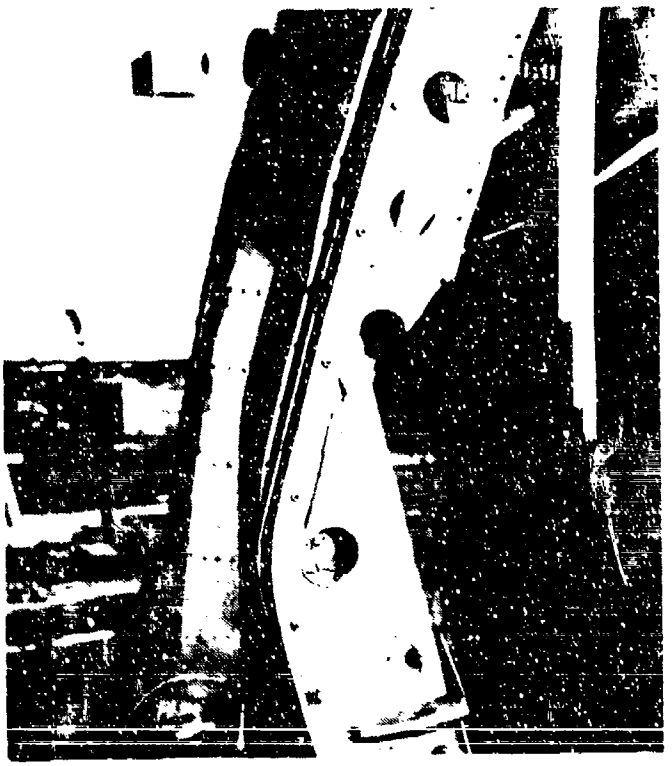

FIGURE 22. FAILURE MODES RESULTING IN JAGGED ELEMENTS PROTRUDING INTO OCCUPIED SPACE IN THE CABIN AREA OF A MEDIUM CARGO HELICOPTER FOLLOWING VERTICAL IMPACT.

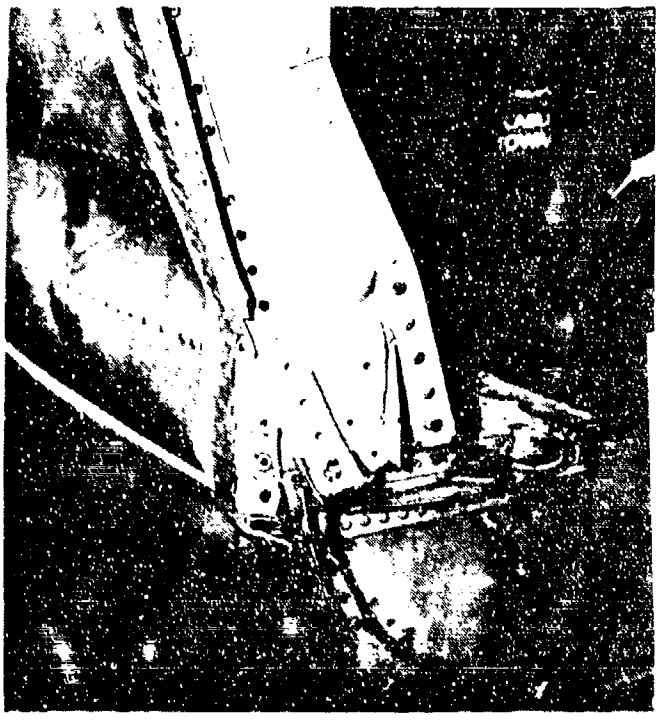

FIGURE 23. ROTATIONAL JOINT FAILURE WITH COMPRESSION AND BENDING IN A MEDIUM CARGO HELICOPTER FOLLOWING VERTICAL IMPACT.

FIGURE 24. FAILURE OF FRAME MEMBER AND JOINT WTH FRAGMENTATION, COMPRESSION, AND BENDING IN A MEDIUM CARGO HELICOPTER FOLLOWING VERTICAL IMPACT.

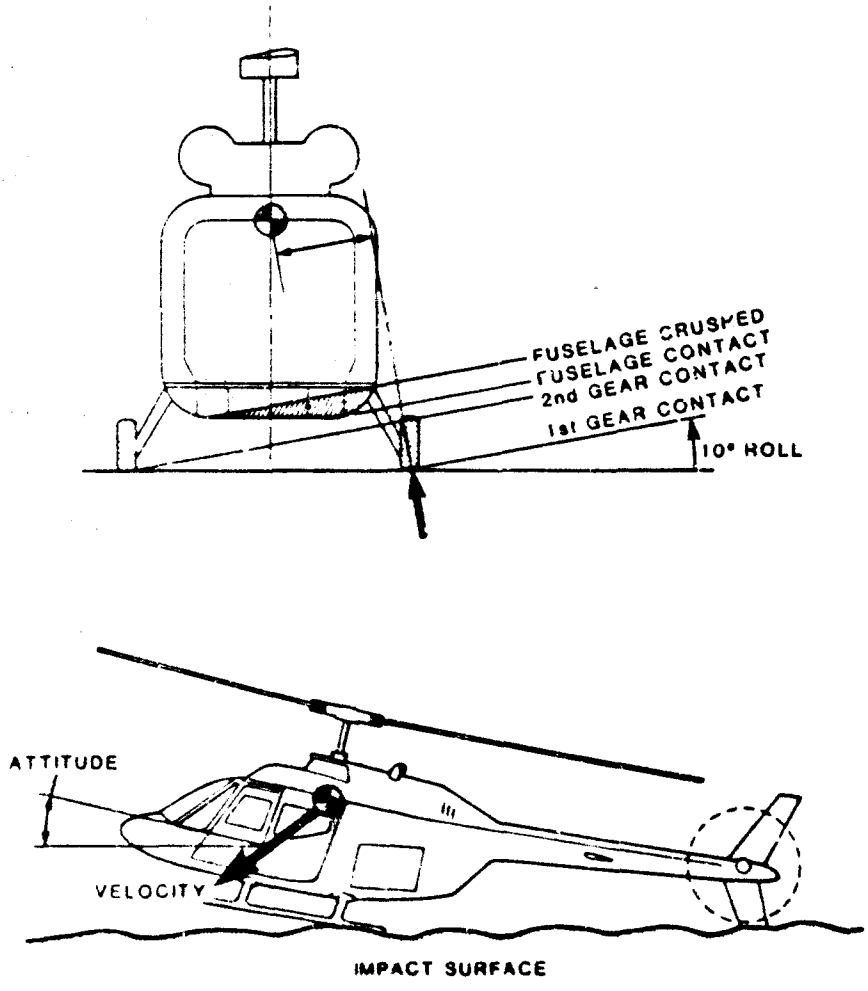

FIGURE 25. DIRECTION AND ATTITUDE OF IMPACT.

5.3.5 Margins of Safety

Safety margins of 0.0 based upon the crash load factors presented elsewhere in this volume will generally be considered satisfactory. Safety factors may be increased as necessary to ensure performance in critical areas, particularly in load paths for occupant retention.

Designs allowing the structure to remain more nearly intact through improved compliance or improved progressive, yet predictable, deformation are sometimes more effective than direct increases of strength. Plastic yielding can relieve stress concentrations before the ultimate strength of members is reached.

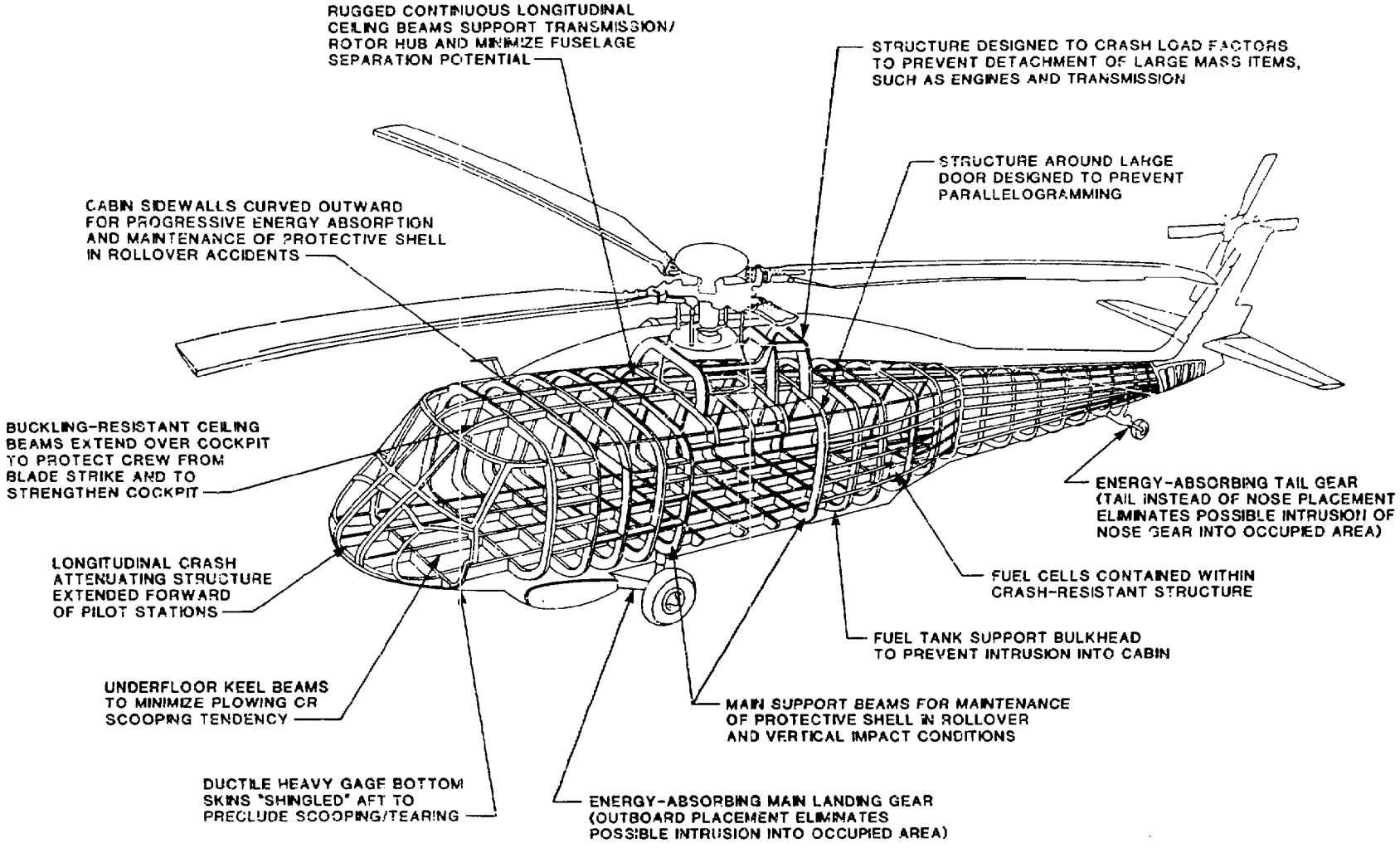

FIGURE 26. STRUCTURAL LAYOUT FOR OCCUPANT PROTECTION DURING CRASH IMPACT CONDITIONS.

5.3.6 Joint Concepts

The joints and attachment fittings of a crash-resistant airframe structure must be able to withstand large deformation without failure and connect items such that structural failure or separation occurs before the joint fails.

Of the two considerations, the first imposes the greater constraint on a joint constructed of composite materials or, for that matter, on a metallic fitting manufactured from a casting or a forging. Joint concepts which cannot themselves meet the above criteria should have redundant or backup load paths to satisfy the above considerations while relying on the airframe structure to absorb the energy and redistribute crash loads. Many composite joints contain some metal for this purpose and are considered hybrids.

Figure 27 shows an example of a joint concept which has been used successfully for transmission retention. It utilizes composite parts which fail progressively in bearing to allow energy absorption without structural separation.

5.3.7 Materials

Most helicopters in the Army inventory are constructed primarily of metallic materials. Some secondary and fairing components are made from nonmetallic materials or composites. However, all composite or largely composite aircraft are in development. Therefore, both materials are applicable for crash-survivable design.

Subsequent sections discuss these requirements with reference to both metallic and composite structures.

5.3.7.1 General. The kinetic energy of an aircraft subjected to a crash is absorbed in a number of ways, including deformation of aircraft structure. Absorption of energy through structural deformation can work effectively as an occupant protective device if the surrounding structure is allowed to deform, thus attenuating the forces transmitted to the occupant. The use of surrounding structure as a buffer can be accomplished more efficiently if the impact causes crushing without complete rupture of structural members. Material properties can greatly affect the degree to which this is actually achieved. Material ductility is required to ensure that crushing, twisting, and buckling can occur without rupture.

5.3.7.2 Material Strength and Elongation Characteristics. Material strength and elongation characteristics are described in applicable military handbooks. MIL-HDBK-17 (Reference 21) and MIL-HDBK-5 (Reference 22) contain basic design data for composite and metallic materials, respectively. In using these properties, one should bear in mind that for some materials, such as steel, handbooks present only guaranteed minimum strength and elongation data; for other materials, such as aluminum, values are presented indicating both minimum guaranteed strength and the strength values which statistics show will be met or exceeded by 90 percent of the materials under consideration. The 90-percent probability values are normally somewhat higher than the guaranteed values. The selection of the strength value should be based upon the consequences of failure. For design of structural members, such as members supporting heavy overhead masses, where failure could result in a

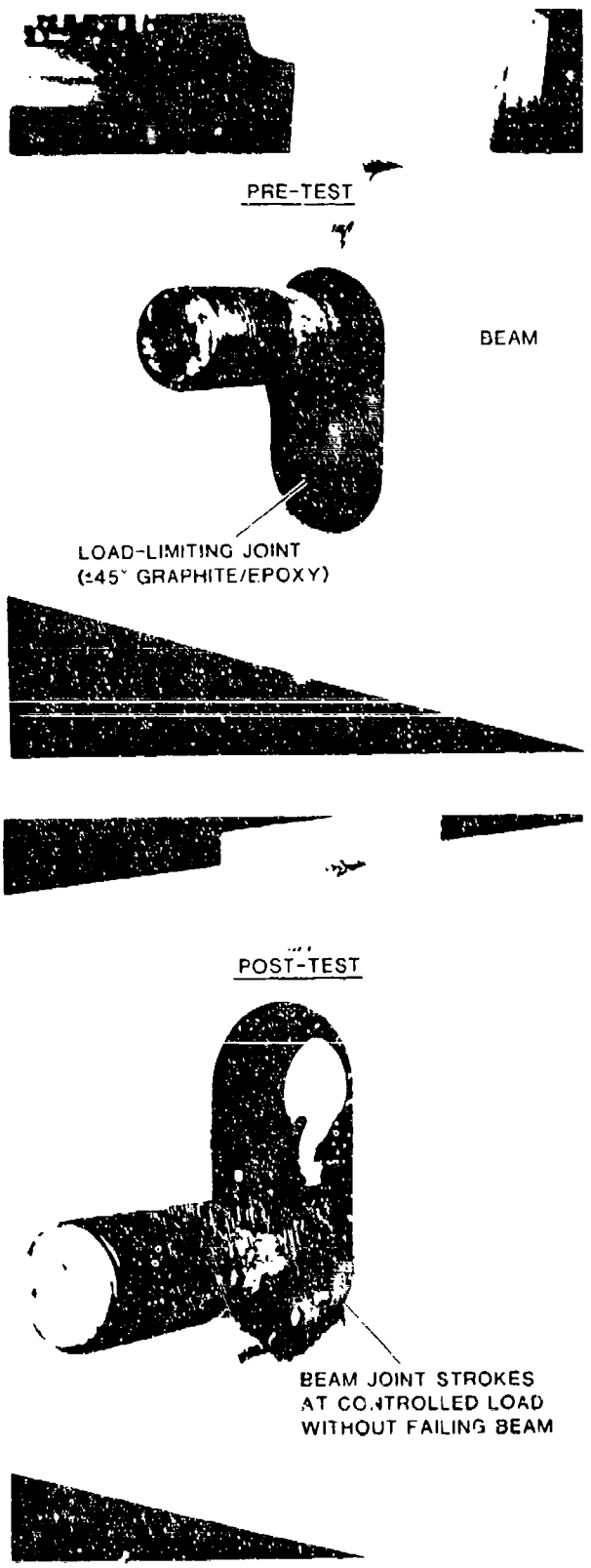

FIGURE 27. ENERGY-ABSORBING JOINT CONCEPT.

severe loss of occupant protection, the use of minimum guaranteed values would be reasonable. For design of structures likely to be subjected to massive crushing, such as airplane nose structures, the use of statistical values would be justified.

5.3.7.3 Composite Materials. Composite materials offer certain advantages over metallic in some areas of helicopter structure, primarily the advantage of reduced weight. However, most composite materials cannot tolerate large strains without fracture as can ductile aluminum. Because of this, crash energy absorption with composites must come from innovative design to enhance material stress-strain behavior.

At present energy-absorbing behavior of composites is not easily predicted. Thus, substructure testing will usually be required in order to verify that a proposed configuration will actually perform as intended.

Figure 28 compares typical stress-strain curves for an aluminum alloy and a graphite/epoxy composite in tension. The shaded areas indicate the potential energy absorption capabilities; the difference between the two materials should be noted: i.e., the ratio $A_{7075}/A_{GE} = 12.3$.

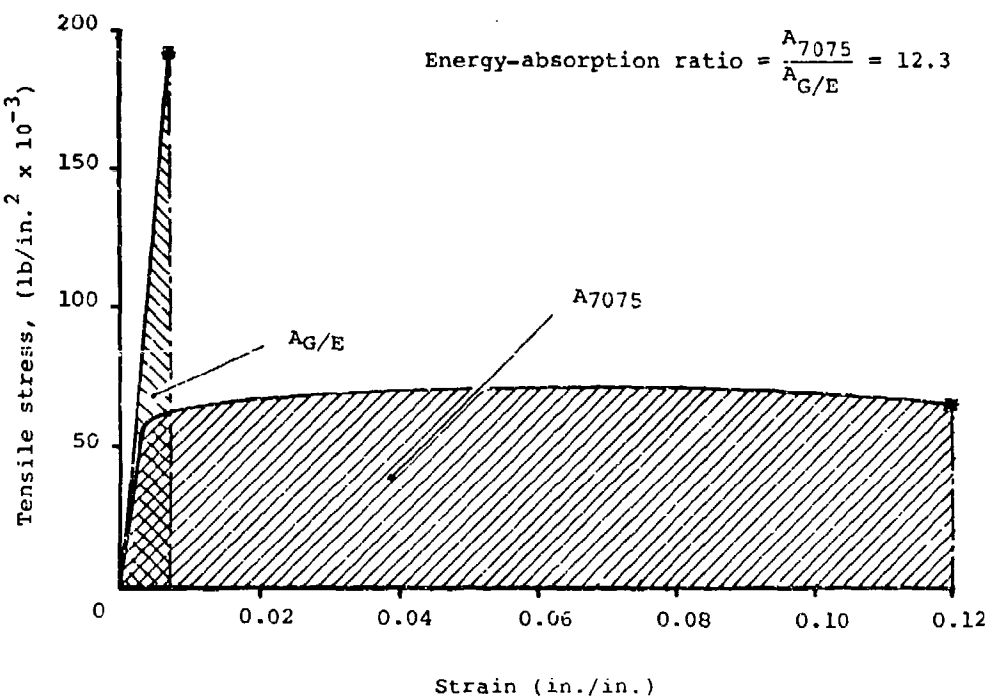

FIGURE 28. STRESS-STRAIN RELATIONSHIP FOR ALUMINUM ALLOY (7075) AND 0-DEGREES GRAPHITE/EPOXY COMPOSITE.

However, if properly designed assemblies of composite materials are progressively crushed, they can exhibit high energy absorption. Figure 29 shows a comparison of Specific Energy Absorption (SEA) for a number of devices with a composite tube having the largest value (Reference 23). In addition to SEA, the failure modes of composite materials should be considered. Typically, graphite/epoxy has poor postcrushing integrity and exhibits fracture and separation during crushing. On the other hand, Kevlar/epoxy typically has good postcrushing integrity.

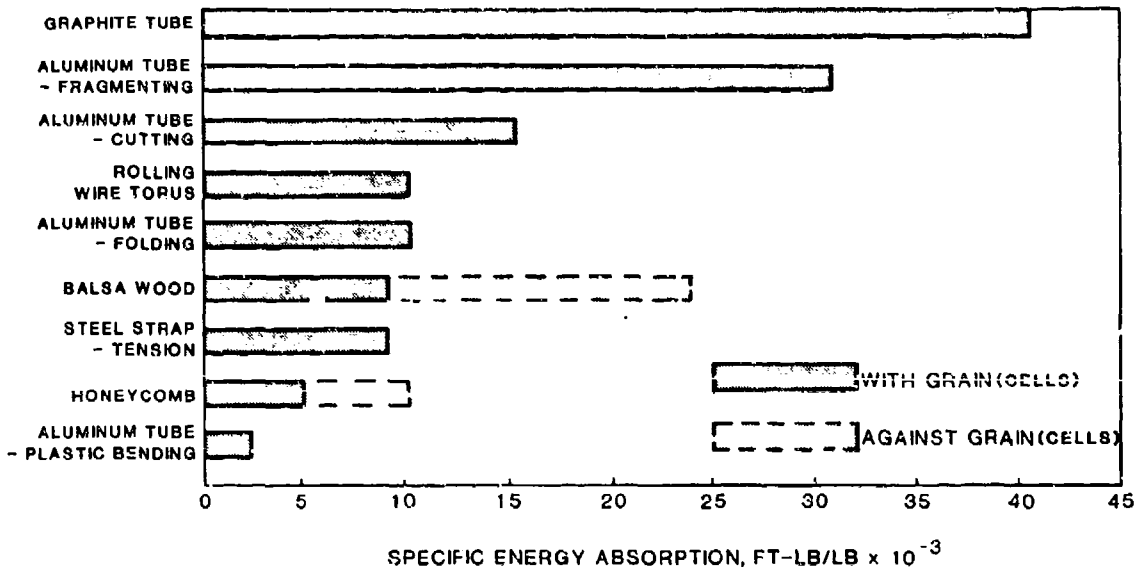

FIGURE 29. SPECIFIC ENERGY ABSORPTION COMPARISONS. (FROM REFERENCE 23)

Table 6 presents values for ultimate strengths and elastic moduli for several typical structural composites.

Much design and development test work has been conducted to find composite geometries that will serve the dual purpose of carrying normal flight and landing loads as well as providing energy absorption when subjected to crash loads. Detailed information may be obtained from References 24 through 42.

Additionally, much information concerning the inclusion of crash resistance in composite aircraft, using the techniques presented in References 24 through 42, is available from the U.S. Army-sponsored Advanced Composite Airframe Program (ACAP). Results from these programs are available in References 36 and 43 through 46. Two U.S. Army ACAP helicopter drop tests, reported in References 47 and 48, have demonstrated the feasibility of crash-resistant composite structures.

TABLE 6. ULTIMATE STRENGTH AND ELASTIC MODULI FOR TYPICAL STRUCTURAL COMPOSITES

Composite	Ultimate Tensile Stress ($lb/in.^2$)	Modulus of Elasticity: Longitudinal ($lb/in.^2$)	Modulus of Elasticity: Transverse ($lb/in.^2$)
Boron/epoxy [0]	192,000	30×10^6 -30×10^6	2.7×10^6 -2.7×10^6
Graphite/epoxy [0] (high modulus graphite)	110,000	25×10^6 -25×10^6	1.7×10^6 -1.7×10^6
Graphite/epoxy [0] (high strength graphite)	180,000	21×10^6 -21×10^6	1.7×10^6 -1.7×10^6
Boron/aluminum	160,000	34×10^6 -30×10^6	20×10^6 -19×10^6
Borsic/aluminum	140,000	32×10^6 -30×10^6	22×10^6 -19×10^6

Another available method of energy absorption that may achieve adequate performance is incorporation of filler materials, such as honeycombs and structural foams. For longitudinal and lateral impacts, it is feasible to incorporate energy-absorption features of this type; for the support of large mass items with high energy content, other techniques are probably necessary.

Limitations on the use of energy absorption techniques will be dependent on the size and overall layout of the aircraft needed to satisfy mission requirements. For a given aircraft, optimization studies may indicate that some major primary structural elements need to be manufactured from metallic materials, whereas composites may find use in other areas. If construction techniques are mixed, the effect of thermal stresses during manufacture and operation must be fully investigated. If curing of the bonding agent at elevated temperatures is required, warpage of the finished product may result. Table 7 gives values of thermal expansion coefficients for composite and metallic materials. Other useful design information can be found in Reference 44.

If the composite crash-resistant primary structure is not designed carefully, it may be less effective than anticipated. If a composite structure with an energy absorption capability less than that of a metallic structure is used, a survivable deceleration environment must be created by the use of landing gear with greater energy-absorbing capacity, energy-absorbing seats, and possibly some forms of floor load attenuation other than through primary

TABLE 7. THERMAL COEFFICIENTS OF EXPANSION FOR COMPOSITE AND METALLIC MATERIALS (REFERENCE 48)

Material	Coefficient of Thermal Expansion (10^{-6} in./in./°F) Longitudinal	Transverse
Boron filament	2.7	NA
Epoxy matrix resin	2.7	27
Graphite fiber	-0.05	NA
E-glass filament	2.8	NA
Boron/epoxy [0]	2.3	10.7
Boron/epoxy [$0_2/\pm45$]	2.4	7.7
Graphite/epoxy [0]	0.3	14.4
Graphite/epoxy [0/±45/90]	1.9	1.9
E-glass/epoxy [0]	4.8	--
E-glass (181 style weave)/epoxy	5.5	6.7
PRD-49/epoxy [0]	-6.0	--
PRD-49 (181 style weave)/epoxy	0.0	--
Aluminum		13
Steel		6
Titanium		5.6

structural deformation. This may introduce additional weight and require extra installation space to allow adequate stroking distances. Reference 50 presents a survey of crash impact characteristics of composite structures and suggests possible design concepts.

5.3.7.4 Spark Generation. Two types of sparks should be considered potential ignition sources. The friction spark is a particle abraded from a parent material through contact with a moving surface. Initially, the particle is heated by friction. If the friction is great enough, the material's combustion temperature will be reached, causing the particle to ignite.

Electrostatic sparks result from the discharge of an electrostatic charge accumulated on parts during normal operation. The discharge may be triggered when crash forces cause separation of the parts. This section is concerned only with material selection to minimize friction spark generation.

Friction sparks become possible ignition sources when portions of aircraft structure scrape along the ground. While all common metals can be abraded, not all sparks are sufficient to ignite spilled fluids; rather, ignition is dependent on the thermal energy of the spark. Thermal energy is a function of the following parameters:

- Bearing pressure of structure on ground.
- Sliding velocity of structure relative to ground.
- Metal hardness.
- Temperature at which metal particles burn.

Table 8 gives some results of research conducted by NASA to determine the minimum conditions under which friction sparks from metallic materials typically used in aircraft construction will ignite (References 51 and 52).

TABLE 8. MINIMUM CONDITIONS UNDER WHICH CERTAIN ABRADED METAL PARTICLES WILL IGNITE (REFERENCES 51 AND 52)

Metal	Minimum Bearing Pressure ($lb/in.^2$)	Drag Speed (mi/hr)
Titanium	21-23	less than 5
Chrome-molybdenum steel	30	10
Magnesium	37	10-20
Stainless steel	50	20
Aluminum	1,455*	40

*Ignition was not obtained with aluminum.

Aluminum alloys are the least likely to cause ignition of spilled fuel; however, the abrasion rate for aluminum is high, which can result in rapid wear and subsequent tearing. This, in turn, exposes other structures that may be manufactured from materials prone to generate sparks. To minimize the probability of belly skin loss, relatively thick skins made of ductile materials are recommended.

Particular attention should be given to attachment points for hoists, landing gears, boarding steps, and other components located in anticipated impact areas. Also, particular attention should be given to steel nuts, bolts, and washers that can contaminate otherwise spark-free areas.

Composites included in aircraft structures have not been considered as potential ignition sources. However, if the aircraft belly primary structure is constructed from composites, the high bearing pressures and sliding velocities may generate sufficient heat for hot spots to ignite spilled flammable fluids. The relevant properties to ensure that ignition temperatures cannot be developed should be fully investigated for any composite located in such an area of sliding contact.

5.3.7.5 Strain Rate Effects. During a crash, rapidly increasing loads, not instantaneous loads, are applied. In most cases, a minimum of 10 msec is required for loads to reach maximum values. Under such conditions, inertia effects may be of importance, but strain rate effects in materials are probably insignificant.

6. SUBSYSTEM DESIGN

6.1 INTRODUCTION

This section offers specific suggestions for achieving the most crash resistance from fuselage, landing gear, and other subsystems. However, it must be recognized that systems integration is essential for optimizing aircraft crash performance. The specification for the performance of each subsystem is presumably created from an aircraft systems model that considers the interaction between subsystems. Conversely, the total systems model requires input about achievable subsystems capabilities. Development of optimum crash resistance performance therefore requires an iterative approach.

Many crash conditions must be considered for a crash resistant aircraft design, including those for which the landing gear cannot be effective as an energy absorber. In such circumstances, the crash performance of the fuselage is most important; for this reason, the fuselage is presented first. Following sections treat the landing gear and other subsystems external to the fuselage (rotor blade, wing, empennage, engine pods, etc.), some of which may be employed as energy absorption devices in a crash or may be shed to reduce kinetic energy.

6.2 FUSELAGE

6.2.1 General

Improved crash resistance begins with improvements in fuselage design, since the fuselage provides the occupants' protective shell and can appreciably control accelerations applied to the seats. In this section, principles for improving fuselage structure and methods for accomplishing these improvements are presented.

A graphic example of cabin collapse is shown in the sequence of photographs shown in Figure 30. These photographs, taken during a NASA fuselage drop test, illustrate how an occupied volume can be briefly reduced to the point where human survival is unlikely even though the postcrash deformations may be small.

Fuselage crash performance can be improved through the following design techniques:

1. Alteration of the structure that makes initial contact with the ground to reduce gouging and scooping of soil, hence limiting accelerations.

2. Reinforcement of cockpit and cabin structure to prevent collapse and to provide adequate tiedowns for occupants and cargo.

3. Modification of fuselage structure to provide energy absorption through controlled deformation.

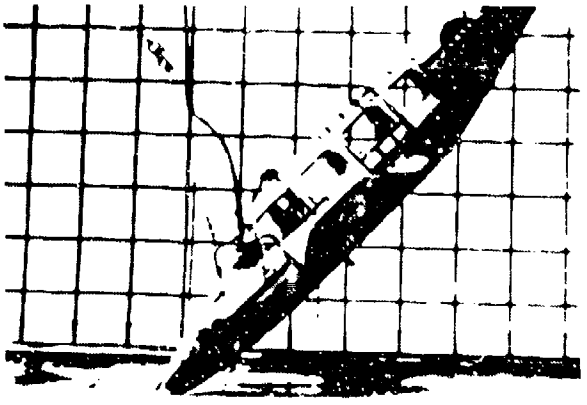

1. INITIAL CONTACT OF NOSE WITH GROUND

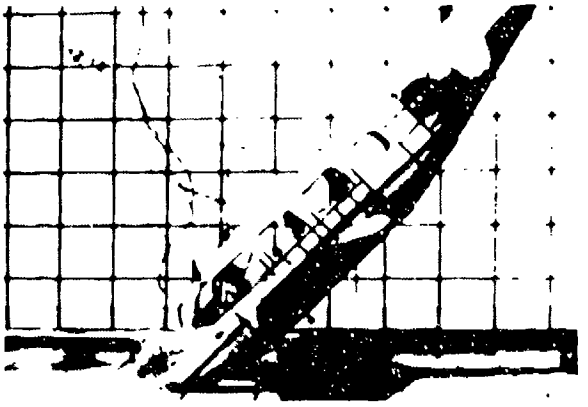

2. COCKPIT LIVABLE VOLUME STILL INTACT

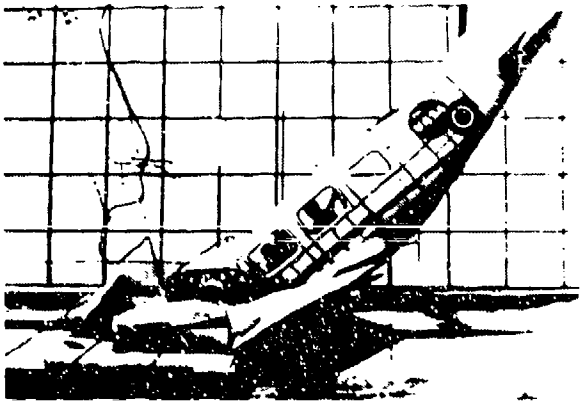

3. COCKPIT LIVABLE VOLUME STARTS TO COLLAPSE

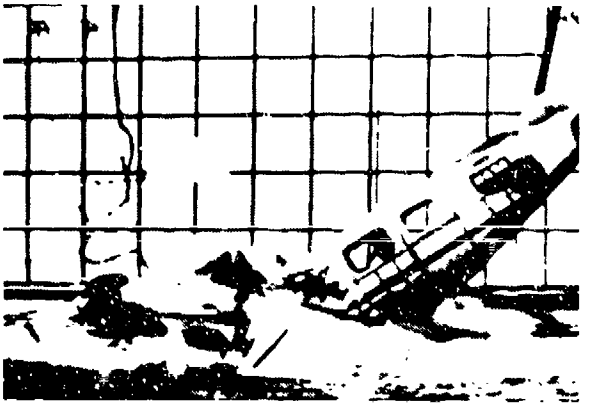

4. COCKPIT LIVABLE VOLUME TOTALLY COLLAPSED

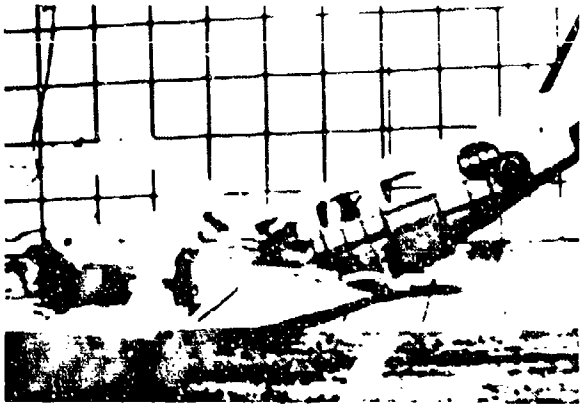

5. COCKPIT LIVABLE VOLUME STILL CLOSED

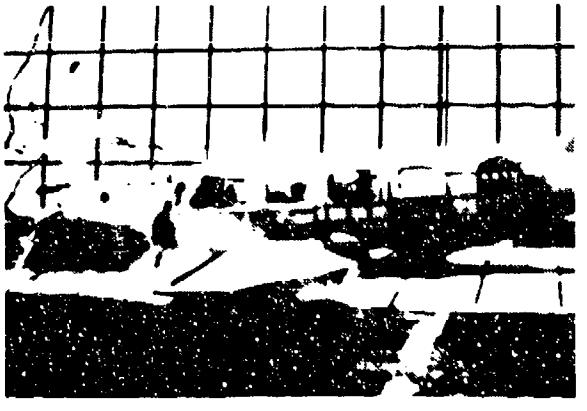

6. COCKPIT LIVABLE VOLUME HAS SPRUNG BACK OPEN

FIGURE 30. NASA DROP TEST OF CIVIL LIGHT TWIN-ENGINE AIRCRAFT.

4. Resistance of fuselage penetration by selective structural reinforcement or by modification of components such as the antitorque rotor blades, empennage boom, support system for the external stores, and the landing gear to ensure that if these parts fail, they fail safely.

5. Provision for component breakaway to effect a reduction in the mass of the aircraft, and reduce the fuselage strength requirements.

Potential benefits from each method depend upon the structural characteristics of each aircraft design and it's mission constraints.

Figure 31 illustrates an approach to maintaining a protective shell and absorbing vertical crash energy. This can be accomplished by providing rollover strength in the form of stiffened ring frames on the top and sides of the fuselage. The crushable webs of the subfloor beams contribute strength and stiffness to satisfy the normal airworthiness criteria; they also function as energy absorbers to attenuate the vertical crash impact forces.

The sections that follow discuss the design of crash resistant fuselages. Load-limiting strategies are discussed first. They are used to reduce the forces on the occupants and to reduce loads within the fuselage, thus preserving the protective shell with minimum weight. Next are methods to avoid unnecessary failures of the protective fuselage shell or blockage of emergency escape routes by crash-induced fuselage deformation. Last, attention is directed to structural interfaces with other subsystems: engines, transmissions, fuel tanks, seats, cargo, and ancillary equipment. Although landing gear, wings, empennage, external engine pylons, and external stores are also mounted to the fuselage, these major external subsystems and their structural interfaces are described in other sections.

6.2.2 Load-Limiting Fuselage Structure

6.2.2.1 General. A basic difference exists between the dissipation of kinetic energy in crashes which are primarily longitudinal (high velocity, low angle) and those that are primarily vertical.* In longitudinal impacts onto relatively flat surfaces, a high percentage of the kinetic energy of the aircraft is dissipated in displacement of earth and in friction between the aircraft and the earth. Consequently, in this type of crash, a relatively low percentage of the kinetic energy is absorbed by structural deformation. In primarily vertical impacts, longitudinal impacts into barriers, and lateral impacts, much more of the kinetic energy must be absorbed by the structure. This leads to separate design concepts for improving crash resistance under primarily longitudinal impact conditions and under other impact conditions.

---

*As used here, "longitudinal" refers to the orientation of the velocity vector with respect to the impact surface, i.e., parallel to the impact surface. The impact surface is presumed to be relatively firm and unobstructed. "Vertical" impact refers primarily to the autorotation type impact for rotary-wing aircraft.

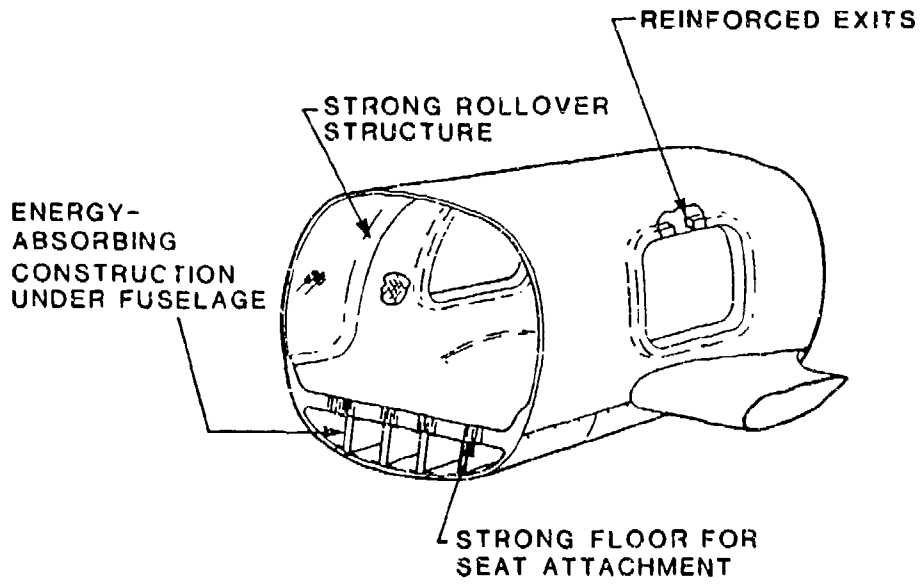

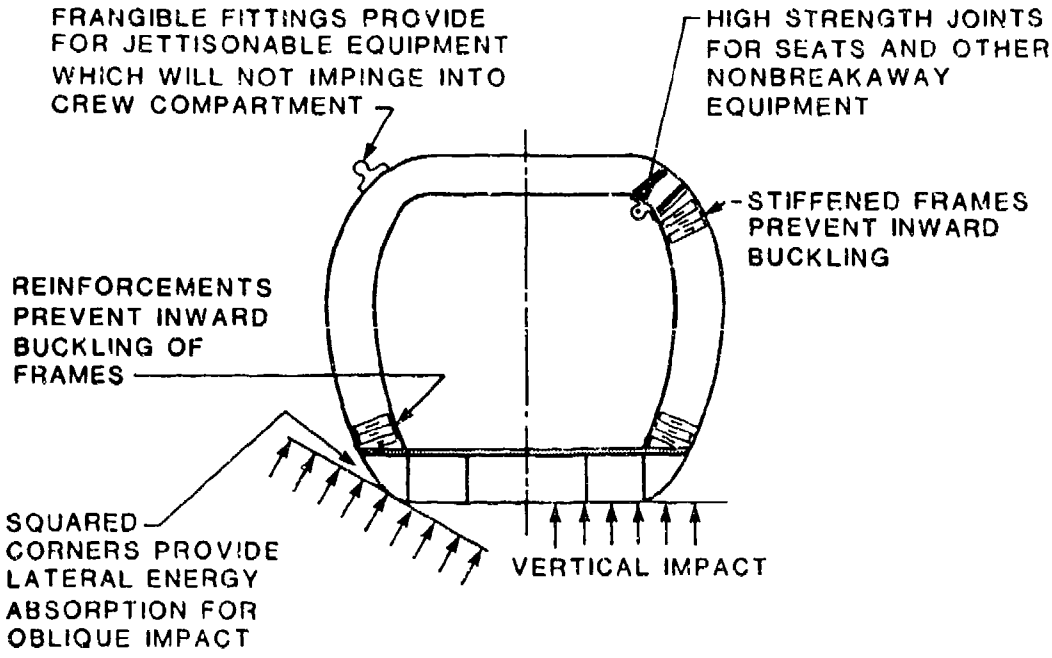

FIGURE 31. OVERALL FUSELAGE CONCEPTS. (FROM REFERENCE 50)

In a longitudinal impact, the main considerations are to ensure the integrity of the structural shell, to minimize earth scooping or plowing of the lower fuselage, and to provide some energy-absorbing material forward of the occupied area to limit forces due to impact with obstacles such as earth berms.

For a primarily vertical impact (or for the vertical component of any impact), structural energy-absorption requirements differ appreciably from those of a longitudinal impact. In a vertical impact against rigid surfaces, there exists no possibility of low-force-level (and hence low-acceleration-level) energy absorption exterior to the aircraft comparable to the frictional energy absorption in a longitudinal skid. The velocity change in the vertical direction must be accomplished in a short time. Consequently, when the vertical velocity component is high, crashes are generally characterized by large structural deformation and high floor accelerations. The floor acceleration can be reduced by incorporating crushable underfloor structure.

The difference in typical vertical and longitudinal impacts is graphically illustrated in Figure 32. The vertical impact in Figure 32(a) shows a constant low level acceleration for an extended period of time as the gear strokes. This is followed by fuselage impact which occurs at a much higher G level for a shorter time. (The gear may still be stroking and contributing to the load during this time.) Seat stroke coincides with fuselage crush and continues afterward until the seat and occupant's energy is expended. Corresponding velocity and displacement are also shown to clarify the dynamics of the system interactions.

Longitudinal impacts are usually relatively simpler with acceleration profiles as shown in Figure 32(b). An initial slide is followed by a higher acceleration pulse with fuselage crush due to impact with an obstacle or earth plowing followed by a long low-level acceleration slide-out period. Impacts with barriers, of course, lack the slide-out period. Usually, there is negligible energy absorption in structure other than the fuselage.

The limiting of loads on the fuselage is directly beneficial since it reduces the decelerations experienced by the seat structure and occupants. Equally important, it is indirectly beneficial by reducing loads on the structure and thus helping to preserve the protective fuselage shell.

6.2.2.2 Vertical Energy Absorption. To evaluate potential improvements in crash resistance of cabin structure for vertical impacts, two idealized extreme configurations are presented. First, consider a fuselage section in which the aircraft mass is concentrated at the top of a fuselage section. This model is schematically illustrated in Figure 33. The fuselage acts as a nonlinear spring which is initially elastic and remains so for a moderate deformation; thereafter, the spring force reaches a critical value that produces a plastic deformation. For such a model, a vertical impact requires that substantially all of the kinetic energy of the mass be converted to deformation energy of the structure.

The concepts shown schematically in Figure 34 include a crushable region below the cabin floor that deforms plastically at forces below the critical load for the upper fuselage sidewalls. To provide further deceleration distance for the overhead mass, an energy-absorbing structure may be placed between the mass and the fuselage (Figure 34) Care must be taken in using

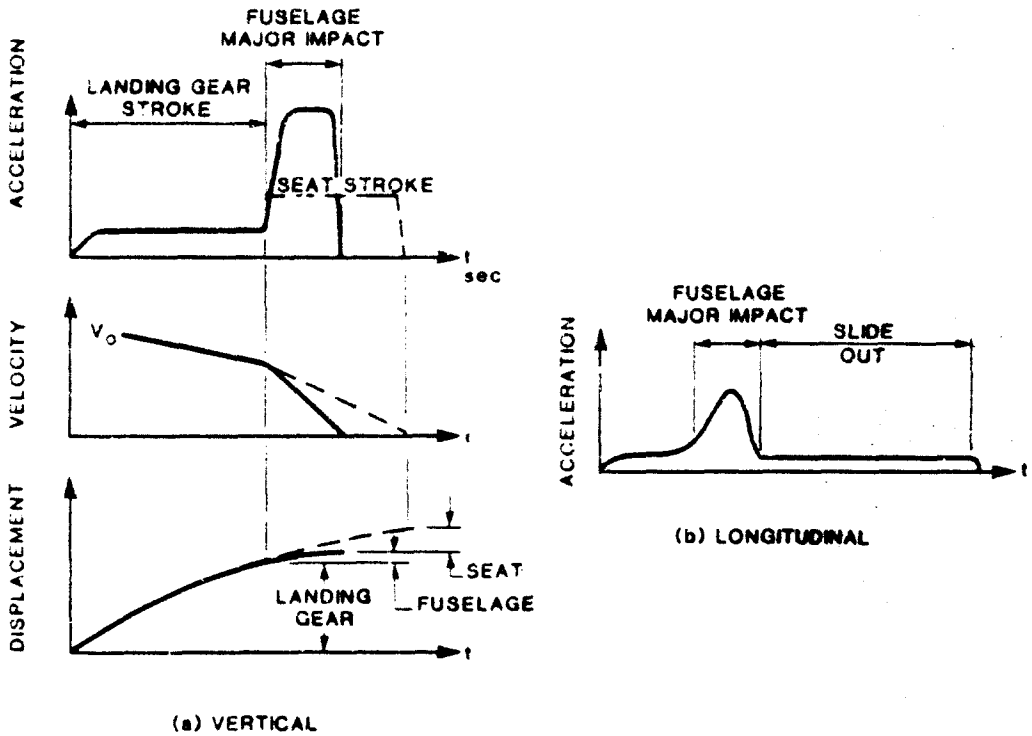

FIGURE 32. TYPICAL VERTICAL AND LONGITUDINAL CRASH PULSES.

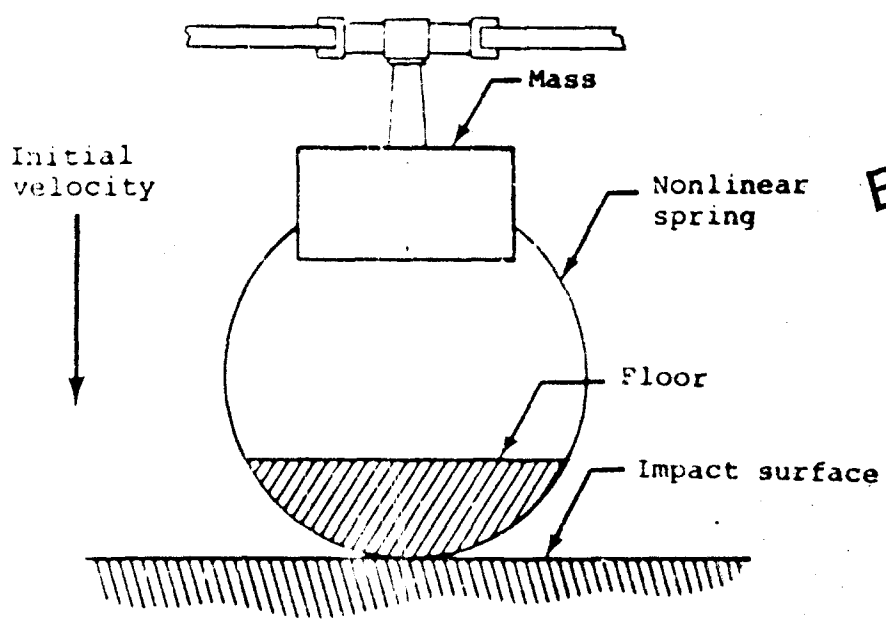

FIGURE 33. FUSELAGE STRUCTURE WITH OVERHEAD LARGE MASS ITEMS (IDEALIZATION).

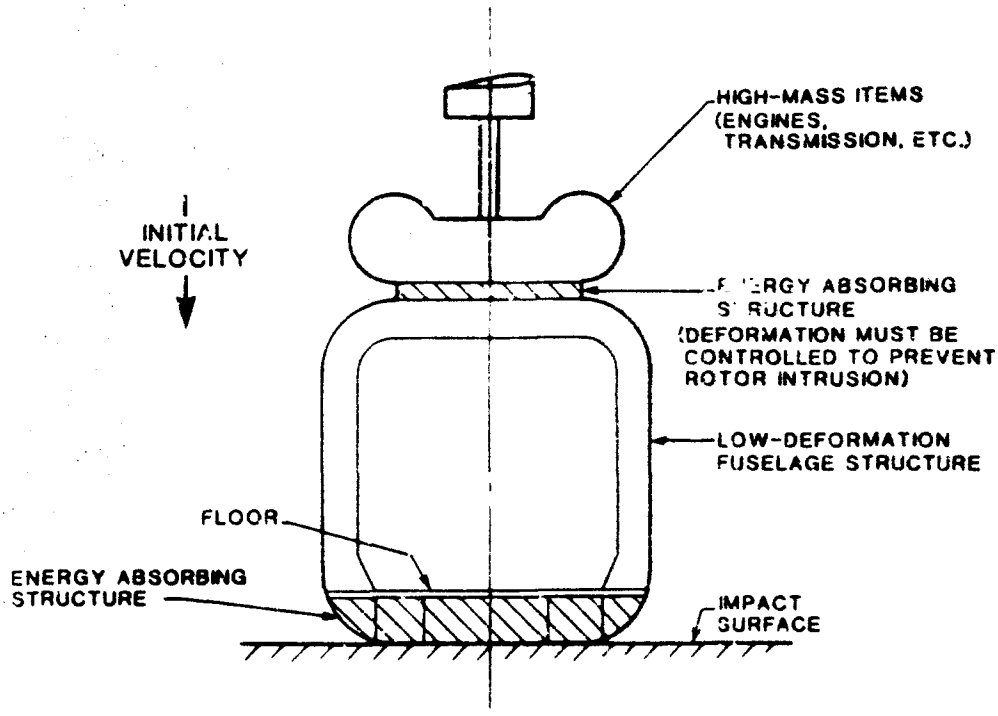

FIGURE 34. DECELERATION OF OVERHEAD HIGH-MASS ITEMS BY ENERGY-ABSORBING MATERIAL.

this concept to ensure that nonuniform deformation of this structure does not lead to rotor blade intrusion into the cockpit.

The opposite extreme consists of an aircraft with the mass concentrated at or near the bottom of the fuselage. Figure 35 illustrates this configuration schematically. The light upper structure in the cabin would be unlikely to collapse even for high-energy impacts. If crushable subfloor structure were included in the model, it could serve to attenuate the floor acceleration.

Actual conditions generally fall between the two extremes presented above. To the extent that large masses and sometimes floor/ceiling-mounted troop seats are secured to the upper fuselage, the possibility of cockpit/cabin collapse should be carefully considered in the design process.

The fuselage underfloor structur can help protect occupants from high decelerations by absorbing energy d ing the crushing process that occurs during vertical impacts. This structure should demonstrate large plastic deformation during the crash. Metal structures generally accomplish this through the process of instabil.ty failures, followed by large plastic deformations. Some components are also capable of absorbing energy following compressive collapse. Some concepts for energy-absorbing structure are shown in Sections 5.3.1 and 5.3.6.3. Methods for calculating the amount of energy absorption capability required are presented in Section 7.3.3. References 53 through 61 provide additional information concerning the mechanics of large-deformation structural energy absorption.

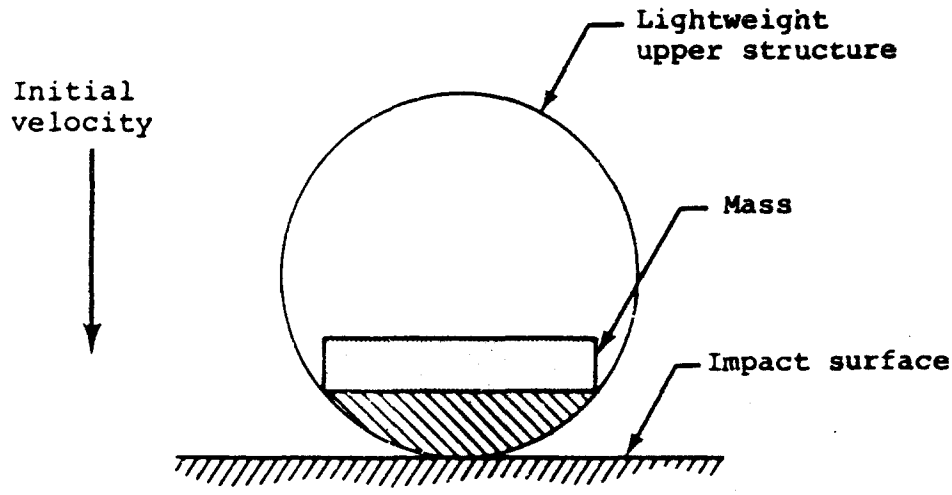

FIGURE 35. FUSELAGE STRUCTURE WITHOUT OVERHEAD MASS ITEMS (IDEALIZATION).

Figure 36 summarizes the design requirements for proper vertical energy absorption design. The load-deformation curve should exhibit a relatively uniform crushing load to provide efficient energy absorption. The stroke-to-length ratio of the involved structure should be such that the useful stroke is sufficient to provide the necessary energy absorption. The crushable structure should not have a high peak load at the initiation of stroking that could cause the fuselage structure to collapse. Also, the underfloor design should possess postcrash structural integrity and should function properly under combined load effects resulting from varying impact conditions.

MIL-STD-1290 now requires that the fuselage be designed to withstand a 42-ft/sec vertical impact with a pitch of +15 to -5 degrees and a roll of ±10 degrees as shown by the crosshatched envelope in Figure 37a. Vertical energy absorption capability is very much a function of impact attitude, and this effect must be carefully considered by the designer. The effect of roll and pitch attitude on survivable vertical impact velocity is illustrated by Figure 37b which shows the resulting 36 ft/sec envelope for an experimental ACAP fuselage designed for the rectangular 42-ft/sec envelope represented by the crosshatched area.

Methods of absorbing energy include the use of crushable material. Honeycombs, expanded foams, or similar materials share the major disadvantage of occupying relatively large volumes. Such space usage can result in system installation compromises, enlarged profiles, and increased primary structure weight to accommodate such energy attenuation methods. They do, however, still provide a method warranting consideration.

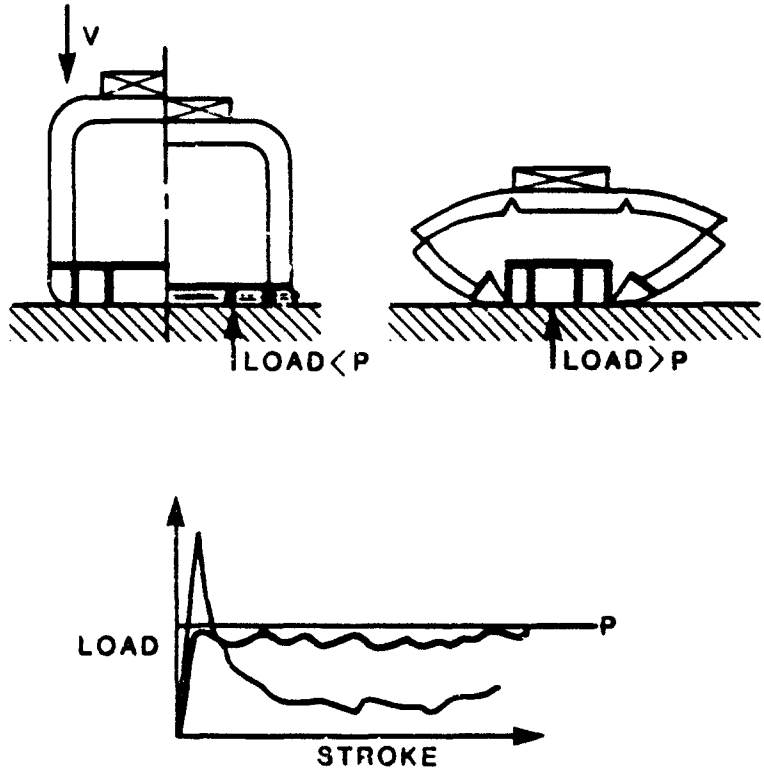

FIGURE 36. VERTICAL IMPACT CRUSHING LOADS.

Considerable work has been done to investigate various underfloor structural geometries capable of sustaining normal flight and landing loads while providing significant energy absorption during a crash with vertical velocity. Examples of such structure are shown in Figures 38 and 39. Other concepts are presented in References 62 through 64. These concepts, when used underneath a strong floor structure, result in the desired combination of a continuous strong floor and an energy-absorbing understructure.

The beam and bulkhead concepts shown in Figure 38 are designed to react to the vertical, longitudinal, and lateral impact loads; however, the most efficient direction for providing a progressive collapse is vertically. In each of the concepts shown, it is assumed that the floor structure would also be designed to react the crash impact forces without failure. The concepts shown are directly applicable to many current fixed- and rotary-wing aircraft, because their structural arrangement is similar.

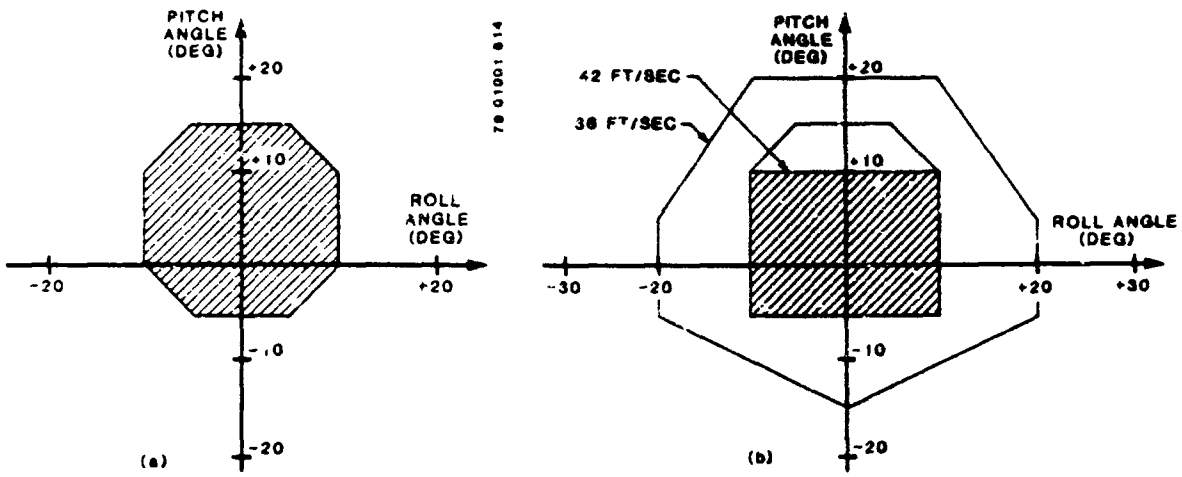

FIGURE 37. ROLL AND PITCH ATTITUDE ENVELOPES.

Concepts 1, 2, and 3 are web designs for floor beams made of composite materials. These webs may be designed so that crushing is initiated at the desired load and the beam absorbs energy through progressive crushing of the web. The sine, circular and square tube features provide enhanced specific energy absorption. Peformance can be analyzed based on a single cell or section of the web, and extensive performance characterization studies have been made for various materials, layups, and dimensions. Further information on the performance of these crushable beam webs is contained in Reference 31.

Concept 4 in Figure 38 shows rib-stiffened floor beams constructed in a manner very similar to metal beams. However, their webs are designed to crush and absorb energy when they are subjected to high vertical loads. The stiffeners provide the buckling resistance necessary to insure that the webs will crush rather than bend laterally under load. Component test results for this configuration are given in Reference 27.

Concept 5 in Figure 38 is a solid laminate approach that utilizes the high strength of graphite fibers to provide the strong load-carrying portion of the floor structure. The crushable portion of the floor takes advantage of the favorable crushing mode of failure of Kevlar to provide the energy-absorbing portion of the structure. Test data and details are presented in Reference 44.

Concept 6, shown in Figure 38, shows schematically a sandwich underfloor construction that consists of Kevlar/epoxy face sheets and a honeycomb core that crushes and provides energy absorption when the beam is subjected to crash loads. Details and further test data are presented in Reference 31.

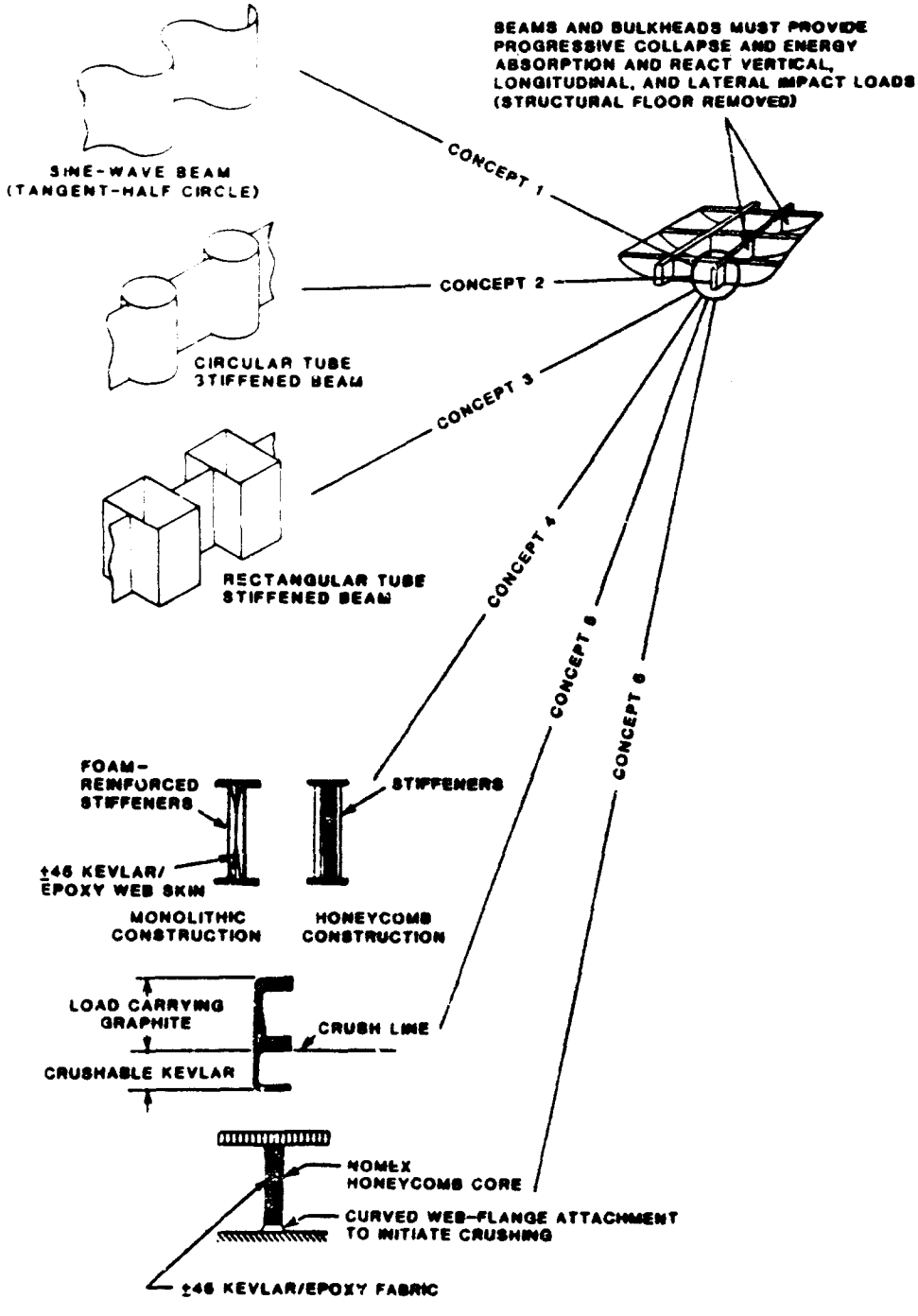

FIGURE 38. ENERGY ABSORPTION CONCEPTS - BEAMS AND BULKHEAD (VERTICAL IMPACT). (FROM REFERENCES 27, 29, 30, 44, AND 50)

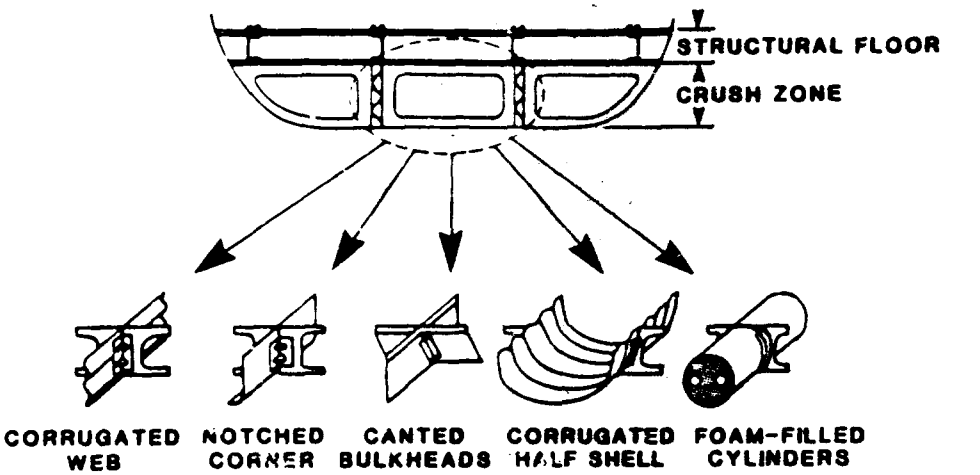

FIGURE 39. UNDERFLOOR BEAMS DESIGNED WITH POTENTIAL ENERGY-ABSORBING CAPABILITY. (FROM REFERENCE 62)

The energy-absorbing concepts shown in Figure 39 are of aluminum construction. Details of these and other metallic concepts may be found in References 56 and 62.

A fuselage concept using crushable composite sandwich underfloor structure to absorb the crash impact kinetic energy is shown in Figure 40. The lightweight crushable underfloor structure is integral to the airframe and serves a dual purpose by providing the structural strength to withstand flight, landing, ditching, and floor loads as well as the energy absorption capacity to dissipate crash-impact kinetic energy and decelerate the aircraft to rest. As shown in Figure 41, the composite energy-absorbing underfloor was developed in a systematic manner proceeding from design support testing to full-scale cabin testing to incorporation in the design of an advanced experimental aircraft (Reference 66). Details of the cabin test configuration are shown in Figure 42. A mix of frangible and crushable structure was used to control crash loads under various impact conditions.

The optimum energy absorption capability of underfloor structure is a direct function of the available stroking distance between the cockpit/cabin floor and underside of the aircraft. This distance varies for different aircraft types and results in differing landing gear-to-structure-to-seat energy-absorption distributions. This emphasizes the need for a crash-resistant seat designed as an integral part of the aircraft.

6.2.2.3 Earth Scooping and Plowing. When the forward sections of an aircraft deform so that a scoop is formed and a large quantity of earth is impulsively accelerated, two adverse effects may occur. First, high acceleration

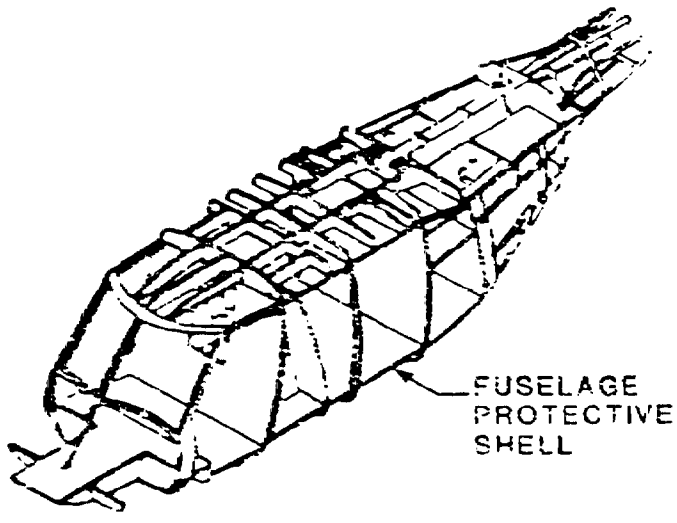

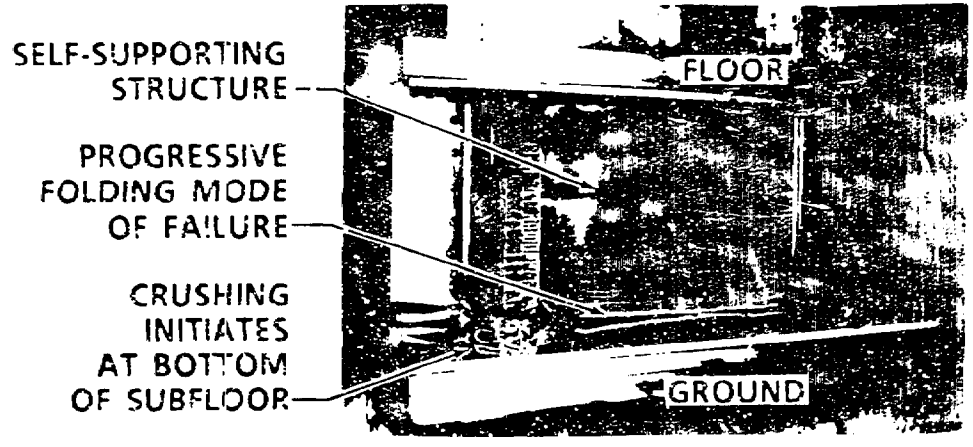

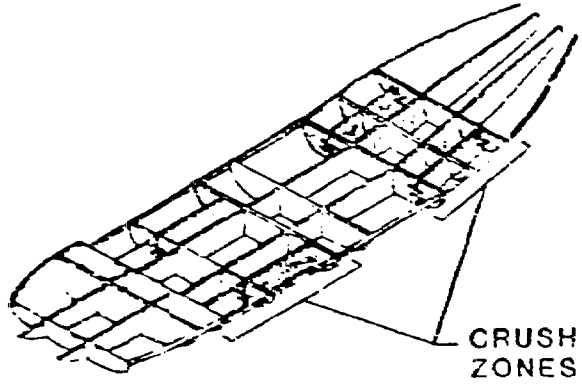

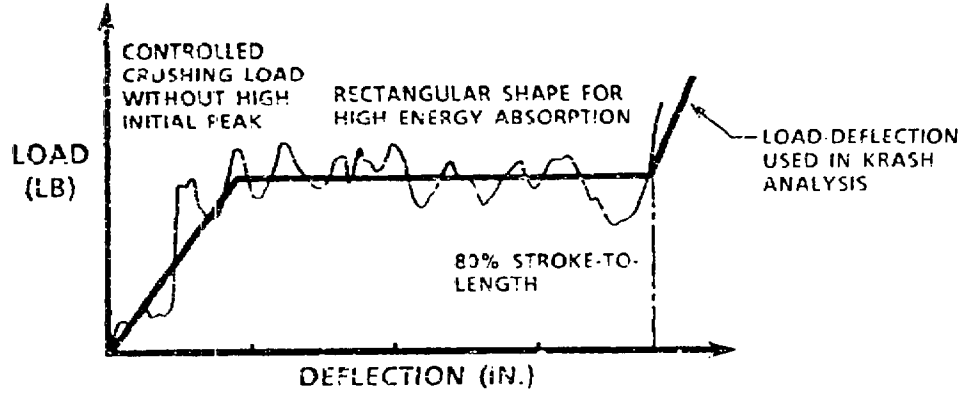

FIGURE 40. ENERGY-ABSORBING UNDERFLOOR STRUCTURE.

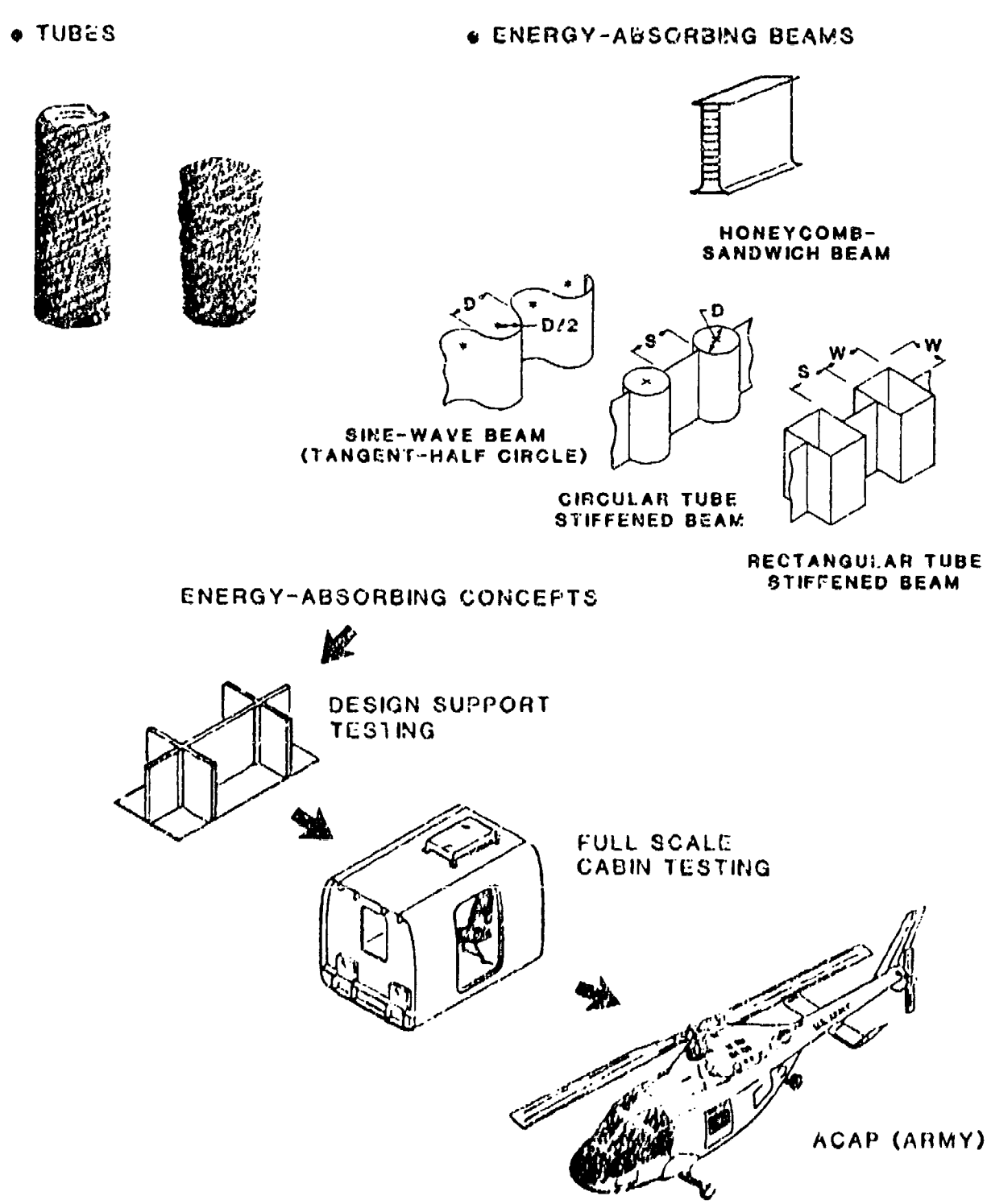

FIGURE 41. DEVELOPMENT OF COMPOSITE ENERGY-ABSORBING UNDERFLOOR STRUCTURE. (FROM REFERENCE 66)

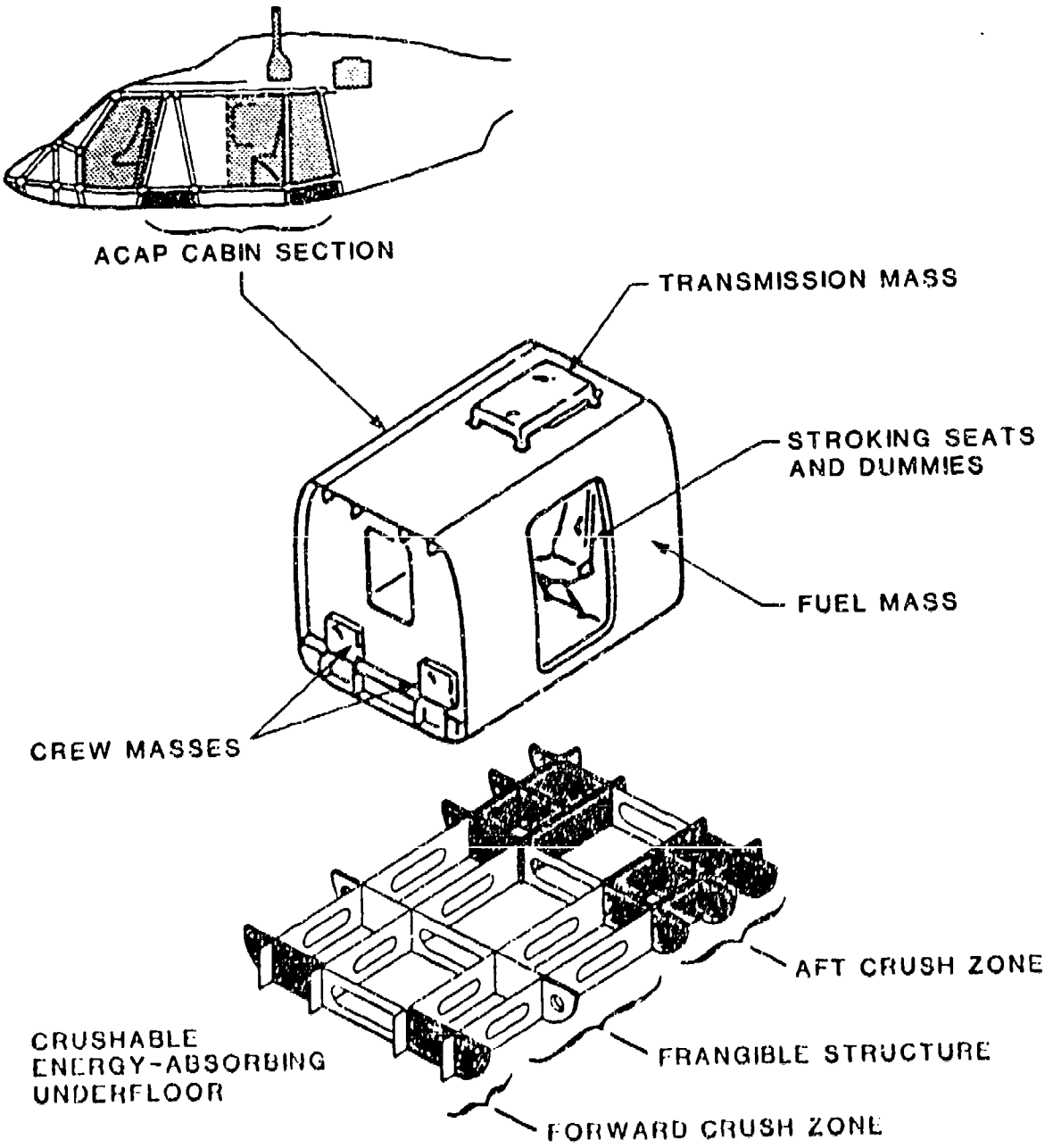

FIGURE 42. COMPOSITE CABIN TEST SECTION.

of the aircraft may occur. Second, the large forces required to accelerate the earth mass may be concentrated in a small area and cause local collapse of the cockpit protective shell.

The earth-scooping process occurs in a very short time interval; therefore, the principle of conservation of momentum may be applied to the system, which includes the mass of soil that must be accelerated, referred to as the effective mass of earth, and the aircraft mass. Accordingly, conservation of momentum leads to the relationship

$$m_A v_o = (m_A + m_E)\, v \tag{5}$$

where m_A = mass of aircraft

m_E = effective mass of accelerated earth

v_o = initial impact velocity of aircraft

v = velocity of combined system immediately after impact.

Solving Equation (5) for v, we obtain

$$v = \frac{m_A}{m_A + m_E}\, v_o \tag{6}$$

To find the interaction force involved in the momentum exchange, an impulse-momentum relationship may be applied to the earth mass as a free body.

$$\int_{t_1}^{t_2} F\,dt = m_E v \tag{7}$$

where F = interaction force

t_1 = time just prior to impact

t_2 = time directly following momentum interchange.

By definition of the average force,

$$\int_{t_1}^{t_2} F dt = F_{av} \Delta t \tag{8}$$

where $$\Delta t = t_2 - t_1$$

Substituting Equations (6) and (8) into Equation (7) yields

$$F_{av} = \left(\frac{m_A m_E}{m_A + m_E} \right) \frac{v_o}{\Delta t} \tag{9}$$

Consequently, the average acceleration of the aircraft mass due to the acceleration of the earth mass is

$$a_A = \frac{F_{av}}{m_A} = \left(\frac{m_E}{m_A + m_E} \right) \frac{v_o}{\Delta t} \tag{10}$$

Also, $$m_E = K A v_o \Delta t \tag{11}$$

where K is a constant and A is the cross sectional area of the gouge in the earth.

Thus,

$$a_A = \frac{K a v_o^2}{m_A + K a v_o \Delta t} \tag{12}$$

which indicates that the deceleration of the aircraft varies with the square of the initial velocity (where the scoop effect is a dominant factor and Δt is small). Thus, at high impact velocities, the scoop phenomenon assumes a greater significance. Experimental evidence substantiates the fact that impact accelerations do increase with the increasing impact velocity; however, maximum aircraft acceleration due to impulsive acceleration of earth is limited by the strength of the aircraft structure. Experimental evidence also indicates that, under high rates of loading, the force transmission ability of structures increases due to the stabilizing effect of lateral inertia during buckling of the structural members.

As an example of the use of Equation (12), assume that the following conditions exist:

$$v_o = 140 \text{ ft/sec}$$

$$\Delta t = 0.02 \text{ sec}$$

$$m_E = 0.185 m_A$$

Then

$$a_A = \frac{m_E}{m_A + m_E} \frac{v_o}{\Delta t}$$

$$a_A = \frac{0.185}{1.185} \frac{140}{0.02}$$

$$a_A = 1{,}092 \text{ ft/sec}^2 = 34 \text{ G}$$

If the impact velocity, v_o, and the time interval, Δt, remain unchanged but the effective earth mass, m_E, is reduced to $0.10\ m_A$, the average impulsive acceleration of the aircraft becomes

$$a_A = \frac{0.1}{1.1} \frac{140}{0.02} = 637 \text{ ft/sec}^2 = 19.8 \text{ G}$$

Increasing the impact velocity, v_o, to 160 ft/sec (under the aforementioned assumption that acceleration varies with velocity squared), when $m_E = 0.185 m_A$, results in an aircraft acceleration

$$a_A = \left(\frac{160}{140}\right)^2 1.092 = 1{,}430 \text{ ft/sec}^2 = 44 \text{ G}$$

And if a mass of earth equal to $0.1 m_A$ is accelerated under an impact velocity of 160 ft/sec, the average acceleration is computed to be 25.8 G.

Figure 43 shows a family of curves relating impulsive aircraft acceleration to the ratio of effective earth mass to aircraft mass for various impact velocities. The duration of the impulsive loading varies with impact velocity, although the curves are based on a single assumed value of 0.02 sec for the 140-ft/sec impact.

In addition to the force associated with momentum exchange, soil penetration by projecting structure gives rise to a drag force, sometimes called the "plowing effect." The plowing force is to be distinguished from the scooping

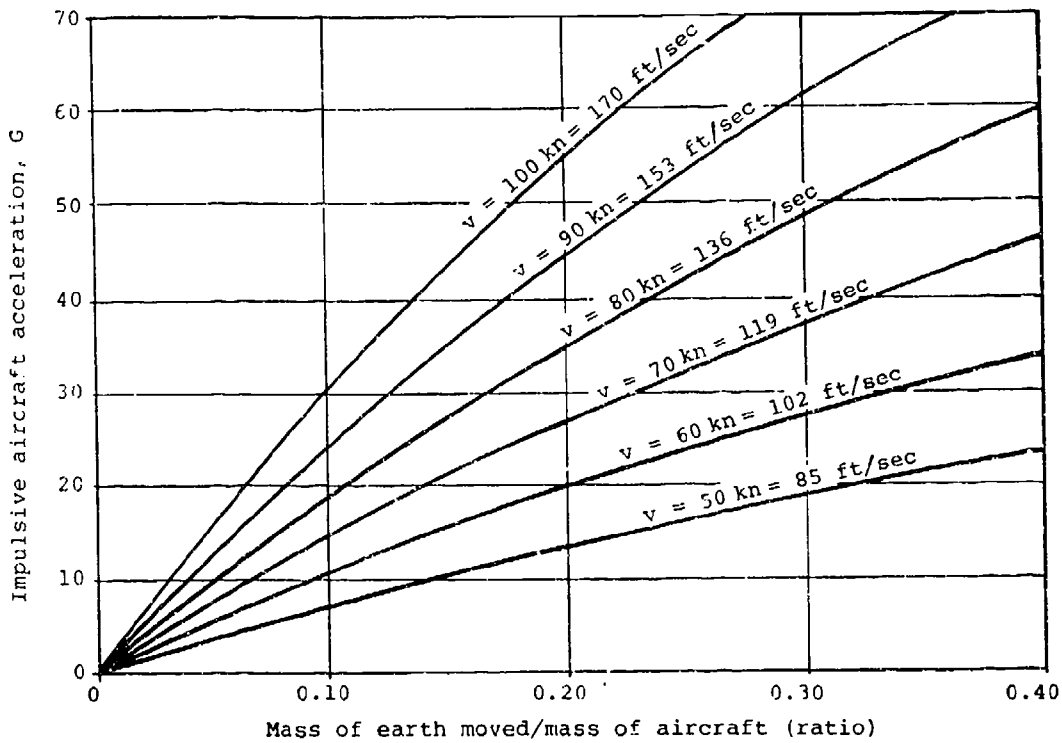

FIGURE 43. IMPULSIVE AIRCRAFT ACCELERATION AS A FUNCTION OF VELOCITY AND RATIO OF ACCELERATED MASS OF EARTH TO AIRCRAFT MASS (BASED UPON ASSUMED TIME, t, FOR ACCELERATION OF EARTH MASS).

force because it is a steady-state force depending upon velocity, soil strength and density characteristics, and projected area of interference.

However, a design which effectively reduces the scoop effect also helps to reduce the plowing effect. As stated in Section 4 and illustrated in Figure 44, the design criterion for the plowing condition is a combination of 10 G up and 4 G aft.

Reduction of earth scooping can be accomplished by structural design which eliminates those surfaces that can gouge or dig into terrain. The structural design should provide a large, relatively flat surface so that the aircraft skids along on top of the terrain. Design techniques include reinforcement of underfloor structure and canting of major structural components as illustrated in Figure 45. If this reinforcement is to be effective, the lower skin should be a ductile, tough material with enough thickness to resist tearing. The skin should remain continuous to provide a skidding surface. Additionally, the underbelly skins, made from thick sheet material, are shingled in an aftward direction to preclude their picking up at the front edge. These features are illustrated in Figure 46. It is recommended that the forward fuselage belly skins on aircraft weighing up to 3000 lb be capable of sustaining loads of 1500 lb/in.; over 3000 lb but under 6000 lb, 2400 lb/in.; and over 6000 lb, 3000 lb/in. The above running loads are to be applied over the forward 20 percent of the basic fuselage length.

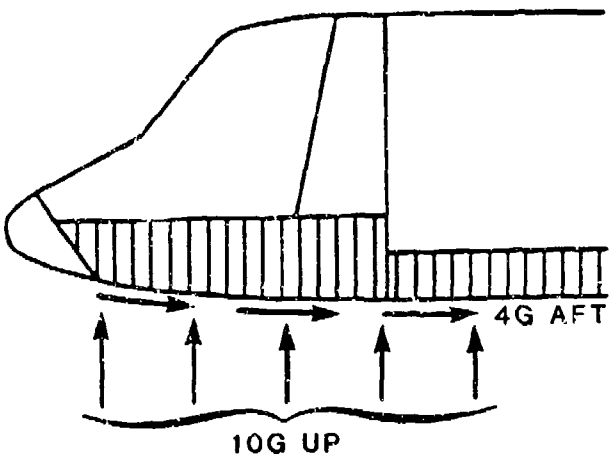

FIGURE 44. DESIGN CRITERIA FOR PLOWING CONDITION.

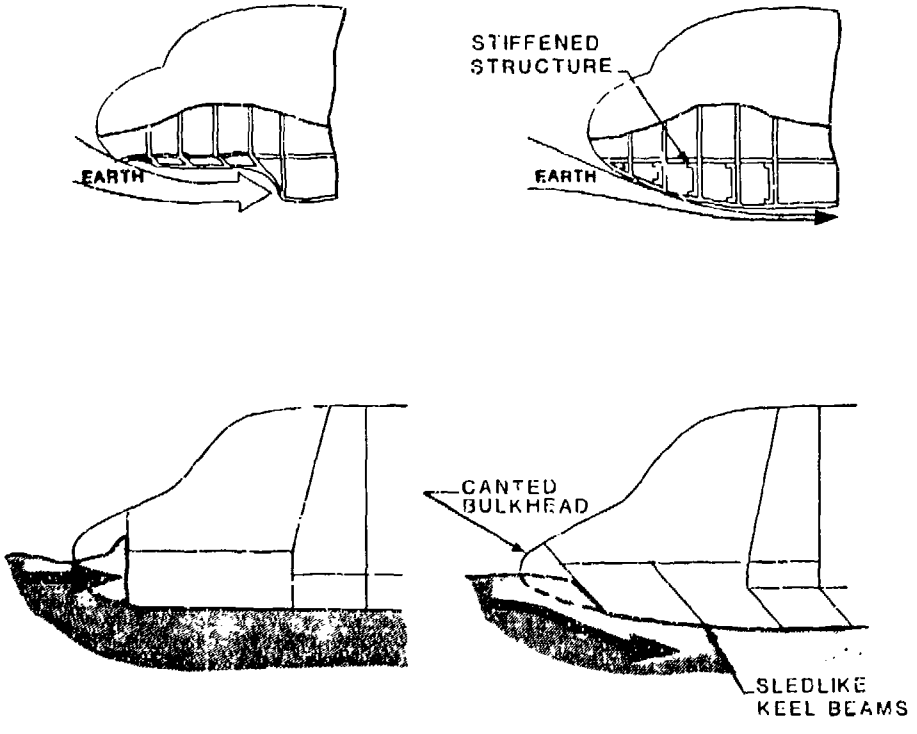

FIGURE 45. METHODS OF DESIGNING NOSE STRUCTURE TO REDUCE EARTH SCOOPING.

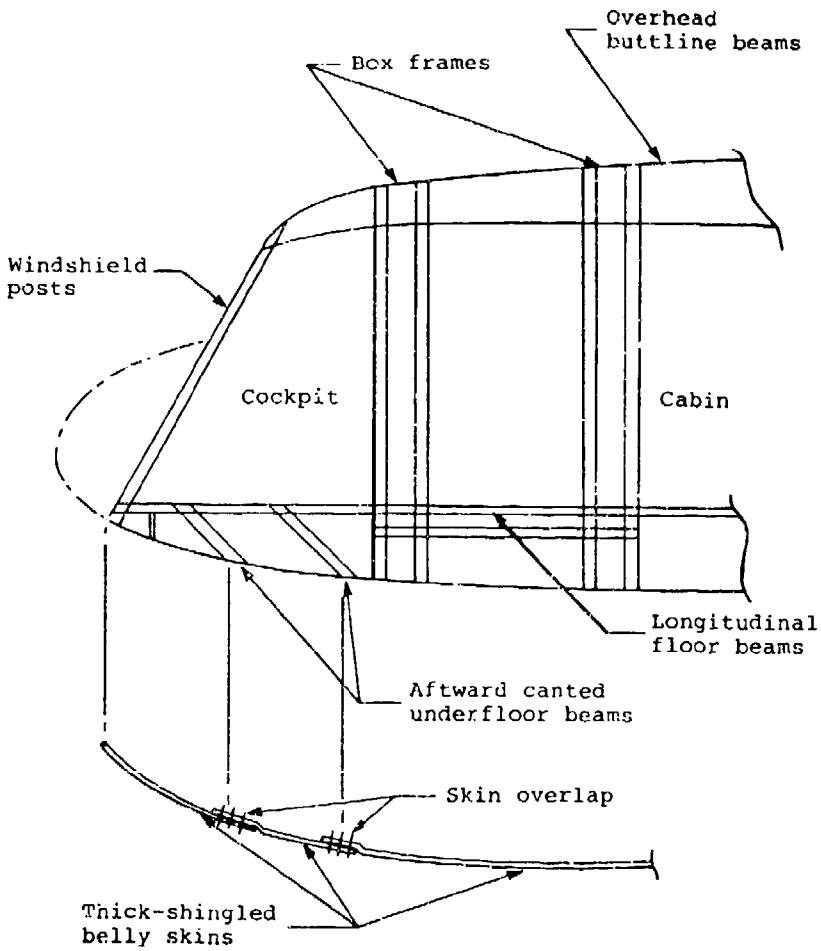

FIGURE 46. FEATURES OF HELICOPTER NOSE SECTION TO PREVENT NOSE PLOWING.

This method for reducing earth scooping increases the deformation strength of the underfloor structure, thus increasing the deceleration levels at the floor level due to vertical velocity components. Therefore, the reinforcement should not be continued back any further than necessary under occupied sections of the fuselage. Modifications to reinforcing structure under occupied regions are presented in Section 6.2.2.2.

Strong structural crossmembers can present abrupt contour changes during deformation, thus forming the lip on the scoop that tends to trap earth. Forward underfloor frame members may be canted aftwards at the bottom to provide an upward load component on the aircraft that tends to prevent, or limit, digging in of the structure. The longitudinal strength of the nose section can be increased by the use of strong continuous structural members running fore and aft in the underfloor section of the aircraft. These beams can be used to support the crossmembers and act as skids to further reduce scooping or digging-in tendencies. Figure 47 illustrates this type of construction.

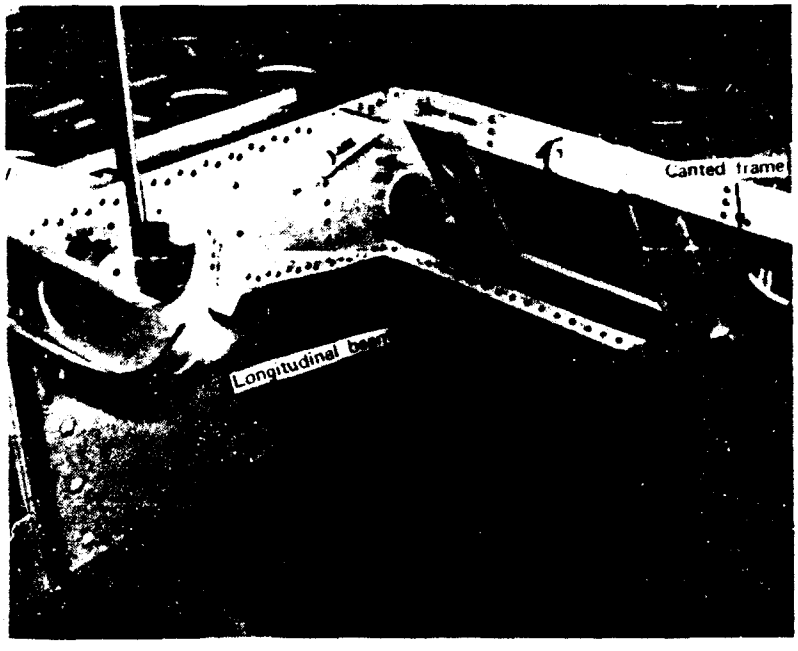

FIGURE 47. TYPICAL UNDERFLOOR CANTED FRAME AND LONGITUDINAL BEAM MEMBER TO MINIMIZE NOSE PLOWING.

In multiengine aircraft, the engine nacelles may present as much of an earth scoop as the nose of the fuselage, and since the engines are often attached to the strong, rigid wing center section, the forces produced by engine earth scooping are transmitted to the fuselage cabin.

The results of full-scale experimental crash tests indicate that longitudinal aircraft accelerations produced by earth scooping can be significantly reduced by the application of the methods discussed above.

6.2.2.4 Energy-Absorption Capacity of Forward Fuselage. In accordance with Section 4 and as illustrated in Figure 48, the fuselage should be designed to preserve a survivable volume in the cockpit at 20 ft/sec and in the cabin at 40 ft/sec for a longitudinal impact.

From a consideration of conservation of energy, the initial kinetic energy of an impacting aircraft must be accounted for in energy dissipated during the deformation of both soil and structure. Therefore,

$$\frac{m_A(v_o^2 - v_f^2)}{2} = U_C + U_S \qquad (13)$$

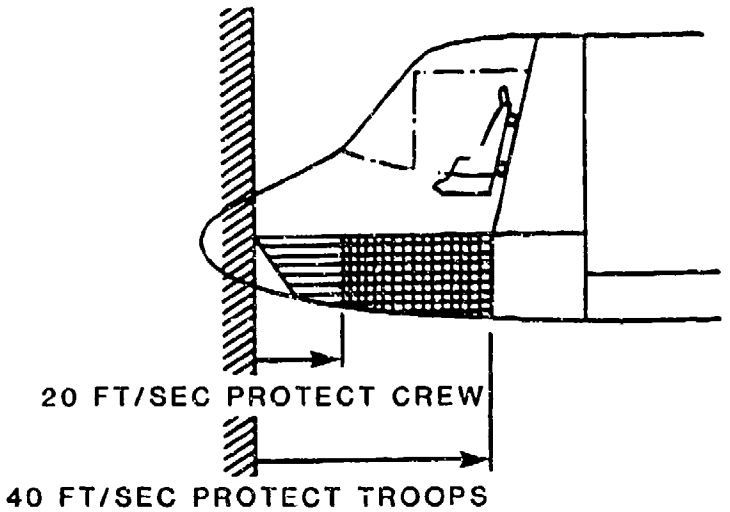

FIGURE 48. LONGITUDINAL IMPACT DESIGN CRITERIA.

where m_A = mass of aircraft

v_0 = initial impact velocity of aircraft

v_f = velocity remaining after impact

U_G = energy dissipated in soil deformation and ground friction

U_S = energy dissipated in structural deformation.

This equation states that the reduction in aircraft kinetic energy must be equal to the energy absorbed by deformation of earth and structure and is simplified by the assumption that there is no change of aircraft mass during the impact.

As a simplified model, the structural energy absorption, U_S, may be expressed as

$$U_S = P_{av}S + U'_S + U_C \qquad (14)$$

where P_{av} = average force developed in collapse of structure forward of the cabin

S = linear deformation (reduction in length) of structure forward of the cabin

U_S' = deformation energy in structure other than in the cabin or structure forward of the cabin

U_C = energy to be absorbed in cabin deformation.

The cabin deformation energy, U_C, represents the quantity of energy absorbed by deformation of cabin structure and may be obtained from Equations (13) and (14):

$$U_C = \left[\frac{m_A (v_o^2 - v_f^2)}{2} - U_G\right] - (P_{av}S + U_S') \qquad (15)$$

This equation for cabin deformation energy is valid if conditions reach or exceed the point of onset of cabin deformation.

Assuming a fixed mass and velocity and ignoring control over energy dissipated outside the aircraft, the factors that are controllable in Equation (15) are P_{av}, S, and U_S'. Consequently, U_C, the energy which must be absorbed in cabin collapse or collapse of the protective shell, may be reduced by:

- Increasing P_{av}, the average crushing force acting during collapse of structure forward of the cabin. P_{av} may be increased by providing a forward structure which will maintain a force as nearly uniform as possible. In addition, P_{av} may be further increased by increasing the maximum force. This latter option is limited, however, by the existing strength of the cabin.

- Increasing the available deformation distance, S, by maximizing the length of the nose on the aircraft.

- Increasing the deformation energy absorbed in aircraft structure other than forward structure or cabin structure.

Application of any of these principles to the airframe design, with a given cabin structural configuration, will make it possible for the aircraft to withstand impact at increased velocity without collapse of the protective shell.

6.2.3 Fuselage Protective Shell

6.2.3.1 General. The fuselage is expected to provide many important functions during a crash, among them:

- Maintaining a livable volume around occupants
- Shielding occupants from contact with outside hazards, such as trees, rotor blades, flying debris
- Providing hard points for attaching seat, cargo, etc.
- Preventing rotorcraft main transmissions from shifting to such an extent that the rotor blades may penetrate occupied areas
- Reacting and distributing point loads from landing gear
- Avoiding rupture of subsystems containing flammable fluid
- Preserving structure around emergency egress openings, to facilitate postcrash egress.

The threat of fuselage collapse under vertical impact may be reduced in any of several ways: first, a transferral of mass from the top of the fuselage to the floor would be beneficial. Second, a general strengthening of cabin structure may be effected including localized strengthening at locations of large concentrations of mass attached to upper structure. Third, elastic energy and plastic energy absorption may be increased at loads less than the collapse load. Fourth, increased energy absorption in the subfloor structure at load levels below the fuselage collapse load further protects against collapse.

The design of floor structure and the floor support structure also has a considerable effect upon the protection offered by the cabin structure as a protective shell. The floor structure should be strong enough to carry the loads which will be applied to it by passenger and cargo restraint systems (see Sections 6.2.6 and 6.2.7) without the need for supports which carry through to the lower fuselage skin and stiffeners. Such supports transfer crash loads applied at the outer fuselage surface directly into the floor. Buckling of the floor produced by such a load transfer can reduce the bending strength of the fuselage and also reduce the effectiveness of restraint systems which depend upon floor integrity. Evacuation of the aircraft can also be impeded by interruptions in the floor surface.

In some situations, such as longitudinal impact with a barrier, the entire fuselage is not expected to remain intact, but rather to progressively crush from the front. In other words, even when partially failed, the fuselage is expected to protect as many of the occupants as possible.

The shape of the fuselage has an inherent influence on survivability. Rectangular cross sections provide more usable interior volume but must be more carefully designed to provide the same crash-resistant characteristics as spherically, cylindrically, or elliptically shaped fuselages. Rectangular-shaped fuselages can provide resistance to rollover after gear failure and

added energy-absorbing structure in an impact with a roll attitude. Figure 49 shows a light observation helicopter shape and component layout advantageous for providing crash impact protection (Reference 67).

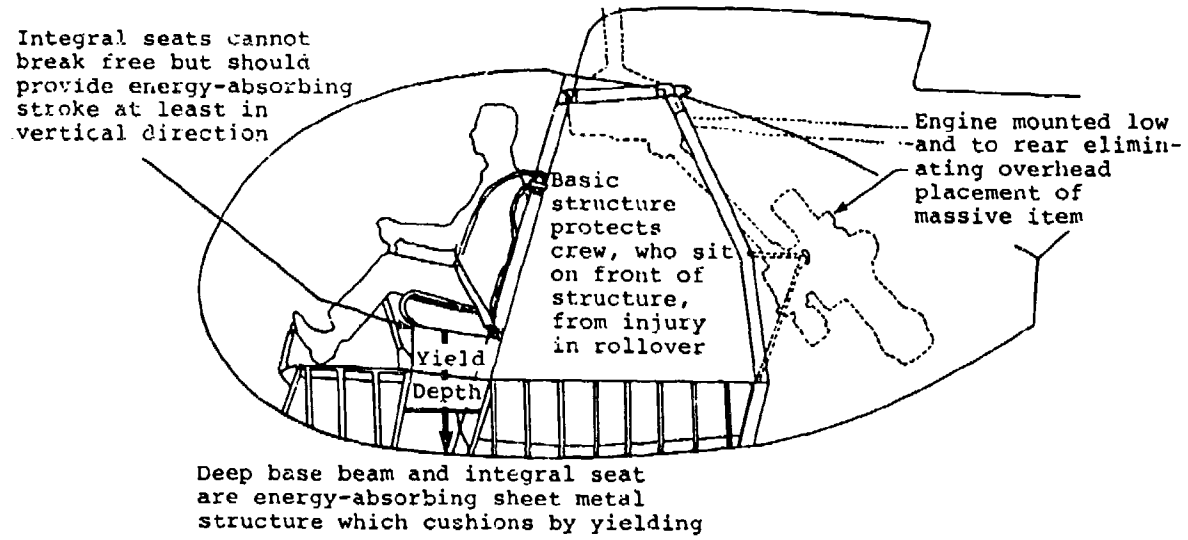

FIGURE 49. OBSERVATION HELICOPTER - LAYOUT OF CRASH-RESISTANT FEATURES. (FROM REFERENCE 24)

Most aircraft crashes occurring at impact angles up to 30 degrees involve a rapid change in pitch attitude to quickly align the aircraft fuselage with the impact surface. The resulting angular acceleration produces a fuselage bending moment which usually causes a compression of upper members of the forward fuselage. This compression is combined with compression of the fuselage due to the longitudinal forces of impact. The result may be a compressive buckling failure.

It is sometimes possible to provide sufficient strength to prevent fuselage bending failure. If this is not practical, it is desirable to determine the probable failure points and to position passengers away from those locations. Cargo tiedown attachments should be designed to prevent loss of cargo restraint, should fuselage bending failure occur.

6.2.3.2 Structural Concepts. The major structural elements of a helicopter designed to satisfy crash resistance requirements are emphasized in Figure 50 for the nose section and in Figure 51 for the cabin/center section. The nose section structure is basically a propped cantilever with the underfloor structure being the cantilever and the props being the windshield posts that extend upward to the transmission support buttline beams. Longitudinal loading is reacted primarily by underfloor beams that resist bending and secondly by windshield posts that transfer loads to the transmission buttline beams. Underfloor frame members and the outer skin assemblies provide lateral stability for the longitudinal members.

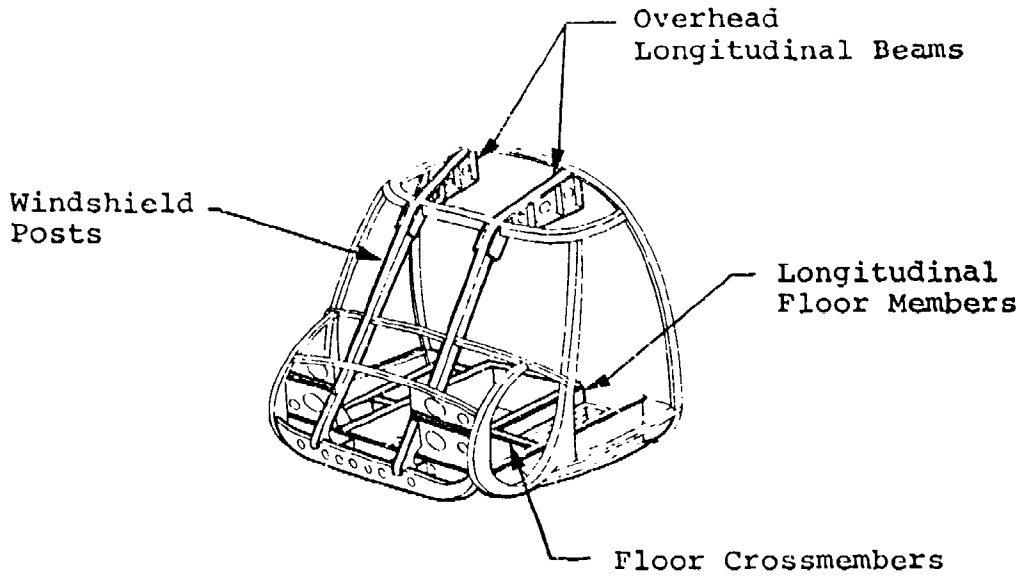

FIGURE 50. LONGITUDINAL IMPACT AND BLADE STRIKE PROTECTION IN NOSE SECTION. THE FIGURE DELINEATES THOSE MEMBERS REQUIRING CAREFUL DESIGN CONSIDERATION.

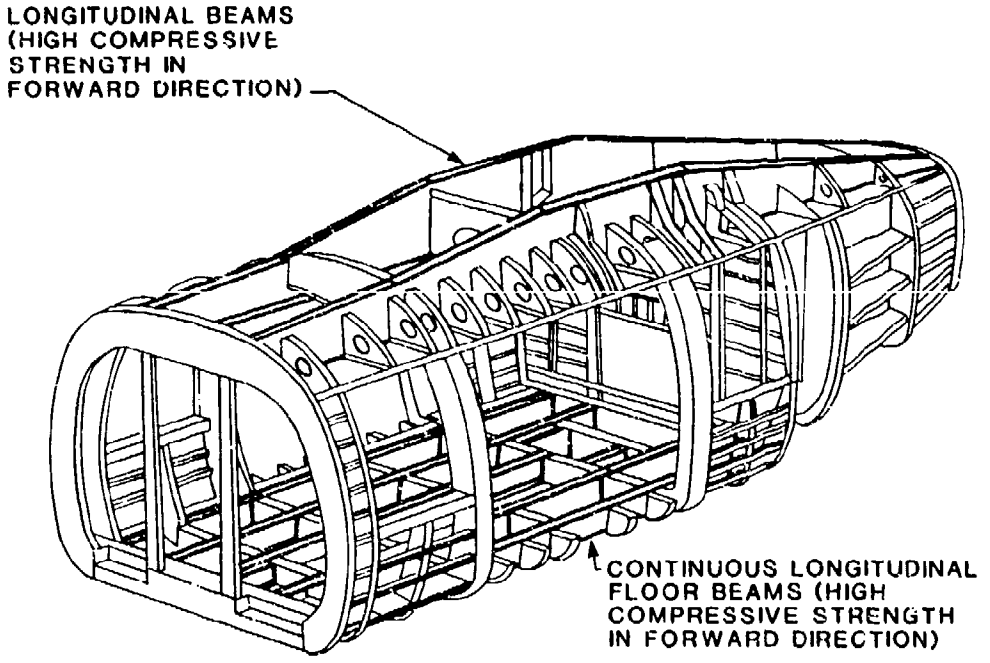

FIGURE 51. LONGITUDINAL IMPACT PROTECTION IN CABIN SECTION.

The cabin structure, by virtue of specific aircraft mission requirements for rapid troop ingress and egress, contains a large area of cutouts necessitating a longitudinal beam system for carrying major loads. In the upper vertical structure, two buttline beams continue into the cockpit section to provide continuous paths for crash loads in the longitudinal direction. Figures 52 and 53 show details of typical beams. Loading at and below the floor level is transferred from the cockpit through the cabin by longitudinal floor beams.

Figure 26, Section 5.3.2, shows a typical structural layout for a single rotor, utility-type helicopter with large mass items mounted overhead and large door cutouts for rapid ingress and egress. To prevent excessive intrusion into the occupied cabin, the support of large mass items is of primary importance. This is achieved by using deep longitudinal buttline beams and built-up box-frame members. The box-frame structure is achieved by adding skin to the inboard and outboard profiles of two adjacent frame members, thus producing a closed-box structure. Such a section is stronger and more stable under compressive loading conditions than two individual frame sections acting together. Figure 54 shows typical sections through box frames of this type; section variation can be tailored to the anticipated loading conditions at any point in the structure. When using this type of construction, care should be taken to provide adequate inspection capability in enclosed areas where corrosion may occur.

Alternatively, adequate protective coating must be used and wet assembly techniques employed to provide protection against corrosion for time periods equivalent to major structural overhaul intervals.

Widely spaced frames that are skinned on the inside profile may be fitted with detachable skin panels to allow the location of equipment and system elements in the space between the frames. However, only nonhazardous equipment should be located in such areas; combustibles and potential ignition sources are not to be installed in such locations.

The load-carrying members indicated for vertical and rollover protection in Figure 26, in general, provide protection against lateral impacts and must be designed for this function. Rollover protection must be adequate to support the aircraft during rotation and also after the aircraft has come to rest in any attitude.

Figure 55 indicates one approach to providing the primary load-carrying structure needed to resist the effects of a post-impact rollover. The structural elements needed for similar protection in the cockpit area are emphasized in Figure 50.

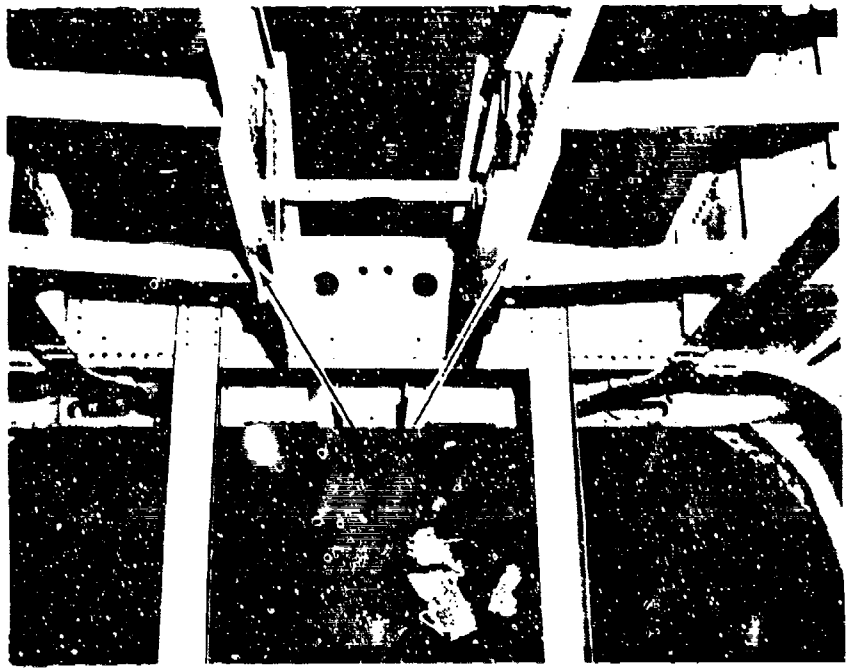

FIGURE 52. TYPICAL LONGITUDNAL BEAMS ADJACENT TO COCKPIT FOR LONGITUDINAL CONTINUITY OF OVERHEAD STRUCTURE.

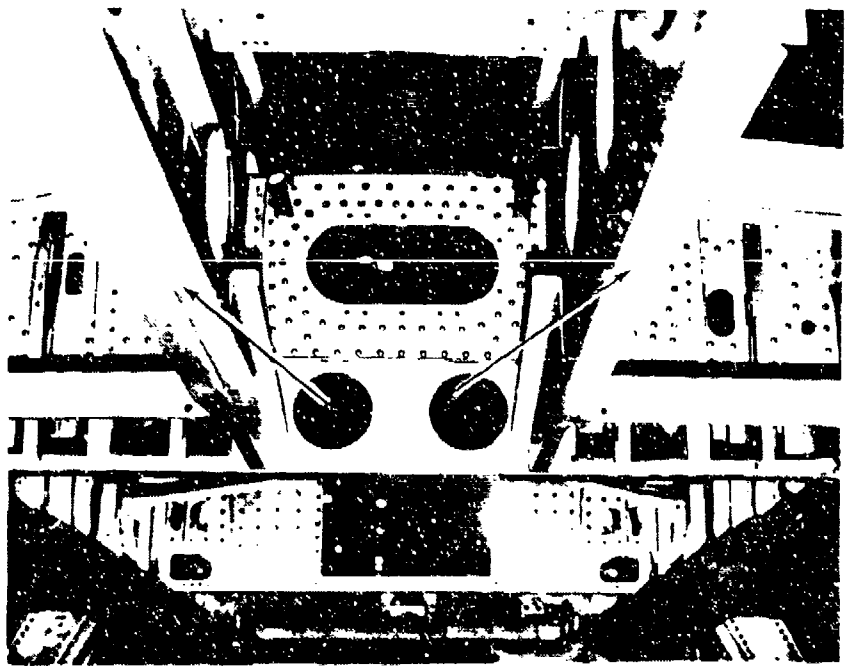

FIGURE 53. TYPICAL FULL-DEPTH LONGITUDINAL BEAMS FOR OVERHEAD SUPPORT OF LARGE MASS ITEMS AND LONGITUDINAL CONTINUITY OF STRUCTURE.

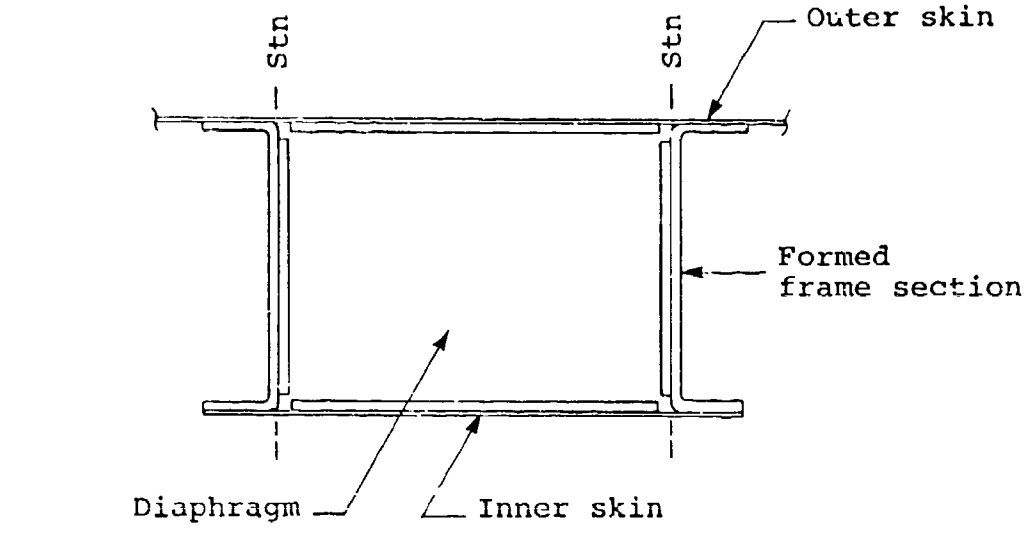

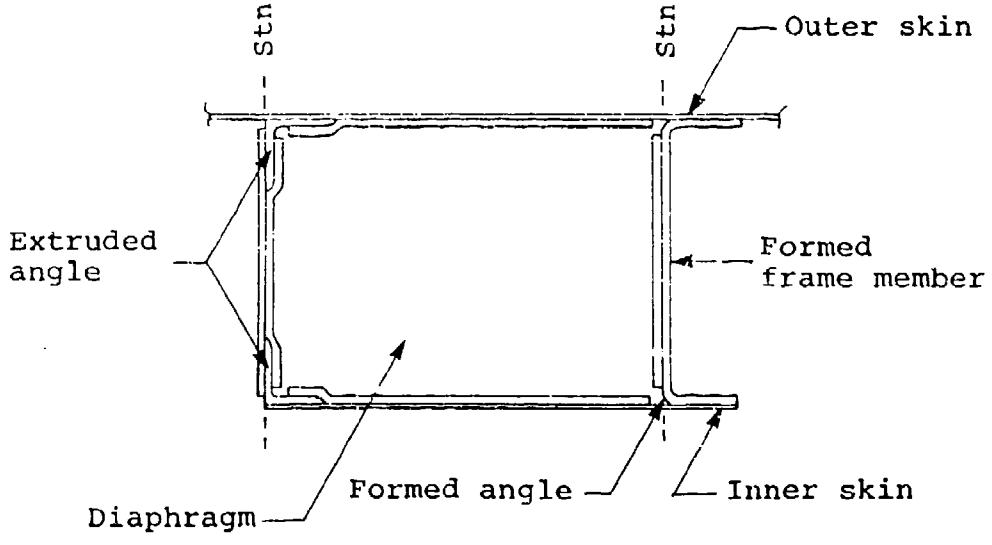

FIGURE 54. EXAMPLES OF CLOSED BOX-BEAM FRAME SECTIONS.

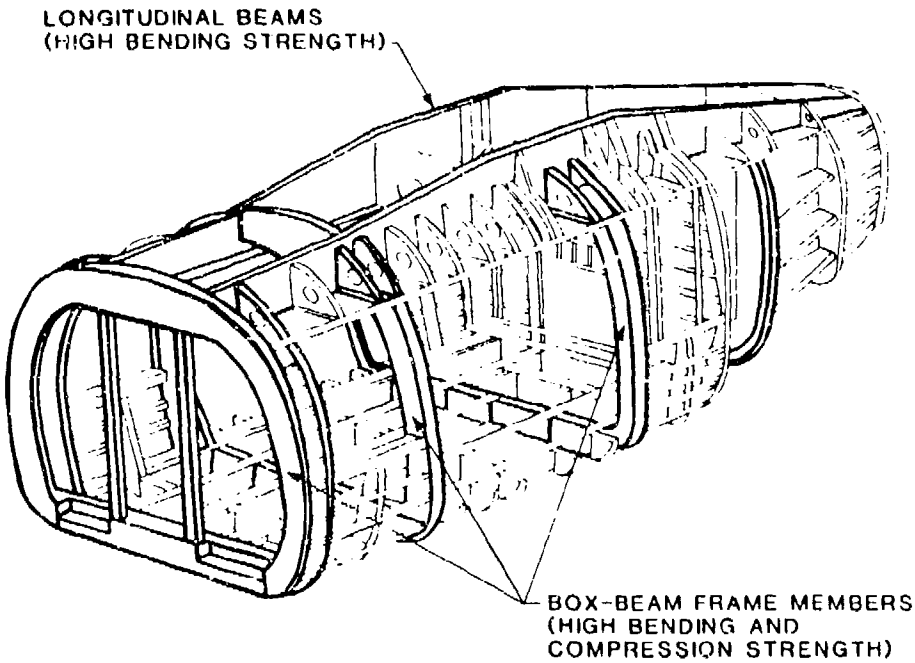

FIGURE 55. PROTECTION FROM OVERHEAD MASS AND ROLLOVER IN CABIN SECTION.

Rollover protection in the cabin section is provided by the buttline beams, longitudinal floor beams, and main box frames. The cockpit of the helicopter shown in Figure 26 is protected by a mesh of structural elements, the majority of which are door and transparency support members. These are shown in Figure 50; details of the sections and materials used are shown in Figure 56. Reference 68 contains more detailed information on lateral rollover protection.

Prevention of main rotor blade entry into the cockpit is an extremely difficult task due to the conflicting requirement of good pilot visibility. Structural members that can deflect a main rotor blade will have to be large in size, thus restricting the pilot's visibility. A roll cage type cockpit that could minimize blade intrusions would include large structural beams overhead and on the outboard sides. High-strength windshield posts and door posts that attach the overhead structure to the floor beams provide the remainder of the roll cage.

Figure 57 shows details of the overhead protection provided by structural continuity of the windshield posts and longitudinal beams mating with the cabin section.

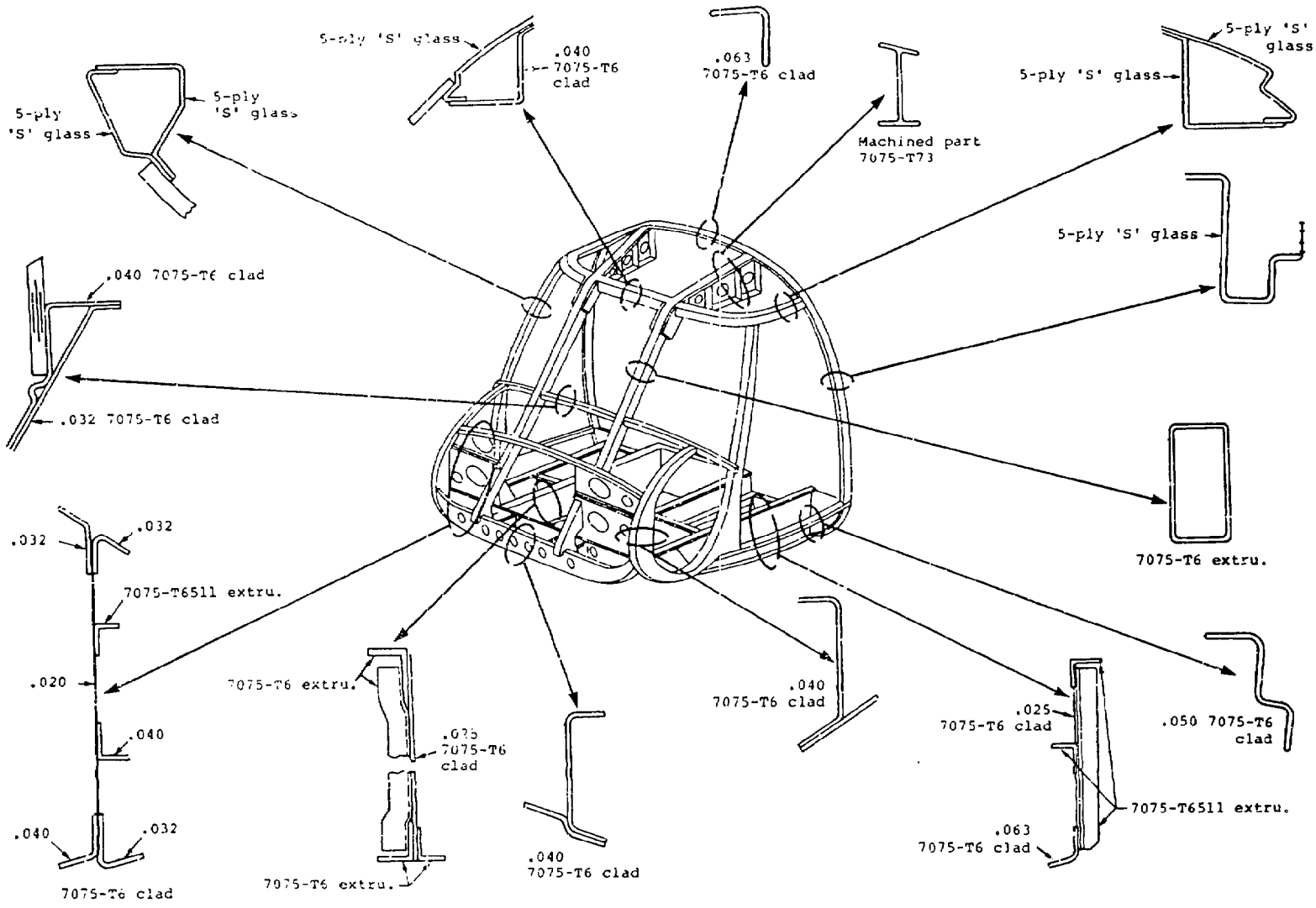

FIGURE 56. TYPICAL STRUCTURAL SECTIONS FOR NOSE SECTION.

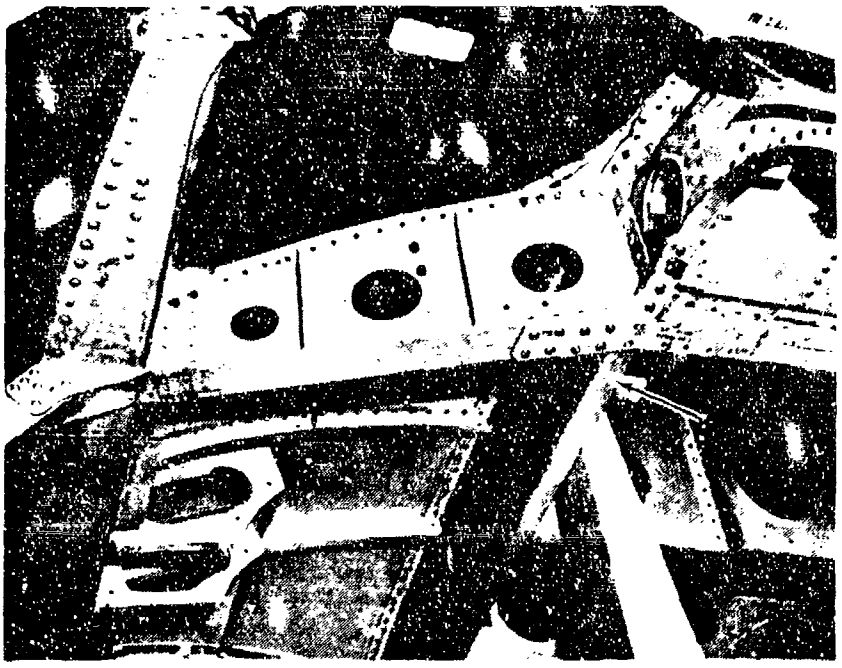

FIGURE 57. TYPICAL COCKPIT OVERHEAD LONGITUDINAL BEAM MEMBER.

High-strength deflector beams might be installed forward of the windshield rather than as windshield posts, as shown in Figure 58. Moving the beams further away from the pilot will minimize the pilot's visibility restriction. Such external deflector beams could also deflect wires up over the cockpit.

6.2.3.3 Emergency Exits. The structural framing should be rigid enough to prevent deformation to such a degree that emergency exits are inoperable. It is desirable that the emergency exit closure be expelled or released by the structure when structural damage does occur.

Exits should be placed in locations which are favorable for rapid egress. If components near exit locations are likely to be damaged to the extent that the exit will be blocked, allowances should be made to compensate for it. An example is the location of an emergency exit near a landing gear attachment. Upon vertical impact, the landing gear could be driven upward into the floor structure, causing severe distortion of the floor structure. Therefore, the floor should be reinforced near the exit or the relative locations changed.

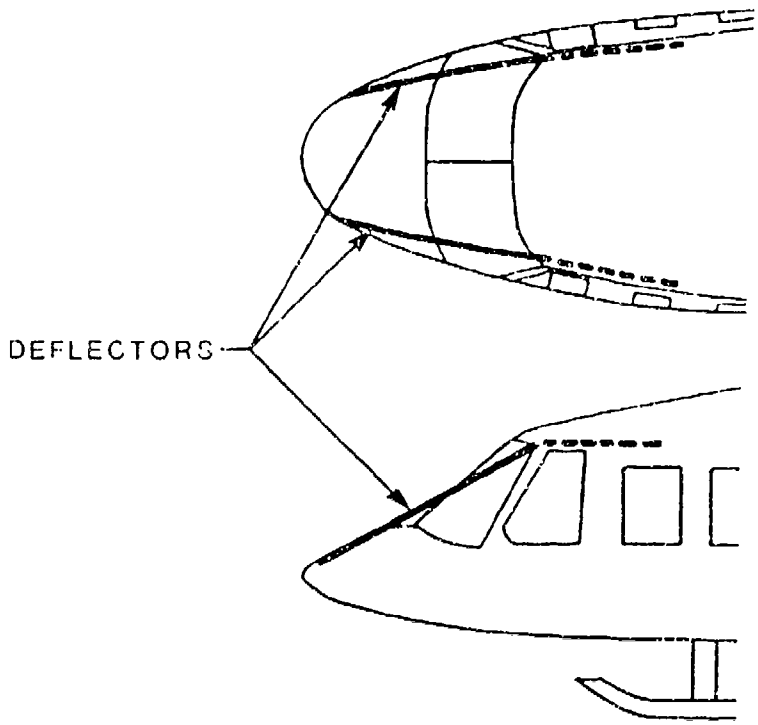

FIGURE 58. EXTERNALLY MOUNTED BLADE STRIKE DEFLECTORS.

To prevent collapse of emergency exits, the hatches could be reinforced with a filament-wound composite tube that would provide the necessary strength and stiffness. This local reinforcement could also serve as a framing member that would redistribute the airloads around the cutouts.

6.2.4 Engine Mounts

For Type I (light fixed-wing) aircraft, engine mounts should be designed to keep the engines attached to the basic structural members supporting the mounts (nose section, wing, aft fuselage section, etc.) under the crash conditions cited in Table 2, even though considerable distortion of the engine mounts and/or support structure may occur. The basic structure supporting the engine should fail or separate before engine mount failure occurs. This will reduce the fire hazard and the localized damage to other structures which occurs when engines break free and are traversed by the aircraft.

For Type II (rotary-wing, including tilt/prop rotor) aircraft, mounting of engines, transmissions, fuel tanks, rotor masts, and other high-mass items should be designed to prevent their displacement in a manner that would be hazardous to the occupants under the crash conditions cited in Table 2. The transmission and rotor hub should not displace in a manner hazardous to the

occupants during the following impact conditions: (1) rollover about the vehicle's roll or pitch axis and (2) main rotor blade obstacle strike that occurs within the outer 10 percent of blade span assuming the obstacle to be an 8-in.-diameter rigid cylinder.

6.2.5 Fuel Tank Installation

MIL-T-27422 (Reference 69) and Volume V define the requirements for the design and installation of crash-resistant aircraft fuel systems.

Tank location is an important factor in minimizing postcrash fire hazard. The location must be considered with respect to occupants, ignition sources, and probable impact areas. Greater distance between occupants and the fuel supply tends to increase potential escape time. The tank also should be separated from probable ignition sources. Whenever possible, tanks should not be installed in or over the engine compartment, the battery, or other primary ignition sources. An extremely important consideration is the location of tanks with respect to probable impact damage. The possibility of penetration by aircraft hardware, such as landing gear, or ground obstacles require that the tank be located where there is minimal probability of penetration.

Tank installations must provide fuel containment for high-G impacts. There should be sufficient distance between the belly of the aircraft and the tank to allow for fuselage crushing and to minimize the potential for tank wall penetration by rocks, tree stumps, posts, etc. Fuel tank supports and system hardware attachments should be designed to allow major structural deformation without tearing the tanks. Structurally generated jagged edges in the area of the tank should be minimized. Fuel tanks should be regular in shape, cylindrical or rectangular, to minimize the effects of internal pressure due to structural compression and to reduce the propensity to snag on structural elements.

Structural deformation around the tank should not exceed the compression capability of the fuel tank under survivable crash impact conditions. Large mass items should be located away from fuel tanks wherever possible to prevent excessive compression of tank volume and/or penetration.

In addition, tank distortion due to inertial loads acting on the contents should be carefully considered. Relatively large fuel masses may cause tank bulging. Extensive damage to adjacent structure and compromised fuselage integrity may result. This effect is discussed further in Reference 70.

Figure 59 shows a typical interior support structure for a fuel tank. Closely spaced frame members are interconnected to provide a uniform support matrix to minimize tank compression and distortion under severe impact conditions.

6.2.6 Seat Installation

Three major categories of seats are used on U.S. Army helicopters: crew (pilot/copilot), gunner, and troop seats. Crash resistance criteria in MIL-STD-1290 require that each seat occupant be provided with a survivable

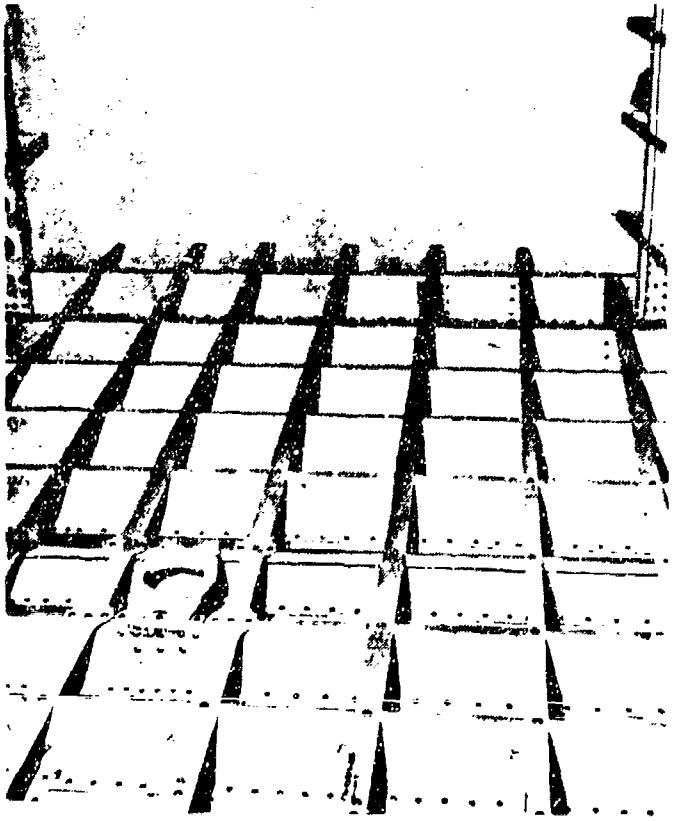

FIGURE 59. TYPICAL INTERIOR SUPPORT STRUCTURE FOR FUEL CELL.

environment when the aircraft is subjected to the design crash impact conditions. To meet this requirement, energy must be absorbed in the vertical direction and living space maintained as the total aircraft system is decelerated. Seats must act as part of the decelerating system and complement the landing gear and deforming fuselage structure. Ideally, each occupant must be brought to a state of rest without incurring debilitating injury that might preclude timely egress. Various energy-absorbing seat concepts are illustrated in Figure 60.

Whichever seat type is used, the total system must be considered when the seat-to-structure interface is evaluated. As extreme examples, if the landing gear and structure could always provide vertical deceleration near the 14.5-G human tolerance limit, the seat-to-structure loading would be moderate, and less seat energy absorption would be needed. Alternatively, if the landing gear and structure combination were either too rigid or too flexible, the seat would need to provide the major portion of the protection to the occupant, and a much longer seat stroking distance would be needed.

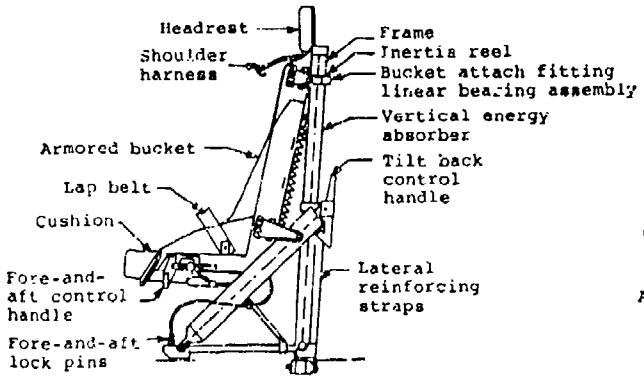

(a) Crewseat, armored bucket, floor-mounted

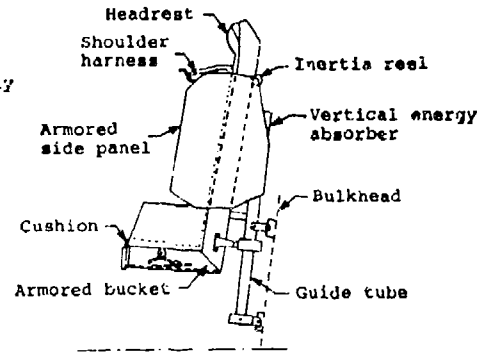

(b) Crewseat, armored bucket, bulkhead-mounted

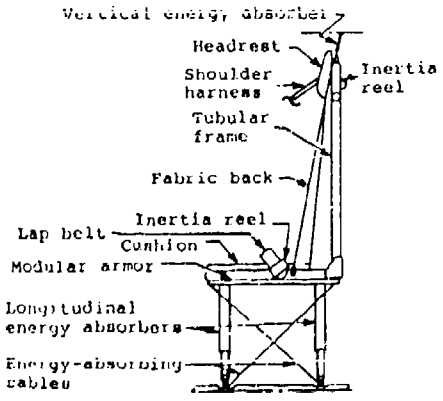

(c) Gunner seat, side-facing frame construction

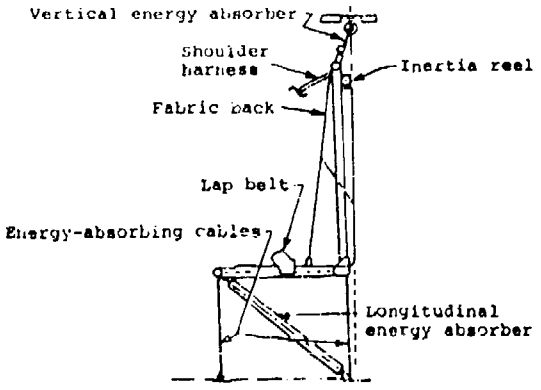

(d) Troop seat, forward-facing, frame construction

FIGURE 60. TYPICAL CRASH-RESISTANT SEAT CONFIGURATIONS.

When assessing the seat installation, it is necessary to know the design impact conditions, the total energy content, and the predicted energy-absorption capability of the landing gear and primary structure.

Where crash-resistant stroking seats are used, the increased occupant strike envelope due to the seat stroke must be considered. The strike envelope is dependent upon whether the seat has the capability for uniaxial, biaxial, or triaxial stroking. Wherever possible, uniaxial stroking in the vertical or near vertical direction is recommended for this reason.

Because availability of energy-absorbing stroke in the vertical direction is mandatory, items that surround the seat, such as consoles and collective controls, should be placed to permit that stroke, even in the presence of forward and lateral displacement. The required clearance will vary depending on the specific seat design and whether the lateral and longitudinal motion results from intentional energy-absorbing stroke or from elastic or plastic deformations of the structure. Three inches of dynamic lateral deflection is common even in an elastic structure designed for vertical stroke alone.

A minimum of 12 in. of vertical seat stroke is recommended (from the lowest vertical adjustment position), as discussed in Volume IV. Because of the desired positioning of the seat in the aircraft, 12 in. may be difficult to provide between the seat bucket and the floor. In these cases a hole, or well, in the aircraft floor should be provided under the seat. Whenever possible, at least 1 in. of clearance should be maintained between the outer edges of the bucket and the innermost parts of the sides and front of the well. Nets or frangible membranes should be employed to prevent flight equipment or personal articles from being stored in the well, where they could interfere with seat stroking.

The underfloor or bulkhead structure, depending on where the seat mounts, and the aircraft attachment hardware should be designed to withstand the loads and moments generated by the seat. The loads and moments should be those applied by the specific seat for all design loading conditions and for all positions in the aircraft. In other words, the design of the aircraft structure and the seat should proceed concurrently, with reaction loads and moments calculated for the specific seat used in designing the aircraft structure. The highest floor reaction loads invariably result from combined loading conditions, that is, dynamic tests 1 and 2 per MIL-S-58095 (Reference 71) and MIL-S-85510 (Reference 72).

6.2.7 Cargo and Equipment Retention

6.2.7.1 General. Cargo should be restrained to enhance survival of the crew and passengers in survivable crashes. To determine the types of cargo-restraining devices needed for U.S. Army aircraft, it is important to consider the type of aircraft, the probable crash modes, and the type of cargo being carried. Crew and passenger locations relative to cargo and cargo tiedown provisions are also significant.

The type of aircraft and its predominant crash mode should dictate the selection of appropriate restraint criteria. The types of cargo to be flown and the restraint criteria will determine the available tiedown clearance. An awareness of aircraft structural response to impact will help to identify

realistic clearance envelopes for specific personnel locations. Consideration should also be given to restraint integrity in the event of local structural deformation, discontinuities and/or secondary or tertiary impacts.

6.2.7.2 Cargo and Equipment Retention Guidelines. Cargo should be restrained to longitudinal loads of 16-G peak with a longitudinal velocity change of 43 ft/sec. Forward and lateral strength deformation characteristics should be in accordance with those indicated in Figures 61 and 62, respectively. If the structure of the fuselage and floor is not strong enough to withstand the cargo crash loads, load limiters should be used to attenuate the loads transmitted to the structure. If load limiters are used, restraining lines should be of a material with low-elongation characteristics to ensure the most efficient energy absorption. Nets used to restrain small bulk cargo should be constructed of material with high stiffness characteristics, in order to minimize dynamic overshoot. Restraining lines without load limiters used for large cargo (3-ft^3 or more) longitudinal restraint should be so arranged that maximum load in all lines occur as simultaneously as possible. Restraining lines having different elongation characteristics should not be used on the same piece of cargo.

6.2.7.3 Cargo Categories and Pallet Systems. U.S. Army cargo has traditionally been divided into two categories, based primarily on size, as listed in Table 5 (Section 4.3.4). This includes small cargo which is usually transported stacked on a pallet and large or bulky cargo which can best be restrained individually by cables, ropes, or chains that are attached to the floor or sidewalls of the aircraft.

Both categories of cargo (including, for example, packs, rifles, rations, and wheeled or tracked vehicles) will often be carried along with troops. Crash protection should then be provided for the troops as well as the crewmembers. Where aircraft are dedicated to cargo shuttle missions, cargo crash restraints should be provided primarily for flight crew protection.

Small cargo (up to approximately 3 ft^3 in size) is routinely transported on wooden Army pallets to expedite handling by fork lifts. Army warehouse pallets provide no restraint; cargo may be loose or only lightly secured to the pallet by banding (a 1-G restraint). These loads can best be restrained by nets attached to aircraft floor fittings.

Cargo netted to 463L pallets (References 73 and 74) are restrained only to USAF flight load criteria (Reference 75). The USAF cargo tiedown criterion requires only 3 G forward. Another deficiency of the present 463L net, however, is its elasticity. The designer should be aware of the basis for the different USAF criteria. Analyses of USAF accidents have suggested that the risk of passenger fatality above the 3-G forward restraint criteria is statistically rare (Reference 76). The same is not true for Army aircraft.

Both pallet systems must be given additional restraint to meet U.S. Army crash resistance criteria.

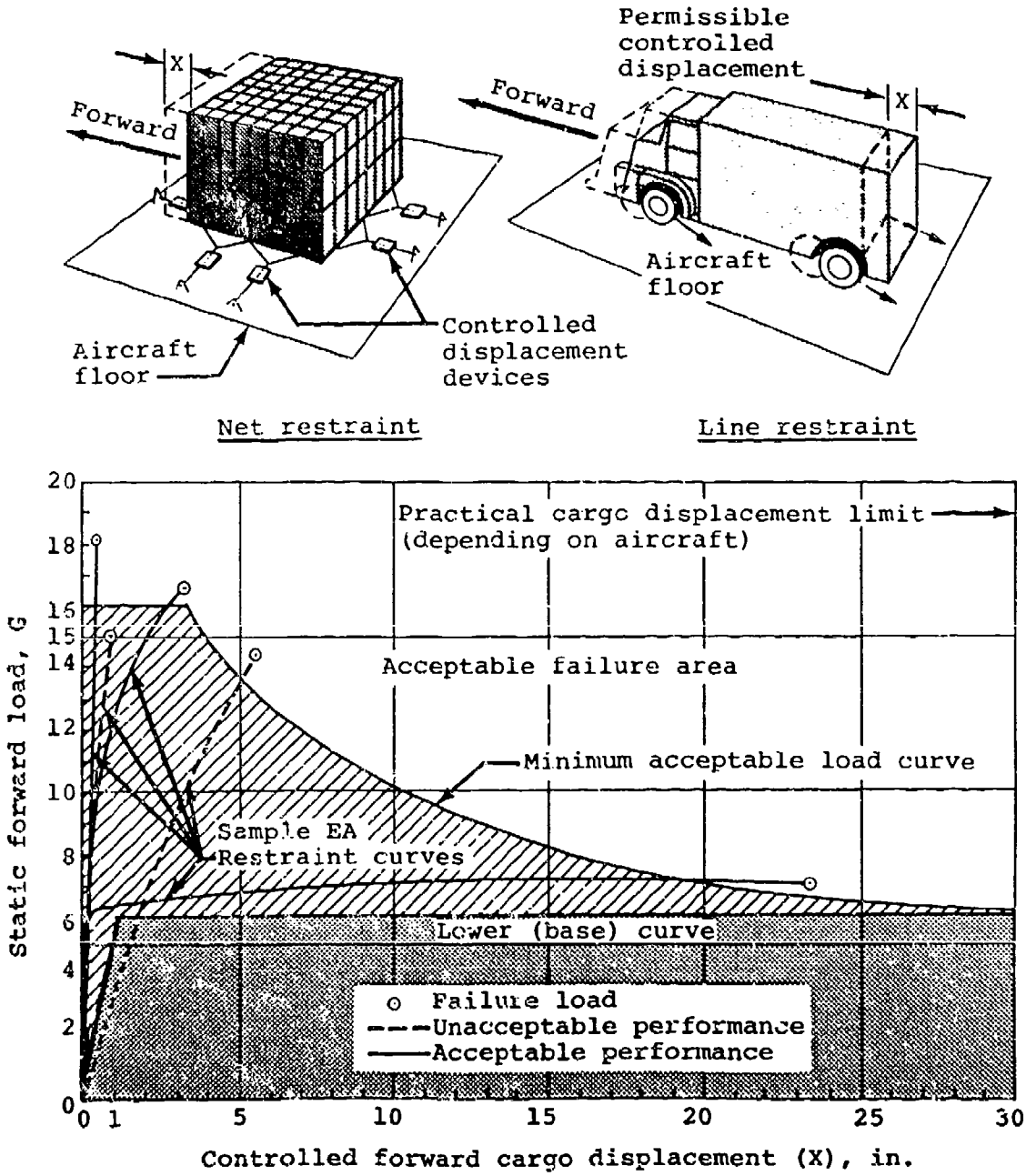

FIGURE 61. LOAD-DISPLACEMENT REQUIREMENTS FOR ENERGY-ABSORBING CARGO RESTRAINT SYSTEMS (FORWARD LOADING OF ROTARY AND FIXED-WING AIRCRAFT).

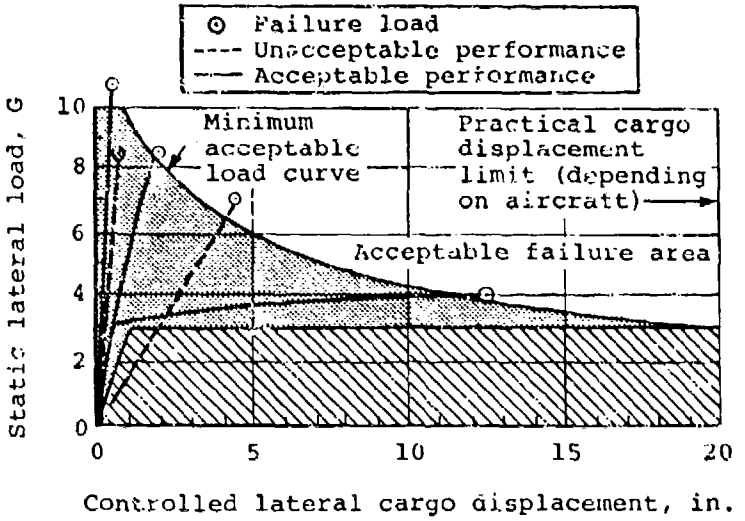

FIGURE 62. CARGO LATERAL LOAD-DISPLACEMENT REQUIREMENTS.

6.2.7.4 Strength. Cargo carried alongside, forward, or aft of troops should perhaps also be restrained to the same G level as are the seats. However, the weight of a restraint system capable of keeping a maximum cargo load in place at such load levels would be high. Several factors other than the expected floor pulses affect the retention strength level required for cargo, in particular the type of cargo, where it is located, and how it is restrained in the aircraft.

Most small cargo probably will be restrained by a single net stretched over any number of items. Therefore, statistically, a net designed for a given load will be loaded to a lower value in most accidents. Furthermore, failure of a cargo's net restraint is not likely to be as large a threat to human survival as the failure of an occupant's seat restraint would be. For example, failure of a single net midway in a row of nets would not become lethal until other nets also failed. Therefore, for practical reasons--i.e., the low actual probability of injuries caused by displaced cargo and the structural problems involved in restraining cargo to levels equal with personnel restraint--it is concluded that the cargo restraint level can reasonably be less than that for occupants.

In the case of large cargo carried behind troops, the above reasoning does not apply. However, a detailed cargo restraint study conducted for the U.S. Army (Reference 77) indicates that most items of large cargo are carried outside the helicopter by sling.

6.2.7.5 Energy Absorption. The use of load limiters for cargo restraint is recommended, provided the cargo cannot stroke into space occupied by personnel. For the aircraft 16-G, 43 ft/sec triangular cabin pulse calculations have been made to show the required restraint G level and the

corresponding stroke for load-limiting restraint systems. The required G-level-versus-displacement relationship, shown in Figure 61, results from minimizing the restraint systems' structural strength (and hence, their weight) and establishing an acceptable load displacement. These results neglect any restraint system elasticity or longitudinal friction.

Recommended performance goals for such load-limiting restraints are shown in the forward longitudinal load-versus-displacement curve for the forward direction (Figure 61) and the lateral load-versus-displacement curve for the lateral (Figure 62).

To meet the necessary energy absorption requirements, restraint forces must rise rapidly to the left of and above the lower base curve, terminating above the minimum acceptable load (ultimate strength) curve.

Similar load-limiter calculations have been made for the lateral direction, and the resulting values are shown in Figure 62. The lateral strength requirements are based on a velocity change of 21 ft/sec and a 10-G triangular pulse.

Figure 63 (Reference 78) shows the results of tests on two load-limited experimental Navy systems, each having different elastic deformation characteristics.

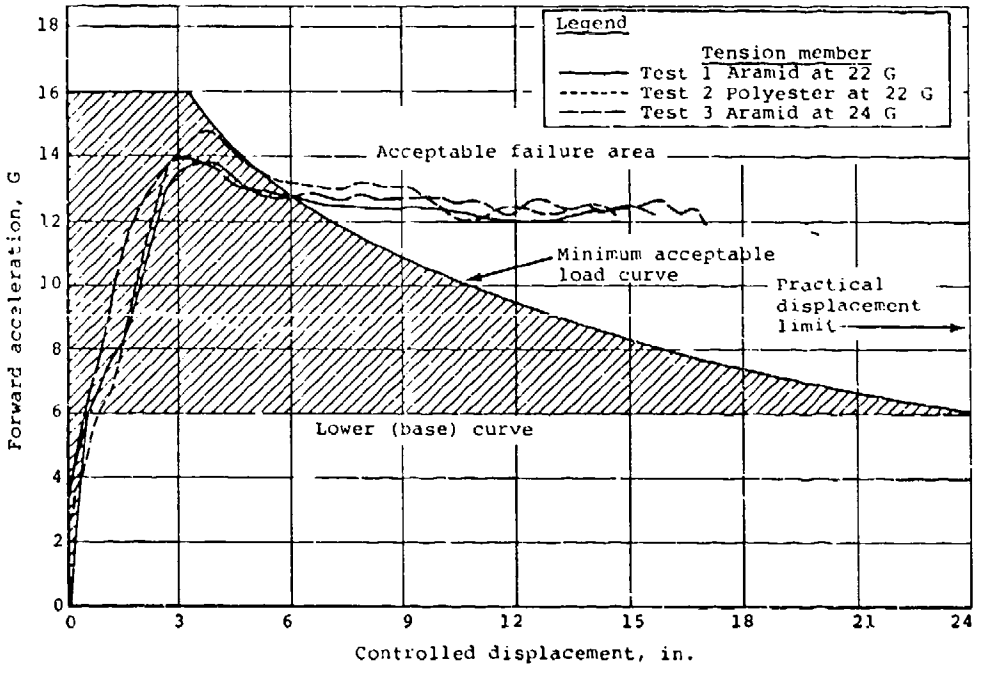

FIGURE 63. RESULTS OF INTEGRATED CARGO RESTRAINT/CRASH SIMULATION TESTS USING ENERGY ABSORBERS AND LOW-ELONGATION TENSION MEMBERS AND FORWARD LONGITUDINAL LOAD-DISPLACEMENT REQUIREMENTS. (FROM REFERENCE 78)

Identical metallic load limiters were used in all tests. The first and third tests employed an aramid, low-elongation restraint device (tension member), and the second test used a polyester restraint (approximately double the strength of the aramid capability to achieve equivalent strain).

Reference 79 describes a design study conducted to identify an advanced cargo restraint system for the Navy Grumman C-2A aircraft. The NADC-sponsored study explored numerous possible tiedown configurations and specific energy absorber and attaching tension member requirements. Energy absorbers considered for the application included the rolling helix, the inversion tube, and the wire bender. In addition to metal-deforming devices, two nonmetallic devices were considered: the plastic extruder and tear webbing. The wire bender (Figure 64) was selected as the optimum design for this application, based primarily on size and weight. For tension members used to attach the energy absorber to the load, both Kevlar and overstrength (low-elongation) polyester were considered. The Kevlar was identified as preferable, based primarily on greater and more constant stiffness.

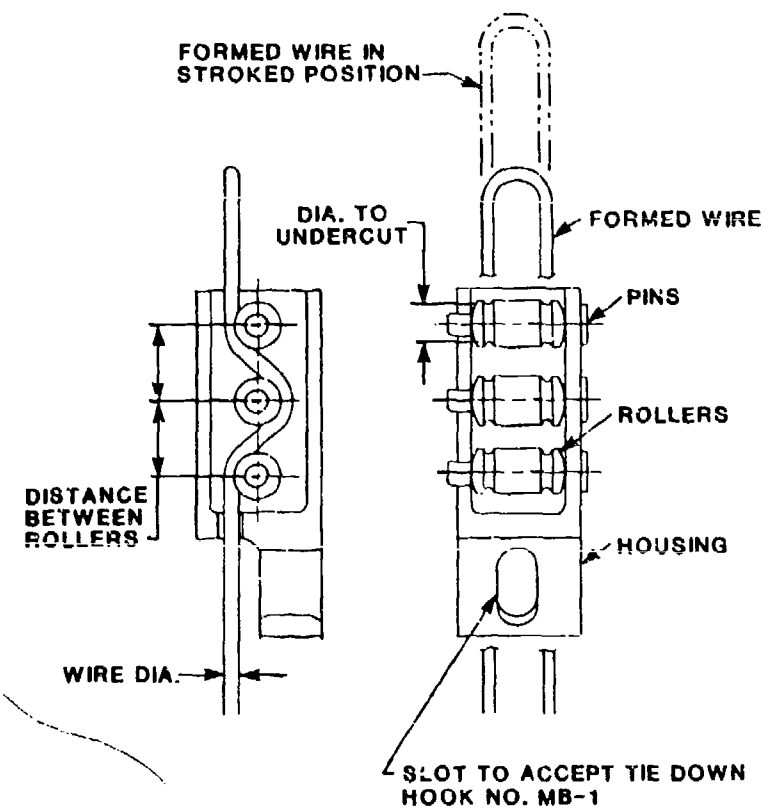

LOAD LIMITER WITH WIRE STORED OUTSIDE HOUSING

FIGURE 64. CARGO RESTRAINT LOAD LIMITER.

The selection of design load levels for load limiters is important to ensure stroking and to protect the aircraft floor tiedowns from ultimate load failure, as evidenced by the results of the U.S. Army/NASA cargo experiment crash test of a CH-47C helicopter (Reference 80). Floor attachments failed as a result of two factors:

- Limiter design load level was less than 2 percent below fitting ultimate strength.
- Inadequate consideration was given to the variability in both the limiter loads and the tiedown fitting strengths.

A load-limiter design that is too conservative, however, is counterproductive, due to longer stroke requirements. This may mean that higher fitting strengths should be considered for new aircraft designs and that old aircraft fittings should be upgraded. Load-limiter attachments and support structures should be designed with a load factor of at least 1.25. Even 1.33, as used in the FAA requirements, may not be too high to cover the variations of performance and strength.

The design strength values for cargo along all axes of loading are summarized in Table 9. The aftward and upward loads in Table 9 are based on expected rebound loads of approximately 30 percent of the peak input values. Hardware designs should not allow disengagement of the restraint during a crash. Restraints usually slacken in the time period between initial impact loading and rebound, and a restraint hook without a keeper can become disengaged.

TABLE 9. CARGO RESTRAINT LOADS AND DISPLACEMENT REQUIREMENTS

Item No.	Load Direction (With Respect to Floor)	Restraint Load	Controlled Displacement
1	Forward	See Figure 61	See Figure 61
2	Aftward	5 G	No requirement
3	Lateral	See Figure 62	See Figure 62
4	Downward	16 G	No requirement
5	Upward	5 G	No requirement
6	Forward and Lateral (Combined)	See Figure 61	See Figure 61
		4 G	No requirement

The 16-G downward loading shown in Table 9 is recommended to ensure that the cargo does not significantly crush the floor, and perhaps destroy the longitudinal restraint for personnel or cargo. This requirement should not be difficult to meet for the net-restrained bulk cargo because this cargo will probably be stacked on pallets that will assist in load distribution. Shoring, however, will be required to prevent floor penetration by wheeled vehicles. Deformation of the floor under the wheels is permissible so long as it does not result in loss of restraint. Combined forward and lateral loads are considered realistic; Item 6 in Table 9 is included to ensure that the system will not fail under this type of loading.

Displacement requirements are not suggested for the aftward, downward, and upward loads shown in Table 9, because these loading directions are not considered to be as potentially hazardous as the loads in the forward and lateral directions. Upward restraint is usually not a problem since all restraints used act in unison for this direction.

For personnel located aftward of the cargo, a buffer spacing to allow for restraint system elasticity under the 5-G loading should be considered. Normal preload is in the range of only 150 to 350 lb; therefore, cargo movement in response to an aftward 5-G rebound load can be expected.

6.2.7.6 Design. Nets should be designed to restrain the small (bulk) cargo up to the specific loads shown in Table 9 with a minimum of elongation to reduce overshoot. Stiff webbing materials such as polyesters and aramids should be used. Their relative elongation and weight advantages over nylon are shown in Table 10 (Reference 78). Present disadvantages affecting the adoption of aramid fibers for tension member application are cost, low abrasion resistance, and fabrication technique development.

TABLE 10. CARGO NET MATERIALS - RELATIVE CHARACTERISTICS

Webbing Fibers	Elongation at 5,000 lb (percent)	Weight (lb)	Breaking Strength (lb)
Nylon	7.5	3.0	1.1
Polyester (Dacron)	2.0	5.9	1.8
Aramid (Kevlar)	1.0	1.0	1.0

An example of an energy-absorbing cargo enclosure that was designed to replace an existing metallic, non-energy-absorbing cargo cage is shown in Figure 65 (Reference 81). The lightweight, flexible, energy-absorbing cargo enclosure was designed for a crash pulse requirement of 17 G and a change in velocity of 60 ft/sec. The new stowable structure consists of fore and aft barriers and side nets fabricated of Kevlar webbing tension members and ballistic membranes to contain small objects. The forward barrier uses 12 load limiters (Reference 77).

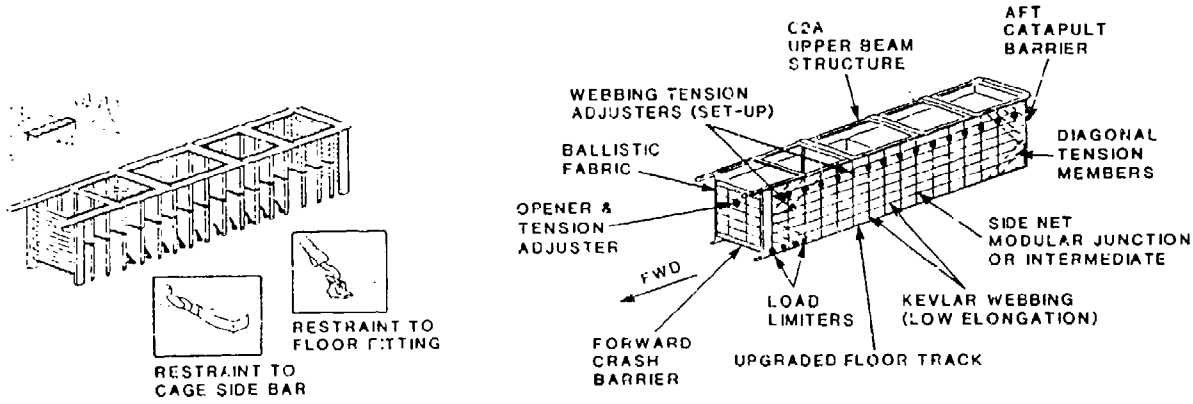

FIGURE 65. ENERGY-ABSORBING RESTRAINT SYSTEM DESIGNED TO REPLACE EXISTING METALLIC CARGO CAGE.

An example of a cargo barrier net using eight load limiters is shown in Figure 66. The eight straps attached to the four corners of the barrier net have wire bending load limiters as shown in Figure 67. Crash test results with these devices are described in Reference 80.

Nets should be designed for the most critical loading conditions, i.e., a high stack with small boxes. Such a loading would tend to cause a larger diaphragm action on the net as the individual boxes slide over each other. More concentrated loads may be encountered in restraining palletized loads on floor rollers.

6.2.7.7 Cable, Rope, Strap, or Chain. Large cargo of the type outlined in Table 5 can be secured most easily by cables, straps, ropes, or chains (lines). In cases where the use of load-limiting devices is not possible, retaining lines for the longitudinal direction should be arranged to simultaneously attain the maximum load in all lines. A combination of fabric ropes and steel cables should not be used on the same piece of cargo because of the difference in their elastic stiffnesses. Also, symmetrical restraint configurations should be used to avoid overloading individual tiedowns and, eventually, failing the system (Reference 82).

With load-limiting devices, it is desirable to use metal cables or other low-elongation tension members stressed below the yield point. Low elongation is essential to ensure that the energy is absorbed efficiently. Metal cables possess handling qualities that discourage their use. Nonmetallic fiber materials are lighter in weight as well as more flexible and stowable.

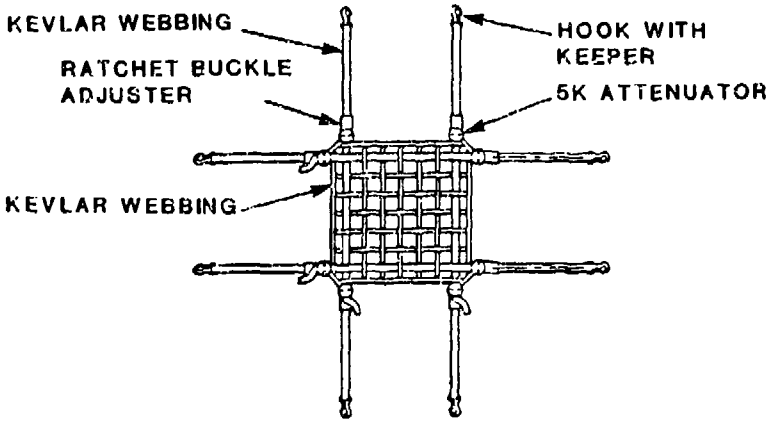

FIGURE 66. CRASH-RESISTANT BARRIER NET.
(FROM REFERENCE 81)

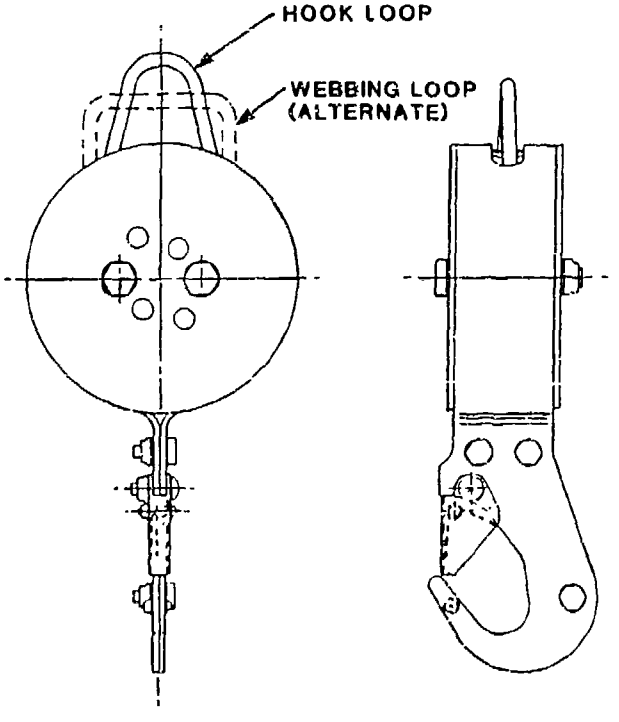

FIGURE 67. LOAD-LIMITING TIEDOWN ASSEMBLY.
(FROM REFERENCE 81)

6.2.7.8 Ancillary Equipment Retention. Objects that are unrestrained or dislodged from their attachment during a crash can cause injuries by striking the occupants directly, or, in the case of larger masses, by striking seats or other retention system components, causing failures of these items. Therefore, all ancillary equipment carried within the occupiable portion of the aircraft must be restrained.

All ancillary equipment frequently carried aboard the aircraft must be provided with integrated restraint devices or anchors. Stowage space for non-restrained items that are not regularly carried aboard the aircraft should also be provided, preferably located where items stored in it cannot become hazards.

To provide adequate protection during severe survivable crashes. As stated in Section 4.3.2.1, restraint devices and supporting structure for ancillary equipment must be designed to restrain the equipment during exposure to the following static loads:

Downward:	50 G	Aftward:	15 G
Upward:	10 G	Sideward:	25 G
Forward:	35 G		

It is a relatively simple task to restrain small items of equipment to withstand the static loads specified above. For larger items, however, significant weight penalties may be incurred or the available supporting structure may not be capable of withstanding the loads. For these reasons, load-limiting devices are recommended for the restraint of heavier equipment. However, load-limiter stroking must not allow any equipment to enter an occupant strike envelope. (Occupant strike envelopes are discussed in Volume II.)

6.2.7.9 Other Considerations. While the troop/cargo mix situation has received the most attention in this portion of the design guide, special cargo missions exclusively involving the aircrew may possibly require other design solutions, i.e., emphasis on forward longitudinal restraint and crew isolation. An extreme case of this nature, involving both crew and passengers, is the Navy C2-A COD fixed-wing aircraft where extremely tight quarters, requirements for high utilization of the volume devoted to cargo, and a forward longitudinal restraint of 20 G prevail (Reference 83). These conditions have dictated the use of a structural locker for multidirectional restraint.

6.3 LANDING GEAR

Landing gear, normally the aircraft's first energy-absorbing subsystem to contact the ground, can contribute significantly to the avoidance of damage to the fuselage and mission equipment in hard landings and to the survival of the crew and passengers in severe survivable crashes. The conditions for this to occur depend heavily on the impacted terrain, as well as on the aircraft velocity and attitude. Ground that is firm, smooth and level is conducive to the proper performance of the landing gear, but only about 20 percent of survivable crashes occur on surfaces that meet these conditions (References 84 and 85). Testing is typically conducted on solid surfaces to achieve repeatability, but a wheel will be punched deeply into soft earth, bog, or sand before developing the resistive forces for which the system is designed.

Landing gear designs optimized for performance on ideal impact surfaces while neglecting the actual crash conditions do not satisfy the intent of the systems approach to crash resistance. The principles and concepts presented in this section are related, whenever possible, to their utility under less-than-ideal conditions.

Optimization of designs must consider both the load profile generated and the associated stroking of the landing gear. These parameters are discussed in the ensuing paragraphs. Also, other design contraints, such as troop step-up height or cargo aircraft ramp angle may place constraints on the landing gear height. In these cases, the systems approach should be used to design compensating energy absorption in the fuselage.

6.3.1 Landing Gear Loads

Landing gear load factors must be selected as a result of a series of trade-offs that consider all system parameters. For each sink rate, landing gear peak load should ideally be selected to enhance crash survival through maximum energy absorption at acceptable levels of acceleration. However, landing gear loads are limited by the strength of the aircraft structure. Within practical ranges, landing gear loads may usefully increase with increasing sink-rate-at-ground-contact (SRAGC). Also, plateaus in the load versus SRAGC curve are useful just below certain damage threshholds. An example of the way peak landing gear loads may vary with SRAGC is shown in Figure 68 (adapted from Reference 86). This curve is qualitative and should not be scaled.

For any given SRAGC, the load should be as constant as possible throughout the stroke of the gear to maximize energy absorption. This is not easy to achieve, due to elasticities and inefficiencies in the components of the system. Examples of achievable load versus stroke curves and the corresponding efficiencies are shown in Figure 69.

As suggested by Figure 68, the SRAGC spectrum may be usefully divided into three landing regimes: normal, hard, and crash. The normal landing regime is shown to make the point that design for the other two regimes must still preserve the soft landing characteristic at low sink rates.

"Normal operation" ranges from slow ascent rates (ground resonance mode) to descent rates of about 10 ft/sec in the battlefield environment or in autorotative landing training (Reference 18). In this regime, relatively low landing gear loads are able to maintain comfortable ground clearance during landings encompassing a wide range of aircraft attitudes and ground conditions.

In the hard landing regime, the issue is prevention of fuselage and mission equipment damage due to either fuselage contact with the ground or loads that exceed the design limit. This range extends from about 10 ft/sec to beyond 20 ft/sec, depending on aircraft attitude, forward velocity, drift, gross weight, impact surface conditions, and other factors. A limited number of landings is expected in this regime. At the low end of the range, the aircraft is expected to be able to fly away with no damage. At the upper end

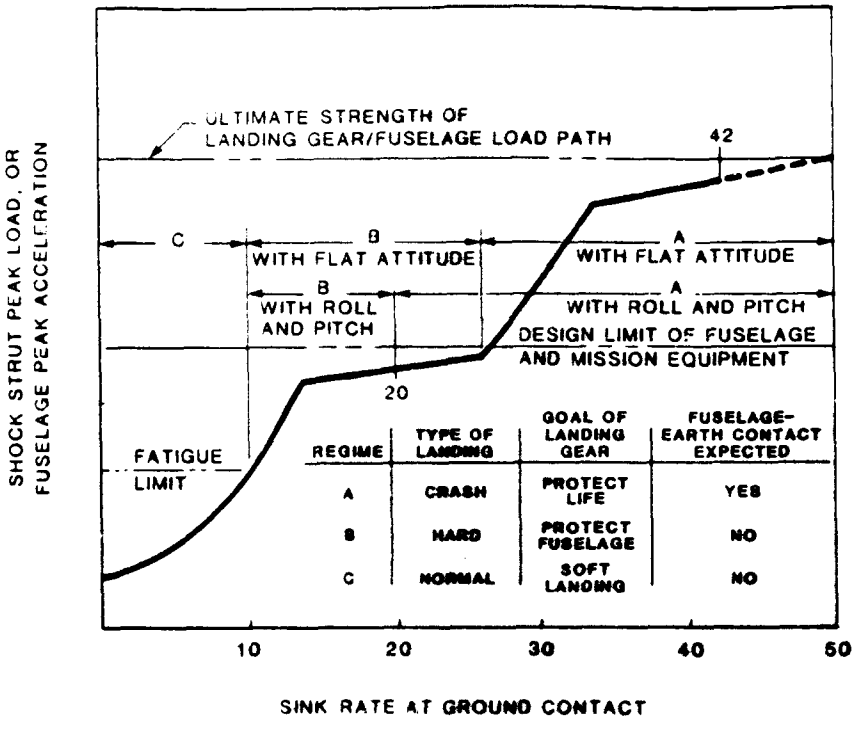

FIGURE 68. LANDING GEAR PEAK LOAD SELECTED TO PROTECT BOTH HUMAN LIFE AND EQUIPMENT. (FROM REFERENCE 86)

of this range, MIL-STD-1290 requires that helicopter landing gear (assisted by rotor lift) be able to decelerate the aircraft from a sink rate of 20 ft/sec onto level, rigid surface without allowing the fuselage to contact the ground and without exceeding the design limit load. Combinations of pitch and roll attitudes for this sink rate are also given in MIL-STD-1290. At the 20-ft/sec condition, plastic deformation of and damage to the landing gear is acceptable; the remainder of the aircraft, except possibly rotor blades, should be flightworthy after the incident.

Landing gear loads producing peak fuselage accelerations of 3 to 6 G have been considered appropriate for the hard landing regime (Reference 87). Landing gear limit load for the flat impact attitude at a 20-ft/sec sink rate may be selected to deliver acceleration of the fuselage equal to the design limit acceleration in the "pull-up" flight maneuver (Reference 18). But this results in the effective fuselage acceleration being cut in half during landings in which load is contributed only by gear on one side of the fuselage, such as during moderate-to-large roll attitude.

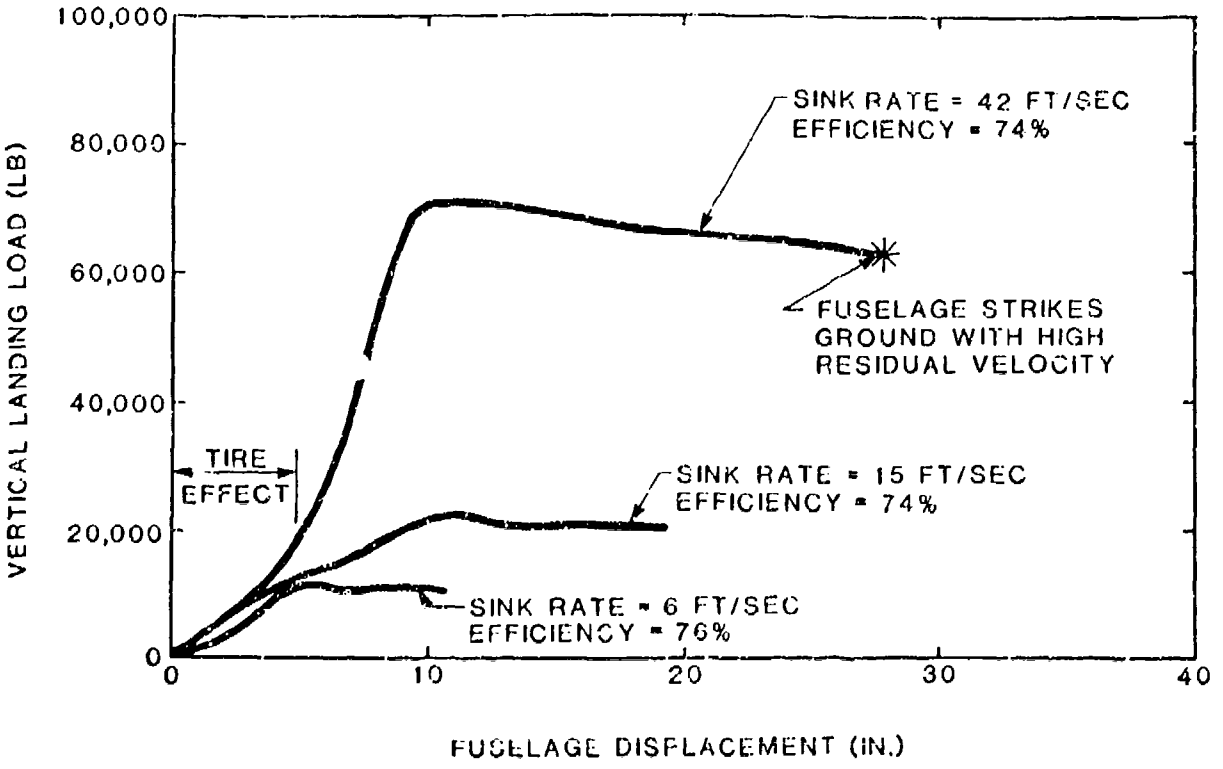

FIGURE 69. EXAMPLE OF ACHIEVABLE LANDING GEAR PERFORMANCE.

As sink rates rise into the crash regime, damage to the fuselage and/or mission equipment becomes unavoidable, and concern shifts to protecting the occupants from injury/death. This range extends from the hard landing range to about 42 ft/sec. At the high end of this regime, gear loads must approach, but not reach, the ultimate load of the fuselage/landing gear. Landing gear loads creating fuselage accelerations of about 10 G have been considered practical on recent development programs. The fuselage is expected to contact the ground in this regime, sometimes with very high residual kinetic energy, which must be absorbed by fuselage crushing. It is also expected that the landing gear loads will damage the fuselage, but will not cause rupture of essential load paths.

Discontinuities in the curve of peak load versus SRAGC in Figure 68 represent possible "staging" occurring in the shock strut. "Staging" refers to the shift of load control within the air-oil oleo from one pressure relief valve to another or from the primary oleo to a separate energy absorber in series with it. The ideal curve shape depends on the aircraft size and configuration, fuselage material (metal or composite), the mission equipment expense and tolerance to acceleration, and the expected crash scenarios (including impact surface). In general, the curve must gradually increase to account for

the increasing kinetic energy. However, two plateaus may be considered useful:

- A load plateau beyond the upper end of the hard-landing regime may avoid unnecessarily exceeding the design limit of the fuselage and/or mission equipment in low-energy crashes that do not result in fuselage contact, such as low-roll, low-pitch conditions onto prepared surface, a common example being a missed autorotation during pilot training.

- A load plateau at the upper end of the crash regime ensures two outcomes: first, during crashes with more than about 35 ft/sec sink rate combined with roll attitude, the down-side landing gear will deliver as much load as the fuselage can tolerate; and second, during low-roll, low pitch conditions onto prepared surface, the ultimate strength of the fuselage/landing gear will not be exceeded at (and even beyond) the design survival sink rate of 42 ft/sec. It is appropriate to do this at the high end of the survivable crash spectrum where total loss of the aircraft and mission equipment is expected; in this range, emphasis should be on protecting the occupants by maximizing the energy absorption available to extend the occupant survival envelope.

6.3.2 Selection of Landing Gear Stroke

The landing condition that most strongly influences landing gear stroke is the MIL-STD-1290 requirement to avoid fuselage damage during a 20 ft/sec sink rate with roll and pitch. The required landing gear stroke is dependent upon:

- Landing gear load (selected as discussed in previous paragraphs)

- Kinetic energy of the fuselage

- Aircraft attitude and rotational inertia that may result in only one gear contributing to energy absorption throughout most of the displacement

- Efficiency of energy absorption.

Analytical modeling using computer simulations, as well as crash tests, have demonstrated little tendency for aircraft roll to be corrected by the initial ground contact of the down-side gear (References 87 and 88). As a result, considerably more stroke is required to decelerate the fuselage during landings with roll attitude. A description of useful computer simulation tools and a quantitative example of landing gear stroke is presented in Chapter 7.

Coupling the left and right main landing gear to one another has been considered to compensate for roll by delivering greater loads to the downside gear. Mechanical, hydraulic, and electrical means may be considered. Mechanical connection through a torque tube was investigated by Sen (Reference 88). The conclusion was that the weight added by the torque tube and the strengthening of other components made the concept impractical.

6.3.3 Fuselage Velocity Change Controlled by Landing Gear

The velocity at which the fuselage will strike the ground can conveniently be found by applying conservation of energy methods. For instance, if a landing gear can fully decelerate the fuselage without fuselage/ground contact for a descent rate of 20 ft/sec with roll and yaw, the energy absorbed equals the kinetic energy of the fuselage at 20 ft/sec. Assume now that the sink rate of the above aircraft is 42 ft/sec, the stroke length of the landing gear is the same, and the average landing gear stroking load is 50 percent greater than it is at 20 ft/sec. The energy absorbed by the landing gear is then 50 percent greater, but the fuselage's kinetic energy at 42 ft/sec is 4.4 times what it was at 20 ft/sec due to the velocity-squared term in the kinetic energy equation. The residual fuselage kinetic energy at ground impact can be found by subtracting the energy absorbed by the landing ge r from the kinetic energy at 42 ft/sec.

$$KE_{impact} = \frac{1}{2} M (42^2 - 1.5 \times 20^2) = \frac{1}{2} M V^2_{impact}$$

Therefore, the fuselage has a residual velocity of 34 ft/sec when the fuselage strikes the ground. This approximation neglects the fact that some gear stroke will likely occur after fuselage crush begins.

6.3.4 Wheel Versus Skid

Depending on the helicopter's mission and performance requirements, a wheeled gear or skid gear may be chosen. Predominate reasons may be cited such as weight, cost, ground handling and taxiing, which are unrelated to crash resistance. The crash-resistant characteristics are discussed in the following sections.

Wheeled gear have the advantage of reduced drag force during landings with forward velocity. Skid gear may offer higher rollover resistance than 3-point wheeled gear and superior soft-ground flotation characteristics, important when considering the high percentage of accidents that occur on terrain other than prepared, solid surface.

Both wheeled and skid gear may not absorb significant energy in a lateral impact. In a primarily vertical impact with significant sideslip velocity and roll attitude, digging-in of the gear can cause rollover and/or collapse of the gear under the belly of the aircraft.

Most research to develop high-capacity energy absorption has been directed at wheeled gear, while skid gear have historically been characterized by simplicity and light weight. Thus, an opportunity may exist for the improvement of skid gear energy absorption.

6.3.5 Wheeled Gear

The gear may be distributed around the fuselage in three primary configurations: four-point (quadricycle), three-point with nose wheel, and three-point with tail wheel. Each configuration has advantages and disadvantages.

The quadricycle configuration puts gear near the corners of the fuselage, positioned well to react most combinations of pitch, roll, yaw, forward velocity and side drift. The extra cost, weight, and aerodynamic drag may make such gear impractical on all but the largest helicopters. Examples are the Sikorsky S-55 and the Boeing Helicopter CH-47 Chanook. The gear can be made retractable to reduce drag at the expense of increased cost and weight.

In the nose-wheel configuration, the two main gear are positioned near the aft end of the fuselage where they share the initial impact in the prevalent positive-pitch attitude. Careful design is necessary to prevent the nose wheel, usually positioned below the cockpit, from being driven into the cockpit by high-sink-rate crashes or by encounters with obstructions during crashes with forward or lateral velocity.

In the tail-wheel configuration, a main landing gear is positioned on each side of the forward fuselage. This is a good position to limit occupant deceleration, prevent rollover, and avoid penetration of the livable volume during high-energy survivable crashes. However, the single tail gear is the first to contact the ground in the prevalent positive-pitch attitude.

The tail wheel can be located either at the junction between the fuselage and tail boom or near the aft end of the tail boom. The disadvantage of the latter is the additional strength needed if the tail boom must react the resulting loads. The more forward location enables the tail gear to absorb more energy, due to its closer proximity to the aircraft c.g. The incorporation of such a design is shown in Figure 70. Note that the vertical stabilizer is extended downward and equipped with a skid to avoid tail rotor strikes.

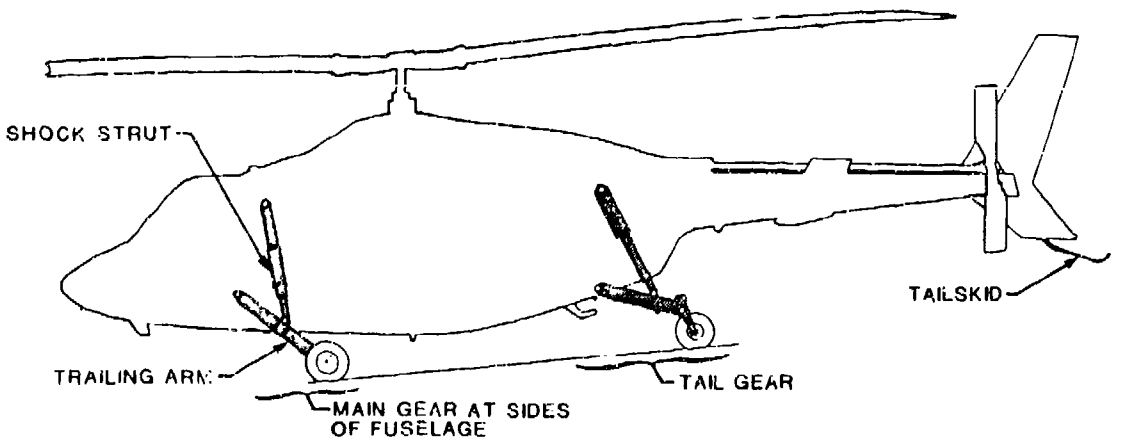

FIGURE 70. LOCATION AND GEOMETRY OF LANDING GEAR.

If an extreme aftward location of the tail wheel is selected, the tail wheel protects the tail rotor well, but is inefficient at decelerating the aircraft due to its great distance from the c.g. Worse, tail wheel contact causes forward pitching which may increase the sink rate at the front of the helicopter.

6.3.6 Weight of Landing Gear

The weights of different crash-resistant landing configurations have been evaluated in References 87, 89, and 90. Weights presented by Crist and Symes in Reference 86 are summarized in Table 11.

TABLE 11. UNINSTALLED WEIGHTS OF EQUIVALENT CRASH-RESISTANT LANDING GEAR

Configuration and Rollover Angle	Weight Each Gear (lb) Forward	Aft	Total	Percent BSDGW*
Tail Wheel (30^{o})	125	80	330	4.13
Tail Wheel (25^{o})	120	60	300	3.75
Nose Wheel (25^{o})	103	127	358	4.48
Quadricycle (30^{o})	107	113	440	5.50
Skid (30^{o})	-	-	367**	5.24

*Basic structural design gross weight.
**Includes 83 lb for skid assemblies, which replaced the wheels and tires on the quadricycle gear.

6.3.7 Components and Load Paths

Wheeled gear may have the wheel motion guided by a swinging arm (drag link) or by the shock strut (cantilever), or by some articulated linkage that may be a combination of the two methods, as shown in Figure 71.

Long axle travel is required of crash-resistant landing gear: the Black Hawk and Apache main gear wheels have 26 and 39 inches of vertical travel, respectively. For such long travels, the drag link design may be more weight-efficient than the cantilever, especially when encounters with obstructions are considered.

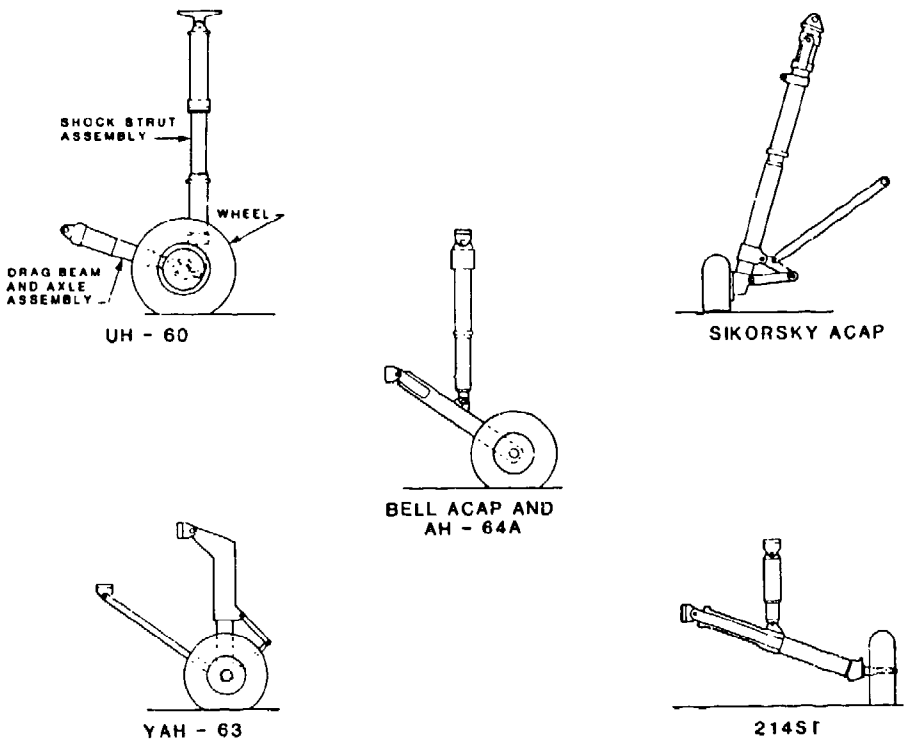

FIGURE 71. WHEEL LANDING GEAR CONCEPTS.

6.3.7.1 Drag Link/Shock Strut Attachment Geometry The locations of the attachment points of the drag link and shock strut to the fuselage can be selected to optimize crash performance. The following principles should be considered:

- Location of the gear beside the fuselage, rather than under it, reduces the probability of intrusion of a failed gear into occupied volume and reduces roll-over danger.

- Wheel motion during normal landing and kneeling may be required (by the procurement specification) to be in the aircraft vertical direction, or to lie within a given vertical-longitudinal plane. This avoids lateral motion of the wheel, with its resultant scuffing of the tire. Thus, the pivot axis of the drag link is usually parallel to the pitch axis of the aircraft.

- Considering the high probability of forward velocity accompanying the downward sink rate and the encounter of wheels with obstructions, a drag link geometry causing combined upward/aftward wheel travel should be given preference.

- Attachment of the drag link to the fuselage at about floor level, slightly above the crush zone of the fuselage, will improve the probability of that critical pivot joint maintaining its integrity throughout the crash. This feature is illustrated in Figure 72.

- Landing gear stroke may usefully continue after fuselage impact and during crushing of the fuselage as shown in Figure 72. The extra stroke is also useful for 20 ft/sec impacts with roll attitude, which require more stroke on the downside gear. (Achieving this may lead to a long-stroke shock strut, attached high on the side wall of the fuselage, and substantially aligned with the vertical axis. By contributing to the deceleration of the overhead masses throughout the crash, such a strut may either reduce the load-carrying requirements of the side walls or reduce the energy-absorbing structural allocation throughout the fuselage).

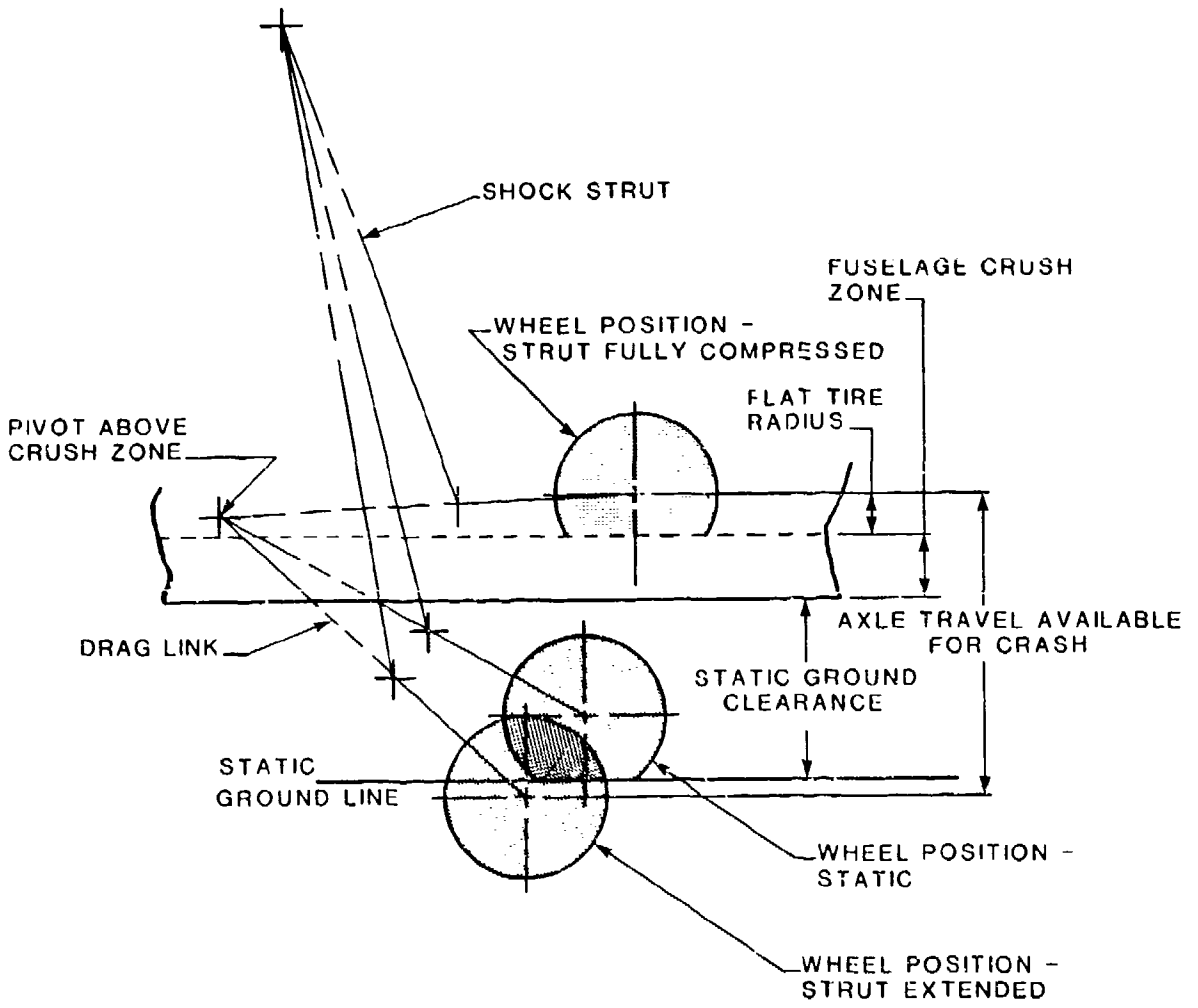

FIGURE 72. GEAR GEOMETRY SELECTED TO CONTINUE ABSORBING ENERGY DURING CRUSHING OF FUSELAGE FLOOR.

- Overreliance on a landing gear configured per the previous paragraph to decelerate the overhead masses can result in an aircraft unsuitable for impact on water or soft earth, due to inadequate fuselage strength and/or energy absorption.

- Length of the drag link must be selected to achieve the required axle travel along a path that avoids extreme loads during all required combinations of attitude, velocity, and wheel obstruction.

- Weight sensitivity analyses performed at Bell Helicopter suggest that attaching the shock strut to an intermediate point on the drag link results in a minimum weight system. Shock strut weight increases more rapidly with increasing stroke than with increasing load.

- Bottoming of the shock strut should result in benign failure of its fuselage attachment point. The failure should not contribute to loss of continuity in longitudinal beams or transverse bulkheads comprising the roll-cage, must not penetrate the livable volume or fuel tanks, and must not sever fuel lines.

- Similarly, attachment points between the drag link and fuselage should be designed and located so that failure will avoid intrusions into livable volume and fuel tanks/lines.

6.3.7.2 Landing Gear Configuration. When defining the landing gear configuration, the layout of the aircraft system and associated structure must be considered. Aircraft type and associated mission constraints, large mass locations, the protection of occupants, and potentially hazardous fluid and munitions should all be taken into account when optimizing landing gear geometry and load path reactions. Additionally, aircraft shaping to minimize signatures may also have to be considered.

By assessing geometrical layouts and varying landing gear track width, inclination, stroke, etc., the most efficient aircraft system can be identified. This not only results in a design that meets the pitch and roll requirements for crash impacts, but also provides an efficient and lightweight aircraft structure.

Such an approach is particularly applicable to small attack types of helicopters when signature reduction, especially for the front, results in the need for a very narrow fuselage. Figure 73 shows the optimization of the main landing gear and structural frames to directly transfer gear loads to frame members for an attack type helicopter with narrow body requirements and some shaping for signature reduction. This philosophy is less applicable to cargo helicopters, utility, medium, and heavy lift, where a rectangular "box" is normally required for occupants and equipment and the opportunities to optimize landing gear installations are restricted.

6.3.8 Skid Gear

The simplest form of skid gear, which offers advantages of low cost and weight, is the bent tube attached to structural frame members. The skid gear can also provide improved support in landings on soft or marshy terrain.

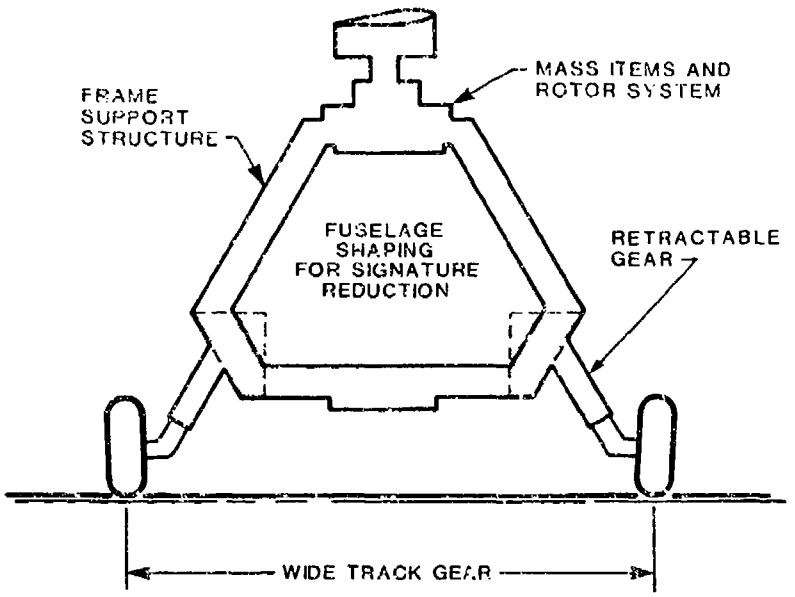

FIGURE 73. POSSIBLE STRUCTURAL LAYOUT FOR ATTACK HELICOPTER WITH SIGNATURE REDUCTION.

This type of gear provides limited energy absorption. The skid system is basically a nonlinear structure providing a constant spring rate for small deflections only. Such a design provides a low-cost means of creating small elastic deflections during normal landings while providing energy dissipation efficiencies comparable to those of an oleo strut. However, in a hard landing or a crash the skids deflect appreciably and the nonlinear plastic characteristics of such a system prevail. During plastic bending the moment arm increases, lowering the loads as the deflection increases until the fuselage contacts the ground.

Improvements to the fixed-skid concept have been designed in an attempt to provide some level of energy absorption with rate damping. In addition, such a system can be tuned to minimize the effects of dynamic excitations that may produce ground resonance. Figure 74 shows the basic skid system used on one observation helicopter and an improved, pitch-interconnected concept (Reference 31). The improved design was initiated to reduce the pitching response of the aircraft and minimize the incidence of blade-tail boom strikes. Although tail boom clearances were improved, the new concept did not satisfy the MIL-STD-1290 requirement for no ground contact by the fuselage for a 20-ft/sec vertical impact (Reference 1). Only 17.5 ft/sec was reached before fuselage contact.

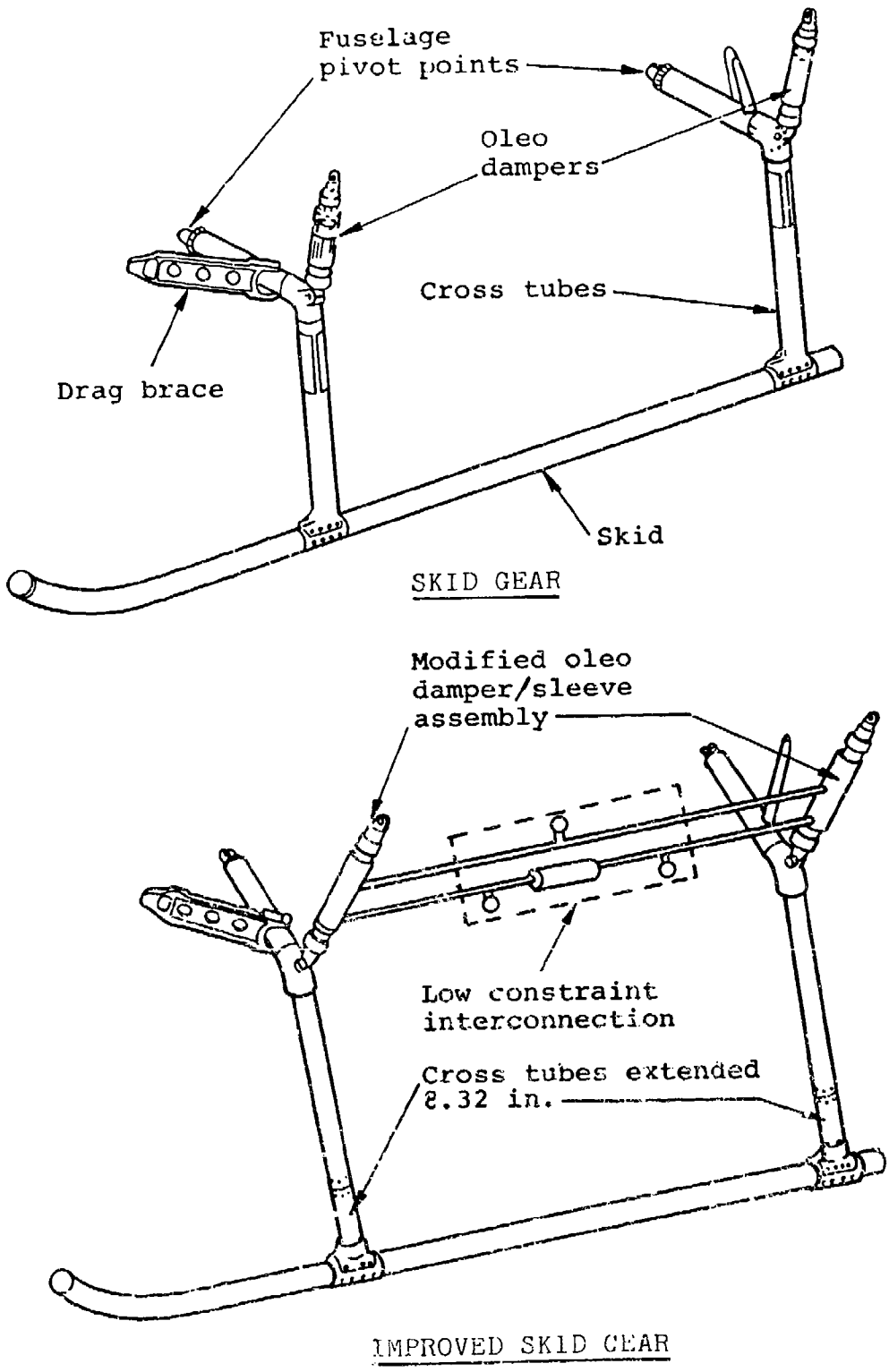

FIGURE 74. HELICOPTER SKID GEAR AND IMPROVED, PITCH-INTERCONNECTED CONCEPTS.

6.3.9 Shock Strut

The shock strut is a component of the wheeled landing gear system that is relied on to supply most of the spring rate and damping characteristics. A skid gear may also be equipped with a shock strut or struts. For normal operations (other than crash situations), a conventional air/oil oleo, such as shown in Figure 75, provides two useful load characteristics: load increases with displacement and with rate of contraction.

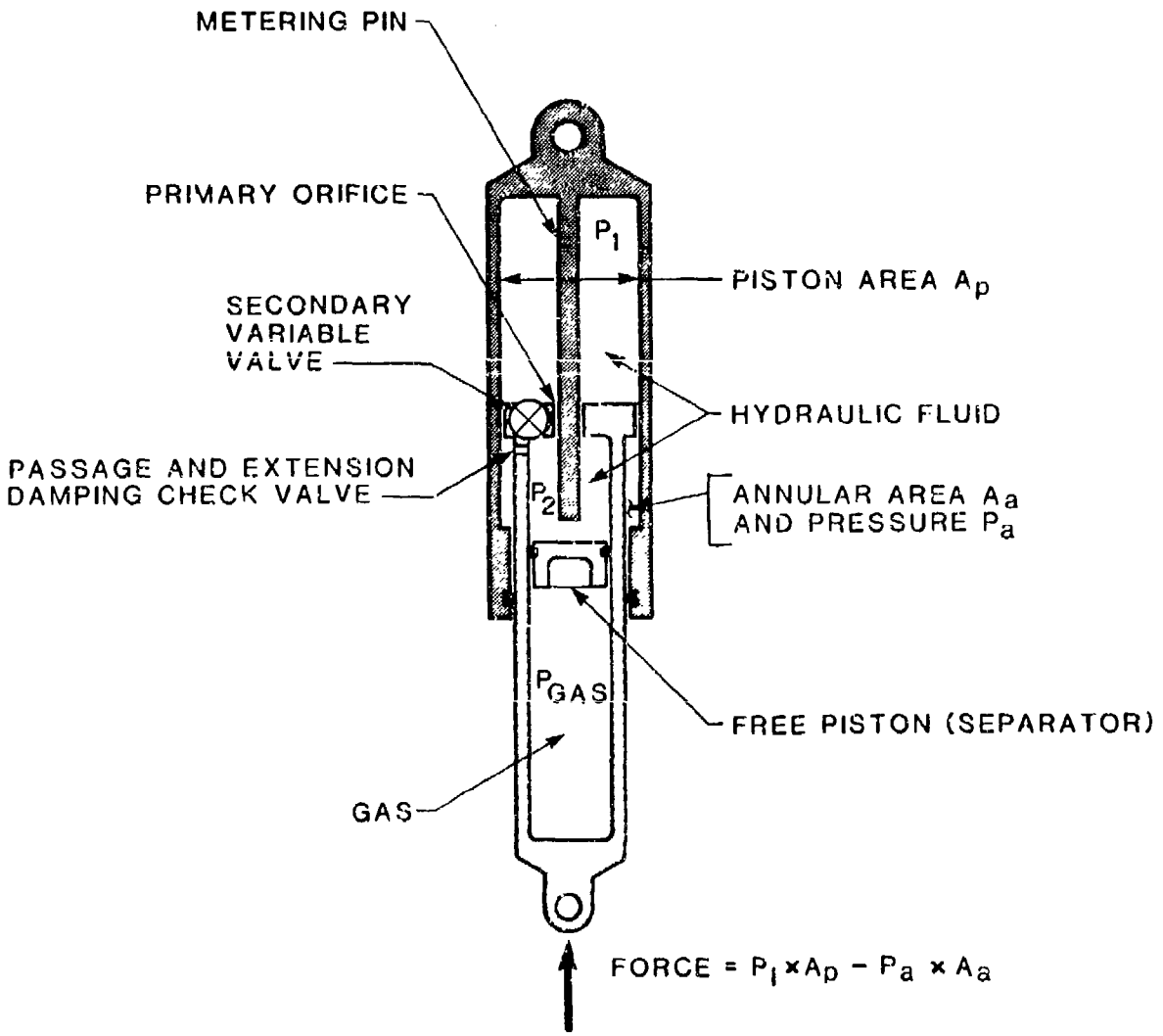

FIGURE 75. AIR/OIL OLEO SCHEMATIC.

6.3.9.1 Load Versus Displacement. Load increases as a function of displacement, due to the compression of the gas. The spring rate is typically tailored by the selection of the initial pressure and volume to satisfy aircraft static ground clearance requirements for the required range of gross weights.

Pressure in the gas chamber is calculated by the equation

$$P_{GAS} = P_0 \times (V_0/V_S)^k \qquad (16)$$

where P_0 and P_{GAS} = gas pressures at initial (fully extended) and final stroke conditions, respectively.

V_0 and V_S = gas volumes at initial (fully extended) and final stroke conditions (at stroke S), respectively.

k = a gas constant, which for air or nitrogen equals 1.0 under static (isothermal) conditions, such as resting on the runway, and 1.4 under dynamic (adiabatic) conditions during a landing or crash.

6.3.9.2 Load Versus Contraction Rate. Load increases as a function of shock strut rate of contraction, due to the pressure differential required to cause flow of hydraulic fluid through the orifice (or valve). Pressure drop across the orifice is given by the equation

$$\Delta P = P_1 - P_2 = (\rho \times Q^2) / (2 \times C_D^2 \times A_0^2) \qquad (17)$$

where ΔP = pressure drop across the orifice

P_1 and P_2 = pressures upstream and downstream of the orifice, respectively

ρ = fluid density

Q = fluid flow rate, expressed in volume per unit time

C_D = flow coefficient depending on the orifice shape

A_0 = the area of the orifice. This area is necessarily the sum of several fixed and variable orifices (pressure relief valves) as explained below.

If the orifice area is fixed (constant), pressure increases as the square of the contraction rate, resulting in the undesirable pressure versus sink rate curves such as those labled A and B in Figure 76. For curve A, initial sink rates only a little greater than 30 ft/sec cause what has been described in most literature as "lock-up", characterized by immediate bursting of the shock

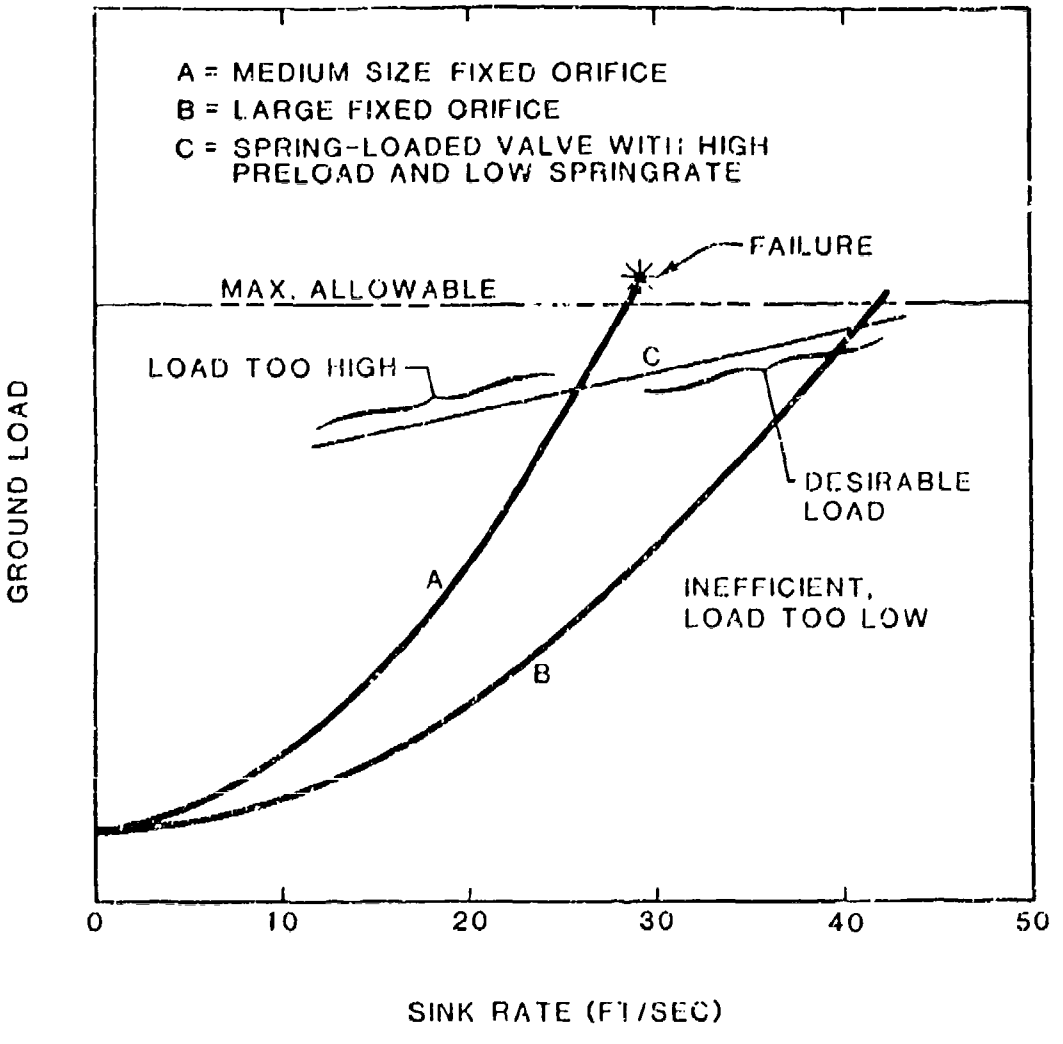

FIGURE 76. EXAMPLE OF EFFECTS OF DIFFERENT ORIFICES ON THE VELOCITY SENSITIVITY OF A HYDRAULIC OLEO.

strut or failure in the fuselage/shock strut load path. Similarly, a larger fixed orifice, sized appropriately for 42 ft/sec, will deliver undesirably low load (hence, insufficient energy absorption) for all lesser sink rates, as shown by curve B.

Therefore, the hydraulic fluid flow path within the oleo must be equipped with one or more valves capable of increasing the flow area as the flow rate increases. In the extreme, a spring-loaded valve with very high preload and very low spring rate achieves the load versus stroke characteristic shown as curve C in Figure 76 (Reference 86). This characteristic is useful at very high crash energies, but imposes excessive loads onto the fuselage and mission equipment at low-to-intermediate sink rates.

With several parallel valves, each can be tailored to a different portion of the sink rate spectrum. In general, fixed orifices and small valves provide low pressure at low flow rates, and larger valves handle the high flow rates. In this way, the desired load versus sink rate characteristic could be achieved over the entire sink rate spectrum, such as was previously shown in Figure 68.

A servo-operated valve has been considered that would be controlled automatically by a microprocessor or other means. This has been described as an "active control" landing gear. The concept was originally developed for fixed-wing aircraft forced to taxi on rough or bomb-damaged runways and has since also been applied to automotive suspensions. For repeated contact with a series of chuckholes, such a system can improve ground clearance while reducing shock loads. However, for the one-event shock of a helicopter hard landing or crash, active control may present unnecessary cost and unreliability.

A low viscosity oil should be chosen to minimize temperature dependence. Viscosity can generally be neglected and is absent from Equation (17).

6.3.10 Shock Strut Oleo Total Load

For dynamic adiabatic conditions, Equations (16) and (17) can be combined by solving Equation (17) for P_1, and noting that $P_2 = P_{GAS}$ for practical values of separator piston mass and friction.

$$P_1 = ((\rho \times Q^2)/(2 \times C_D{}^2 \times A_0{}^2)) + (P_0 \times (V_0/V_S)^{1.4}) \qquad (18)$$

In Equation (18) the group of terms $((\rho \times Q^2) / (2 \times C_D{}^2 \times A_0{}^2))$ is most strongly dependent on aircraft sink rate. Recall that Q is the volume rate of flow through the orifice, a function of the piston area and shock strut contraction rate. The shock strut contraction rate is itself dependent upon the geometry of the articulated gear mechanism. The squaring of the flow term makes the pressure a strong function of shock strut contraction rate, unless compensated by a variable orifice.

The group of terms $(P_0 \times (V_0/V_S)^{1.4})$ is exponentially dependent on the degree of shock strut contraction, unless at some predetermined pressure, gas from volume V_S begins to be discharged to limit the peak gas pressure.

In the hydraulic fluid flow path, orifice area A_0 may most effectively be the total of several fixed and variable orifices:

- A fixed orifice, such as that suitable for normal, low-energy landings
- One or more variable orifices (spring-loaded pressure relief valves) that open with increasing pressure to compensate for rate sensitivity

- A variable orifice that changes with degree of contraction, such as provided by a metering pin, most suitable for optimizing performance in the normal and hard landing regimes.

6.3.11 Shock Strut Load Transients and Failure Conditions

The load delivered by the shock strut oleo has been shown in Equation (18) to increase with both increasing rate of contraction and degree of contraction. Contraction rate tends to be highest near the beginning of the gear stroke and diminishes as the gear decelerates the fuselage. The degree that the contraction rate diminishes becomes less as initial sink rate increases (for energetic crashes, considerable residual velocity exists after all landing gear stroke is exhausted).

During the initial high contraction rate, a pressure-regulating orifice is required to discharge sufficient hydraulic fluid from the high pressure chamber to avoid exceeding the ultimate safe pressure. Safe design pressure of about 8000 psi has been used in the shock struts of the AH-64A and UH-60A. An inadequate pressure-regulating orifice will result in immediate failure of the strut at high sink rates, before a useful amount of energy is absorbed (curve A of Figure 76).

Assume now that an adequate pressure regulating orifice is installed in the flow path of the hydraulic fluid, to avoid failure during high sink rates. Another hazard exists in the latter portion of the stroke due to the buildup of gas pressure, if this is combined with a high shock strut contraction rate. This is the result of two circumstances:

1. Common practice has been to optimize strut performance for intermediate sink rates by utilizing the fact that the contraction rate diminishes to zero before the stroke is complete. Figure 77(a) shows an oleo optimized at an intermediate sink rate by adjusting the rate and degree characteristics to make their sum as near constant as possible. A metering pin is sometimes also used to tune the characteristics to achieve this.

2. This same oleo at high sink rates will exceed the ultimate load before stroking the entire distance, as shown in Figure 77(b). The reason for the failure is that the high contraction rate (thus high hydraulic ΔP) is maintained throughout the stroke, while the gas pressure is also increasing.

Reference 86 suggests limiting the buildup of gas pressure to some predetermined maximum to avoid the overpressure condition shown in Figure 77(b). When the threshold gas pressure is reached, the (inert) gas begins to be discharged to the atmosphere through a pressure relief valve. The threshold at which discharge begins should be selected high enough to avoid maintenance after moderate hard landings.

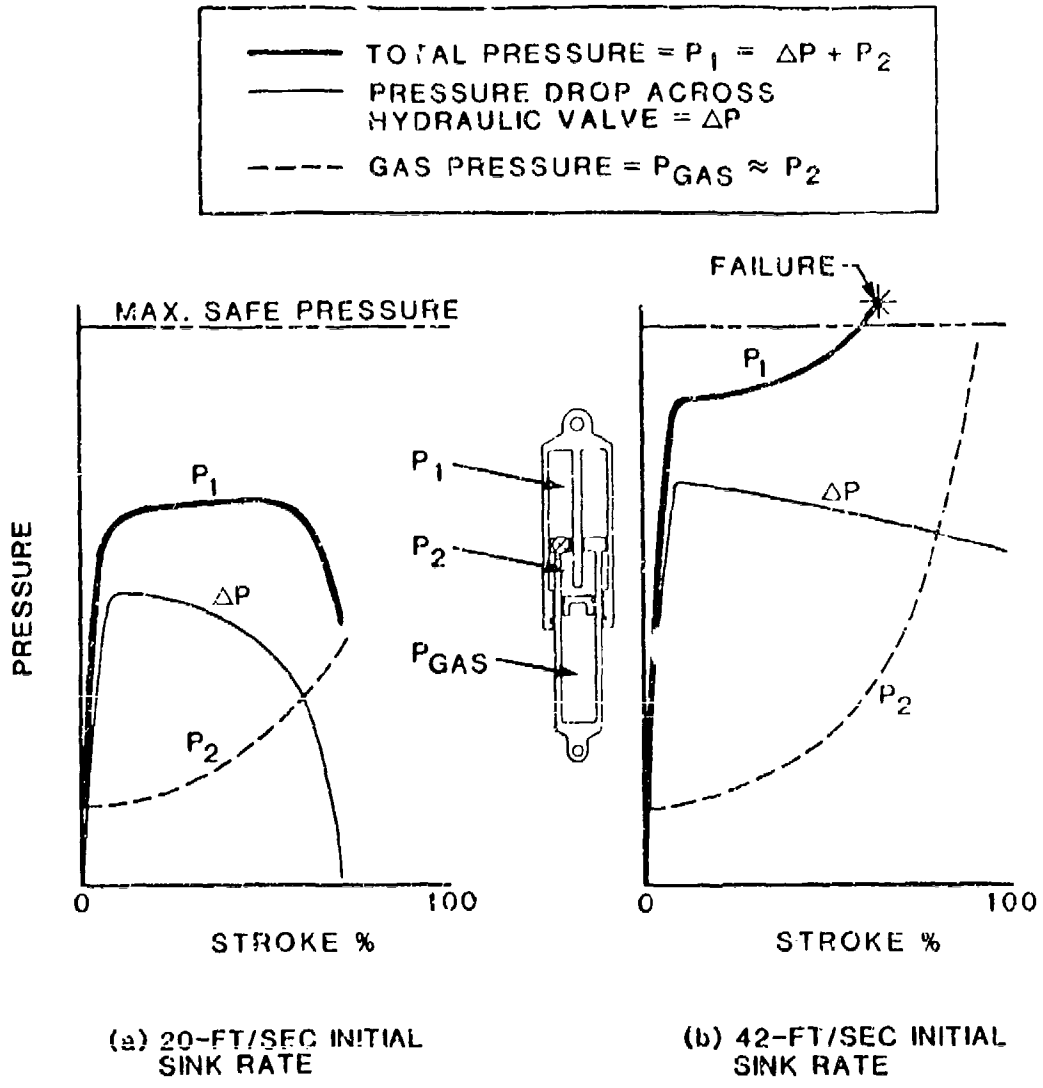

FIGURE 77. RESPONSE OF A SIMPLE OLEO TO TWO TEST CONDITIONS.

6.3.12 Containment of Flammable Hydraulic Fluid

Fire-resistant hydraulic fluid per MIL-H-83282 (Reference 92) is still flammable, especially when vaporized by discharge at high pressures through an orifice or valve. Therefore, the oil must be contained within the shock strut or piped to a reservoir.

Containment of hydraulic fluid within the shock strut presents a design problem that must be solved for each system. The obvious place to discharge the fluid is into the space ordinarily occupied by gas; however, because the

volume of gas must be selected by 1-G static spring rate considerations, the gas volume is grossly inadequate to accept the large amount of fluid displaced during the full stroke. Piping the fluid to a reservoir in the fuselage raises the problems of leakage, extra maintenance, and potential severing of the lines in a crash.

6.3.13 Series Coupling of Shock Strut Energy-Absorbing Devices

The mismatch between gear performance characteristics required for normal landings and crashes has historically been solved by building the shock strut as a stack of two, relatively independent, energy-absorbing devices (or stages) in series with one another. The first stage is an air/oil oleo with its gas volume and gas pressure sized to deliver the proper spring rate needed to achieve the required 1-G static ground clearance. The variable orifices controlling flow of the hydraulic fluid in this first stage can be optimized to deliver the required load characteristics for sink rates up to 10 or 15 ft/sec.

The second stage strokes during crashes to supplement the displacement of the first stage and to avoid initial load spikes that would otherwise occur due to rate sensitivity of the first stage. The second stage can be another air/oil oleo, or a hydraulic damper, or a mechanical energy absorber, as shown conceptually in Figure 78(a), (b), and (c), respectively. Each concept has advantages and disadvantages.

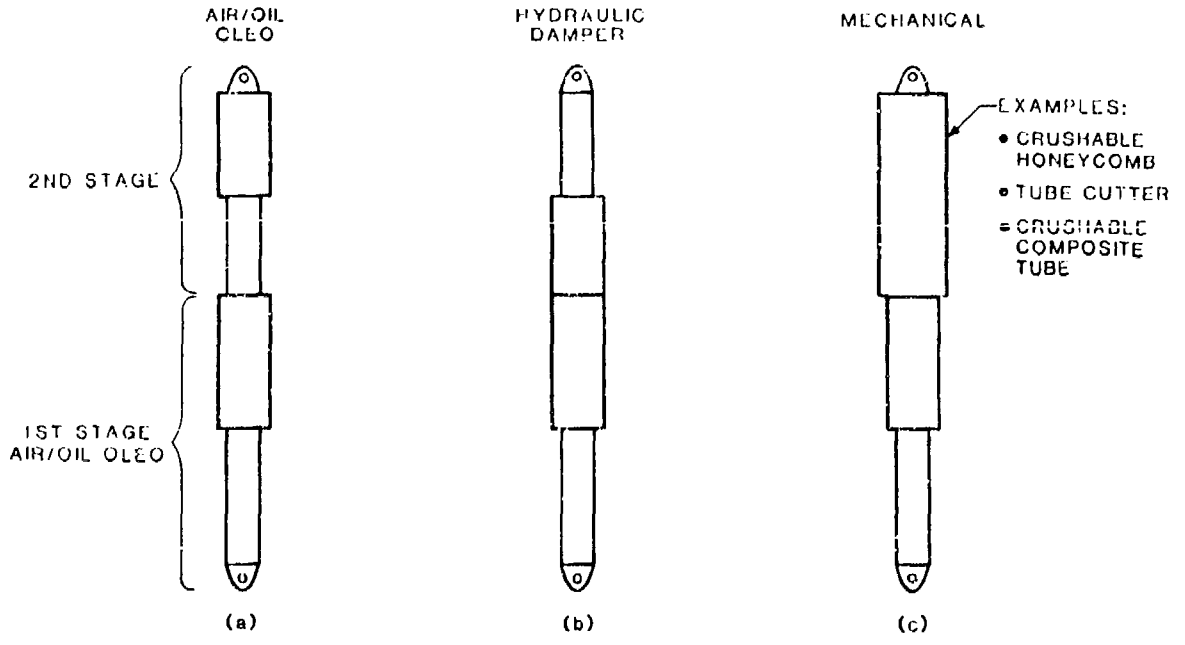

FIGURE 78. TWO-STAGE SHOCK STRUT CONCEPTS.

In concept (a) of Figure 78 the second stage gas volume may, for instance, be charged to 900 psi, while the first stage is charged to 300 psi. During normal landings the second stage will therefore not deflect until the first has compressed several inches. During hard landings, it is entirely acceptable for the second stage to stroke somewhat to assist the first. After the event, the gas pressure in the second stage reextends that stage, resetting it automatically. The primary advantage is the ability to fly away after hard landings without service to the landing gear. Disadvantages include relatively high weight and cost due to duplication of components in the first and second stages.

In concept (b) of Figure 78 the first stage by itself must absorb the energy in all normal landings. The second stage is normally held in its extended position by shear rings, calibrated to avoid breaking until some predetermined hard landing load occurs. Once the shear rings have broken, the second stage begins to contract, forcing hydraulic fluid through a valve(s). The design has the advantage of requiring no gas pressure to maintain the normal degree of extension of the second stage, therefore avoiding the potential failure mode caused by buildup of gas pressure near the end of the stroke. Also, no separator piston is needed to prevent mixing of the fluid and gas. One disadvantage is that the second stage must stroke during some hard landings and will not reset itself automatically after that event; shear rings, fluid, and valve need to be replaced and/or refurbished before the helicopter can be flown again.

Concept (c) of Figure 78 utilizes a mechanical energy absorber for the second stage. Shear pins or rings may be used to maintain the fully extended position of the second stage during normal landings. The energy absorbing device can be selected for high energy absorption per unit weight and for high ratio of available stroke to overall length. Attractive energy absorbing concepts include crushable graphite tubes, crushable aluminum honeycomb, and tube-cutting devices. Properties of these materials (and others) and methods of constructing energy absorbers may be found in Volume IV. The primary advantages of a mechanical energy absorber for the second stage are: light weight, no maintenance as long as the stroking load is not exceeded, and insensitivity of load to contraction rate.

A performance requirement unrelated to crash resistance is the need for military helicopters to kneel for storage aboard cargo aircraft and ships. To accomplish this, the shock strut can be shortened by ground personnel. Because of the long stroke of the gear, both the first and second stages may need to be shortened. Concept (a) facilitates this by enabling the pumping of hydraulic fluid to a remote reservoir. Concept (b) requires the shear rings to be disengaged before the fluid is pumped out. Concept (c) may be less amenable to shortening.

6.3.14 Transient Effects and Efficiency

At initial impact of the gear with the ground, the shock strut does not instantly reach its peak contraction rate (thus delaying development of peak load). Inefficient compression of the tire at comparatively low loads delays the transfer of motion to the shock strut. Tires such as are used on the AH-64A or UH-60A deflect about 6 in. prior to wheel rim contact. Flexibility

in the drag link further delays the transmittal of motion to the shock strut. The compressibility of hydraulic fluid in the shock strut is also significant especially during the initial motion.

After contraction of the oleo shock strut is finally underway, it does not deliver perfect efficiency, although 90 percent efficiency can be exceeded for selected conditions. Considering all factors, overall efficiency of the landing gear is expected to be only about 75 to 80 percent.

Flexibility of the fuselage should also be considered, especially if large masses are located remote from the landing gear, such as in the case of the engine nacelles on a tilt-rotor aircraft. In developing landing gear for the V-22, the subcontractor discovered that landing loads predicted by a flexible aircraft model were 20 percent lower than those predicted by a rigid aircraft model (Reference 93).

6.4 SUBSYSTEMS EXTERNAL TO THE FUSELAGE OTHER THAN LANDING GEAR

6.4.1 General

Plastic deformation of aircraft elements outside the occupied area is an additional method of absorbing aircraft energy. Elements such as rotor blades, wings, tail sections, and even external stores can be bent, battered, or destroyed in the process of bringing the occupied section to a successful halt. When trees, ground obstacles, or uneven terrain are involved, impacts with blades, wings, etc., often occur. Energy is expended in breaking the impacted object and/or failing the aircraft element.

6.4.2 Rotor Blade

Rotor blades on helicopters can significantly contribute to energy absorption if the aircraft impacts into trees. The rotating blades incrementally chop the trees until rotor motion stops or until blade separation occurs. In either case, an appreciable quantity of energy can be absorbed, providing that the attachment strength to the basic fuselage is adequate to prevent the blades from being detached or the rotor mast and transmission system from being torn out of the aircraft.

Composite blades often offer a desirable degree of energy absorption. When a composite blade impacts tree limbs, progressive delamination between the axial fibers occurs due to adhesive failure. This process, called brooming, does not destroy the longitudinal load-carrying elements in the blade; these elements can continue to flail the tree and dissipate energy.

An additional property of other composites that can be used to advantage is the high modulus of elasticity achievable by using certain fibers, such as graphite or boron. A stiffer blade that reduces deflections and reduces the probability of a blade strike on the fuselage crown can thereby be designed.

When rotor blades with metal spars are subjected to tree impacts, successful energy absorption takes place until a tree element too strong for the blade to sever is impacted. Then the blade will fail by plastic bending or by completely detaching from the rotor. During these failure sequences, blades

may impact the fuselage. Titanium spars perform better than earlier aluminum spar blades, but some failures are unavoidable, and overhead fuselage structure should be designed to resist penetration.

Blade tips can be made frangible to crush upon impact. Deformation of the tip should be as controlled as possible. For example, if a frangible tip with tip weight fractures and leaves the blade, the resultant main rotor centrifugal unbalance may cause severe pylon damage. Therefore, the blade should retain its balance during the blade tip strike. A replaceable frangible blade tip concept (from Reference 94) is shown in Figure 79.

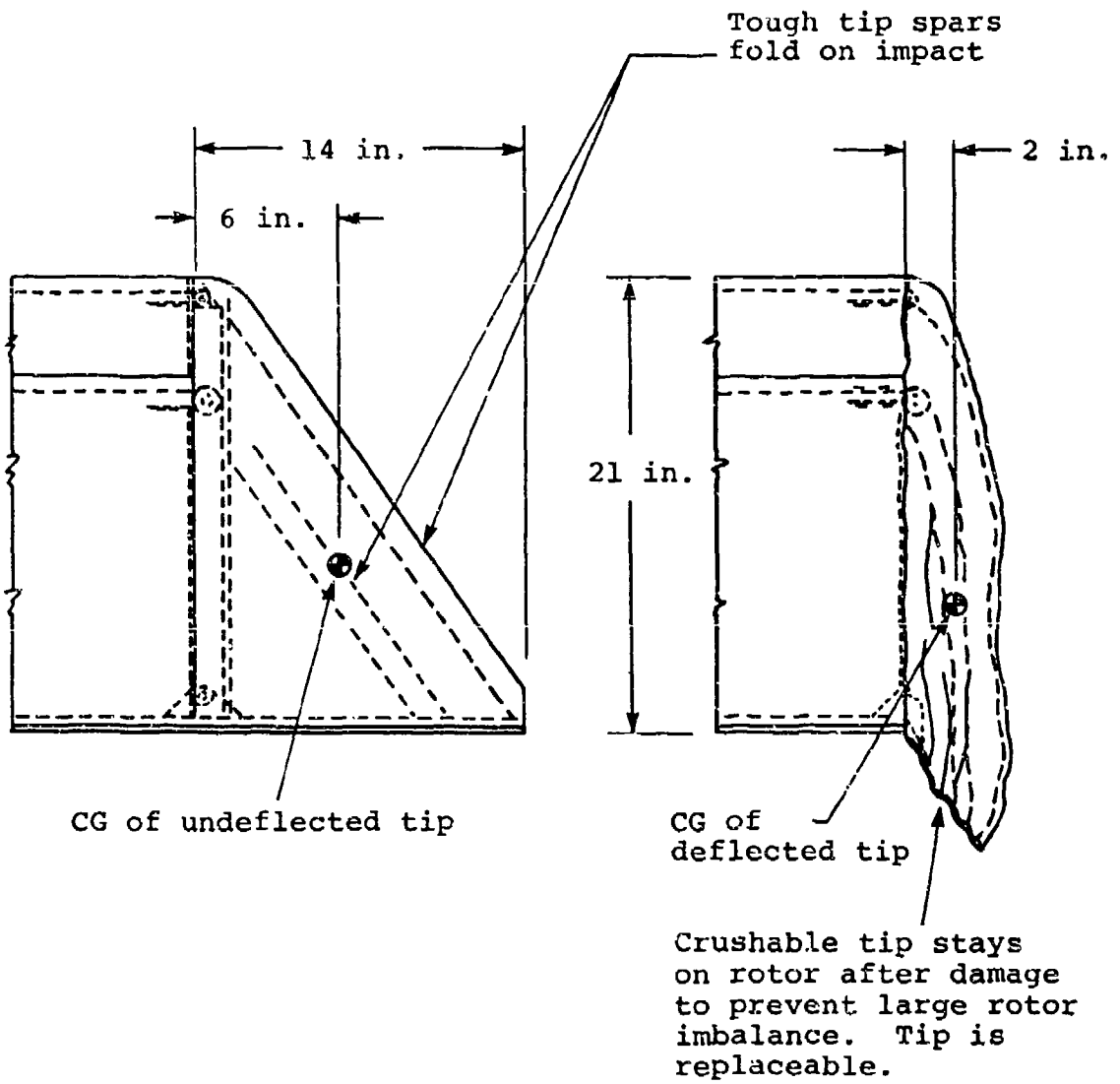

FIGURE 79. FRANGIBLE MAIN ROTOR BLADE TIP. (FROM REFERENCE 94)

For future main rotor blades, it may be possible to design a blade that can accept localized destruction during a blade strike such that harmful blade strike loads are not transmitted to the mast. The blade should progressively fail inward, starting at the blade tip. Filament-reinforced composite materials could accept the failure of the resin material, yet retain some of the load-carrying capability of the fibers (Reference 68). Some means for blade balance weight retention should be included.

6.4.3 Wing, Empennage, Engine, and External Stores

Wing impacts usually occur in one of two ways. Either a tree, pole, or similar object is hit, producing highly concentrated loading, or the wing strikes a barrier, such as an earthen mound or a dike, which produces loading that is more evenly distributed along the wing's leading edge. Crushing and shear strength, for typical wings, will allow trees or poles to cut into the wing as the aircraft moves forward, until the wing is cut off or until the pole breaks. The fore-and-aft loads under these conditions are low in terms of their effect on fuselage accelerations. In fact, even the more evenly distributed loads can produce fuselage accelerations of perhaps only 5 G.

Wing failures in fixed-wing aircraft typically account for only 5 percent, or less, of the total kinetic energy which may be present in a crash of moderate velocity (Reference 95). Therefore, the use of the wing structure as an effective energy absorber does not appear to be promising. Increasing this energy-absorption capability would involve adding material to structural members which can already withstand normal loading. In all likelihood, most of the added material could not be used effectively for any particular crash.

However, the wings could be designed to break free from the fuselage structure under high longitudinal impact forces. This could reduce the mass considerably, especially if the wings contain fuel. As discussed earlier, this reduction could effectively reduce the energy absorption requirements for the cabin structure. Wing removal may also provide the possibility of removing flammable fluids away from the fuselage and occupants.

Empennage structure or, for that matter, any structure aft of the occupiable cabin, seldom provides beneficial effects during a longitudinal crash. Instead, the mass tends to increase the loads which must be supported by the cockpit/cabin structure. Therefore, if empennage structures can be designed to collapse during a longitudinal impact, the requirements for cockpit/cabin structural strength and energy-absorption capability are reduced.

Stub wing or sponsons can be designed to absorb lateral impact loads. In addition, the stub wing/sponsons help keep the emergency exits off the ground and thus useable when the aircraft comes to rest on its side.

All external systems should be designed so that their crash-induced failure will not lead to penetration or rupture of the fuselage protective shell.

6.4.4 Special Tilt-Rotor Considerations

Crash resistance design considerations for tilt-rotor aircraft share many common items with conventional helicopter and fixed-wing aircraft. These include the items listed in Table 1.

On conventional helicopters, the main rotor pylons and engines generally are located near the occupied areas, and adequate tiedown strength is required to prevent potentially hazardous displacement of the large mass items into the occupied areas. On tilt-rotor aircraft the pylons and engines may be located near the wing tips, well away from the occupied areas. If so, allowing the wings to fail in a controlled manner will reduce the aircraft mass, and less material is required in the fuselage structure to absorb the reduced aircraft kinetic energy (Reference 65).

For tilt-rotor aircraft with wing-mounted engines, the design approach to control the wing, pylon, and rotor failure modes is illustrated in Figure 17. By proper choice of the prop-rotor direction of rotation, rotor ground strikes are directed away from the occupied areas. Some debris from the ground and rotor blade fragments may still impact the fuselage sidewalls in the vicinity of the tip path plane. The seating arrangements and the design of the structure in those areas adjacent to the tip path plane should consider this possibility (Reference 65).

To maintain the occupied volume within the fuselage, the fuselage should be designed stronger than the wings. Similarly, the wings should be designed stronger than the pylon. Consequently, the pylon and wing should fail prior to the fuselage, preventing collapse of the occupant compartment (Reference 65). A tilt-rotor design using fuselage-mounted engine(s) would be more like a helicopter as far as crash resistance is concerned.

7. ANALYTICAL METHODS

7.1 INTRODUCTION

The complexity of dynamic structural deformation makes analysis both difficult and essential to the design process. In this chapter are presented basic dynamic analysis techniques as well as material which directly supports the aircraft design process, such as discussions of energy absorption tradeoffs for the preliminary design phase, semiempirical methods for preliminary sizing of structure, and analytical methods of crash simulation.

7.2 DYNAMICS OF THE CRASH IMPACT CONDITIONS

7.2.1 Kinematic Relationships

Relationships among the kinematic quantities of position, velocity, and acceleration form the basis for the study of dynamic phenomena. Although these relationships are generally well known, use of their precise definitions facilitates an understanding of the crash event and its analysis. Therefore, a discussion of these relationships as applied to crash impact conditions follows. The reader primarily concerned with aircraft design may wish to proceed to Section 7.3.

Consider first an aircraft impacting a rigid vertical barrier as shown in Figure 80. The position of the reference point fixed in the aircraft relative to a point fixed on the ground is referred to as X. A change in position is referred to as displacement S. In this case, assume that the displacement of the reference point is measured from its position at the time when the aircraft just contacts the wall.

If a change in displacement ΔS occurs in a time interval Δt, then the average velocity of the aircraft over that interval is

$$\bar{v} = \frac{\Delta S}{\Delta t} \tag{19}$$

As the time increment is taken to be very small, Equation (19) yields the instantaneous velocity

$$v = \lim_{\Delta t \to 0} \frac{\Delta S}{\Delta t} = \frac{dS}{dt} \tag{20}$$

Note that velocity has the units of length per unit time, i.e., feet or meters per second.

If in the same time interval the aircraft undergoes a change in velocity Δv, the average acceleration over the interval is given by

$$\bar{a} = \frac{\Delta v}{\Delta t} \tag{21}$$

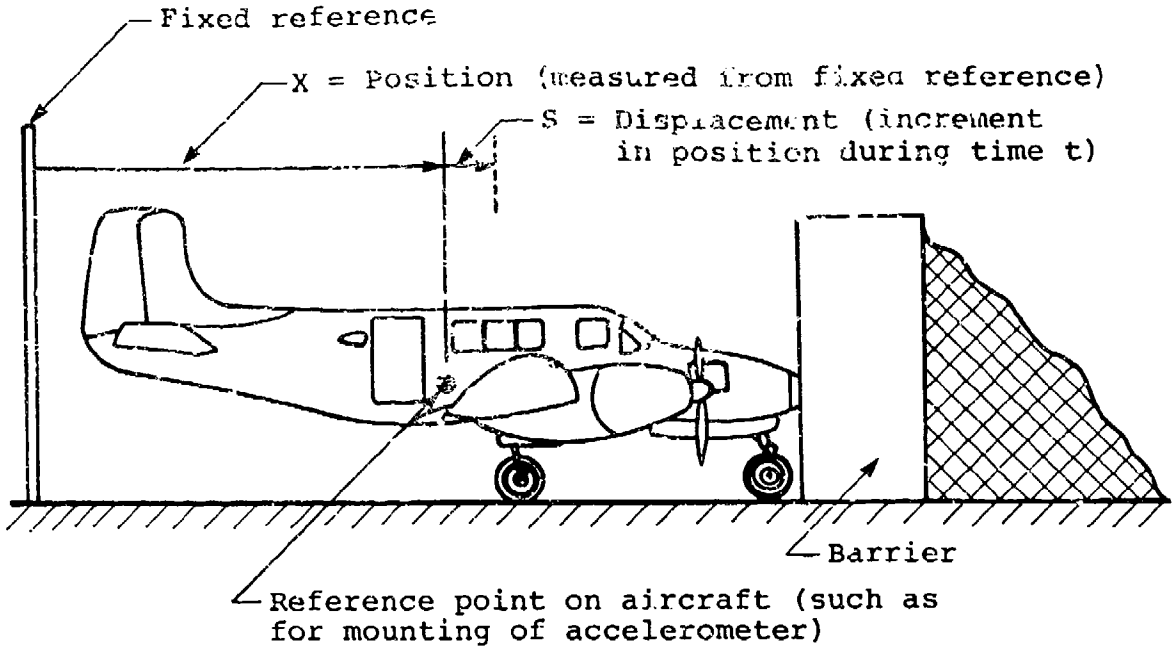

FIGURE 80. DEFINITION OF POSITION AND DISPLACEMENT FOR CRASHING AIRCRAFT.

and the instantaneous acceleration by

$$a = \lim_{\Delta t \to 0} \frac{\Delta v}{\Delta t} = \frac{dv}{dt} \qquad (22)$$

Note that acceleration has units of velocity per unit time, i.e., feet or meters per second per second.

A graphical examination of the relationships among position, velocity, and acceleration will aid in understanding their application in the crash impact conditions. Referring to Figure 81, assume that the aircraft of Figure 80 has a velocity v_0 just prior to contacting the barrier and that the velocity of Point C, fixed in the aircraft, varies with time as shown in Figure 81(b).

First note that in Equation (22) defining acceleration that "a" is the height of the a-t curve and $\Delta v/\Delta t$ (for small Δt) is the slope of the v-t curve in

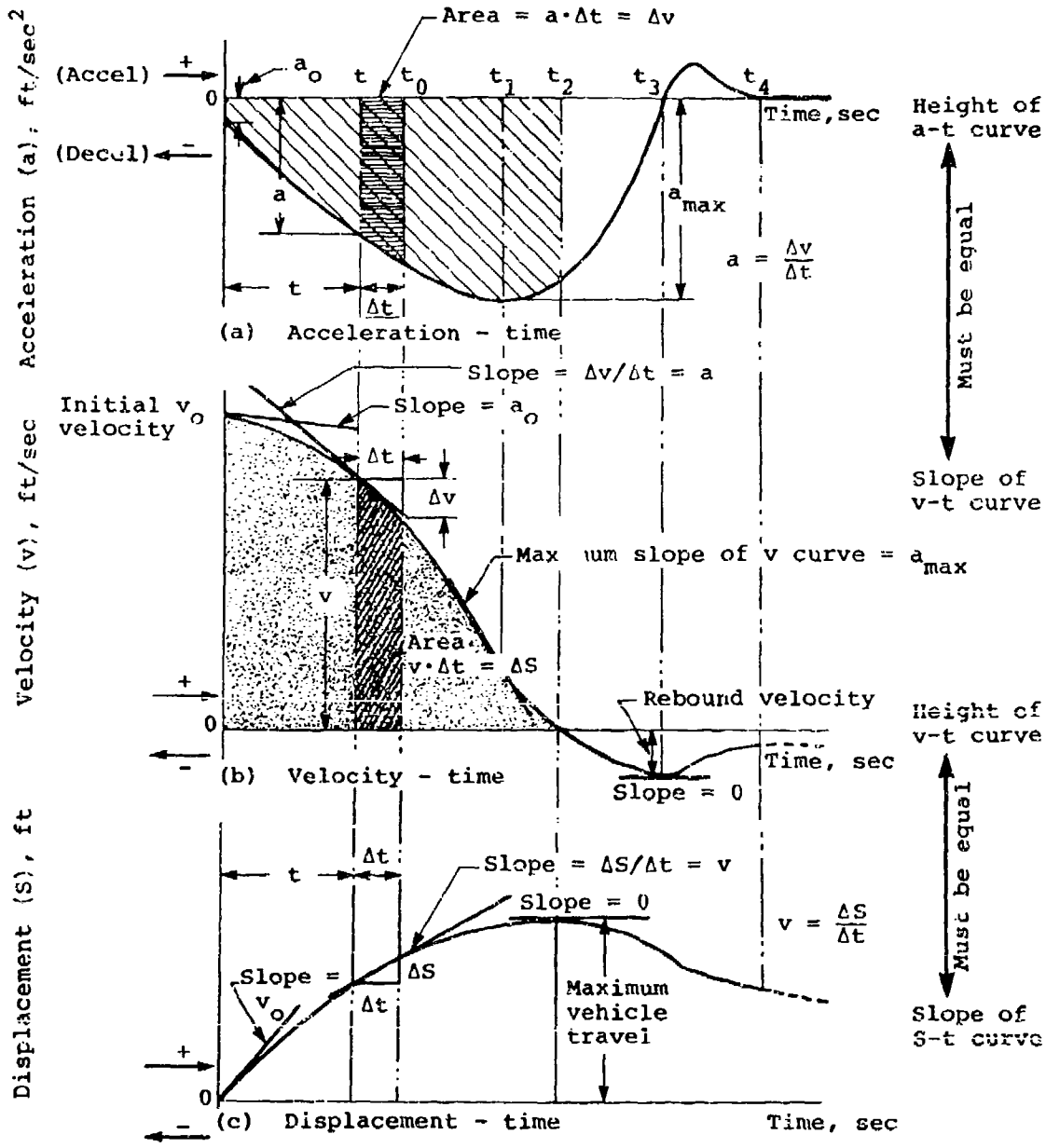

FIGURE 81. ASSUMED RELATIONSHIP FOR ILLUSTRATION OF CRASH KINEMATICS.

Figure 81. Thus Equation (22) indicates that the height of the a-t curve is equal in magnitude and sign to the slope of the v-t curve, that is

$$a = \frac{dv}{dt} \tag{23}$$

This is an invariant relationship, and any data, whether experimentally or theoretically obtained, must meet this criterion to be valid.

In a similar way Equation (20) indicates that the height of the v-t curve is equal to the slope of the S-t curve.

Rewriting Equation (23) and integrating, the change in velocity over any time interval between t_0 and t is

$$\Delta v = v - v_o = \int_{t_o}^{t} a\,dt \tag{24}$$

Therefore, the total change in velocity during a given interval is equal to the area under the a-t curve in the interval. As an example, consider the total crosshatched area between $t = 0$ and $t = t_2$ in Figure 81(a). Assuming $V_2 = 0$, this area is equal to the initial velocity v_o, that is the change in velocity between $t = 0$ and $t = t_2$.

Note that the acceleration in Figure 81 is negative (deceleration), thus producing a negative velocity change or reduction in velocity from v_o to 0. A positive acceleration, on the other hand, produces an increase in velocity.

The same condition exists between the velocity and displacement curves, that is

$$\Delta S = \int_{t^0}^{t} v\,dt \tag{25}$$

or, in other words, the total distance travelled is equal to the area under the v-t curve. Thus the maximum vehicle travel, as in Figure 81(c), would be equal to the area shaded with dots under the v-t curve of Figure 81(b).

The following important points may be noted in Figure 81:

- The velocity is changing at its most rapid rate when the acceleration (or deceleration) is maximum, at time t_1.
- The displacement reaches a maximum when the velocity becomes zero, time t_2.
- The velocity need not necessarily be zero (time t_2) when the acceleration is maximum (time t_1).
- The area contained within the deceleration pulse (from t_0 to t_3) is equal to the initial velocity plus the rebound velocity (the total velocity change).
- The area under the deceleration curve between t_2 and t_3 is equal to the rebound velocity.

7.2.2 Energy Absorption During Deceleration

According to Newton's second law of motion, the resultant force (F) acting on mass (m) produces an acceleration (a) according to

$$F = ma = m \frac{dv}{dt} \tag{26}$$

Applying Equation (20),

$$F = m \frac{dv}{dS} \frac{dS}{dt} = mv \frac{dv}{dS} \tag{27}$$

Multiplying by the incremental displacement dS and integrating,

$$\int_{S_1}^{S_2} F dS = \int_{v_1}^{v_2} mv\, dv = \frac{1}{2} mv_2^2 - \frac{1}{2} mv_1^2 \tag{28}$$

which states that the work done on a mass m by resultant force moving through a change in displacement from S_1 to S_2 changes the kinetic energy of the mass, which is defined as

$$\text{Kinetic Energy, } T = \frac{1}{2} mv^2 \tag{29}$$

Work done by force F during the change in displacement is defined as

$$\text{Work} = \int_{S_1}^{S_2} F dS \tag{30}$$

which is equivalent to the area under the curve of force versus displacement between any two displacements, as illustrated in Figure 82.

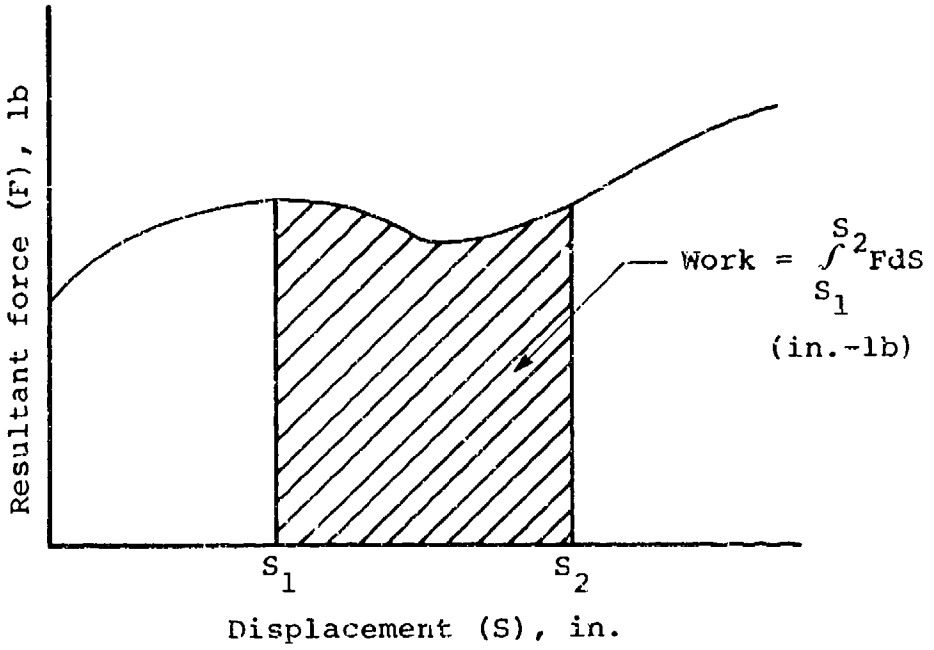

FIGURE 82. DEFINITION OF WORK.

In application of Equation (28) to the crash environment, an aircraft moving with initial velocity v_o can be slowed to a reduced velocity v (which is zero when the aircraft comes to rest) by application of a force through a distance S

$$\int_0^S FdS = \frac{1}{2} mv_o^2 - \frac{1}{2} mv^2 \qquad (31)$$

where the force acts in a direction opposing the velocity, as shown in Figure 83. Referring to Figure 83, it might be said that the kinetic energy of the aircraft is absorbed by crushing of its forward structure as its velocity is reduced.

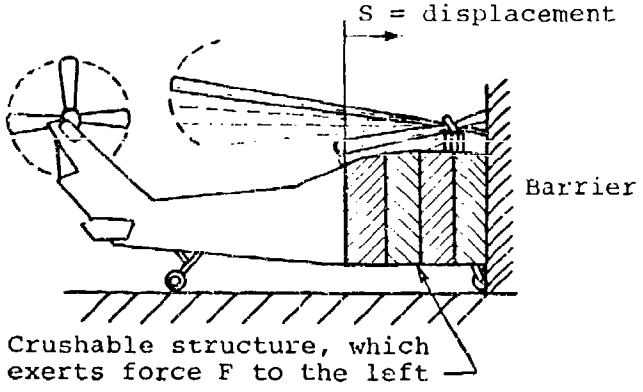

(a) Idealization of impact into barrier

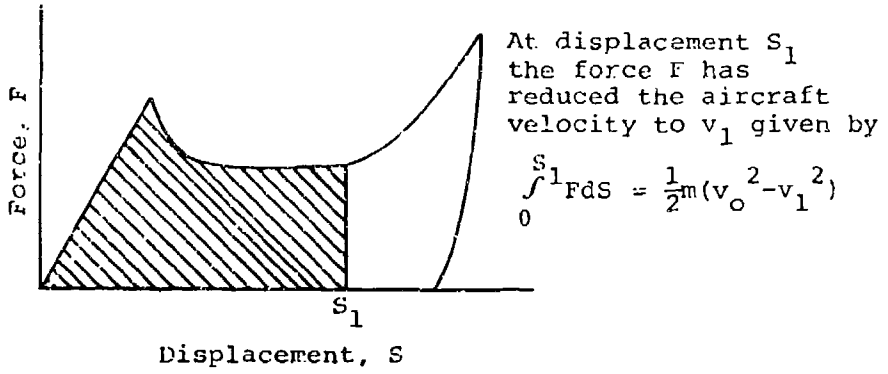

(b) Force versus displacement for barrier impact

FIGURE 83. ILLUSTRATION OF IMPACT REDUCING AIRCRAFT KINETIC ENERGY.

If a constant stopping force were applied, the velocity would be reduced at constant deceleration as shown in Figure 84(a) and the force-displacement curve would be as shown in Figure 84(b).

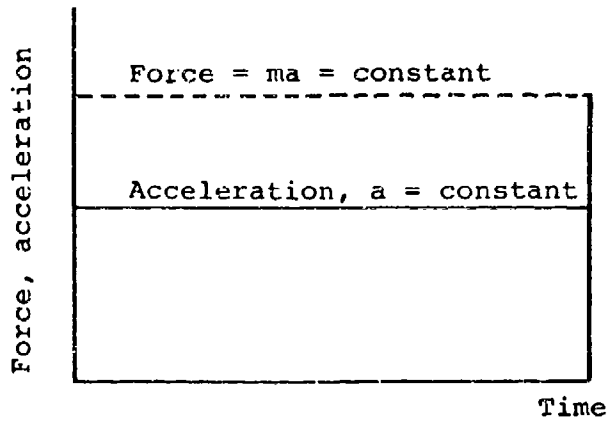

(a) Constant acceleration versus time

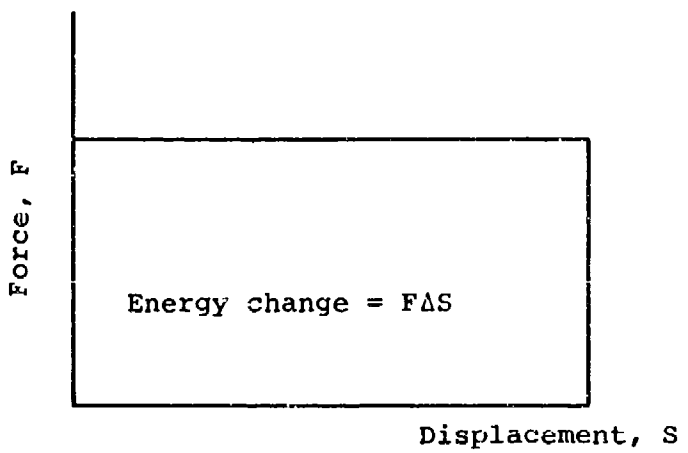

(b) Constant force versus displacement

FIGURE 84. ILLUSTRATION OF DECELERATION BY CONSTANT FORCE.

Often, for protection of occupants, it is desirable to limit the decelerating force to some prescribed value. Given a maximum force, the most efficient energy-absorbing system would be the one requiring the smallest displacement, S, which would be the constant-force system. Therefore, energy absorption by a constant force is often referred to as "ideal" energy absorption. The

devices shown in Volume IV exert a nearly constant force and thus act as nearly ideal energy absorbers. They are desirable for use where concentrated loads are applied and the transmitted force must be limited, such as in seats and landing gear.

Structural systems and certain materials, such as plastic foams and honeycomb materials, approach the ideal force-displacement curve to the extent shown in Figure 85.

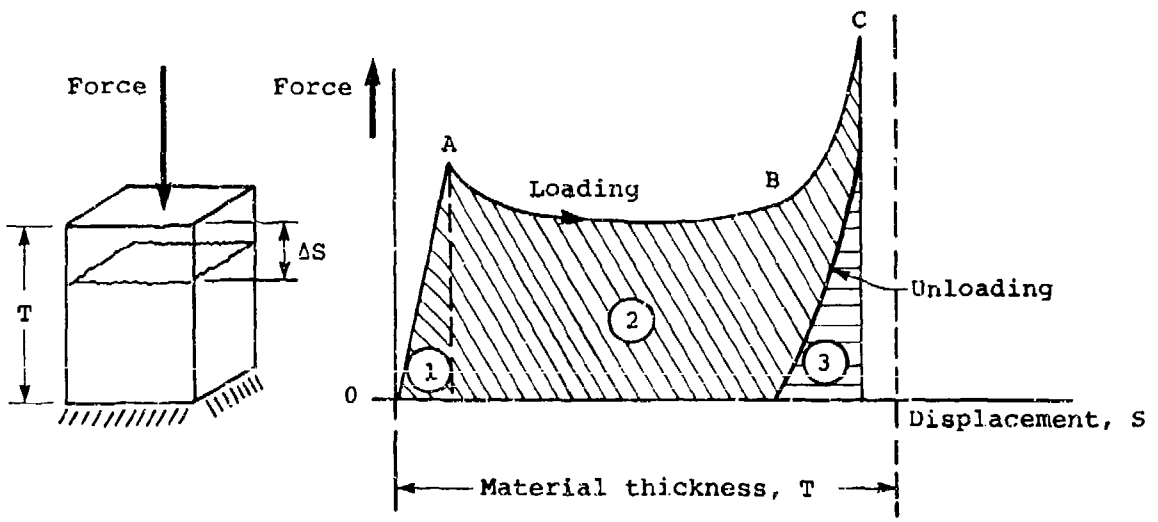

FIGURE 85. FORCE-DISPLACEMENT CURVE FOR HONEYCOMB MATERIALS.

Again, the area under this curve represents energy absorbed. The area can be divided into three important regions. If loading results only in reaching Point A in Figure 85, then unloading generally occurs along the elastic curve OA, and the energy indicated by Area "1" is restored to the system just as a spring releases its energy when it is unloaded. Area "2" represents inelastic, or plastic, energy absorption, and if loading reached Point C, the energy corresponding to Areas "1" plus "2" plus "3" is absorbed. However, as unloading occurs, the energy of Area "3" is restored in the form of rebound.

Loading in the region from B to C in the figure is often referred to as "bottoming," a condition in which the deforming structure or material has become compacted and the load increases rapidly with very little further deformation.

The energy dissipated in locked-wheel skidding is of interest in calculating, for example, the initial velocity when the skidding distance is known. This is readily obtained from Equation (31) if it is assumed that during skidding

the sliding forces are constant and are the only significant forces present. Thus, the work done by the sliding force is simply the force times the distance and from Equation (31), for $v_{final} = 0$,

$$FS = \frac{1}{2} mv_o^2 \tag{32}$$

or

$$v_o = \sqrt{\frac{2FS}{m}} \tag{33}$$

The sliding force F can be assumed to equal an average coefficient of friction times the normal force between the vehicle and the sliding surface, or the weight of the vehicle if the surface is horizontal, thus

$$F = \mu N = \mu W \tag{34}$$

and

$$v_o = \sqrt{\frac{2\mu WS}{W/g}} = \sqrt{2g\mu S} \tag{35}$$

where μ = coefficient of kinetic (sliding) friction

W = weight of vehicle

S = stopping distance

g = acceleration due to gravity = 32.2 ft/sec^2 or 9.81 m/sec^2.

For the case $v_f \neq 0$ we can use the work-energy principle to obtain

$$\text{Work} = \Delta\text{Kinetic Energy}$$

$$-\mu WS = \frac{1}{2}\frac{W}{g}\left[v_f^2 - v_o^2\right]$$

From which

$$v_f = \sqrt{v_o^2 - 2g\mu S} \tag{36}$$

and

$$v_o = \sqrt{v_f^2 + 2g\mu S} \tag{37}$$

For sliding on a slope of angle θ to the horizontal

$$v_o = \sqrt{v_f^2 + 2gS[\mu \cos \theta \pm \sin \theta]} \tag{38}$$

For sliding uphill the + sign applies; for sliding downhill, the - sign.

Example: The landing gear on an aircraft collapses and the aircraft slides 1200 ft, at which point it is estimated to have a residual speed of 50 kn. By dragging the wreckage with a tank retriever through a load-measuring device it is found that the required load to move the aircraft is 0.7 times the weight of the aircraft. To determine the speed when the gear collapsed

$$v_f = 50 \text{ kn} = 1.69 \times 50 = 84 \text{ ft/sec}$$

$$\mu = 0.7$$

$$v_o = \sqrt{(84)^2 + 2\ (32.2)(0.7)(1{,}200)}$$

$$v_o = 247 \text{ ft/sec}$$

$$= 146 \text{ kn}$$

7.2.3 Stopping Distance

For a complete aircraft system, or a subsystem such as seat and occupant, average deceleration values (G) can be determined for given velocity changes as demonstrated above, and from these data an average stopping distance can be computed.

$$v_o^2 - v_f^2 = 2g\bar{G}S \tag{39}$$

where v_o = impact velocity

v_f = final velocity (usually zero)

g = acceleration of gravity (32.2 ft/sec^2)

$\bar{G}$ = deceleration in "G" units (average)

S = stopping distance.

Solving for S gives

$$S = \frac{v_o^2 - v_f^2}{2g\bar{G}} \tag{40}$$

This expression is useful for assessing the required stroking distance for a seat when impact velocity and acceleration limitations are known; however, it must be noted that this relation yields the total stroking distance, including deformations of the impacted surface and deflection of the gear, fuselage, and seat. Superposition of the seat, structure, and impacted surface characteristics can be used to assess the net average deceleration experienced by a seat occupant.

Figure 86 shows the variation of stopping distance as a function of G and velocity change (Δv) derived from the standard Newtonian equations for assumed constant acceleration.

These characteristics assume 100 percent efficiency, but a real structure will react somewhat differently, requiring larger stopping distances for given velocity changes and/or deceleration levels. The elapsed time values can be used for assessing human tolerance potential when human injury criteria are known as functions of G level and exposure time.

Figure 86 is useful for the initial assessment of motion envelopes needed to provide occupants with a survivable decelerative environment and for the requirements of various structural energy-absorption elements.

It is interesting to compare several deceleration pulse shapes (negative acceleration) to show the effect pulse shape has on deceleration distance. Rectangular, triangular, and sinusoidal pulses are considered.

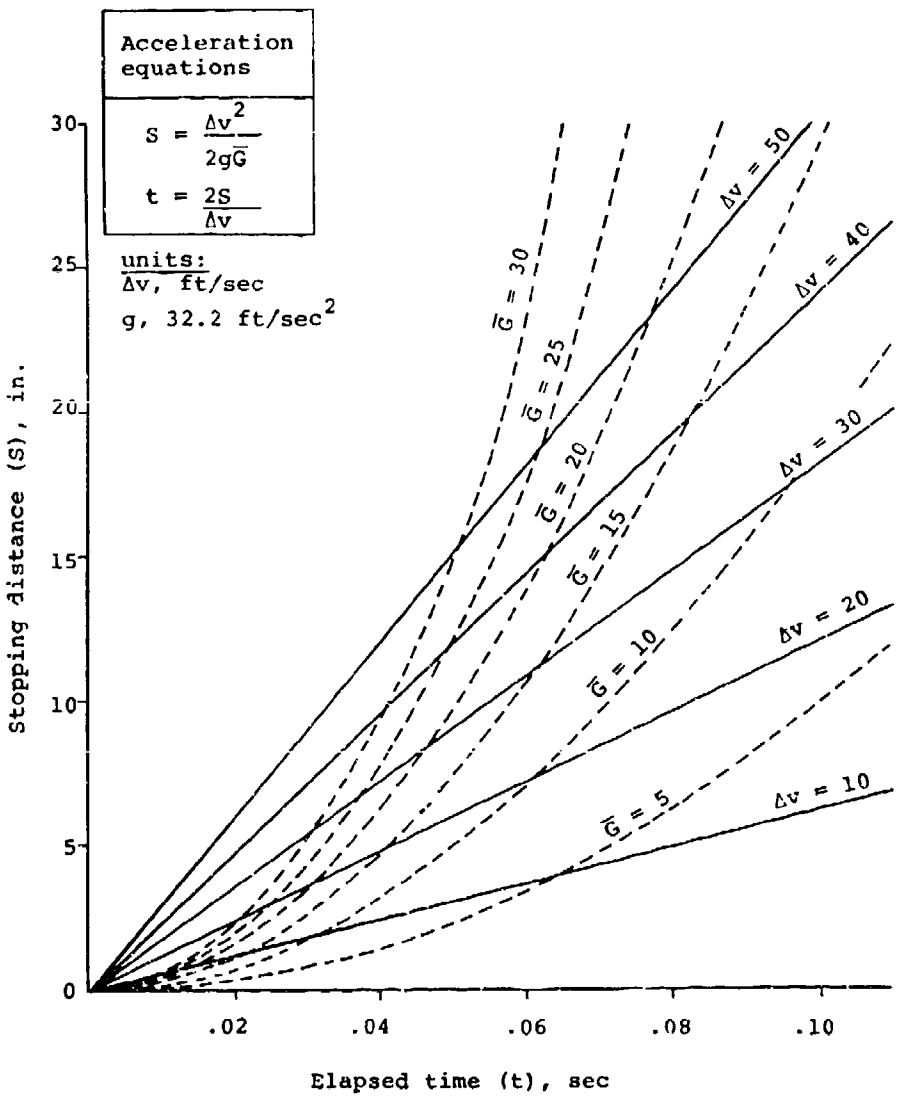

FIGURE 86. THEORETICAL STOPPING DISTANCE AS A FUNCTION OF VELOCITY CHANGE AND AVERAGE DECELERATION LEVEL.

7.2.3.1 Rectangular Deceleration Pulse

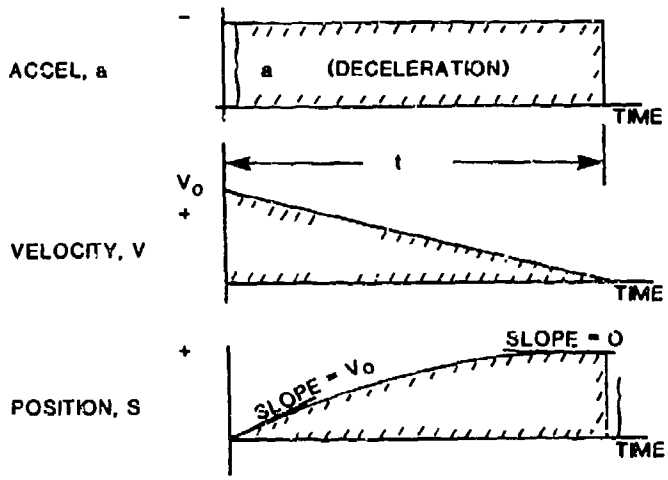

From Equation (24) $$v_o = at \tag{41}$$

Then, $$t = v_o/a$$

From Equation (25) $$S = \frac{1}{2} v_o t \tag{42}$$

So that $$S = \frac{1}{2} v_o \cdot \frac{v_o}{a}$$

or $$v_o^2 = 2aS \tag{43}$$

and $$S = \frac{1}{2} \frac{v_o^2}{a} \tag{44}$$

The implications of Equations (43) and (44) are that for a large v_o, a very large stopping distance would be required. With a small deceleration, a large stopping distance is also required.

7.2.3.2 Triangular Deceleration Pulse

Comparing two triangular pulses here, one with zero rise (onset) time and another with zero offset time,

Zero Rise Time	Zero Offset Time
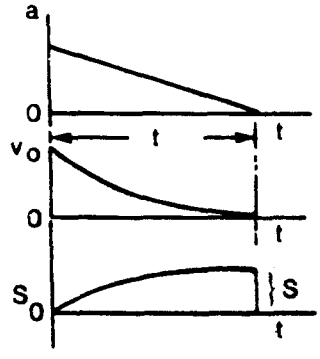	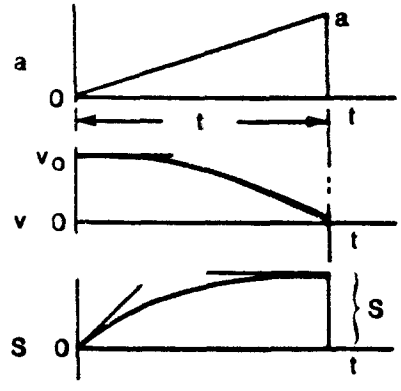
$\frac{1}{2}at = v_o$	$\frac{1}{2}at = v_o$
$t = \frac{2v_o}{a}$	$t = \frac{2v_o}{a}$
$S = \frac{1}{3}v_o t$	$S = \frac{2}{3}v_o t$
$= \frac{1}{3}v_o \cdot \frac{2v_o}{a}$	$= \frac{2}{3}v_o \cdot \frac{2v_o}{a}$
$S = \frac{2}{3}\frac{v_o^2}{a}$	$S = \frac{4}{3}\frac{v_o^2}{a}$

Note that the deceleration pulses are equal in time ($t = 2v_o/a$) but that the zero-rise-time case requires twice the deceleration distance of the zero offset time case.

7.2.3.3 Symmetrical Triangular Pulse

For a symmetrical (isoceles) triangular pulse,

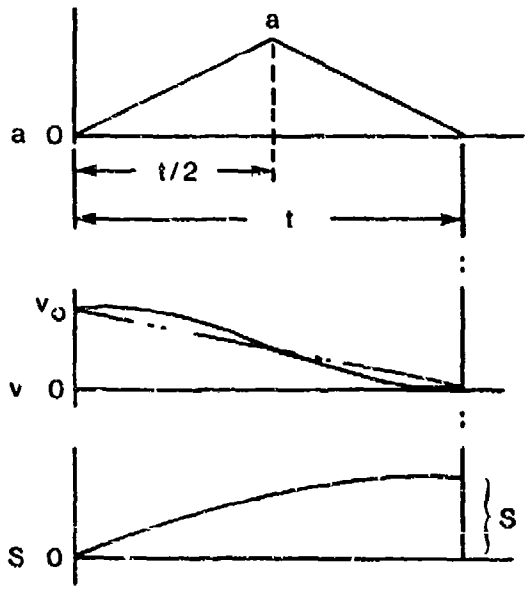

$$\frac{1}{2} at = v_o$$

$$t = \frac{2v_o}{a}$$

$$S = \frac{1}{2} v_o t$$

$$S = \frac{1}{2} v_o \left(\frac{2v_o}{a}\right) = \frac{v_o^2}{a}$$

7.2.3.4 Summary for the Case of Final Velocity, v_f, = 0

Summaries for various shaped pulses are included below:

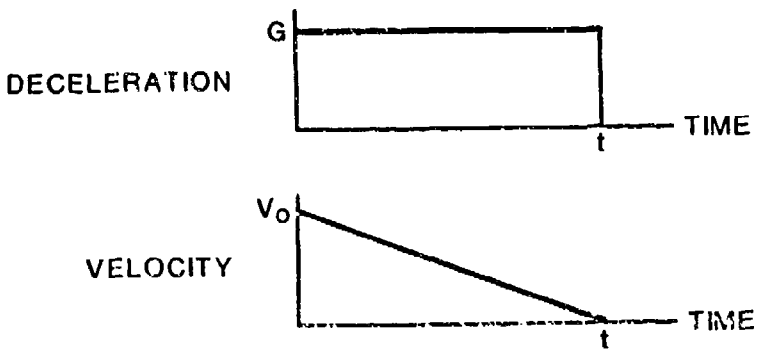

	Rectangular Pulse
Pulse Duration:	$t = \frac{v_o}{32.2G}$
Deceleration Level:	$G = \frac{v_o^2}{64.4S}$
Stopping Distance:	$S = \frac{v_o^2}{64.4G}$
or	$S = \frac{32.2Gt^2}{2}$

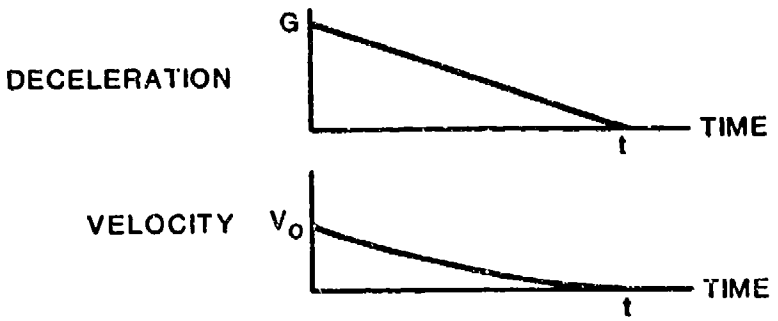

Triangular Pulse No. 1

Pulse Duration: $t = \frac{2v_o}{32.2G}$

Deceleration Level: $G = \frac{2v_o^2}{96.6S}$

Stopping Distance: $S = \frac{2v_o^2}{96.6G}$

or $S = \frac{32.2Gt^2}{6}$

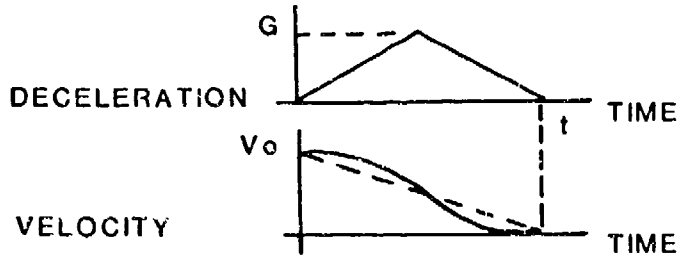

Triangular Pulse No. 2

Pulse Duration: $t = \frac{2v_o}{32.2G}$

Deceleration Level: $G = \frac{v_o^2}{32.2S}$

Stopping Distance: $S = \frac{v_o^2}{32.2G}$

or $S = \frac{32.2Gt^2}{4}$

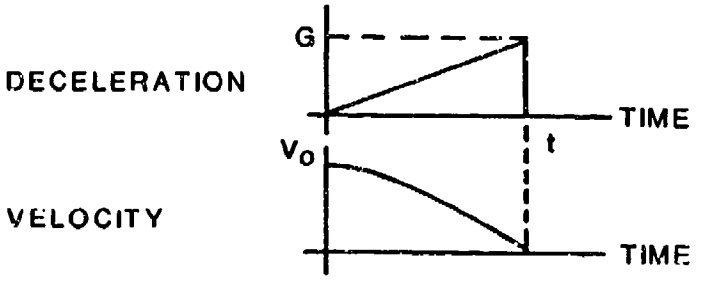

Triangular Pulse No. 3

Pulse Duration: $t = \frac{2v_o}{32.2G}$

Deceleration Level: $G = \frac{4v_o^2}{96.6S}$

Stopping Distance: $S = \frac{4v_o^2}{96.6G}$

or $S = \frac{32.2Gt^2}{3}$

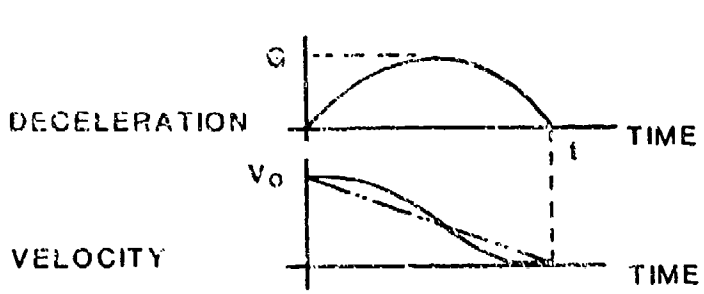

Half-Sine Pulse

Pulse Duration: $t = \frac{1.57v_o}{32.2G}$

Deceleration Level: $G = \frac{0.7854v_o^2}{32.2S}$

Stopping Distance: $S = \frac{0.7854v_o^2}{32.2G}$

or $S = \frac{32.3Gt^2}{3.14}$

A plot of these equations is given in Figure 87. Relative times and stopping distances are shown in Figure 88 for convenient visual comparison.

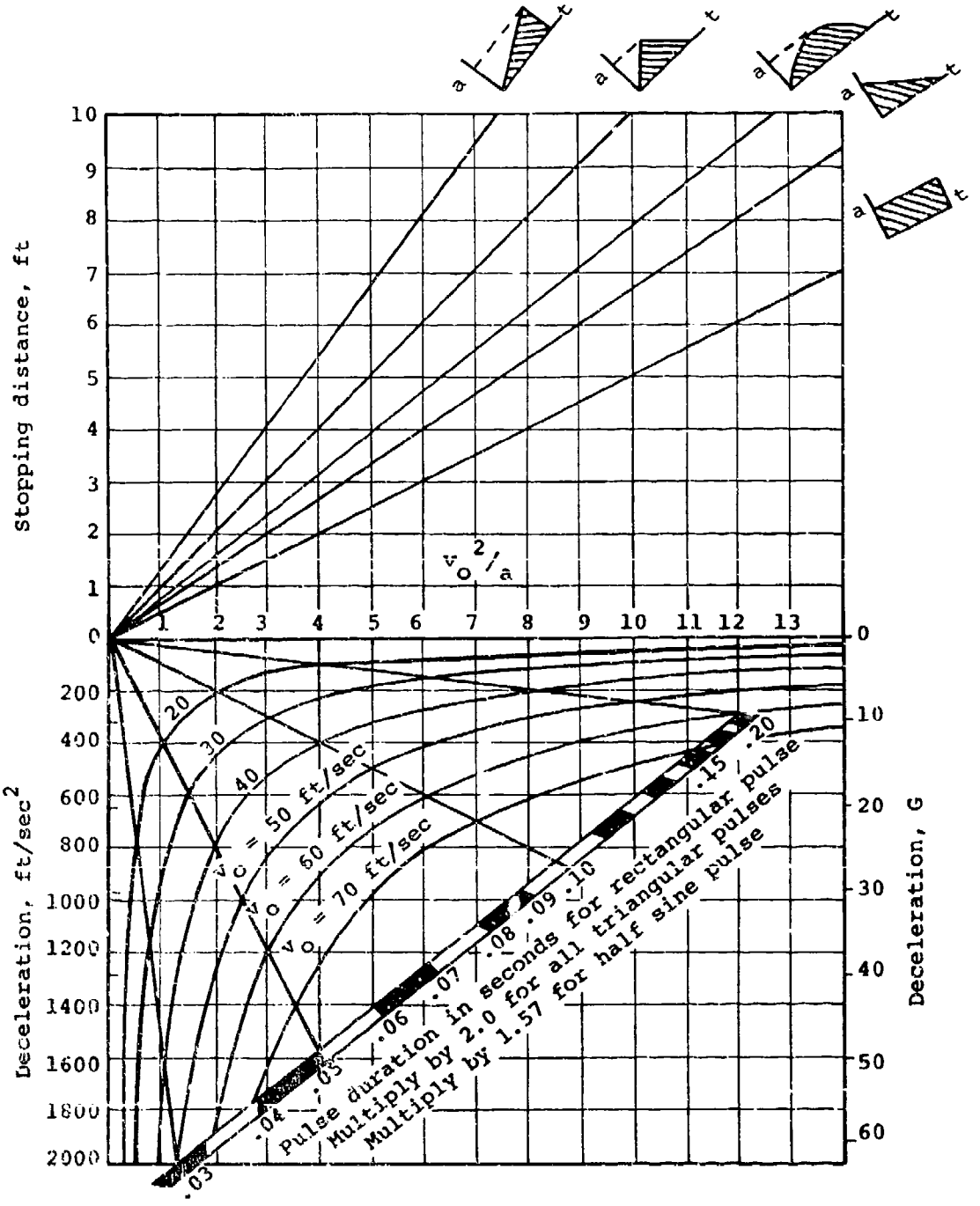

FIGURE 87. DECELERATION, VELOCITY, AND DISTANCE AS FUNCTIONS OF TIME FOR FIVE PULSE SHAPES.

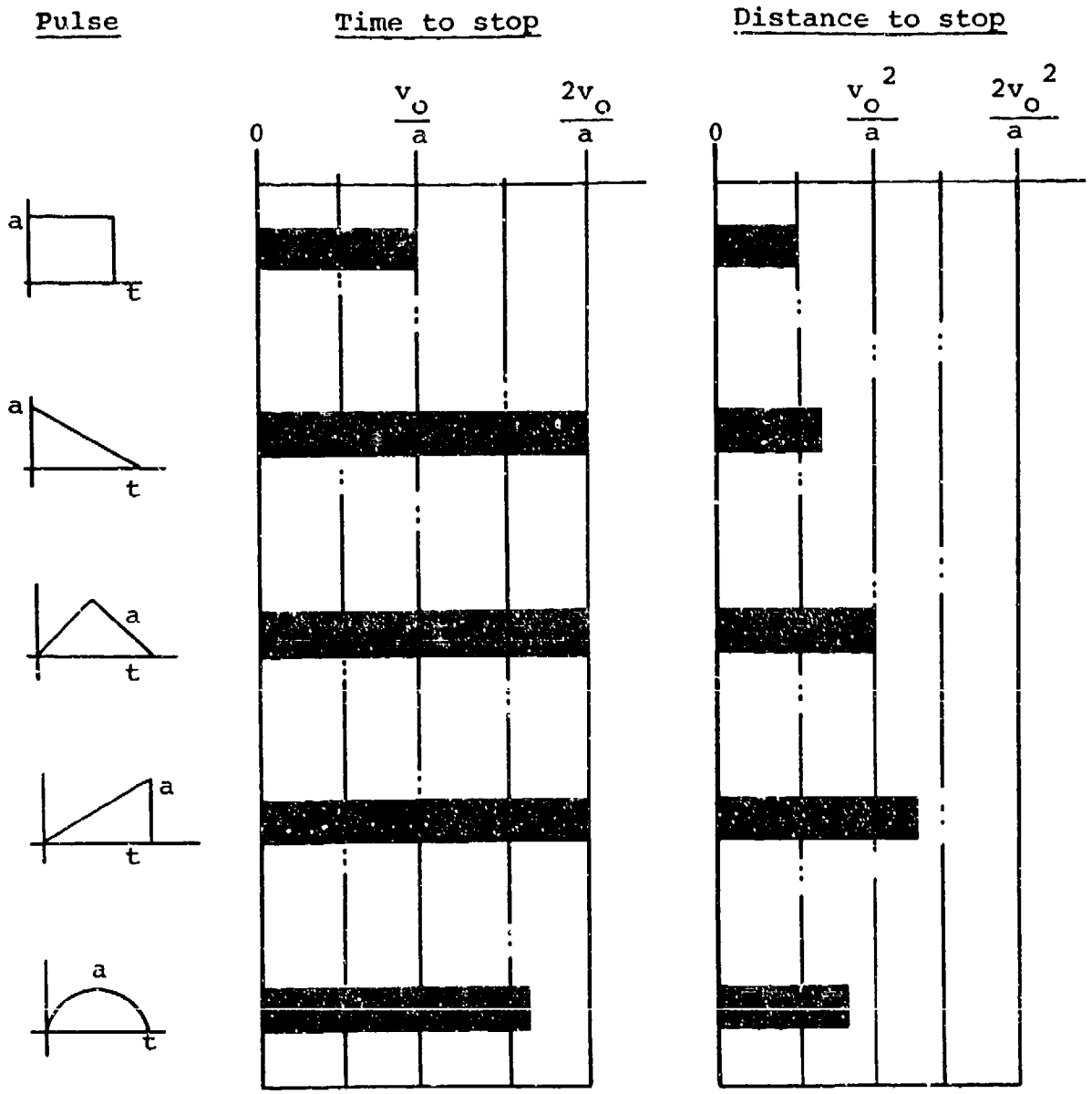

FIGURE 88. COMPARISON OF STOPPING DISTANCE FOR VARIOUS DECELERATION PULSE SHAPES.

Note that the time to stop is equal for all three triangular deceleration-time pulses, but that the stopping distances are not. Minimum stopping distance is achieved with the rectangular pulse and hence it is the most desired pulse shape from a consideration of deceleration from maximum velocity at a given deceleration level in the shortest possible distance.

7.2.3.5 Summary for the Case of Final Velocity, $v_f \neq 0$

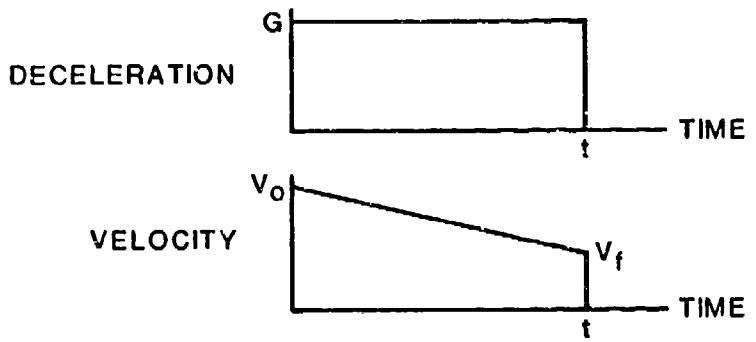

Rectangular Pulse

Pulse Duration: $$t = \frac{v_o - v_f}{32.2G}$$

Deceleration Level: $$G = \frac{v_o^2 - v_f^2}{64.4S}$$

Stopping Distance: $$S = \frac{v_o^2 - v_f^2}{64.4G}$$

or $$S = v_o t - \frac{32.2Gt^2}{2}$$

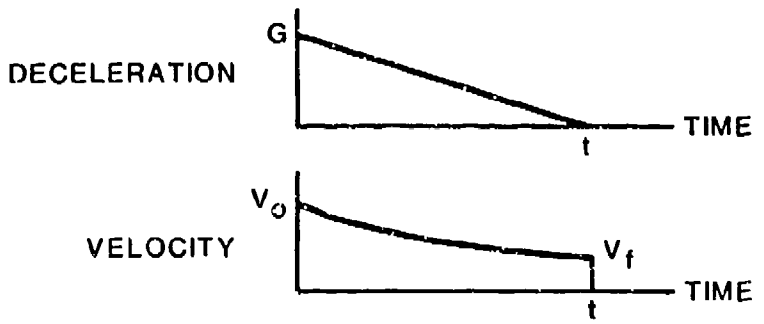

Triangular Pulse No. 1

Pulse Duration: $$t = \frac{2(v_o - v_f)}{32.2G}$$

Deceleration Level: $$G = \frac{2v_o^2 + 2v_o v_f - 4v_f^2}{96.6S}$$

Stopping Distance: $$S = \frac{2v_o^2 + 2v_o v_f - 4v_f^2}{96.6G}$$

or $$S = v_o t - \frac{32.2Gt^2}{3}$$

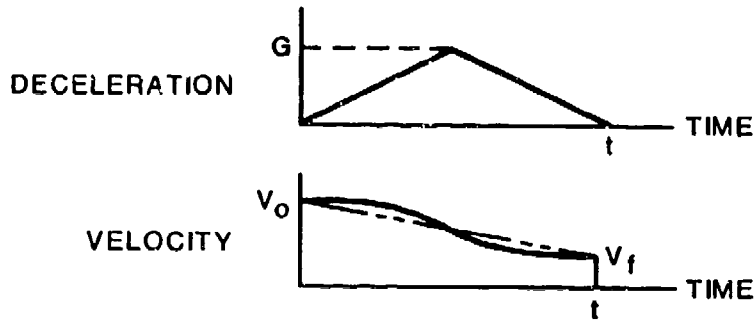

Triangular Pulse No. 2

Pulse Duration: $$t = \frac{2(v_o - v_f)}{32.2G}$$

Deceleration Level: $$G = \frac{v_o^2 - v_f^2}{32.2S}$$

Stopping Distance: $$S = \frac{v_o^2 - v_f^2}{32.2G}$$

or $$S = v_o t - \frac{32.2Gt^2}{4}$$

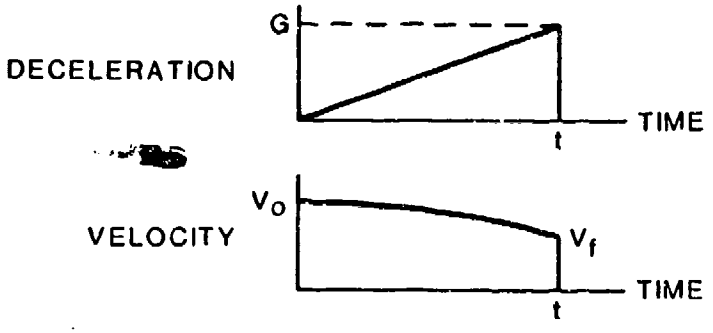

Triangular Pulse No. 3

Pulse Duration: $$t = \frac{2(v_o - v_f)}{32.2G}$$

Deceleration Level: $$G = \frac{4v_o^2 + 2v_o v_f - 2v_f^2}{96.6S}$$

Stopping Distance: $$S = \frac{4v_o^2 + 2v_o v_f - 2v_f^2}{96.6G}$$

or $$S = v_o t - \frac{32.2Gt^2}{6}$$

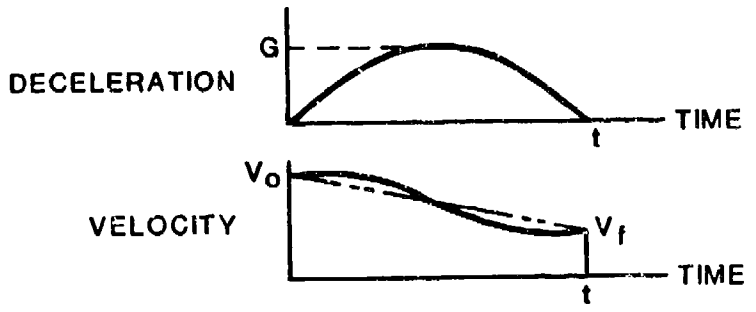

Half Sine Pulse

Pulse Duration: $$t = \frac{1.57\ (v_o - v_f)}{32.2G}$$

Deceleration Level: $$G = \frac{0.7854\ (v_o^2 - v_f^2)}{32.2S}$$

Stopping Distance: $$S = \frac{0.7854\ (v_o^2 - v_f^2)}{32.2G}$$

or $$S = v_o t - \frac{32.2Gt^2}{3.14}$$

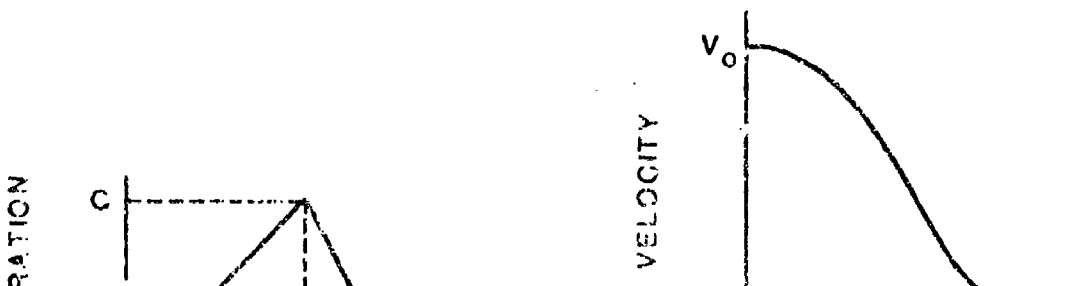

2/3T TRIANGULAR PULSE

2/3t Triangular Pulse

Pulse Duration: $t = \frac{2(v_o - v_f)}{32.2G}$

Deceleration Level: $G = \frac{10\,v_o^2 - 2\,v_o v_f - 8\,v_f^2}{289.9S}$

Stopping Distance: $S = \frac{10\,v_o^2 - 2\,v_o v_f - 8\,v_f^2}{289.9G}$

or $S = v_o t - \frac{32.2Gt^2}{4.5}$

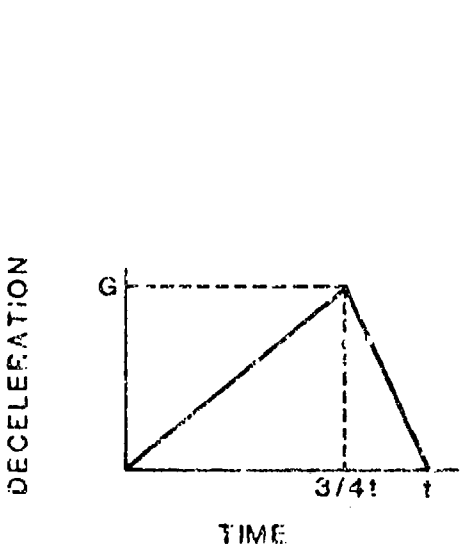

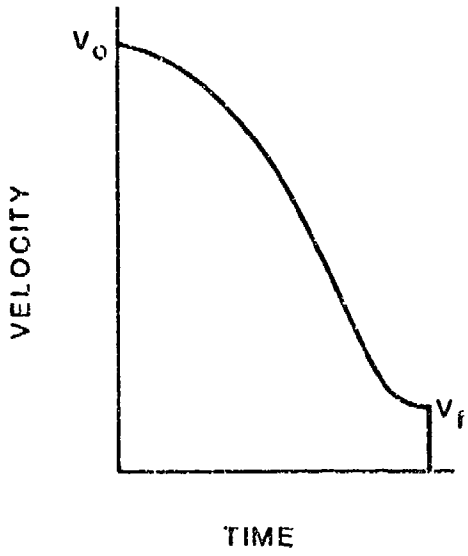

3/4T TRIANGULAR PULSE

3/4T Triangular Pulse

Pulse Duration: $t = \frac{2(v_o - v_f)}{32.2G}$

Deceleration Level $G = \frac{3.5\, v_o^2 - v_o v_f - 2.5\, v_f^2}{96.6S}$

Stopping Distance $S = \frac{3.5\, v_o^2 - v_o v_f - 2.5\, v_f^2}{96.6S}$

or $S = v_o t - \frac{32.2Gt^2}{4.8}$

7.3 APPLICATION OF KINEMATIC RELATIONSHIPS AND ENERGY ABSORPTION PRINCIPLES TO PRELIMINARY DESIGN STUDIES

In order to design an effective crash-resistant system it is necessary to make initial decisions regarding the percentage of pre-impact kinetic energy to be absorbed by the landing gear, fuselage, and seat systems. These decisions must be made early in the design process because they can be the driving factors in setting fuselage ground clearance (landing gear geometry) and depth of fuselage underfloor structure.

This section presents two examples illustrating an energy balance analysis that can be used for preliminary design of the landing gear, seat system, and fuselage structure. The examples are representative of two different fuselage design philosophies.

The first example is a structure designed such that the underfloor structure absorbs energy through plastic deformation, while the structure supporting the large overhead masses (engine, transmission, etc.) is strong enough to resist the crash-induced loads without plastic deformation. The second example illustrates the effect of designing a structure such that both the underfloor and overhead support structure deform plastically. Both concepts can provide occupant protection.

In both examples the stroking characteristics (load factor and length of stroke) are selected for the landing gear and seat system before sizing the fuselage energy-absorbing capabilities. The system is designed in this order, because the landing gear and seats often have to meet specific requirements, such as MIL-STD-1290, MIL-S-58095 (Reference 71), and MIL-S-85510 (Reference 72). The fuselage structure must then be designed to absorb the remaining energy not absorbed by the landing gear or seat system. (However, energy absorption in the fuselage should by given preference when possible, because the gear will not be effective on soft soil or water.)

Sections 7.3.1 and 7.3.2 are general discussions of landing gear and seat system design criteria and procedures. Section 7.3.3.3 presents an example of designing fuselage structure such that the support structure for overhead masses does not plastically deform, and Section 7.3.3.2 presents an example of designing fuselage structure so that both the underfloor and overhead structure absorb energy through large plastic deformations. The elements of the energy-absorbing system (landing gear, seat, fuselage structure, and available stroking distance) are illustrated in Figure 89.

Some values in the following illustrative calculations are taken from appropriate military specifications. Others are typical values used for illustration. They do not represent design requirements. Systems specifications and referenced military specifications should provide all design parameters for an actual application.

7.3.1 Selection of Seat System Stroking Forces

To limit occupant spinal injury MIL-S-58095 and MIL-S-85510 require that occupant vertical decelerations not exceed 23 G for a total of 0.025 sec. To compensate for dynamic overshoot effects, the seat system vertical load-limiting device must be designed to stroke at a load factor that is significantly less

S_{LG} = DISTANCE SEAT AND OCCUPANT MOVE WHILE BEING DECELERATED BY LANDING GEAR STROKING

S_F = DISTANCE SEAT AND OCCUPANT MOVE WHILE BEING DECELERATED BY CRUSHING OF FUSELAGE UNDERFLOOR STRUCTURE

S_S = DISTANCE SEAT AND OCCUPANT MOVE DURING STROKING OF THE ENERGY ABSORBING SEAT SYSTEM. THIS MAY OCCUR SIMULTANEOUSLY OR AFTER CRUSHING OF FUSELAGE STRUCTURE.

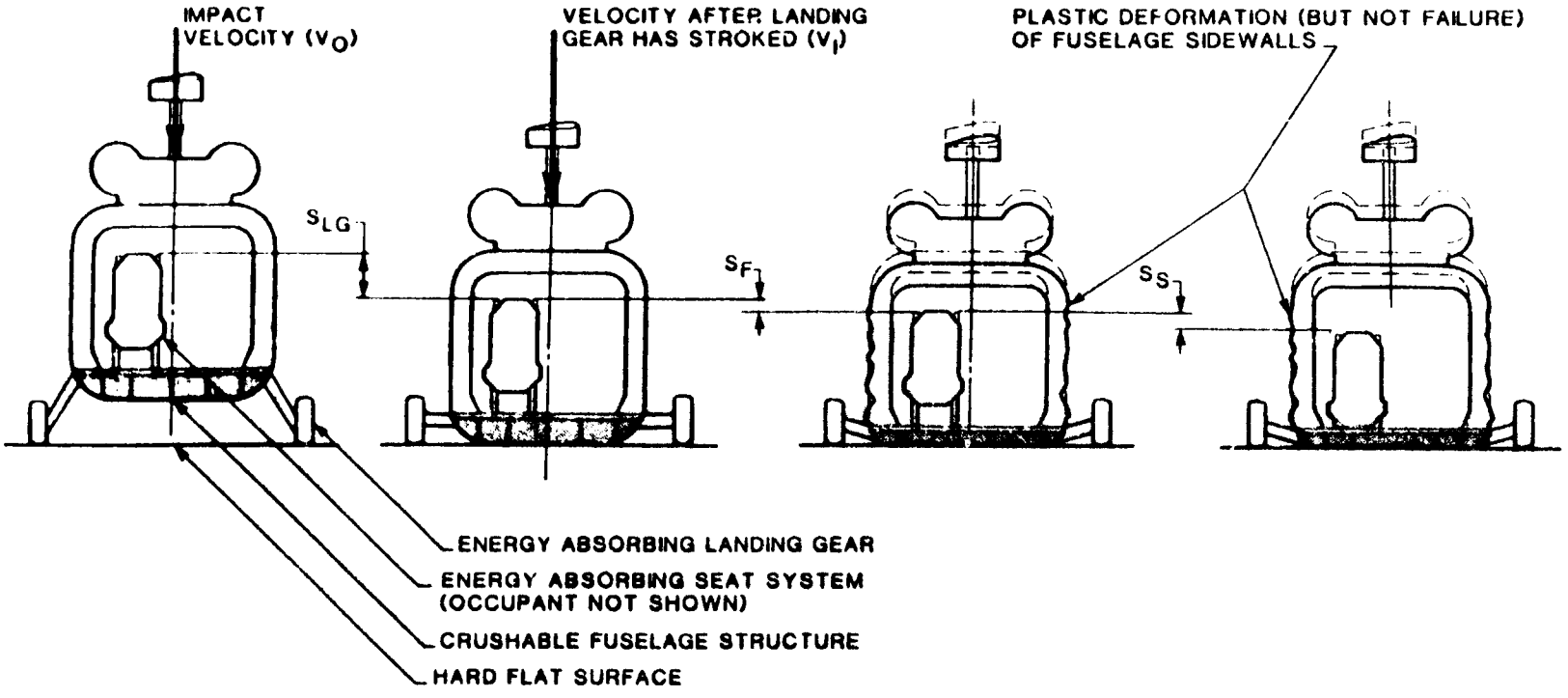

FIGURE 89. ENERGY ABSORPTION SEQUENCE DURING VERTICAL CRASH OF A CRASH-RESISTANT AIRCRAFT SYSTEM.

than 23 G. For most military helicopters 14.5 G has been selected for the seat system stroking load factor. This value has been found to prevent the occupant dynamic deceleration from exceeding the 23-G, 0.025-sec criteria.

The seat system stroking distance is generally limited by the distance from the bottom of the seat bucket to the floor structure. This distance can be increased in some cases by designing a well in the floor so that the seat bucket can stroke into the well. MIL-S-58095 and MIL-S-85510 require that a minimum of 12 in. stroking distance be provided with the seat bucket in the full-down adjustment position. It is, of course, desirable to provide as much stroking distance as possible, since the seat provides the most reliable occupant energy-absorption capability. It can usually function within stroking limits even when the energy absorption of the airframe and landing gear are unable to perform as desired because of impact conditions.

According to MIL-S-58095 and MIL-S-85510, the test criteria for an energy-absorbing seat includes a 50-ft/sec vertical impact with a 30-degree nose-down pitch and a 10-degree roll. The vertical velocity component of this impact is 42 ft/sec, which is the same as that specified for the fuselage in MIL-STD-1290. The seat test criteria includes lateral and vertical components to assure that the seat mechanism will stroke in a combined-load condition.

If the seat had to absorb all occupant/seat energy in a 42 ft/sec vertical impact with the seat stroking at a uniform 14.5-G load, it would have to stroke about 24 in. Since that distance generally cannot be made available, the seat, fuselage, and landing gear must be designed as a complete energy-absorbing system in order to provide adequate protection for the occupant.

7.3.2 Selection of Landing Gear System Stroking Forces

MIL-STD-1290 requires that the landing gear protect the fuselage from damage following touchdown at a 20-ft/sec sink rate with a pitch of +15/-5 degrees and roll attitudes up to ±10 degrees. To prevent fuselage damage and to allow the landing gear to decelerate the aircraft effectively, the landing gear must be designed to stroke at a load that is low enough to prevent overstressing the fuselage structure. If, for instance, the fuselage design limit-load factor were 5.5 G, the landing gear would be designed to stroke at a lower-load factor, such as 5 G. The highest decelerations will occur when the impact attitude is level, causing all landing gear to stroke simultaneously. If the landing gear were designed to produce a 5-G deceleration following impact with no roll, each landing gear would have to be designed to produce only a 2.5-G deceleration if acting separately from the other gear. As illustrated in Figure 90, one gear can indeed act alone following impact with 10 degrees of roll.

The length of the landing gear stroke must be long enough to absorb the pre-impact kinetic energy even with a 10-degree roll attitude at impact. In the example shown in Figure 90, the majority of the kinetic energy must be absorbed by only one landing gear.

The length of landing gear stroke needed to protect the fuselage can be calculated using the assumption that (neglecting friction) the preimpact kinetic energy will be totally converted to work during stroking of the landing gear (see Section 7.2.2).

$$\text{Kinetic Energy (KE)} = 1/2(W/g)V_o^2$$

$$\text{Work (E)} = \bar{F} \times S$$

For complete conversion of kinetic energy to energy-absorbing work,

$$KE = E$$

$$1/2(W/g)V_o^2 = \bar{F} \times S = \bar{G} \times W \times S \qquad (45)$$

where W = effective stroking weight of the entire aircraft (lb)

g = gravity constant (32 ft/sec^2)

V_o = vertical velocity at impact (ft/sec)

$\bar{F}$ = average stroking force (lb)

S = stroking distance (ft)

$\bar{G}$ = average load factor caused by stroking energy absorber

For example, let

W_F = effective weight of the fuselage and its payload

G_{LG} = maximum landing gear load factor

S_{LGS} = landing gear stroking distance (sum of LH and RH gear stroking)

η = efficiency = $\bar{F}/F_{max} = \bar{G}/G_{max}$

The required stroking distance that must be designed into the landing gear can be calculated by substituting into Equation (45) and solving as shown below:

$$1/2(W_F/g)V_o^2 = G_{LG} \times \eta \times W_F \times S_{LGS}$$

$$S_{LGS} = V_o^2/(2 \times G_{LG} \times \eta \times g) \qquad (46)$$

For most gear geometries it is probable that upon impacting with a 10-degree roll attitude both main landing gear will stroke, but not the same distance. The downside landing gear will stroke farther than the upside gear, as illustrated in Figure 90. The exact amounts must be determined from the geometric relationship of the fuselage and landing gear.

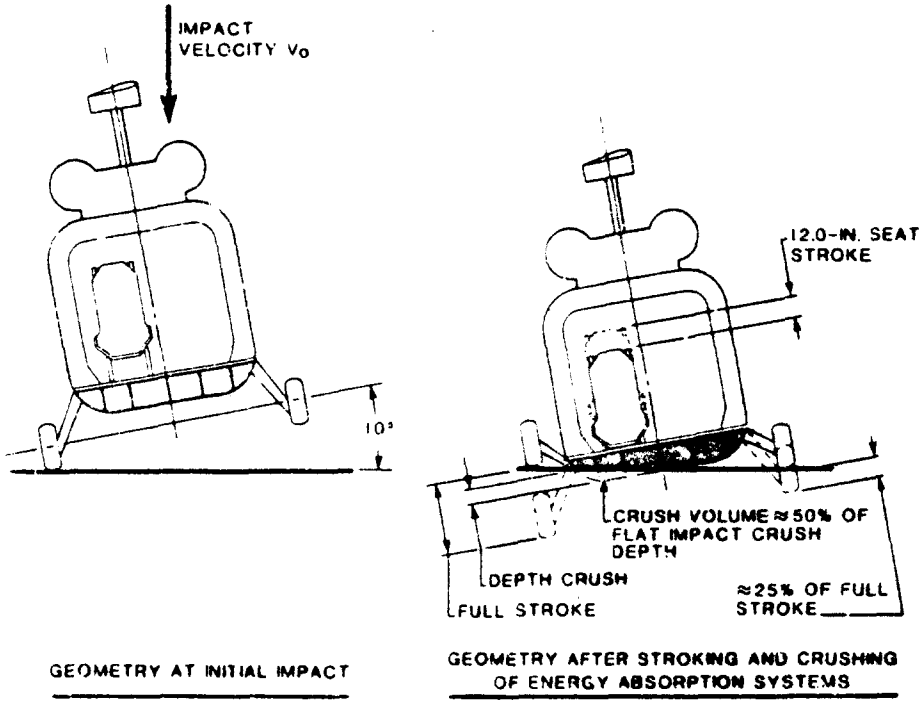

FIGURE 90. EXAMPLE CRASH GEOMETRY WITH 10-DEGREE ROLL ATTITUDE AT IMPACT.

It should also be recognized that in some crashes the gear will fail to provide any appreciable deceleration to the fuselage. This will be true of an impact on water or soft soil. It may also be true in crashes having airframe dynamics that cause the gear to fail before appreciable stroke has occurred. An example might be a crash with a high lateral velocity component.

The sample calculations shown here illustrate the effect of an energy-absorbing gear impacting on a hard level surface. However, because the gear is the least reliable contributor to the energy-absorbing process (due to variability of impact surfaces), the eventual design should be as conservative as possible in the areas of seat and fuselage energy absorption, so that the maximum possible survivability remains if the gear does not contribute to the energy-absorption process. Helicopters with retractable landing gear will accentuate the need for energy absorption in the structure and seat. Any self-righting of the aircraft is ignored for simplicity and conservatism.

For example, if the landing gear shown in Figure 90 were designed to limit maximum fuselage loading to 5 G, with an efficiency of 80 percent, at impact velocities up to 20 ft/sec, the required length of available landing gear stroking distance would be calculated as follows.

$$G_{LG} = 1/2 \times 5G = 2.5G$$

To protect the fuselage with a 10-degree roll attitude, the downside gear would stroke its full distance, while the upside gear would only stroke approximately 25 percent of its full available stroking length (see Figure 90). If S_{LG} is the maximum stroking travel available for each gear, then

$$S_{LGS} = 1.0 \times S_{LG} + 0.25 \times S_{LG} = 1.25\ S_{LG}$$

Neglecting the 10-degree misalignment between the velocity vector and the direction of gear stroke, the SLG can be approximated by substituting into Equation (46),

$$1.25\ S_{LG} = (20\ \text{ft/sec})^2/(2)(2.5)(.8)(32.2\ \text{ft/sec}^2)$$

$$S_{LG} = 2.5\ \text{ft}$$

If the same aircraft were to impact at a 0-degree roll attitude, fuselage protection would be provided up to a higher impact velocity. The calculations using Equation (46) would be as follows:

$$2(2.5)\text{ft} = V_o^2/(2)(2.5)(.8)(32.2\ \text{ft/sec}^2)$$

$$V_o = 25.3\ \text{ft/sec}$$

Thus, for the example helicopter, the landing gear must be designed to stroke a minimum of 2.5 ft, at 2.5 G (per gear), with 80 percent efficiency, in order to prevent fuselage damage following impact at 20 ft/sec with a 10-degree roll. This same landing gear design will prevent damage to the fuselage following impact at 25.3 ft/sec, if the impact occurs in a level attitude onto a solid level surface.

7.3.3 Fuselage Structure

The fuselage structure must be designed to absorb the kinetic energy that will not be absorbed by the landing gear and seat systems (ignoring the energy that will be absorbed by the touchdown surface). There are five variables involved in designing the basic characteristics of the crushable underfloor structure:

1. Maximum vertical velocity at impact
2. Maximum fuselage deceleration load factor
3. Average deceleration, related to maximum by an efficiency factor
4. Depth of underfloor structure
5. Fraction of depth that is crushable.

7.3.3.1 Impact Velocity. MIL-STD-1290 specifies that the aircraft be designed to protect the occupants following impact on a hard smooth surface at a vertical velocity of 42 ft/sec with pitch and roll attitudes of up to +15/-5 and ±10 degrees, respectively. For aircraft not designed to meet MIL-STD-1290, a review of accident statistics for similar aircraft, used in the same manner, will provide guidance in determining the degree of protection that is required.

7.3.3.2 Design of Fuselage Underfloor Structure for Use With Rigid Fuselage Sidewalls. A schematic of a crash-resistant aircraft with rigid side walls (not designed to absorb energy through plastic deformation) is shown in Figure 91. The fuselage structure must be designed to absorb the preimpact kinetic energy that will not be absorbed by the landing gear and seat system.

A well-designed landing gear can, under ideal conditions, stroke and absorb energy during the crushing of the fuselage. However, the following analysis assumes for simplicity that the landing gear ceases to contribute energy-absorbing strokes after the fuselage contacts the earth.

With the above assumptions, the following relationship applies:

$$KE = 1/2(W/g)V_1^2 = \bar{F}_F S_F + \bar{F}_S X_S \qquad (47)$$

where W = combined weight of the fuselage, seat, and occupant

KE = kinetic energy

g = gravity constant (32.2 ft/sec^2)

V_1 = velocity of fuselage after completion of landing gear stroking

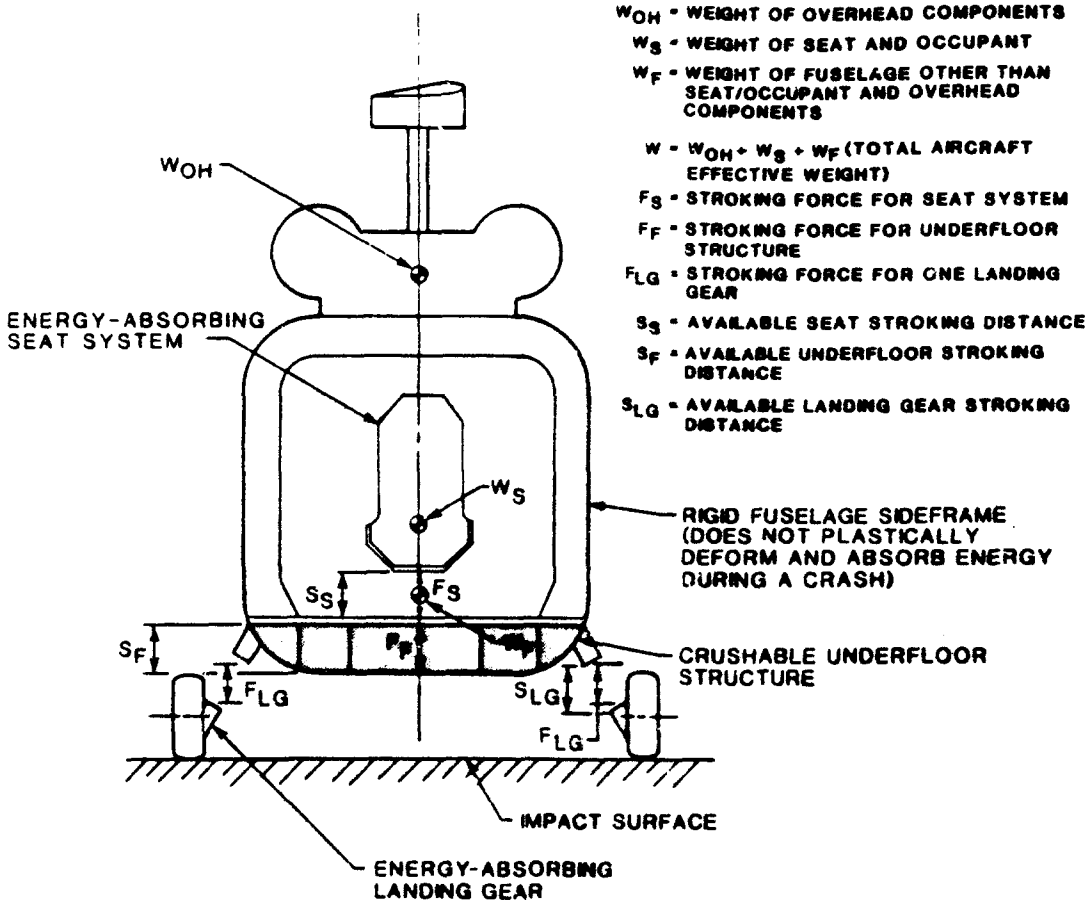

FIGURE 91. SCHEMATIC OF AIRCRAFT CRASH-RESISTANT SYSTEM USING RIGID FUSELAGE SIDEWALLS.

$\bar{F}_F$ = average force required to crush the fuselage underfloor structure

S_F = crush depth of underfloor structure

$\bar{F}_S$ = average force required to stroke the seat energy absorber

X_S = distance stroked by the seat energy absorber (relative to fuselage).

As shown by Equation (47), there are an infinite number of combinations of F_F and S_F that will absorb the kinetic energy. However, there is a

maximum value of $\bar{F}_F$ that will be compatible with the stroking force and distance already selected for the seat system (see Section 7.2.1). If the value of $\bar{F}_F$ exceeds this value, the seat system will not be able to limit the G loads on the occupant throughout the crash. This is because the occupant would still have residual velocity when the seat stroke bottoms, leading to a sudden high deceleration and possible injury. (The same problem will occur if $\bar{F}_F S_F$ is too low and the underfloor structure absorbs insufficient energy.)

The required deceleration rate for the fuselage structure can be calculated using the following relationship:

$$\bar{G}_{Fmax} = V_1^2 \bar{G}_S / (V_1^2 - 2g\bar{G}_S S_S) \qquad (48)$$

where $\bar{G}_{Fmax}$ = maximum fuselage deceleration rate (g's) that will allow the seat system to bring the occupant to rest before the seat bottoms

V_1 = velocity after completion of gear stroking, but prior to initiation of fuselage underfloor structure crushing

g = gravity constant (32.2 ft/sec^2)

$\bar{G}_S$ = seat system average stroking load factor

S_S = maximum available seat system stroking distance.

Equation (48) can be derived by substituting the appropriate values of G and W into Equation (47) for $\bar{F}_S$ and $\bar{F}_F$ ($\bar{F}_F = W_F\bar{G}_F + W_S\bar{G}_S$, $\bar{F}_S = W_S\bar{G}_S$) and noting that $X_S = S_S$ and $S_F = V_1^2/2g\bar{G}_F$ (reference Equation 40).

The second factor that must be considered when defining the fuselage underfloor structure crushing depth and force is the effect on retention of high-mass items, such as engines, transmission, etc., during a crash. For this reason the floor structure for aircraft required to comply with MIL-STD-1290 might be designed to crush at a load factor of 15 to 20 G, because this value corresponds to the requirement in MIL-STD-1290 that potentially hazardous high-mass items be designed to withstand a vertical load factor of +20/-10 G (see MIL-STD-1290 for a complete listing of high-mass retention requirements). Thus, the floor structure crushing helps protect against loss of retention of high-mass items.

To determine the required crush depth for the fuselage underfloor structure, the following steps are required:

1. Define the crash design conditions.

   a. Maximum initial impact velocity
   b. Aircraft impact attitude limits

2. Define landing gear design requirements and calculate the velocity of the aircraft at initiation of fuselage crushing.

$$\Delta KE = 1/2(W/g)(V_o^2 - V_1^2) = \bar{G}_{LG} W S_{LGS} \qquad (49)$$

where W = weight of fuselage and occupant

g = gravity constant (32.2 ft/sec^2)

V_o = initial impact velocity when landing gear first contacts the ground

V_1 = velocity when the fuselage first contacts the ground

$\bar{G}_{LG}$ = average stroking load factor of landing gear (per side)

S_{LGS} = sum of the distances stroked by the LH and RH main landing gear (the distances are equal only for impact at a 0-degree roll attitude).

3. Determine the crush distance required to bring the fuselage structure to rest at a constant rate of deceleration.

$$S_F = V_1^2/2\bar{G}_F g \qquad (50)$$

where S_F = required crush depth for fuselage underfloor structure

$\bar{G}_F$ = average deceleration rate of fuselage.

4. Use Equation (48) to calculate the maximum allowable value for G_F to ensure that the selected value will provide occupant protection.

As an example, consider a helicopter design with the following characteristics:

1. Landing gear - designed to stroke at 4.0 G (per main gear) with 2.5 ft of available stroke (see Section 6.2 for explanation of why landing gear load factor at the 42-ft/sec impact condition may be expected to be higher than at the 20-ft/sec condition).

2. Seat system - 12 in. of stroke at 14.5 G (meets MIL-S-58095 and MIL-S-85510 requirements).

3. Fuselage structure - designed to crush at 20 G (level attitude at impact).

4. Vertical velocity at initial impact = 42 ft/sec (MIL-STD-1290).

Calculations:

1. Determination of fuselage velocity after landing gear stroke:

   The critical case (neglecting pitch) is impact at 10-degree roll attitude, since not all of the landing gear energy absorption capability will be used. See Figure 90 for example landing gear geometry after stroking. The actual value of stroking distance will vary for different designs and must be determined from a kinematic study of each proposed gear configuration.

$$1/2(W/g)(V_o^2 - V_1^2) = \bar{G}_{LG} W S_{LGS}$$

$$1/2(W/32.2\ ft/sec^2)((42.0\ ft/sec)^2 - V_1^2) = 4.0W(1 + 0.25)\ 2.5ft$$

$$V_1 = 31.0\ ft/sec$$

2. Determination of crush distance (S_F) required to bring the fuselage to rest at 20-G deceleration rate:

   For the example geometry shown in Figure 9C, approximately half the underfloor structure will be effective if a 10-degree roll attitude exists at impact. Thus a structure designed to produce 20-G deceleration for a level impact will only produce a 10-G deceleration at a 10-degree roll attitude.

$$S_F = V_1^2/2\bar{G}_F g = (31\ ft/sec)^2/(2)(10)(32.2\ ft/sec^2)$$

$$S_F = 1.49\ ft$$

3. Verify that the design fuselage deceleration rate of 20 G is less than the maximum deceleration that would still allow the system to fully absorb the occupant's kinetic energy without bottoming out the seat.

$$\bar{G}_{Fmax} = V_1^2\bar{G}_S/(V_1^2 - 2g\bar{G}_S S_S)$$

$$= (31.0 \text{ ft/sec})^2(14.5)/((31 \text{ ft/sec})^2$$

$$-2(32.2 \text{ ft/sec}^2)(14.5)(1 \text{ ft}))$$

$$= 512$$

The design value for $\bar{G}_F$ of 20 is less than the maximum allowable for the assumed helicopter characteristics, so the system will be able to absorb effectively the occupant's kinetic energy.

It should be noted that the above system has been designed to provide occupant protection for a 42-ft/sec impact with 10 degrees of roll. If this same aircraft were to impact with a 0-degree roll attitude, the occupant would be provided protection for a higher impact velocity.

The magnitude of the impact velocity allowable with a 0-degree roll attitude and the stroking loads and distances specified in the above example can be calculated as follows:

1. Determine the allowable fuselage impact velocity based on G_F and S_F.

$$\bar{G}_F = 20$$

$$S_F = 1.49 \text{ ft}$$

$$S_F = V_1^2/2\bar{G}_F g) = 1.49 \text{ ft} = V_1^2/((2)(20)(32.2 \text{ ft/sec}^2))$$

$$V_1 = 43.81 \text{ ft/sec}$$

2. Determine the velocity prior to gear stroking.

$$V_1 = 43.81 \text{ ft/sec}$$

$$S_{LGS} = S_{LGRH} + S_{LGLH} = 2.5 \text{ ft} + 2.5 \text{ ft} = 5.0 \text{ ft}$$

$$\bar{G}_{LG} = 4 \text{ G}$$

$$1/2(W/g)(V_o^2 - V_1^2) = \bar{G}_{LG} W S_{LGS}$$

$$1/2(W/32.2 \text{ ft/sec}^2)(V_o^2 - (43.81 \text{ ft/sec})^2) = (4.0)(W)(5.0 \text{ ft})$$

$$V_o = 56.63 \text{ ft/sec.}$$

3. To verify that the available seat stroking distance would be adequate:

$$X_S = V_1^2/2g\bar{G}_S - S_F$$

$$= (43.81 \text{ ft/sec})^2/2(32.2 \text{ ft/sec}^2)(14.5) - 1.49 \text{ ft}$$

$$= 0.57 \text{ ft}$$

Since the available seat stroking distance of 1.0 ft is greater than the 0.57 ft needed, the system will be capable of absorbing a level impact at 56.63 ft/sec.

Thus, for the example shown above, the aircraft would provide occupant protection following an impact at 42 ft/sec with a roll attitude of 10 degrees. The same aircraft would provide occupant protection at an impact velocity of 56.63 ft/sec with a 0-degree roll attitude.

In the above example, the depth of underfloor structure was sized to bring the fuselage to rest at a constant rate of deceleration following impact with a 10-degree roll attitude. Since the underfloor structure was designed to crush at a deceleration rate of 20 G in a level impact, the structure gave a deceleration rate of only 10 G for a 10-degree roll attitude impact. Because the underfloor structure was designed to bring the fuselage to rest at 10 G, the seat system would never be exposed to the 14.5-G level needed to make it stroke during a crash with a 10-degree roll.

From the standpoint of occupant protection it would not be necessary to have the underfloor structure capable of bringing the fuselage to rest at a constant rate of deceleration. Rather it would only be necessary to decelerate the floor to a low enough velocity (at completion of underfloor stroking) so that the seat/occupant kinetic energy would be equal to or less than the remaining capacity of the seat system energy absorber. If this design approach is chosen, the structure that supports the high-mass overhead items (engines, transmission, etc.) must be capable of absorbing the remaining kinetic energy of these components without letting them intrude into the survival space required by the occupants.

If the aircraft in the above example were to impact at level attitude with a velocity of 48 ft/sec and landing gear were totally ineffective, the depth of underfloor crushing and length of the seat system stroking could be calculated as follows:

1. Since the fuselage will be brought to rest at a constant deceleration of 20 G,

$$X_F = V_o^2/2\bar{G}_F g = (48 \text{ ft/sec})^2/2(20)(32.2 \text{ ft.sec}^2)$$

$$X_F = 1.79 \text{ ft} = \text{depth of underfloor crushing}$$

However, 1.79 ft of crush is not possible since there is only 1.49 ft of underfloor structure available. Therefore, S_F = 1.41 ft must be used to calculate the stroke.

2. The seat will be brought to rest at a constant deceleration of 14.5 G. The actual seat stroke relative to the underfloor structure must allow for the distance traveled by the underfloor structure. Therefore,

$$X_S = V_o^2/2\bar{G}_S g - X_F = (48 \text{ ft/sec})^2/2(14.5)(32.2 \text{ ft/sec}^2) - 1.49 \text{ ft}$$

X_S = 0.98 ft or 11.7 in. = distance required for seat to stroke without bottoming

7.3.3.3 Calculation of Required Fuselage Structural Energy Absorption Parameters if Energy Absorption is Provided for Overhead Masses. The crushing load of the underfloor structure need not necessarily be limited by the retention strength for overhead components. However, to utilize a higher underfloor crushing load factor, the structure that supports the high-mass overhead components must be designed to absorb energy through plastic deformation and/or be capable of sustaining high-G forces without failure. An example of this would be the system shown in Figure 92. In the following description, the location of the energy absorbers for the overhead masses is assumed to be in the upper sidewalls. Other energy-absorber locations, such as within the engine mounts, would use the same technique. Crushable sidewalls must, of course, also satisfy other requirements for percentage contraction of livable volume, rollover protection, and postcrash emergency egress.

Design of this system would follow steps similar to those outlined for the example of Section 7.3.3.2:

1. Define the crash design conditions.

   a. Maximum impact velocity
   b. Aircraft impact attitude limits

2. Define landing gear design requirements (see Section 7.3.2).

3. Define seat system design requirements (see Section 7.3.1).

4. Choose the fuselage crushing and overhead mass retention parameters that will absorb the kinetic energy not absorbed by the landing gear and seat system.

The landing gear and seat systems for this example will be the same as those in the example of Section 7.3.2. These values are:

V_0 = 42 ft/sec = initial impact velocity

V_1 = 31.0 ft/sec = velocity after landing gear has stroked (see Section 7.3.3.2)

S_{LG} = 2.5 ft

$F_{LG} = 4.0\ G\ (W_F + W_S + W_{OH})$

S_S = 1.0 ft

$F_S = \bar{G}_S W_S$

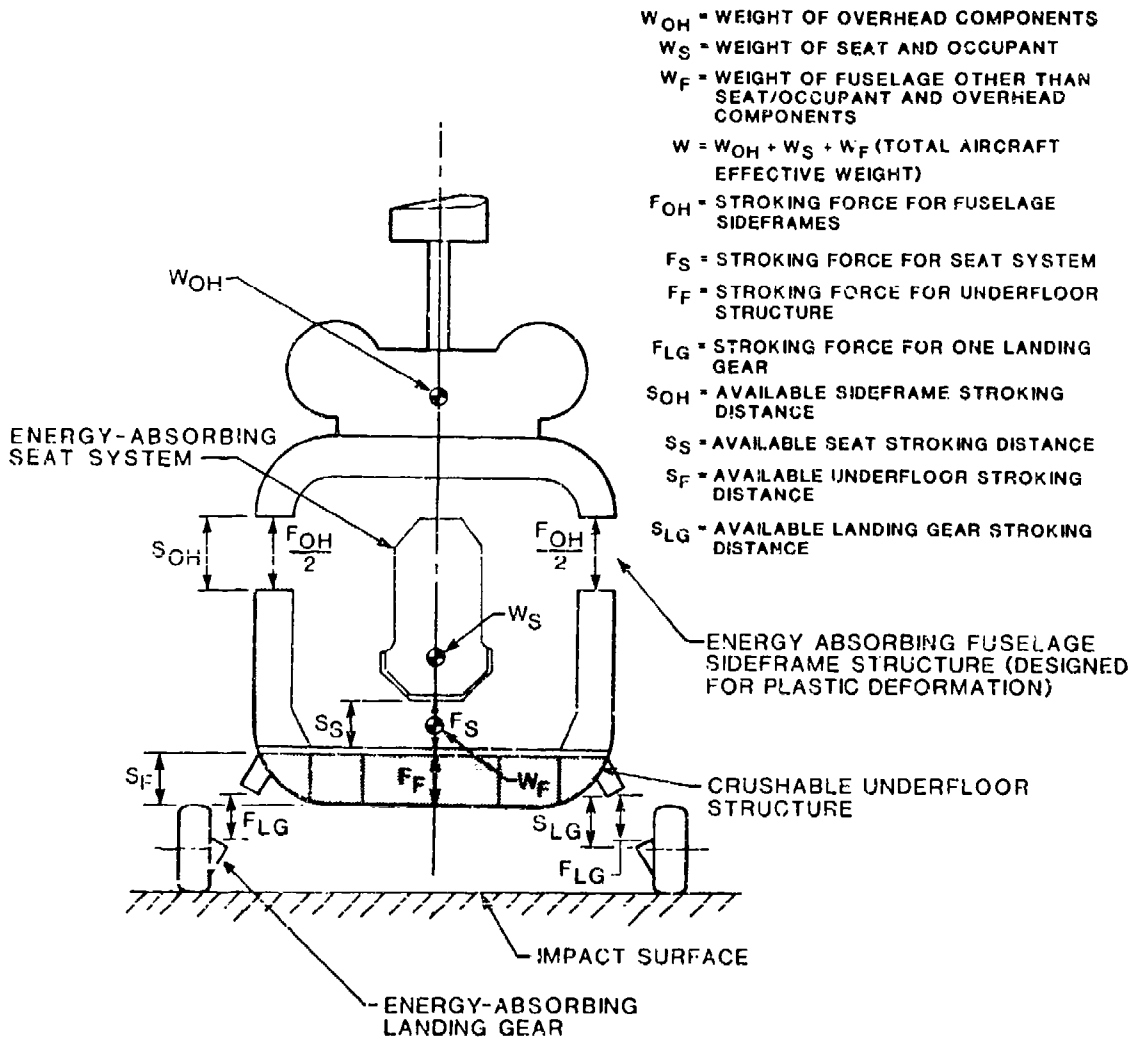

FIGURE 92. SCHEMATIC OF AIRCRAFT CRASH-RESISTANT SYSTEM USING DEFORMABLE FUSELAGE SIDEWALLS.

The relationship between the stroking distances and deceleration rates of the three energy-absorbing systems (seat, underfloor, sidewall) of the model shown in Figure 92 is as follows:

$$\bar{G}_F = (\bar{G}_S + k\bar{G}_{OH})V_1^2/((1+k)V_1^2 - 2g(\bar{G}_S X_S + k\bar{G}_{OH}X_{OH})) \qquad (51)$$

$$k = W_{OH}/W_S$$

$$X_S = (V_1^2/2g)(1/\bar{G}_S - 1/\bar{G}_F) = \text{distance stroked by seat}$$

$$X_{OH} = (V_1^2/2g)(1/\bar{G}_{OH} - 1/\bar{G}_F) = \text{distance stroked by overhead masses}$$

The above relationship assumes that the underfloor structure is deep enough to bring the fuselage to rest for the design values of G_F, G_S, G_{OH}, and V_1. Equation (51) is based on the system shown in Figure 92 and can be derived by substituting into the following energy relationship (recall that X indicates actual distance stroked and S indicates distance available for maximum stroke).

$$KE = 1/2 \ \frac{W}{g} \ V_1^2 = \bar{F}_F S_F + \bar{F}_{OH}X_{OH} + \bar{F}_S X_S \qquad (52)$$

V_1 = velocity of fuselage after completion of landing gear stroking

$$W = W_{OH} + W_S + W_F$$

$$\bar{F}_F = W_{OH}\bar{G}_{OH} + W_S\bar{G}_S + W_F\bar{G}_F$$

$$\bar{F}_{OH} = W_{OH}\bar{G}_{OH}$$

$$\bar{F}_S = W_S \bar{G}_S$$

$\bar{G}_i$ = average stroking load factor of component denoted by subscript

Substituting into the above relationship, noting that $S_F = \frac{V_1^2}{2g\bar{G}_F}$ and solving for $\bar{G}_F$, will yield Equation (51).

As in the example shown in Section 7.2.3.2, the maximum allowable value for $\bar{G}_F$ that will allow the seat to absorb the occupant kinetic energy without bottoming can be calculated with

$$\bar{G}_{Fmax} = \bar{G}_S V_1^2/(V_1^2 - 2g\bar{G}_S S_S)$$

$$\bar{G}_{Fmax} = (14.5)(31.0 \text{ ft/sec})^2/((31.0 \text{ ft/sec})^2 - 2(32.2 \text{ ft/sec}^2)(14.5)(1 \text{ ft}))$$

$$\bar{G}_{Fmax} = 512.3$$

In order to allow for nonuniform surfaces, etc., the example underfloor structure will be designed to decelerate at 40 G. This will assure that the seat will have adequate energy-absorbing ability for the case cited.

If $\bar{G}_F = 40$ and $k = 3$, substituting in Equation (51),

$$40 = ((14.5 + 3(20))(31.0 \text{ ft/sec})^2/((1+3)(31.0 \text{ ft/sec})^2 - 2(32.2 \text{ ft/sec}^2)\ ((14.5)(1.0 \text{ ft}) + (3.0)(20)S_{OH})))$$

and solving for S_{OH} gives

S_{OH} = 0.29 ft = the minimum distance that the sidewall must be able to safely plastically deform.

With a 10-degree roll attitude at impact the underfloor structure will crush at only half of its 40-G design crushing load. Therefore,

$$S_F = V_1^2/2g\bar{G}_F = (31.0 \text{ ft/sec})^2/(2)(32.2 \text{ ft/sec}^2)(20)$$

S_F = .75 ft = stroking distance of crushable underfloor structure.

The results of this analysis indicate that the preliminary design should allow for:

Landing gear: 2.5 ft of usable stroke before fuselage impact
2.5-G load factor per main gear at 20 ft/sec
4.0-G load factor per main gear at 42 ft/sec

Seat system: 1.0 ft of usable energy-absorbing stroke
14.5-G load factor for stroking

Fuselage:
Underfloor structure: 0.75 ft of crushing depth
40-G deceleration rate

Sidewalls: 0.29 ft of allowable plastic deformation
20-G load factor to produce plastic deformation.

The system shown above will provide occupant protection for an initial impact velocity of 42 ft/sec with a 10-degree roll attitude. If this system were to impact in a level attitude, the fuselage would still only provide protection for a fuselage impact velocity of 31.0 ft/sec, because this was the condition for which the sidewalls were designed.

However, both landing gears would fully stroke and absorb more energy than with a 10-degree roll attitude. The calculation of allowable initial impact velocity would be

$$E_{LG} = G_{LG}WS_{LGS} = W(V_o^2 - V_i^2)/2g$$

$$4.0W(2.5 \text{ ft} + 2.5 \text{ ft}) = W(V_o^2 - (31.0 \text{ ft/sec})^2)/2(32.2 \text{ ft/sec}^2)$$

$$V_o = 47.4 \text{ ft/sec}$$

Thus the system in the example would provide crash resistance up to 47.4-ft/sec impact velocity with a level impact versus 42.0 ft/sec with a 10-degree roll attitude at impact.

As a check to ensure that the selected values will work satisfactorily, a calculation can be performed to see if the pre-impact kinetic energy will be entirely absorbed by the proposed system. For example, assume that a helicopter with the following weights is being designed for the values of G_{OH}, $\bar{G}_S$, $\bar{G}_F$, and V_o used in the example calculation:

Engine and transmission (W_{CH}) = 900 lb

Occupant and seat (W_S) = 300 lb

Effective weight of fuselage excluding W_{OH} and W_S = 5,100 lb

Then the pre-impact kinetic energy would be

$$KE_c = WV_o^2/2g = (900 + 300 + 5,100)lb(42\ ft/sec)^2/2(32.2\ ft/sec^2)$$

$$KE_o = 172,565\ ft\text{-}lb$$

Assuming

roll attitude = 10 degrees

stroke of RH gear = 2.5 ft

stroke of LH gear = 0.625 ft

$\bar{G}_{LG} = 4.0\ G$

Then the energy absorbed by the landing gear is

$$E_{LG} = 4.0(900 + 300 + 5,100)lb \times (2.5\ ft + 0.625\ ft)$$

$$E_{LG} = 78,750\ ft\text{-}lb$$

To calculate the energy absorbed by the seat, fuselage underfloor structure, and sidewall structure, the distance stroked by each must be calculated. To do this, the velocity (V_1) of the fuselage immediately after gear stroking and prior to fuselage impact must be calculated.

$$KE = W(V_o^2 - V_1^2)/2g$$

$$KE = 78,750 \text{ ft-lb} = (900 + 300 + 5,100)\text{lb}((42 \text{ ft/sec})^2 - V_1^2))/2(32.2 \text{ ft/sec}^2)$$

$$V_1 = 31.0 \text{ ft/sec}$$

The deceleration rate of the fuselage ($\bar{G}_F$) due to the 10-degree roll attitude will be (1/2)(40 G) = 20 G, and the depth of the fuselage crushing at 10 degrees of roll will be:

$$S_F = V_1^2/2\bar{G}_F G = (31.0 \text{ ft/sec})^2/2(20)(32.2 \text{ ft/sec}^2)$$

$$S_F = 0.75 \text{ ft}$$

Crushing load, $\bar{F}_F = \bar{G}_F W_F + \bar{G}_S W_S + \bar{G}_{OH} W_{OH}$

$$F_F = 20(5,100 \text{ lb}) + 14.5(300 \text{ lb}) + 20(900 \text{ lb})$$

$$F_F = 124,350 \text{ lb}$$

$$E_F = 124,350 \text{ lb } (0.75 \text{ ft}) = 93,263 \text{ ft-lb}$$

The seat stroking distance, S_S, and corresponding energy absorption, E_S, will be

$$S_S = V_1^2/2\bar{G}_S g - S_F = (31.0 \text{ ft/sec})^2/2\ (14.5)(32.2 \text{ ft/sec}^2) - 0.75 \text{ ft}$$

$$S_S = 0.28 \text{ ft}$$

$$E_S = \bar{F}_S S_S = \bar{G}_S W_S S_S = 14.5(300 \text{ lb})(0.28 \text{ ft}) = 1{,}218 \text{ ft-lb}$$

The fuselage sidewall crushing distance, S_{OH}, and corresponding energy absorption, E_{OH}, will be

$$S_{OH} = V_1^2/2\bar{G}_{OH} g - S_F = (31.0 \text{ ft/sec})^2/2(20)(32.2 \text{ ft/sec}^2) - 0.75 \text{ ft} = 0.00 \text{ ft}$$

Therefore, $E_{OH} = 0.00$ ft-lb , which means that no plastic deformation of the sidewalls will occur unless the fuselage deceleration rate exceeds G_{OH}.

$$\sum E = E_F + E_{OH} + E_S + E_{LG} = (93{,}263 + 0.0 + 1{,}218 + 78{,}750)\text{ft-lb}$$

$$\sum E = 173{,}231 \text{ ft-lb}$$

The pre-impact kinetic energy, KE_o, is calculated as follows:

$$KE_o = 1/2(W/g)V_o^2 = 1/2(6{,}300 \text{ lb})(42 \text{ ft/sec})^2/(32.2 \text{ ft/sec}^2) = 172{,}565 \text{ ft-lb}$$

This amount is a check within rounding-off errors of the above summation of the energy absorbed by the various parts of the aircraft.

The above calculations show that:

1. The work done compressing the landing gear, seat system energy absorber, and fuselage structure will be equal to the pre-impact kinetic energy.

2. The seat will only stroke 3.4 in. if the impact occurs with 10 degree of roll attitude. Similar calculations show that the seat will stroke 4.0 in. following an impact with 0-degree roll.

Similar calculations for a level impact with an initial velocity of 42.0 ft/sec gives the following results:

$$KE_o = 172,565 \text{ ft-lb}$$

$$E_{LG} = 126,000 \text{ ft-lb}$$

$$E_F = 40,743 \text{ ft-lb}$$

$$X_F = 0.18 \text{ ft}$$

$$E_S = 1,436 \text{ ft-lb}$$

$$X_S = 0.33 \text{ ft}$$

$$E_{OH} = 3,420 \text{ ft-lb}$$

$$X_{OH} = 0.19 \text{ ft}$$

$$\Sigma E = 171,599 \text{ ft-lb}$$

These calculations show that the system can absorb the pre-impact kinetic energy without exceeding any of the available stroking distances.

Results from the above calculations will not be applicable to any specific aircraft, but the methodology is. All energy-absorbing components should be designed as a system to assure that adequate protection is provided. If operational constraints limit the performance of some components, compensation should be provided in others to maintain the required system performance. Also, preference should be given to components which will most reliably absorb energy: the seat and the fuselage. The gear is least reliable because it will not function as intended on soft surfaces or at high roll angles. Also note that efficiencies must be incorporated to ensure achievement of the assumed G levels.

7.4 LANDING GEAR ANALYSIS

Simple analytical methods for wheel-type gear are merged with detail design concepts in Section 6.3. Methods of analyzing performance of both wheel- and skid-type landing gear were surveyed and described in Reference 96. Applicable techniques for skid landing gear are summarized below.

As indicated in Figure 12, the skid-type landing gear has been used for many years on lightweight helicopters. It is a low-cost means of creating small elastic deflections with energy dissipation efficiencies comparable to those

of the oleo strut during normal landings. The design problem associated with skids is that they are nonlinear structural elements. The skid has linearly related applied force and resulting deformation over the small amount of stroke that results in normal landing impact velocities. Beyond that point it is necessary to consider the plastic deformation of the skid.

The simplest design technique assumes the vehicle is supported by tubular members that cross horizontally at the bottom of the fuselage. The vehicle impact is in a horizontal attitude and dissipates all energy by the strain energy required for bending of the tubes.

The skid stiffness is idealized as a bilinear curve with slope decreasing to a small value after yielding to duplicate the load-deflection curve. This is derived from an idealized stress-versus-strain curve for the particular material used.

Since the load-deflection curve is piecewise linear, it is easily integrated to determine the potential energy as a function of skid deflection. The energy absorbed in the elastic region of the gear is

$$E_1 = \int_0^{\delta_y} P(\delta)d\delta = C\delta_y^2/2 \tag{53}$$

where $P(\delta)$ = applied load (lb)

δ = deformation of skid (ft)

δ_y = deformation at elastic limit (ft)

C = slope of the elastic range of the load-deflection curve (lb/ft)

E_1 = energy absorbed (ft-lb).

For the plastic portion of the curve the energy absorbed is

$$E_2 = \int_{\delta_y}^{\delta} P(\delta)d\delta$$

$$= \int_{\delta_y}^{\delta} [C\delta_y + C_1 (\delta - \delta_y)] \, d\delta$$

$$= C\delta_y (\delta - \delta_y) + \frac{C_1}{2} (\delta - \delta_y)^2 \tag{54}$$

where C_1 = slope of plastic range (lb/ft).

By equating kinetic and potential energies, equations are developed to relate applied loads, elastic limits, vehicle masses, weights applied per skid, and impact velocities.

For a perfectly plastic material,

$$\delta = \frac{\frac{\delta_y}{2} + \left[\frac{RW}{(C - C_1)\delta_y}\right]\left(\frac{6v^2}{Rg}\right)}{1 + \frac{RW}{(C - C_1)\delta_y}} \qquad (55)$$

where $R = 1 - \frac{\text{rotor lift}}{\text{weight}}$

W = effective weight on skids (lb)

g = gravitational constant (ft/sec^2)

v = impact velocity (ft/sec).

Therefore, for varying impact velocities, rotor lift values, and desired effective weights on the skids, the deformation can be calculated. The load factor applied is then the ratio of applied force to effective weight:

$$n = \frac{F}{W} \qquad (56)$$

The procedure requires approximating the stress-strain curve of a material, then approximating the resulting load-deflection curve for the integration process in the energy equations. The results of this type of approach have produced reasonable results when compared with test data

The procedure shown has several distinct steps:

- Establish the stress-strain characteristics of the tube material.
- Calculate the force-displacement characteristics of the tube.

- Incorporate the force-displacement characteristics into an energy relation or set of dynamic response equations.

- Calculate the vehicle response.

7.5 SEMIEMPIRICAL ANALYSIS OF AIRFRAME STRUCTURAL CRASH RESISTANCE

The use of analytical tools to aid designers would be most beneficial during the preliminary stages of design when meaningful trade-offs can be made among weight, cost, space, and crash-resistance capability. It is at this time in the design process that potential changes can be achieved with the least cost penalty to a project. At this stage in the design, only a limited amount of data exists; usually little more than basic weights, stiffnesses, strengths, configurations, and sizing are available. To maximize the effectiveness of preliminary design analytical tools, the crushing characteristics of the typical vehicle structure must be estimated with reasonable accuracy using relatively simple techniques. This information is especially essential if any degree of accuracy is to be achieved with computer simulations described in later sections.

Reference 97 describes such a procedure for prediction of crushing characteristics of primary energy-absorbing metal structure and is as summarized below.

7.5.1 Analysis Procedure

The general procedure for determining the total load-deflection characteristics, including failure and postfailure behavior for a given substructure, is discussed below. The procedure was demonstrated for a test specimen built to represent a section of a utility helicopter lower fuselage. The location of the segment in the lower fuselage and the four-edge support representative of the manner in which loads are transmitted from the fuselage to the transmission housing are shown in Figure 93. Included in the procedure is a step-by-step process with the following sequence:

1. Prediction of failure loads for stiffened panels.

2. Postfailure analysis of stiffened panels.

3. Main beam and bottom skin analysis.

4. Total substructure load-deflection curve.

In predicting the failure load of the model substructure, the work of Needham (Reference 98) and Gerard (Reference 99) was used extensively. For the postfailure analysis, the concept of D'Amato (Reference 100) was used as a base; however, a somewhat different failure mechanism was employed. Subelement crushing characteristics were superimposed in a piecewise sense to yield the total load-deflection curve. Depending upon the rivet pitch, spacing, and strength, a given structure may fail in one of several ways. Therefore, the procedure described herein takes into account monolithic, wrinkling, and interrivet failure modes. Although developed for angle-type stiffened panels, the procedure is reported to be applicable to a variety of panel types, including T-type stiffeners, formed angle stiffeners, extruded angle stiffeners, formed multicorner sections, hat-formed stiffened panels, and extruded-Y stiffened panels.

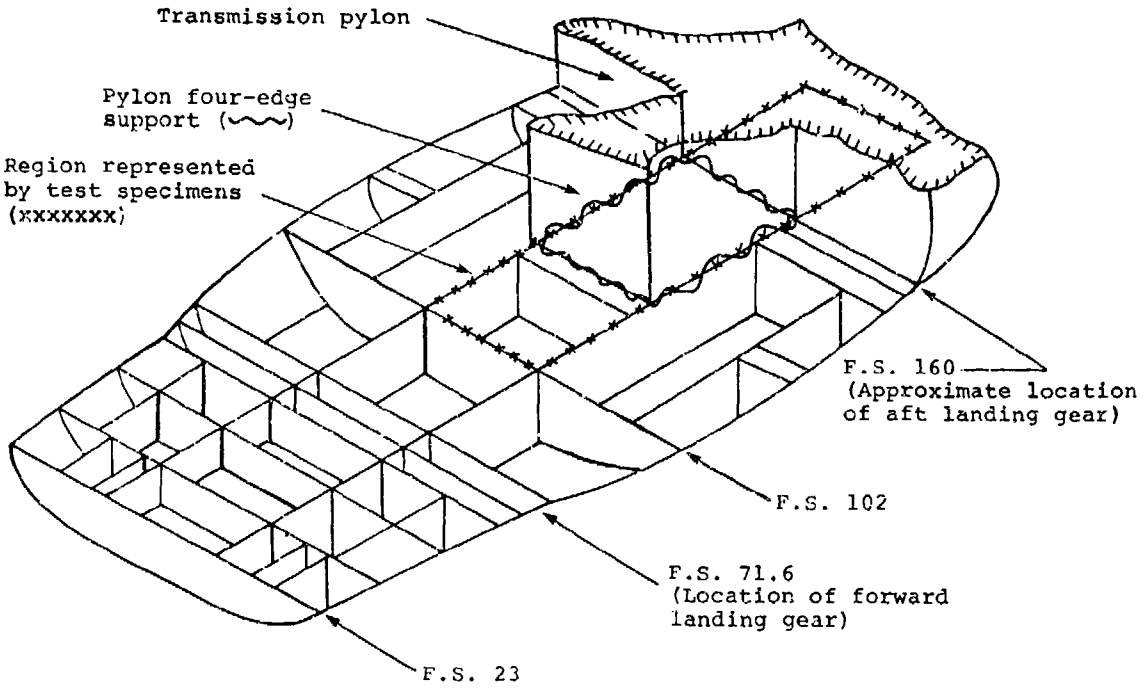

FIGURE 93. LOWER FUSELAGE BULKHEAD AND STIFFENER ARRANGEMENT. (FROM REFERENCE 97)

The failure loads were estimated using the semiempirical/analytical methods described in References 98, 101, and 102 for stiffened short panel elements. The analysis, as outlined, is based on two assumptions: (1) at the threshold of the failure load, full plastic hinges are developed at the constrained supports and the midsection of the panels, and (2) the free warping energy of the flange of the stiffening angles can be neglected.

As is discussed in Section 7.4.3 and in detail in Reference 96, these assumptions are considered, on the average, reasonable. The analysis neglects the effect of strain hardening, the influence of the axial force on the plastic hinge mechanisms of the stiffened panel, the changes in local failure pattern during the postfailure stage, and the effect of geometrical imperfections caused by manufacturing and/or damage. In light of the test results and correlation with analysis, these effects are probably not significant for this type of substructure.

7.5.2 Substructure Test Results

To verify the analytical results, experimental data were obtained during the same study by testing twelve specimens, representative of typical helicopter lower fuselage structure, under the following conditions: static load, dynamic impact ($\leq$30 ft/sec), four-edge support, two-edge support, skin web

thickness from 0.025 in. to 0.064 in., number of angle stiffeners from 12 to 40 ea., and specimen depth of 6.125 in. and 12.125 in. The test specimens were 46 in. long, included five bays, and were 18 in. wide with a side panel at each side. Each specimen was supported in its normal manner. All comparative static and dynamic tests on similar specimens were performed at equal energy input levels. Instrumentation consisted of several strain gages to measure compression and bending, a linear variable differential transducer to measure deflection, accelerometers mounted on the impact head and load cells installed between the test specimen support and the ground for the dynamic tests.

The test program results yielded valuable information for future consideration. For example, for these types of structural elements, static testing to determine load-deflection characteristics should yield sufficiently accurate results when compared to dynamic test results, but in a more economical manner. A static test can provide the desired information with regard to shape of the load-deflection curve, peak failure load (in the program described herein the dynamically obtained failure loads are between 9 and 24 percent higher than the loads measured in static testing and the loads from predicted static calculations, respectively), deflection at which failure load occurs, and energy-absorption capability of the structure.

The test results show that during a dynamic test the amount of springback from the maximum deflected value is immediately evident. After a static test, the structure will relax slowly (up to several days) to its permanently deformed position. The springback in the dynamic test was as high as 40 percent of the maximum deflected value for a test performed with an impact velocity of 30 ft/sec. This observation could be of consequence in areas such as doors, where distortion of structure affects occupant egress after a crash.

7.5.3 Correlation of Test and Analysis Results

Comparison of test and analytical data showed reasonable agreement with respect to peak failure load and energy-absorption capability, particularly for the dynamic tests in which load cells are installed. Figure 94 shows a comparison of the analytically predicted load-deflection curves with test data and illustrates good correlation with regard to shape of the curve as well as peak load and energy absorption. As can be noted in Figure 94, the typical response of the type of structure tested in this study is a relatively sharp load build-up in the elastic region up to the peak failure load (at approximately 0.35 in. or less of deflection). After failure, the load decreases at a rate less rapid than the initial build-up until the deflection reaches approximately 0.75 to 1.0 in. Thereafter, the load decreases gradually until the structure being crushed is confined and once again stiffens. This region, wherein confined crushing takes place, is very significant because the stiffness at this point can greatly influence the response of the upper masses (the transmission and engine of the test vehicle). The initial peak failure load, while of a substantial level, is of short duration and as such may not greatly influence the upper mass response.

Figure 95 shows a comparison of test and analytical results for three groups of specimens. A detailed discussion of the correlation between analysis and test is presented in Reference 97. The energy absorption was predicted within 8 percent of the test results for three specimens that were tested dynamically with load cells installed.

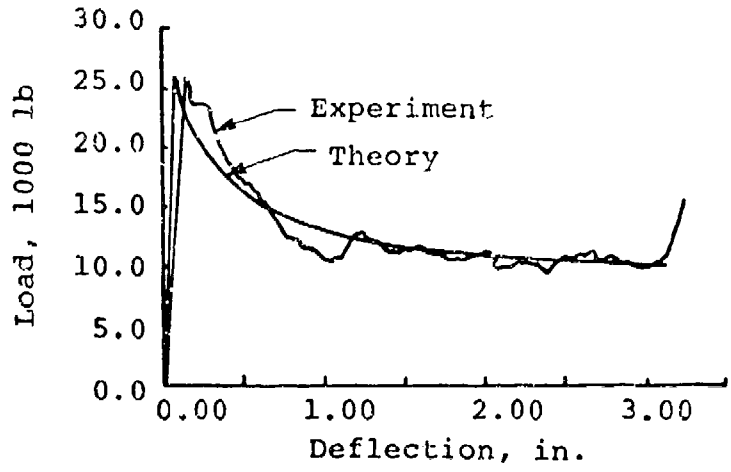

FIGURE 94. PREDICTED VERSUS TEST LOAD-DEFLECTION CURVES FOR A REPRESENTATIVE SPECIMEN. (FROM REFERENCE 97)

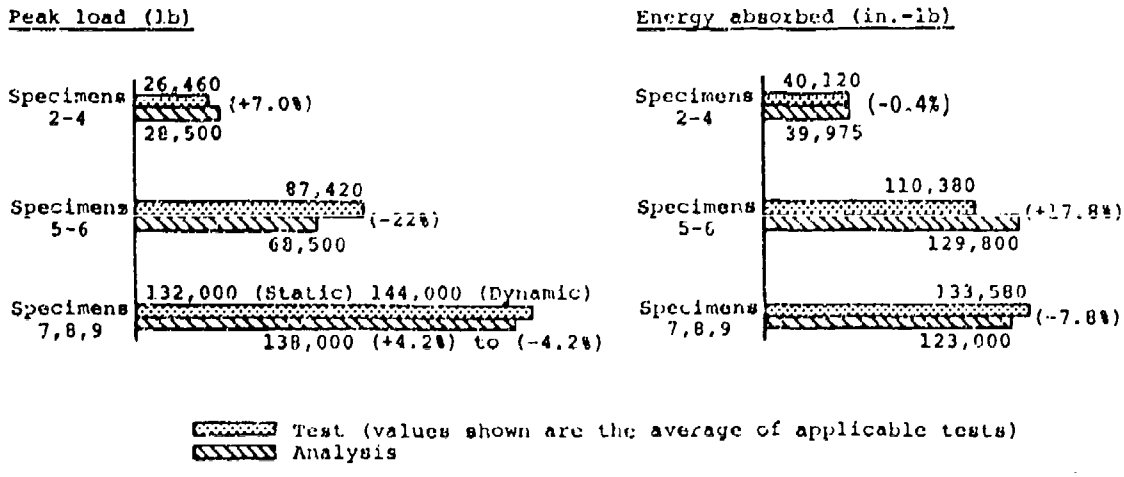

FIGURE 95. COMPARISON OF TEST AND ANALYSIS RESULTS FOR "LIKE" SPECIMENS.

The results of the correlation studies indicate that it is practical to use relatively simple techniques to determine load-deflection characteristics of multiweb, angle-stiffened panels, typical of the lower fuselage of an existing utility model helicopter. The overall crushing behavior of the substructure can be predicted within reasonable accuracy although the failure mode of each individual stiffener cannot consistently be accounted for. The analytical procedure described herein is capable of determining satisfactorily the two most significant parameters for crushable structure, i.e., peak failure load and energy-absorption capability. The approach, as developed in this study, has limitations with regard to accurately predicting the deflection at which failure occurs and the deflections at which postfailure stiffening is encountered. Although the predicted failure deflection is a consistently lower value than that obtained from tests, it represents an extremely small percentage of the total crushing energy, to the extent that it is not significant as long as the peak failure load and load-deflection characteristics are properly defined. The analytical assumptions regarding the mode of failure in the postfailure region and the hinge formation at failure are considered valid in view of the test results. For example, although test results indicate that failures can occur in both the asymmetrical and symmetrical modes, the predicted energy-absorption capability of the structure, which considers only the symmetrical mode, is still very close to test results. Thus, the assumption of a symmetrical failure is, on the average, reasonable.

7.5.4 Example of Analysis for Vertical Impact

The example given here is an analysis to predict major structural collapse for the crash of a medium cargo helicopter. This analysis was performed for the full-scale crash test of a cargo helicopter conducted on 6 March 1975 at the NASA Langley Research Center's Impact Dynamics Research Facility, Hampton, Virginia (Reference 103). The impact velocity components selected for the test were 40 and 30 ft/sec for vertical and longitudinal velocities, respectively, producing a 50-ft/sec resultant velocity.

The structural response and failure modes in crash impact conditions are not easy to predict using static analytical techniques. Initially, the underfloor structure absorbs energy by crushing, but the amount of energy absorbed is dependent upon the type of surface impacted. Soft ground or water can displace and provide a reasonably uniform loading on the base of the structure, but a rigid surface results in more direct loading of the frame members. This difference is illustrated in Figure 96(a), where possible types of load distribution are shown for soft and hard ground impact planes. Figure 96(b) illustrates that the subfloor energy absorption is also dependent upon the surface.

The helicopter occupants, assuming otherwise survivable crash impact conditions, must be protected from injury due to the collapse of basic structure or the penetration of occupied areas by large mass items. The following calculations demonstrate a semiempirical method of predicting overall reduction in the height of occupied areas.

Data obtained from past major accidents, either actual values or estimated impact conditions, have been used in conjunction with deformation information to obtain a simplified relationship between the static and dynamic load-carrying capabilities for structural elements. The case considered here involved the absorption of 135,000 ft-lb of energy with a 42.2-in. structural collapse.

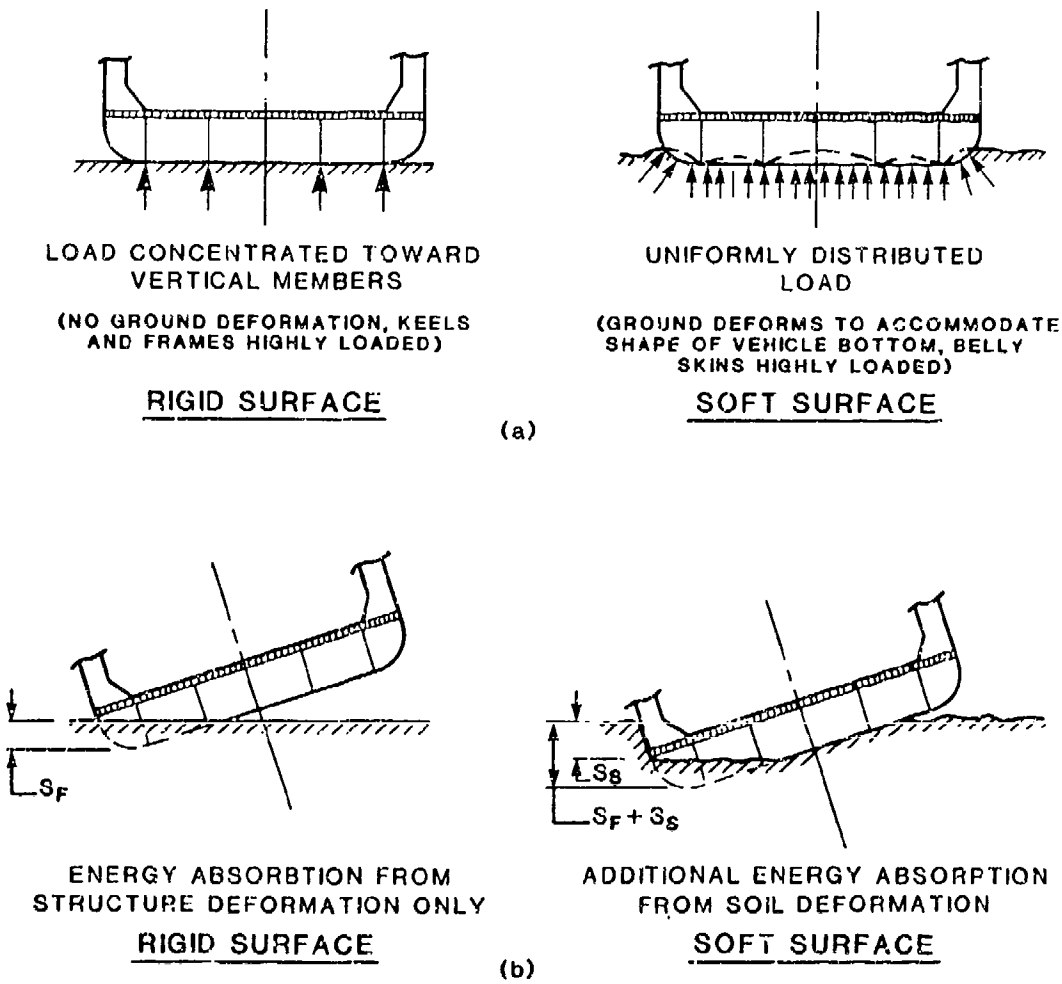

FIGURE 96. LOAD DISTRIBUTIONS ON HARD AND SOFT SURFACES.

The general nature of the energy-absorbing characteristics of an element of airframe structure can be of the form shown in Figure 97. When stability is not the limiting criterion, the curve in Figure 97(a) is applicable; Figure 97(b) represents the response for stability-limited load capability.

In severe impact conditions, stability is the limiting criterion for many structural elements of interest. Figure 98 shows simplified load-deflection characteristics for static load application to a stringer-skin combination subjected to compressive loading (Reference 104).

The area under a load-deflection curve determines the energy-absorption capability for the structure under consideration.

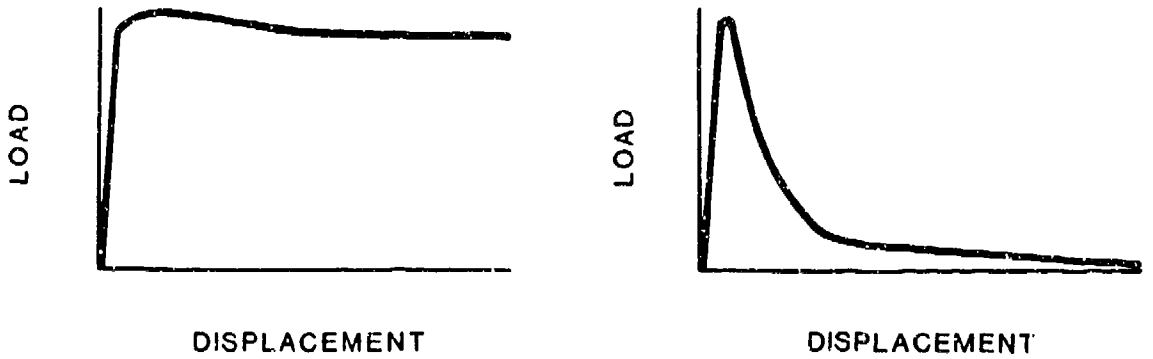

FIGURE 97. TYPICAL LOAD-DISPLACEMENT CHARACTERISTICS FOR AIRFRAME STRUCTURE.

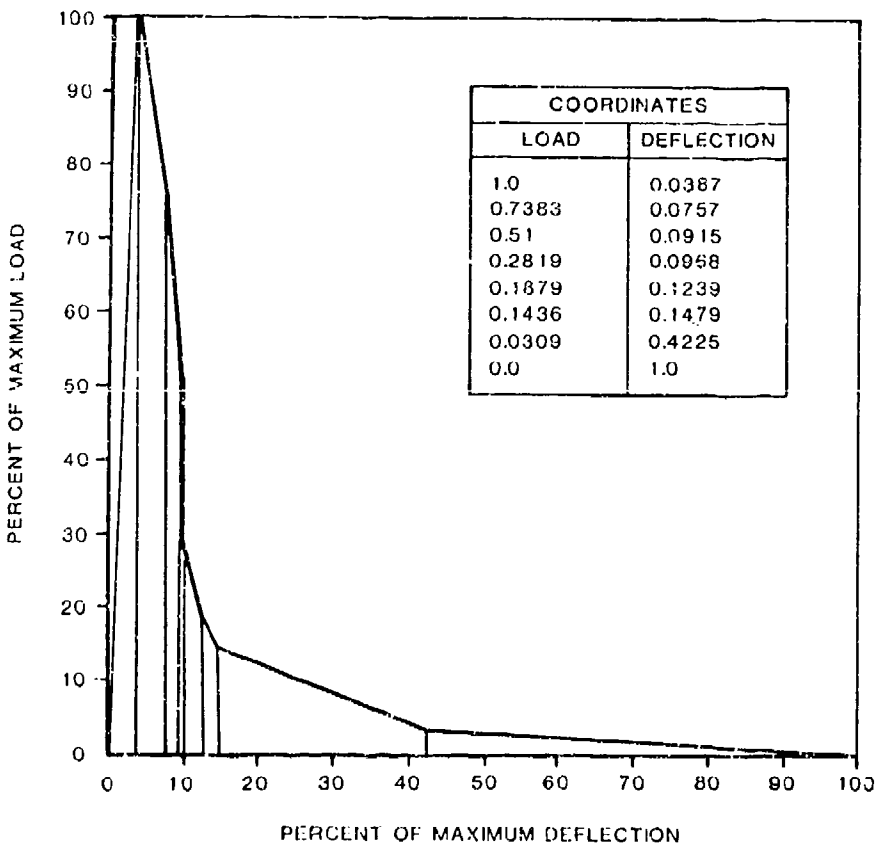

FIGURE 98. SIMPLIFIED LOAD-DEFLECTION CHARACTERISTICS FOR A STATICALLY LOADED STRINGER-SKIN COMBINATION. (FROM REFERENCE 104)

The basic section of a typical side frame member is shown in Figure 99. The crippling stress is computed as follows:

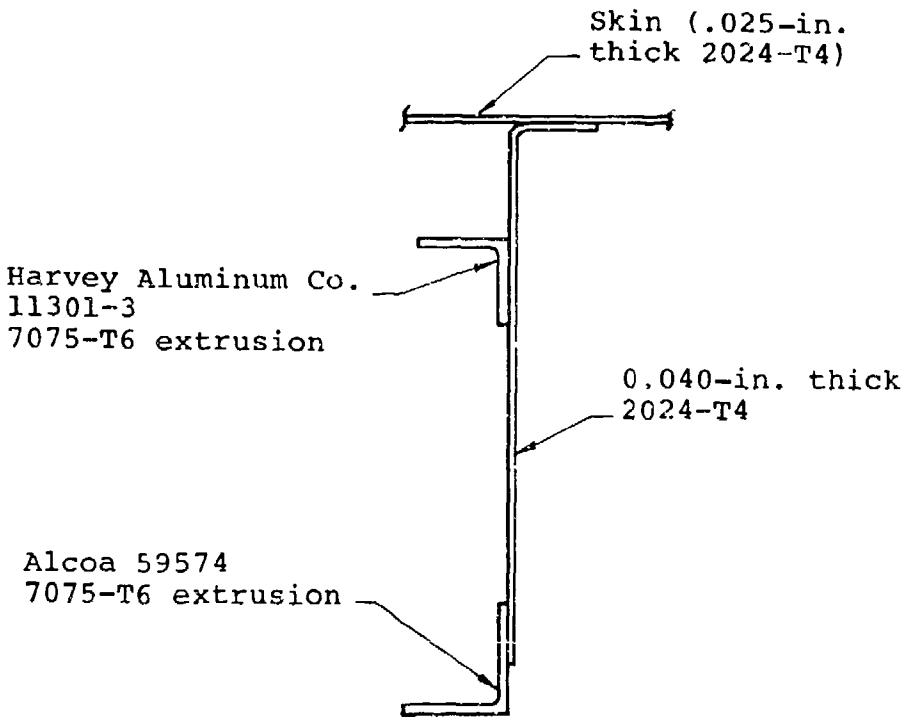

FIGURE 99. TYPICAL FRAME SECTION OF SIDE ELEMENT OF A MEDIUM CARGO HELICOPTER CENTER FUSELAGE.

For Harvey Aluminum Company extrusion 11301-3,

$$\frac{A}{\sum t^2} = \frac{0.210}{0.094^2 + 0\ 125^2} = 8.59$$

$F_{cc} = 62{,}000$ lb/in.^{2} (From Figure 100)

For Alcoa 59574,

$$\frac{A}{\sum t^2} = \frac{0.289}{0.188^2 + 0.125^2} = 5.67$$

$F_{cc} = 70{,}000$ lb/in.^{2}

FIGURE 100. CRIPPLING ALLOWABLES FOR TYPICAL ALUMINUM ALLOY EXTRUSIONS.

For the flanged web,

$$\frac{A}{gt^2} = \frac{(1.5)(0.040)}{(2)(0.040^2)} = 18.8$$

F_{cc} = 19,000 lb/in.^{2} (From Figure 101)

The total compressive capability of the frame element is computed as follows:

Capability of stringer elements = (62,000)(0.210)

+ (70,000)(0.289)

+ (19,000)(1.5)(0.04)

= 34,390 lb

Capability of adjacent skin = (37,000)(0.034)

+ (37,000)(0.032)

+ (19,000)(0.024)

= 2,898 lb (From Figure 102)

Total compressive capability = 37,288 lb

This value is for one section through a typical frame member. For a symmetrical fuselage section, the total compressive capability is twice this value, or 74,576 lb.

From the photographs of helicopter crashes under known impact conditions, the average crushing of the typical frame section was 42.2 in. for the impact velocity considered.

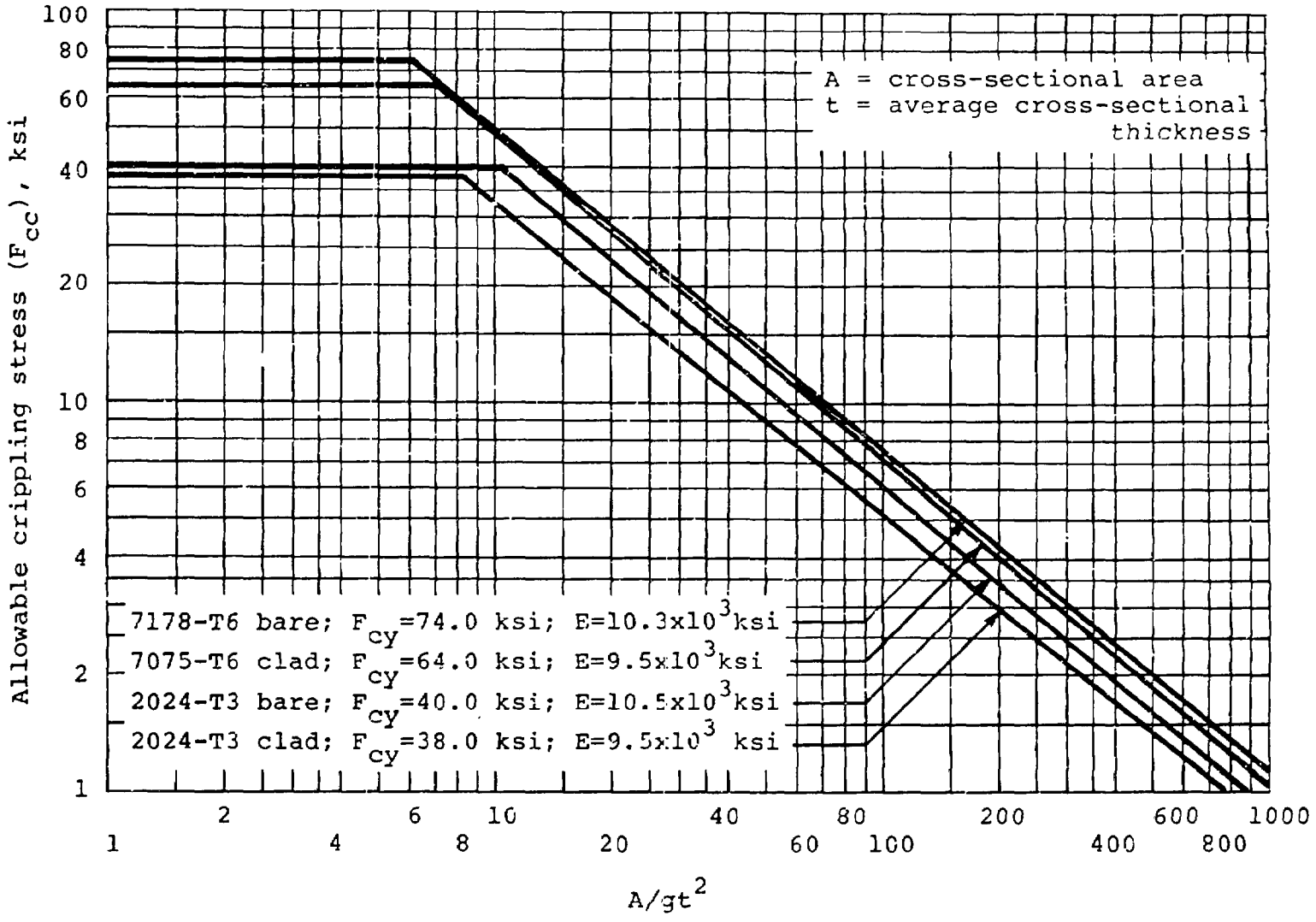

FIGURE 101. CRIPPLING ALLOWABLES FOR ALUMINUM ALLOY FORMED SECTIONS OTHER THAN SIMPLE ZEES AND CHANNELS.

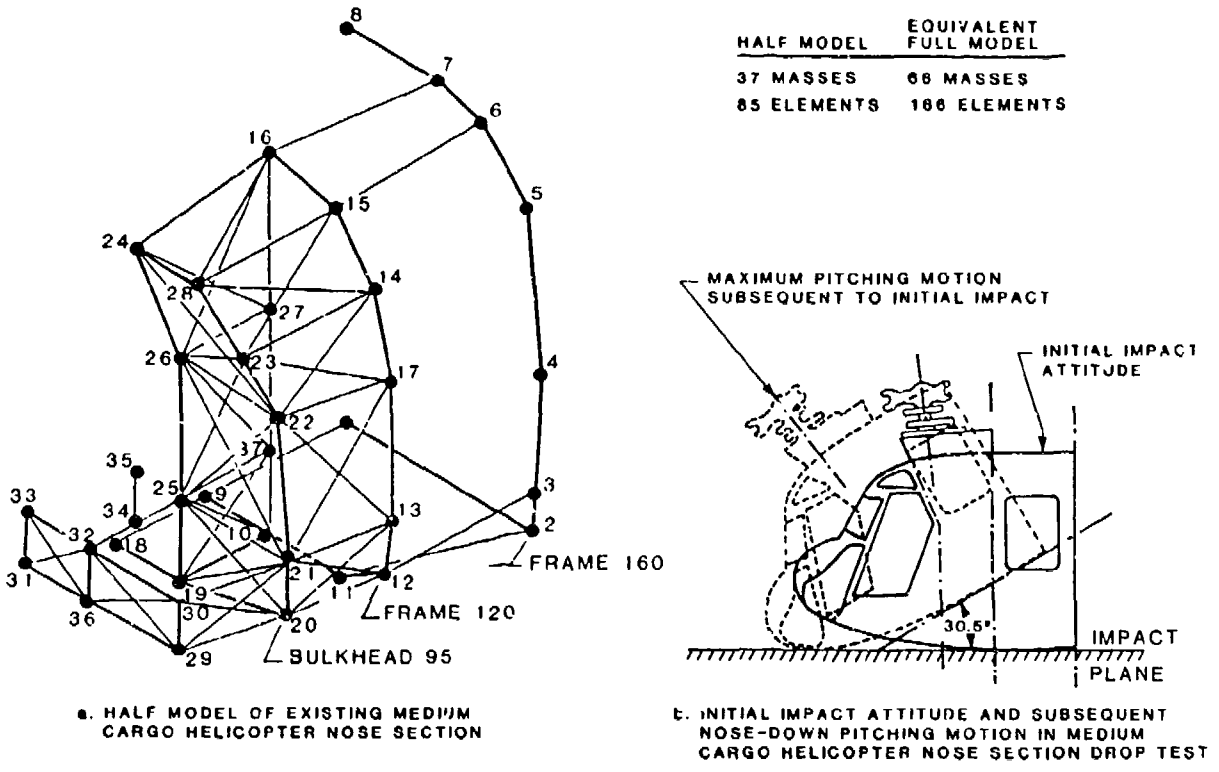

a. HALF MODEL OF EXISTING MEDIUM CARGO HELICOPTER NOSE SECTION

b. INITIAL IMPACT ATTITUDE AND SUBSEQUENT NOSE-DOWN PITCHING MOTION IN MEDIUM CARGO HELICOPTER NOSE SECTION DROP TEST

FIGURE 102. EFFECTIVE AREA OF SKIN FOR ALUMINUM ALLOY STRINGER-SKIN COMBINATIONS.

Using this load value and total displacement in conjunction with the typical stringer-skin compression static characteristic shown in Figure 98, an estimation can be made for the correction required for dynamic energy-absorption capability. Using Figure 98 data, the energy absorbed is given by:

$$E_A = P\, y \sum A$$

$$= (74,576)\ (\tfrac{42}{12}) \sum A \qquad (57)$$

where A = incremental area under curve in Figure 98

$$= (74576)(3.5) \quad (1.0)\left(\frac{0.0387}{2}\right) + \left(\frac{1.0 + 0.7383}{2}\right)0.037$$

$$+ \left(\frac{0.7383 + 0.5100}{2}\right)0.0158 + \left(\frac{0.51 + 0.2819}{2}\right)0.0053$$

$$+ \left(\frac{0.2819 + 0.1879}{2}\right)0.0271 + \left(\frac{0.1879 + 0.1436}{2}\right)0.0240$$

$$+ \left(\frac{0.1436 + 0.0309}{2}\right)0.2746 + (0.0309)\left(\frac{0.5775}{2}\right)$$

$$= 261{,}016\ (0.01935 + 0.03216 + 0.00986 + 0.00210$$

$$+ 0.00637 + 0.00398 + 0.02396 + 0.00892)$$

$$= \underline{27{,}850\ \text{ft-lb (STATIC)}}$$

This result shows that the static collapse energy computation does not agree with the empirical value of 135,000 ft-lb.

Assuming rectangular characteristics would produce an overly optimistic energy-absorption value of 261,016 ft-lb. An assumption of triangular characteristics yields an energy-absorption capability of 130,508 ft-lb, and a comparison of this value with the actual kinetic energy of 135,000 ft-lb yields an error of only 3.34 percent, which is well within an acceptable range for such an analysis. Figure 103 shows the differences between the static and assumed dynamic energy-absorption capabilities of a typical structural element; the result is based on actual test and accident data.

7.5.5 Example of Analysis for Longitudinal Impact

In the previous example, structural resistance to loading was assumed to be in the vertical plane of the helicopter. Additional structural crash-resistance requirements for the primarily longitudinal-lateral impacts are specified in MIL-STD-1290 (Reference 1) and Section 4.3.1 of this document.

A similar method of analysis can be employed after defining the primary structural members assigned to resist the applied loading and after computing load-carrying limitations and potential stroking distances.

As a further example, the nose section of a developmental utility helicopter was used. In the initial design definition phase, the requirements of MIL-STD-1290 were specified for both the 20- and 40-ft/sec longitudinal impact conditions (see Table 3, Section 4.1). These requirements delineated the maximum acceptable intrusions into occupied space for the given impact velocities for longitudinal impacts into a vertical abutment. The basic

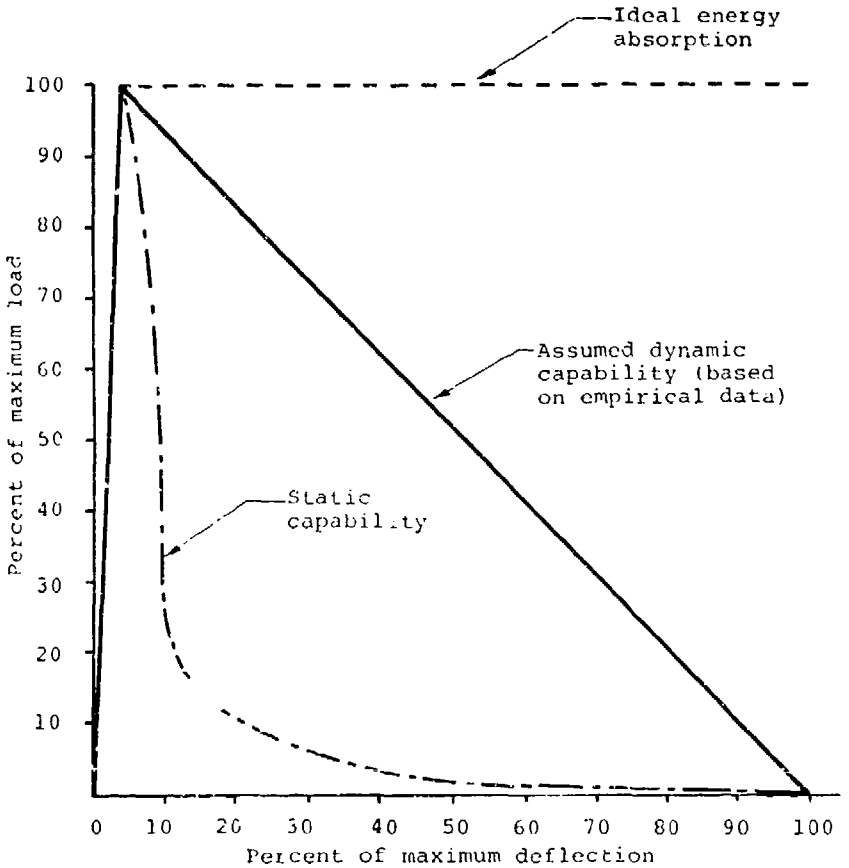

FIGURE 103. ESTIMATED DYNAMIC ENERGY ABSORPTION CAPABILITY OF TYPICAL FUSELAGE STRUCTURE.

design philosophy is that the kinetic energy involved in a 20-ft/sec crash impact velocity is absorbed by the 25 in. of structure forward of the rudder pedals. For a 40-ft/sec crash, energy is absorbed by the structure forward of Station 78 (see Figure 104); the area aft of Station 78 constitutes the cabin area.

7.5.5.1 <u>20-ft/sec Impact</u>. Figure 104 shows the basic structural elements to be considered; the analyses are summarized below:

Longitudinal impact velocity changes = 20 ft/sec

Basic structural weight = 15,587 lb

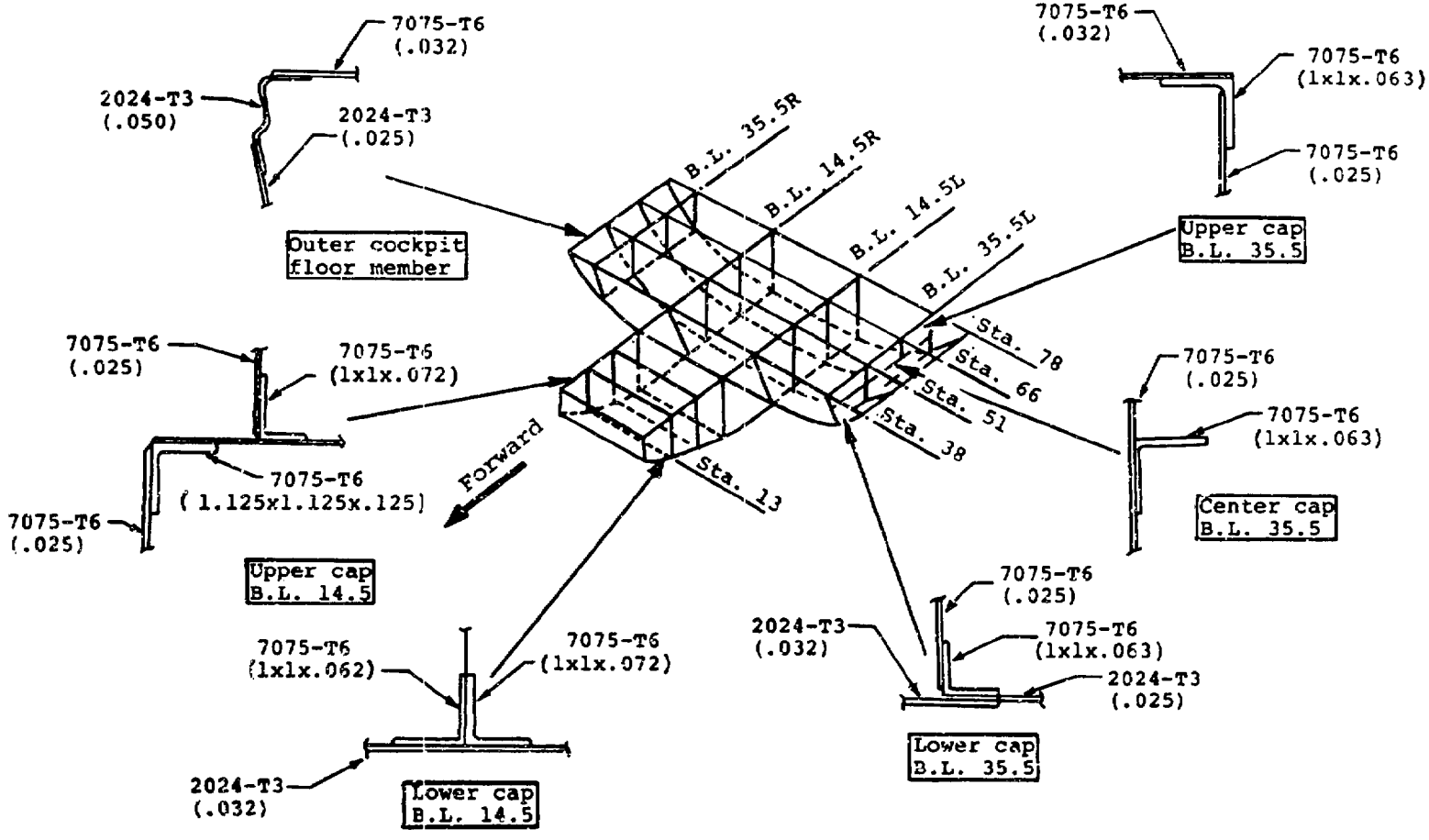

FIGURE 104. EXAMPLE OF LONGITUDINAL IMPACT RESISTANCE ANALYSIS.

Kinetic energy to be absorbed = $(\frac{1}{2})(\frac{15577}{32.2})(20^2)$

= 96,813 ft-lb

Figure 104 shows the basic structural sections that resist longitudinal loading. It should be noted in Figure 104 that these members are stabilized by formers located at approximately a 6-in. pitch.

Using standard methodology for computing the crushing strength of each section yields:

Crushing strength of upper cap, BL 14.5 (left and right sides) = 25,569 lb

Crushing strength of lower cap, BL 14.5 (left and right sides) = 17,919 lb

NOTE: When these values are computed, the amount of effective skin actively participating is dependent on whether interrivet buckling occurs. If interrivet buckling is considered likely, the effective width of skin must be reduced as follows:

$$W_{corrected} = W_{eff} \frac{F_{ir}}{F_{cs}} \quad (58)$$

where F_{ir} = interrivet buckling stress

F_{cs} = crippling stress of stringer.

Summation of the strength capabilities of the four longitudinal sections yields:

Total crushing strength, Station 13 to 38

= 2 (25568 + 17919)

= 86,976 lb

Energy-absorbing capability

$$= 0.5 \times \frac{25}{12} \times 86796$$

$$= \underline{90,600 \text{ ft-lb}}$$

Equivalent Impact Velocity = 19.4 ft/sec

This value, within 3 percent of the desired 20-ft/sec capability, is acceptable when considering the assumptions made and the use of an empirical dynamic factor of 0.5.

7.5.5.2 40-ft/sec Impact. Similar computations were used for this analysis, but additional structure was involved. After the section from Station 13 to 38 has collapsed, members from Station 38 to 78 picked up the loads. The members involved are indicated in Figure 104, but the computations are not given since the process is the same as for the 20-ft/sec case.

7.5.6 Lateral Impact

Once again, resisting structure is identified and energy-absorption capability computed for the frame member sections in the crown and floor that resist volume reduction due to loading in the lateral direction. Summation of the buckling strengths, as demonstrated in Section 7.5.4, is used to determine volume reduction for the specified impact velocity to conform with the MIL-STD-1290 requirements (Reference 1) summarized in Section 4.3.1.3.

7.5.7 Rollover

Postimpact rollover design requirements for load applications and for structural areas that must withstand that loading are specified in MIL-STD-1290 and summarized in Section 4.3.1.4. Basically, a 4W requirement is defined; this can be satisfied by normal static structural analysis techniques.

Since a rollover maneuver is a secondary event occurring after initial impact, an energy-absorption analysis is unnecessary. The 4W postimpact static analysis is adequate for substantiating the rollover performance of the helicopter, because normally the primary impact will absorb most of the energy.

Crash resistance technology can be extended beyond simple concepts by simulation of the crash phenomena. As shown in MIL-STD-1290, there are several sets of crash conditions that must be investigated in support of the design

process. Additional sets of impact conditions may appear critical for certain specific systems, and these require examination as well. These conditions may be simulated by analytical models, scale models, and full-scale tests.

However, during the early design stages of the new aircraft, full-scale testing is untimely and costly. In fact, the testing of full-scale airframes has been confined to technology development, rather than design.

The objective of simulation is to provide a rational basis for the sequence of events and the modes of failure of vital elements of structure during the crash. Complex interactions of crash, inertial, and structural forces which contribute to the structural distortion and the acceleration environment experienced in a crash can be observed. Dissipation of the potential and kinetic energy of the aircraft can be studied for conditions that exist in the crash sequence. Structural distortion with subsequent ruptures, volumetric reductions, and penetration of occupied spaces can be assessed, and estimates of the acceleration levels on critical components and occupants obtained.

In terms of fidelity, the dynamic testing of full-scale structures most closely approximates actual crash conditions, especially if velocity components and impacted surface conditions can be realistically represented.

7.6 STRUCTURAL CRASH RESISTANCE SIMULATION COMPUTER PROGRAMS

Analysis of the crash behavior of aircraft structures is a complex process due to the material and geometric nonlinearity of the structural response. Large deflections and rotations in the deformed structure, regions of intense curvature (wrinkling), material strain rate effects, and interference and contact between structural components during a crash are some of the difficulties found in modeling the crash response of aircraft structures.

A number of computer programs for analysis of aircraft structures in crash impact conditions have been developed, and some of these are being used in the design process. The more significant programs have been critically reviewed by several authors, including Saczalski (Reference 105), Hayduk, et al. (Reference 106), McIvor (Reference 107), and Kamat (Reference 108). These programs, representing different levels of capability and applicability, can be grouped into two main classes:

- Hybrid programs
- Finite element programs.

Hybrid programs combine experimental and numerical methods in which the structure is divided into a number of relatively large sections and subassemblies. The crash behavior of individual components is determined by test or sepa-

rate analyses. These programs are cost effective and sufficiently accurate for evaluation of gross vehicle responses, design trends, structural design and impact parameters, and gross energy dissipation.

Several simple hybrid simulation programs are available where the vehicle is modeled by one to ten lumped masses and up to 50 degrees of freedom. Large structural assemblies are modeled as nonlinear springs. Typical of these programs is that authored by Gattlin, et al. (Reference 109). The Gattlin program (CRASH) simulates the vertical crash impact of the helicopter fuselage modeled with rigid masses connected to nonlinear axial and rotary springs in a predetermined arrangement. These simulations are two-dimensional.

The more advanced hybrid programs employ beam and spring elements and lumped masses in either two- or three-dimensional configurations. Typical of the advanced hybrid programs are those developed by researchers at Lockheed-California (Reference 110), Calspan (Reference 111), and Philco-Ford (Reference 112). In the aircraft industry the Lockheed California program, KRASH, developed by Wittlin, et al., is the most widely used advanced hybrid crash simlation program.

The finite element programs attempt to surpass the limitations of the lumped-parameter approach of the hybrid programs by employing more formal approximation techniques in modeling of the structure and a greater reliance on the fundamental principles of structural mechanics. The stiffness characteristics of the individual elements are calculated by the programs and depend on the loading path, material properties, and the changing shape and position of the structure. The finite element programs are suitable for analysis of designs where the detailed behavior of the individual components is critical, obtaining loads required for input to other analyses, and detailed stress analysis in sizing structural components. The limitations of the finite element approach are found in the inherent tendency toward more complicated and expensive computations.

Finite element programs suitable for crash simulation include WRECKER by Yeung, et al. (Reference 113), ACTION by Melosh, et al. (Reference 114), DYCAST by Pifko, et al. (Reference 115), and PAM-CRASH by Engineering System International (Reference 69).

Reference 106 presents the results produced by three programs, KRASH, ACTION, and DYCAST, used to analyze the dynamic response of a twin-engine low-wing airplane section subjected to a 27.5-ft/sec vertical impact velocity crash condition. The report contains brief descriptions of the three computer programs, the respective aircraft section mathematical models, pertinent data from the test performed at NASA Langley, and a comparison of analysis results versus test results. Cost and accuracy comparisons among the three analyses are presented to illustrate the possible uses of each of the programs. Application of PAM-CRASH programs to analysis of helicopter structures including crushing of stiffened panels and fuel tanks is described in Reference 70.

While accurate and versatile computer programs are essential for crash-resistance analyses, particularly for hybrid programs, some expertise in modeling a vehicle for nonlinear dynamic analysis is also necessary. The remainder of this section discusses in detail the programs KRASH and DYCAST that are most widely used in the aircraft industry.

7.6.1 Program KRASH

The computer program KRASH was originally developed by Lockheed-California Company under U.S. Army support to analyze the dynamic response of helicopters subjected to a multidirectional crash environment. Subsequent to the U.S. Army-sponsored efforts (Reference 110), KRASH was upgraded under an FAA contract (Reference 116), and its capabilities were directed toward the analysis of light fixed-wing aircraft subjected to crash impact conditions. The updated version was called KRASH79 and contained many new features, while retaining its original formulation. Recently completed FAA-sponsored research (Reference 117) has resulted in additional program enhancements. Although the current version, denoted KRASH85, contains features that are directed toward the analysis of large transport airplane crash scenarios, it is also applicable to both helicopters and tilt-rotor aircraft.

Program KRASH is a hybrid program that solves coupled Euler equations of motion for interconnected lumped masses, each with six degrees of freedom defined by inertial coordinates x, y, z, and Eulerian angles ϕ_i, θ_i, ψ_i. The equations of motion are explicitly integrated to obtain the velocities, displacements, and rotations of lumped masses under the influence of external forces such as gravity, aerodynamic and impact forces.

Program KRASH utilizes nonlinear spring and beam elements and lumped masses arranged in a three-dimensional framework to simulate the fuselage structure. The nonlinear characteristics needed to describe the structural elements are derived from component testing and other analyses and input to KRASH.

Major features of the KRASH program are summarized below:

- Aircraft major mass items and occupants are modeled as lumped masses.
- Nonlinear external spring elements are used to model crushable structures, tires, and landing gear.
- Linear and nonlinear beam elements are used to model the airframe structure. Stiffness reduction factors are used to represent the nonlinear properties. Structural failure can be modeled by specifying forces or displacements at failure.
- Initial conditions of linear and angular velocity about three axes and impact into a horizontal ground and/or inclined slope can be specified. Interface to NASTRAN is also available to facilitate initial equilibrium in the presence of aerodynamic forces.
- Symmetric and unsymmetric impact conditions can be specified.

- Large structural displacements and rotations can be simulated.
- Mathematical model can contain up to 80 lumped masses, 50 massless node points, and 180 nonlinear degrees of freedom.
- Restart capability.

Major output parameters available from program KRASH are as follows:

- Mass point and node point response time histories (displacement, velocity, and acceleration).
- Beam load time histories.
- Distribution of kinetic and potential energy by mass item, distribution of strain and damping energy by beam element, and crushing and sliding friction energy associated with each external spring.
- Occupant survival indicators: livable volume change, mass penetration into an occupiable volume, probability of injury indicated by Dynamic Response Index (DRI).
- Overall vehicle center-of-gravity translation velocity.
- Energy distribution by mass, beam, and spring elements.

A comprehensive discussion of theoretical development of program KRASH is presented in Reference 118. A discussion of program KRASH input-output techniques is presented in References 117 and 119. Reference 120 provides a discussion of design guidelines which may be used with program KRASH in the structural crash-resistance analysis of general aviation airplanes. Information related to the program's system requirements and functional organization is contained in Reference 121. Reference 117 applies to the most recent version, KRASH85, and References 118 through 121 were published with previous versions, KRASH and KRASH79. A comparison of the capabilities of three versions of KRASH is presented in Table 12 (Reference 122). A KRASH model of the Sikorsky ACAP helicopter is shown in Figure 105 (Reference 123).

The experimental data used in the validation of program KRASH is summarized in Table 13. Reference 124 describes the use of program KRASH to model a CH-47A crash test. Recent applications of program KRASH include preliminary design of helicopter structures (Reference 123 and 125), landing gears (Reference 126), and evaluation of transport aircraft crash scenarios (Reference 127).

Figure 106 illustrates the iterative analysis and component test process used to predict a complete system response with program KRASH. The system design itself is then modified in an iterative process with the use of the program to obtain the required system performance.

Figures 107 and 108 show the output of the KRASH model alongside actual test photos for corresponding times in the drop test of an experimental cabin section and the Bell ACAP helicopter respectively (Reference 128).

TABLE 12. COMPARISON OF CAPABILITIES OF THREE VERSIONS OF PROGRAM KRASH (FROM REFERENCE 122)

Features	Version KRASH	KRASH 79	KRASH 85
1. Energy Distribution	Yes	Yes[d]	Yes[e]
2. Element Rupture	Yes	Yes[d]	Yes[d]
3. Injury Criteria (DRI)[a]	Yes	Yes[d]	Yes
4. Plot Capability/Summaries	Yes	Yes	Yes[e]
5. Volume Penetration	Yes	Yes	Yes
6. Plastic Hinge Algorithm	No	Yes	Yes[d]
7. Shock Strut	No	Yes	Yes
8. Flexible and/or Sloped Terrain	No	Yes	Yes
9. Acceleration Pulse Excitation	No	Yes	Yes
10 Unsymmetrical Beam Representation	No	Yes	Yes
11. Standard Material Properties	No	Yes	Yes
12. External Spring Damping	No	Yes	Yes
13. Mass Location Plots	No	Yes	Yes
14. Pre- and Post-data Processing	No	Yes	Yes
15. Restart Capability	No	Yes	Yes
16. Symmetrical Model Capability	No	Yes	Yes
17. CG Force Motion History	No	Yes	Yes[d]
18. Volume Change Calculations	NO	Yes	Yes
19. Standard Nonlinear Curves	No	5	6
20. Stiffness Reduction Feature (KR)[b] Applicable to Damping	No	No	Yes
21. Combined Failure Load (LIC)[c]	No	No	Yes
22. Initial Balance Nastran	No	No	Yes
23. Tire Vertical Spring	No	No	Yes
24. Arbitrary Mass Numbering	No	No	Yes
25. External Force Loading	No	No	Yes
26. Oleo Metering Pin	No	No	Yes
27. Addition of Descriptive Names to Identify Input Data	No	No	Yes

a. Dynamic Response Index
b. Stiffness Reduction Factor
c. Load Interaction Curve
d. Enhanced One Level
e. Enhanced Two Levels

7.6.2 Program DYCAST

The computer program DYCAST (Dynamic Crash Analysis of Structures) is one module of the PLANS (Plastic and Large deflection Analysis of Structures) system of nonlinear finite element structural analysis computer codes. These programs have been developed under contract to NASA Langley Research Center as part of a joint NASA/FAA program in general aviation crash resistance. The PLANS modules for static analysis of structures are described in Reference 129 and program DYCAST is described in Reference 115.

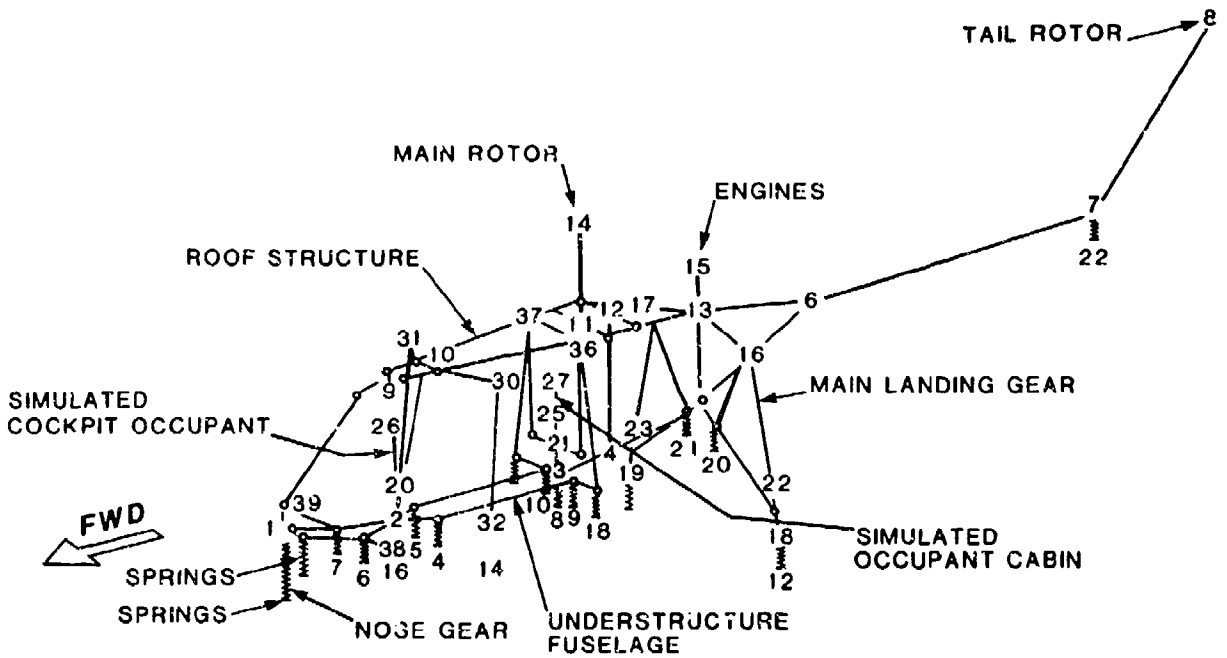

FIGURE 105. PROGRAM KRASH MODEL OF THE SIKORSKY ACAP HELICOPTER. (FROM REFERENCE 123)

Major features of program DYCAST are as follows:

- Nonlinear material capability. Material types available include isotropic plane stress, orthotropic with ideal plasticity, and orthotropic with orthotropic strain hardening.
- Element library that includes stringers, beams, membranes, plates, and springs.
- Capability to model very large displacements and rotations.
- Four different numerical integration methods, three with internally varied time steps.
- Detection of failed members.
- Restart capability.

TABLE 13. EXPERIMENTAL VALIDATION OF PROGRAM KRASH (FROM REFERENCE 122)

Test No.	Aircraft	Gross Weight (lb)	Impact Velocities (ft/sec) Vertical	Longitudinal	Lateral
	Rotary Wing				
1	Utility Type	8,600	23	-	18.5
2	Cargo Type	24,300	42	27.1	-
3	Multi-Purpose	3,800	19.7	19.7	-
4	Multi-Purpose	3,620	32.8	-	-
5	Composite Substructure	3,530	30.0	-	10.3
6	Composite Substructure	3,530	28.2	-	10.3
NA	Bell ACAP (Ref 47)	7,279	41.4	26.4	-
NA	Sikorsky S75 ACAP (Ref 48)	-	38.0	-	-
	Light-Fixed-Wing				
7	Single-Engine, High-Wing	2,400	46	70	-
8	Single-Engine, High-Wing	2,400	42	71.3	-
9	Single-Engine, High-Wing	2,400	49	70	-
10	Single-Engine, High-Wing	2,400	43	89.9	-
11	Twin-Engine, Low-Wing Substructure	2,400	43	-	-
	Transport				
12	Medium Size*	159,000	18	-	172
13	Medium Size	195,000	17.3	260	-

*Test performed on soil; all other tests on rigid surface.

DYCAST accounts for two types of nonlinearities: material and geometric. The nonlinear material behavior, exhibited by materials yielding plastically, is accounted for by the stress-strain curves specified as part of the input data. Three types of stress-strain curves are permitted: elastic-perfectly plastic, elastic-linearly hardening, and elastic-nonlinearly hardening. DYCAST uses a flow theory of plasticity. Basic to this approach is defining an initial yield criterion as well as flow and hardening rules. The initial yield criterion used is based on Hill's equations for orthotropic material behavior which reduces to Von Mises yield criterion for isotropic materials.

The element stiffness during the simulation is determined using the tangent moduli corresponding to the current stress and strain, generalized for multi-axial states at various points on the element cross section (Reference 115).

Geometric nonlinearities due to large deformations of the structure change the effective stiffness of the structure and are treated in DYCAST by an up-dated Lagrangian formulation (Reference 115). The essentials of this method are that the solution is obtained incrementally, solving for increments in

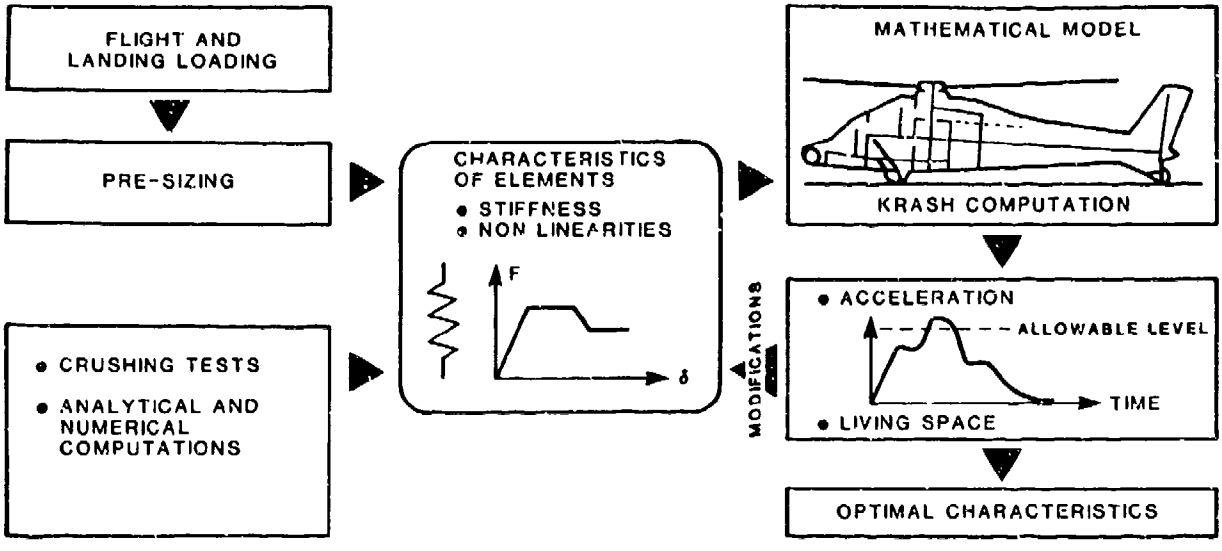

FIGURE 106. PREDICATION OF CRASH BEHAVIOR WITH PROGRAM KRASH.

displacement, stress, and strain at each increment. These quantities are all referenced to the undeformed initial conditions so that the incremental stresses and strains represent the second Piola Kirchoff stress and Green's strain tensor respectively.

The incremental global equations of motion for the system written in matrix form are:

$$[M]\{\Delta\ddot{u}\} + [K]\{\Delta u\} = \{\Delta P\} + \{R\} \qquad (59)$$

where $[K]$ = Stiffness Matrix

$[M]$ = Consistent Mass Matrix

$\{\Delta u\}$ and $\{\Delta\ddot{u}\}$ = displacement and acceleration increments

$\{\Delta P\}$ = Incremental external load vector

$\{R\}$ = Vector of equilibrium force corrections

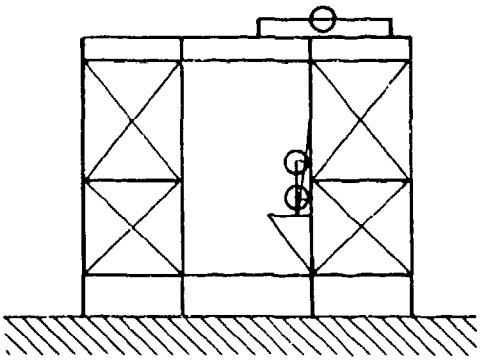

INITIAL CONTACT
WITH GROUND
T = 0 SEC

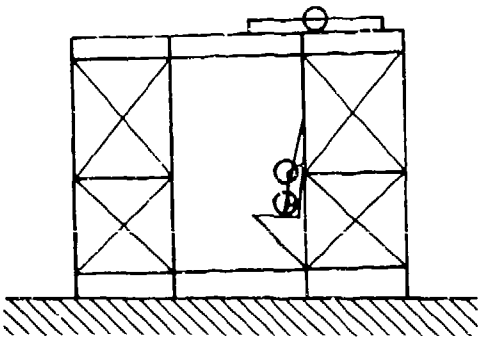

MAXIMUM
FUSELAGE CRUSHING
T = .023 SEC

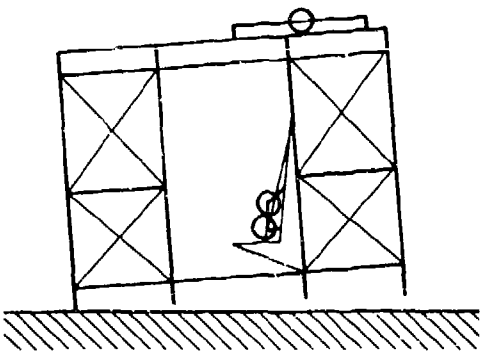

MAXIMUM
SEAT STROKE
T = .071 SEC

FIGURE 107. COMPARISON OF STRUCTURE DEFORMATION FOR FLAT DROP TEST.

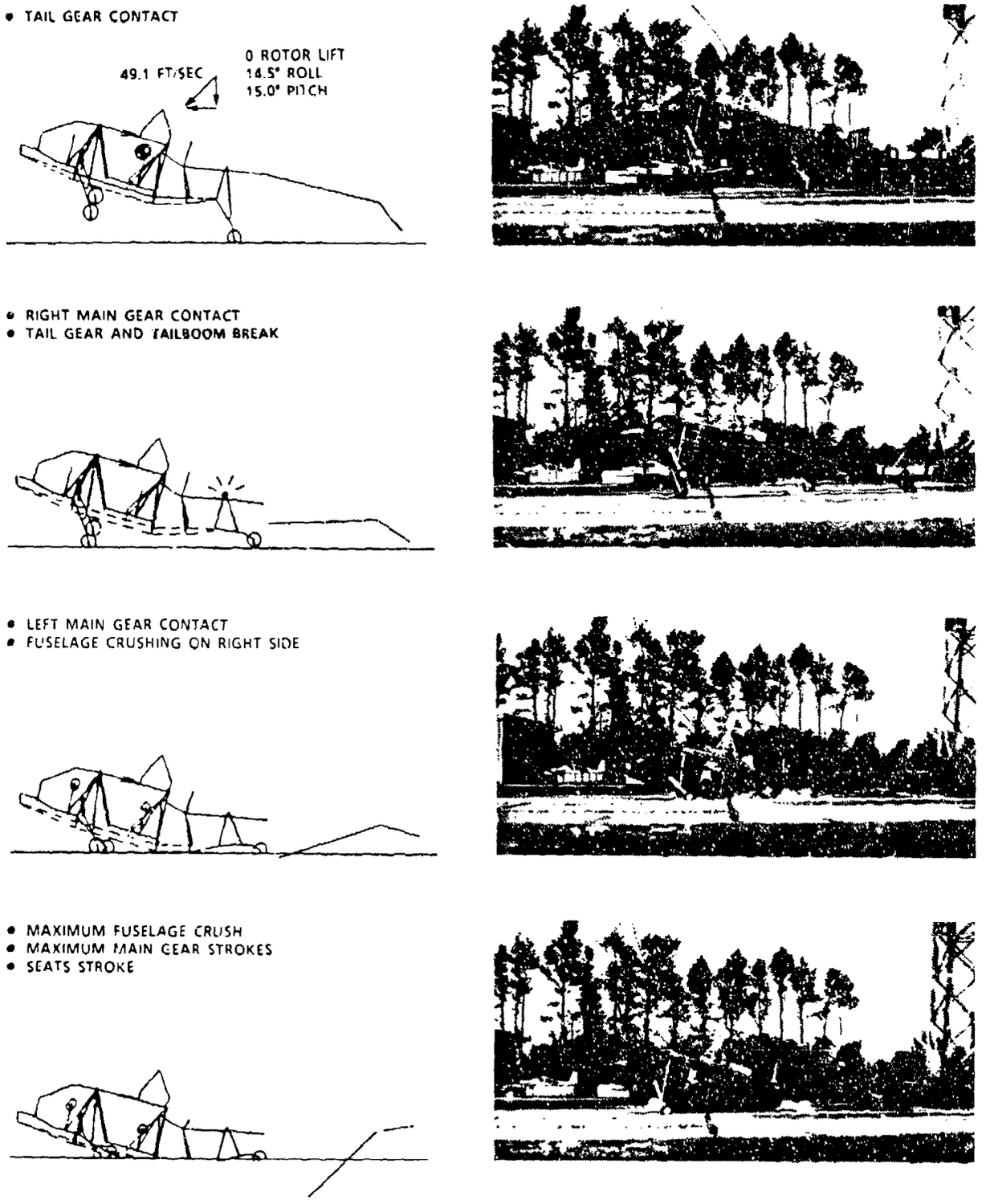

FIGURE 108. BELL ACAP KRASH VERSUS TEST COMPARISON.

Both material and geometric nonlinear effects are accounted for in the equations of motion through formulation of the stiffness matrix [K]. This system of equations is numerically integrated to obtain the response of the structural model.

Both implicit and explicit numerical integration methods are implemented in DYCAST. Central Difference and modified Adams Predictor-Corrector methods are the explicit algorithms, and Newmark-β and Wilson-θ methods are the implicit algorithms. All methods but Central Difference permit a variable time step throughout the analysis.

For solution of nonlinear problems with constant time step, the explicit methods lead to constant coefficient matrices, but the implicit methods may require the formulation of coefficient matrices at each time step. The choice of which method to use involves trade-offs between smaller but computationally less intensive time steps for explicit integrators versus larger but computationally more intensive time steps for implicit integrators.

The element library consists of the following elements:

- Stringers - Two types of stringer elements are available: a two-node element developed from a constant axial strain assumption and a three-node element developed from a linearly varying strain assumption.

- Beams - Twelve different beam cross sections are available. Distinct cross sections are required to calculate the extent of the plastic behavior within the beam cross section.

- Membranes - Three types of triangular membrane elements are available: a three-node constant strain, a six-node linear strain, and four- and five-node transitional elements. The transitional elements permit mixed strain conditions, i.e., constant strain along an edge with linear strain along other edges.

- Springs - An axial force element with force-deflection characteristics specified in a tabular form. This element can be used to simulate structural sections with known force-deflection behavior, to represent an energy-absorbing device, or as a gap element with zero stiffness over a certain range of deflection and nonzero thereafter.

DYCAST restart feature allows a large problem to be run in several parts. This reduces the demand on computer resources and allows the user to examine the results of the simulation as it progresses. The output data from DYCAST include the following:

- Nodal displacements, velocities, and accelerations.

- Element strains and stresses through the cross sections.

- System energy distribution.

- Plots of time histories of displacements, velocities, and accelerations at user-specified nodes.

- Plots of the deformed structure at any time and from any viewing angle.

Further information on DYCAST is given in References 115, 129, and 130. Reference 106 presents a comparison of DYCAST and KRASH modeling of the same section of a light aircraft fuselage structure. DYCAST analyses of helicopter fuselage structures constructed of composite materials are presented in References 50 and 131. A DYCAST model of a helicopter composite cabin section is shown in Figure 109 (Reference 131). Modeling strategies with DYCAST as well as program execution times on various computer systems are given in Reference 131. Reference 132 describes the use of program DYCAST to model sections of transport fuselage which were drop tested at NASA Langley.

7.6.3 PAM-CRASH

PAM-CRASH is a highly nonlinear explicit three-dimensional finite element code for analyzing large deformation dynamic response. It has been widely used in the automotive industry due to its capability to accurately predict automobile crash impact response. This type of analytical tool has been applied to problems in the areas of stiffened panel crushing, fuel tank impact, etc. (Reference 133). Figure 110 shows the correlation of drop test results with the dynamic analysis of a fuel tank.

7.7 POTENTIAL SOURCES OF BASIC STRUCTURAL DATA FOR CRASH-RESISTANCE ANALYSIS

A major obstacle to analyzing structural crash resistance is the difficulty of obtaining adequate data concerning the dynamic failure mechanisms of structural assemblies and elements. Such data are necessary for the analysis techniques described earlier, with the possible exception of the finite element methods. A previous section described semiempirical analysis of airframe components which can be used to provide structural characteristics for computer simulation. Data useful for structural analysis can also be obtained from sources discussed within the following paragraphs.

7.7.1 Estimates

An estimate of the dynamic capability of a structural element or system can be obtained by using standard static failure criteria and multiplying the result by a dynamic correction factor. This method has limited usage since the factor usually specified for the overall failure sequence is representative of the energy-absorption variation between static and dynamic failure modes.

Consequently, a time history of element failure is not usually considered, but the net effect, in terms of energy absorption, is used to determine the gross capability of the structure considered. Such analyses are useful in defining the gross crash-resistance contributions of structural layout prior to the use of more complex analysis techniques.

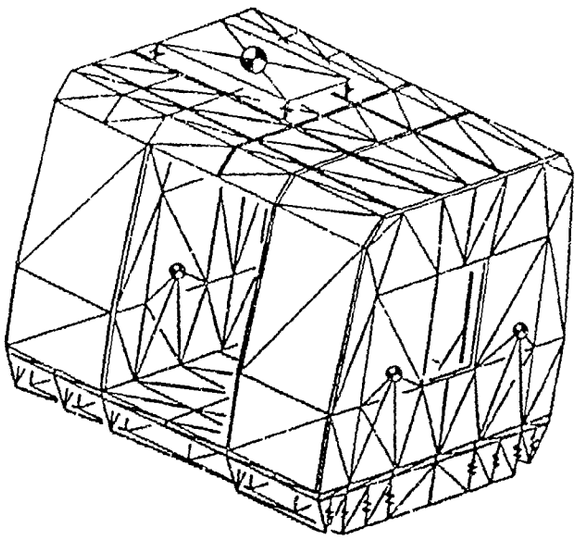

a. FINITE ELEMENT MODEL OF THE COMPOSITE CABIN SECTION

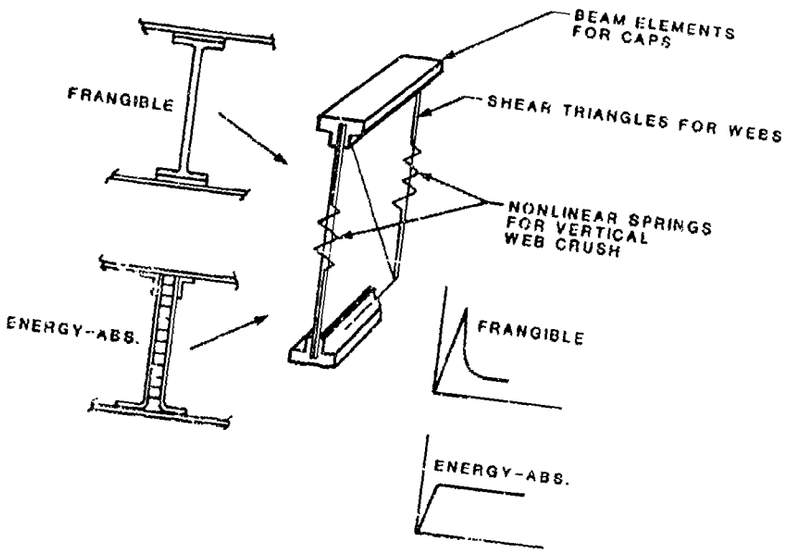

b. SUBFLOOR MODELING DETAIL

FIGURE 109. PROGRAM DYCAST MODEL OF COMPOSITE HELICOPTER STRUCTURE. (FROM REFERENCE 131)

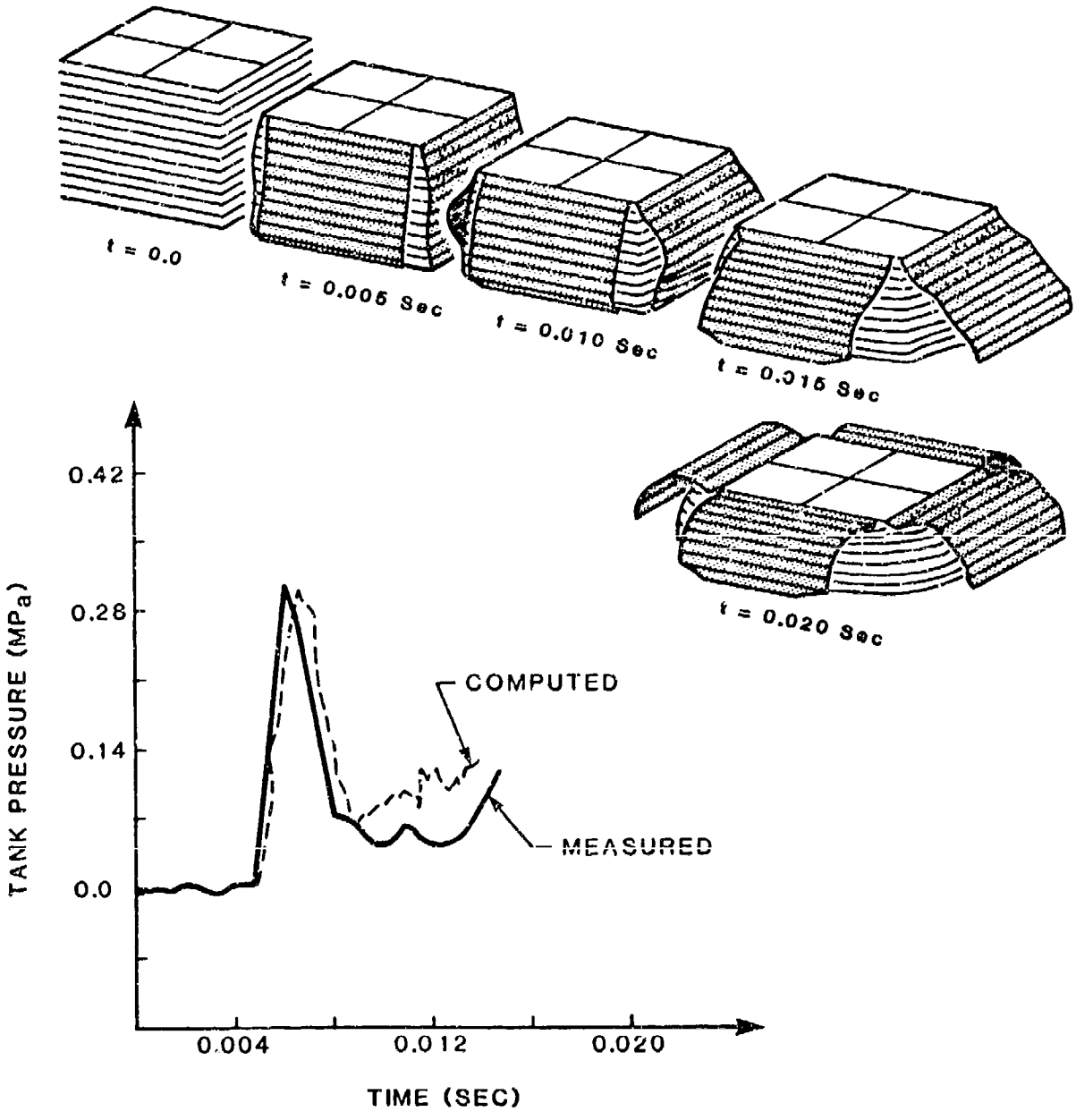

FIGURE 110. 14 M/SEC IMPACT OF A STRUCTURE-FUEL TANK SYSTEM (PAM EFHYD 3D). (FROM REFERENCE 70)

Care must be exercised when using such a technique since structural elements exhibit differing failure modes, and these modes may vary depending on the rate of load application. Additionally, the total load-carrying capability of a member also will be dependent on the rate of load application.

7.7.2 Aircraft Accident Data

Aircraft accidents can provide useful data concerning structural response if the wreckage can be examined in detail before it is disturbed from its post-impact location. Examination of the wreckage can yield data concerning the failure modes and sequences; the effectiveness of energy-absorbing features, if any; and the occupant crash impact conditions experienced in terms of space, extremity flailing, acceleration levels, and injury causes.

Such a relatively subjective review also requires other data to enable the investigator to determine a complete crash scenario. Some of these data can be determined from the crash site itself, particularly terrain hardness, ground obstacles, impact attitude, mass item breakaway, flammable fluid containment, egress potential, etc. However, more important parameters that are harder to obtain include the impact velocity components and the acceleration conditions in the occupied areas. In fact, these data probably will not be available in a recorded format unless the crashed aircraft happened to be a test vehicle with on-board instrumentation. As a result, the velocity components at impact are often estimated using the gross deformations of the structure and the motion of the aircraft relative to the ground. Simple energy and momentum techniques are used to do this; and although the resultant velocity and acceleration estimates are the best available, such an analysis cannot apportion the energy absorption through the aircraft, i.e., in the landing gear, structure, seats, etc.

Reference 110 describes an examination of 3657 U.S. Army rotary-wing aircraft accidents that occurred between 1967 and 1971 and a detailed review of 32 of these. References 134 and 135 describe investigation of general aviation accidents and the information that can be obtained.

A major contribution to the quest for better aircraft crash resistance made by crash analyses is the delineation of the good and bad features of a particular design. By compiling accident data, qualitative assessment of the desirable and undesirable features exhibited by various aircraft types can be made. Once a reasonable data base is compiled, the desirable features can be pinpointed and included in future designs or redesigns. Undesirable features can be suitably identified to ensure their use is not continued.

The most accurate means of validating crash analysis is full-scale crash testing. However, scale-model testing may also be used to advantage. Both are discussed in the following sections.

8. TESTING

8.1 INTRODUCTION

Testing is needed to support many phases of the design of a crash-resistant structure. Initially, crash tests are used to gather data to assist in development of performance criteria. In analytical work, testing is needed to evaluate properties of structural component, and to validate analytical models. In the design process, component tests are essential to proper sizing and configuration of crash-resistant structures. Finally, qualification tests verify that an airframe or components of an airframe will satisfy the crash-resistance performance requirements.

Tests may be either static or dynamic. A static test is usually performed by applying force(s) to a structural test component anchored to a rigid fixture, but can also be performed on a centrifuge. It is suitable for many component design tests. Dynamic tests utilize high-rate deformation typical of a crash. They are usually conducted by impacting the test specimen into a mechanism or material which will deform in a controlled manner to simulate the dynamic response of the appropriate structural interface. For example, in seat tests the fixture is decelerated in a manner which simulates the response of the aircraft underfloor structure in a crash.

Tests may be conducted with a full-scale structure or with a scale model of a structure. A complete structure may be tested, or just a component of the structure. The type of test must be matched to the specific need for information. Typical possibilities are shown in Table 14. Scale-model testing is mostly useful for supporting analytical development efforts.

TABLE 14. TYPE OF TEST POSSIBILITIES

	Static				Dynamic			
	Full Scale		Scale		Full Scale		Scale	
Application	Complete Structure	Component	Complete Structure	Component	Complete Structure	Component	Complete Structure	Component
Performance Criteria Development					X			
Analysis - Component Characterization		X		X				
Analysis - Validation			X				X	
Design Support		X				X		
Qualification					X			

Full-scale component tests are primarily useful for design support including analytical component characterization. Full-scale complete structure tests are appropriate for criteria development and system qualification.

8.2 STRUCTURAL STATIC TESTING

Compatibility is important at the structural interfaces between the airframe and all attached components. The design of the fuselage structure, including the hard points and load distribution structure around the hard points, must be coordinated with the design of the attaching components. Structural properties for all loading conditions and design features, such as structural releases, must be coordinated to achieve the desired compatibility.

A comprehensive system design approach requires that such compatibility be demonstrated. Ideally, static tests of components attached to the fuselage structure by their normal attachment provisions should be performed to demonstrate compatibility. Components such as seats, cargo restraints, engines, and transmissions mounts, landing gear, and attachments for any ancillary or heavy equipment located in an area which could create a hazard for the occupants if freed during a crash should be tested. The ultimate design crash loads should be applied in all hazardous loading directions to demonstrate that the attachment points as well as the load-bearing sections of the fuselage are capable of maintaining structural integrity during a crash. As a minimum, all components and their attaching hardware should be tested on suitable fixtures and hardpoints for their mounting, and the fuselage should be verified by a combination of analysis and complete aircraft system qualification testing.

8.3 LANDING GEAR CRASH TESTING

Instrumented drop tests should be conducted: (1) to verify landing gear crash force attenuation and crash loading strength characteristics analytically predicted and (2) to substantiate the capability of the aircraft landing gear to meet the criteria of Section 4.2.1.7. Drop testing of wheel and skid landing gear should be conducted in accordance with paragraph 9-2.3 of AMCP 706-203 (Reference 136). The 20-ft/sec sink speed drop test should be conducted with the landing gear oriented in a 5-degree nosedown and 10-degree roll attitude and drop tested onto a level, rigid surface with a sink speed of 20 ft/sec at ground contact. Landing gear should also be drop tested in a 0-degree roll, pitch, and yaw attitude onto a level, rigid surface with a sink speed of 42 ft/sec at ground contact to demonstrate crash impact energy-absorption capability. Simulated rotor lift for all drop tests should not exceed one DGW. Tests with a pair of gear mounted on an "iron bird" fixture simulate the aircraft crash conditions more accurately than do tests on a single gear.

8.4 CARGO RESTRAINT

Design loads are specified in Section 6.2.7. Static tests to these loads are recommended. All deformation measurements are to be made at the floor level. Sufficient dynamic tests should be made to assure that design predictions can be accurately based on static test results.

8.5 SEAT AND RESTRAINT SYSTEM

Since proper performance of these items is critical for occupant survival, extensive qualification testing is required by MIL-S-58095 and MIL-S-85510. Testing requirements for seats and occupant retention systems are also described in Volume IV.

8.6 FUEL SYSTEM

Testing requirements for fuel systems are described in Volume V.

8.7 ANCILLARY EQUIPMENT RETENTION

Design loads are specified in Section 6.2.7.8. As a minimum, static tests to these levels are recommended. If appreciable dynamic overshoot is likely, dynamic tests should be conducted.

8.8 FULL-SCALE TESTING

Instrumented, full-scale crash test(s) may be conducted: (1) to verify analyses performed. (2) to substantiate the capability of the aircraft system to meet crash-resistance specifications, and (3) to gather further engineering data on the impact response of aircraft structures.

The present state of the art in analysis of structural behavior under crash impact conditions is such that predictions of location and modes of collapse and failure and predictions of impact forces, accelerations, and deformations have limited accuracy. For this reason, full-scale dynamic crash testing to complement and substantiate analytic simulation of airframe behavior is highly recommended. Such crash tests should be conducted under conditions representative of a severe survivable crash, and testing should demonstrate that the required design specifications are met.

Full-scale tests of the complete aircraft can demonstrate proof of compliance for fuselage and related structures such as landing gear, engines, transmissions, seat tiedown provisions, and fuel tanks and systems. Full-scale testing will validate that the entire energy absorption system of landing gear, fuselage structure, and seats operate satisfactorily.

When full-scale crash tests are conducted, test results should also be carefully studied to provide information for design improvement and for background to improve future designs.

Controlled testing has been done in the past on a variety of aircraft to demonstrate the capabilities of structure, landing gears, fuel systems, etc., in typical crash impact conditions. (See, for example, References 78, 102, and 137 through 140.) Initially, such tests were often performed using powered aircraft that were remotely controlled or prealigned for impacts into selected terrain conditions. Useful data were obtained from many of these tests, although some resulted in postimpact fires and information loss.

A more recent approach for vertical impacts has been to drop test specimens from a fixed site or a moving carrier. Structural assemblies, small aircraft, and helicopters have been tested in this manner. Representative

impact conditions and velocities can be achieved by adjusting the vertical drop height and/or the longitudinal velocity of the carrier as well as roll and yaw attitudes.

The largest facility used for full-scale crash testing of light aircraft and helicopters is the Impact Dynamics Research Facility at NASA Langley Research Center (Reference 141), shown in Figure 111. Here aircraft are allowed to swing on cables that are preset to determine the overall impact attitude. Velocity components are controlled by varying the drop height, cable length, and cable anchor locations. Immediately prior to impact, the aircraft is released from the cables by pyrotechnic means. The ground impact and subsequent motions are then completely unrestrained. A schematic of the NASA Langley crash facility is shown in Figure 112, where the test setup is that used for the full-scale drop test of the YAH-63 helicopter.

The sequence of photographs in Figure 113 shows the drop test of the YAH-63 helicopter impacting at a pitch angle of +9.25 degrees and vertical and horizontal velocities of 48.0 and 26.2 ft/sec, respectively. The test provided data for a helicopter with designed-in crash resistance, including energy-absorbing seats, fuselage structure, and landing gear. Test results are detailed in References 137 and 125.

The primary advantage of testing full-scale aircraft is that there is no need to interpret the data or attempt to extrapolate the results to other structural formats. All data such as velocities, attitudes, accelerations, and structural strains are measured directly as functions of time from impact. In addition, high-speed cameras can record displacements from various locations inside and outside the aircraft in order to provide visual time histories of structural and occupant response during the crash sequence. Instrumented anthropomorphic dummies positioned and restrained in seats with actual restraint systems aid in the evaluation of the occupant's potential for impacting the aircraft interior and for occupant survival. Postcrash review of damage also provides a direct indication of the aircraft's performance with respect to occupied volume penetration, seat and landing gear performance, large mass item retention, and flammable fluid containment.

For very small helicopters, such as the R-22 where seats are not separable but are part of the fuselage, full-scale testing may be the only way to obtain an assessment of the system's crash performance. The above description of full-scale testing may imply that this is the only technique worth using to attain realistic crash simulation. However, such tests are expensive to run, and aircraft, especially new design prototypes, are difficult to obtain. In addition, such tests require careful planning with a redundancy of recording equipment because of the probability that data may not be obtained from all instrumentation channels.

8.9 SCALE-MODEL TESTING

Scale-model testing has been used extensively when investigating the aerodynamic characteristics of aircraft, bridges, buildings, etc. Scale-model testing for structural strength and deflection verification also has been used where material sizes allow. For evaluating crash resistance, however, scale-model testing becomes a more difficult problem, especially when severe plastic deformation and element rupture occur.

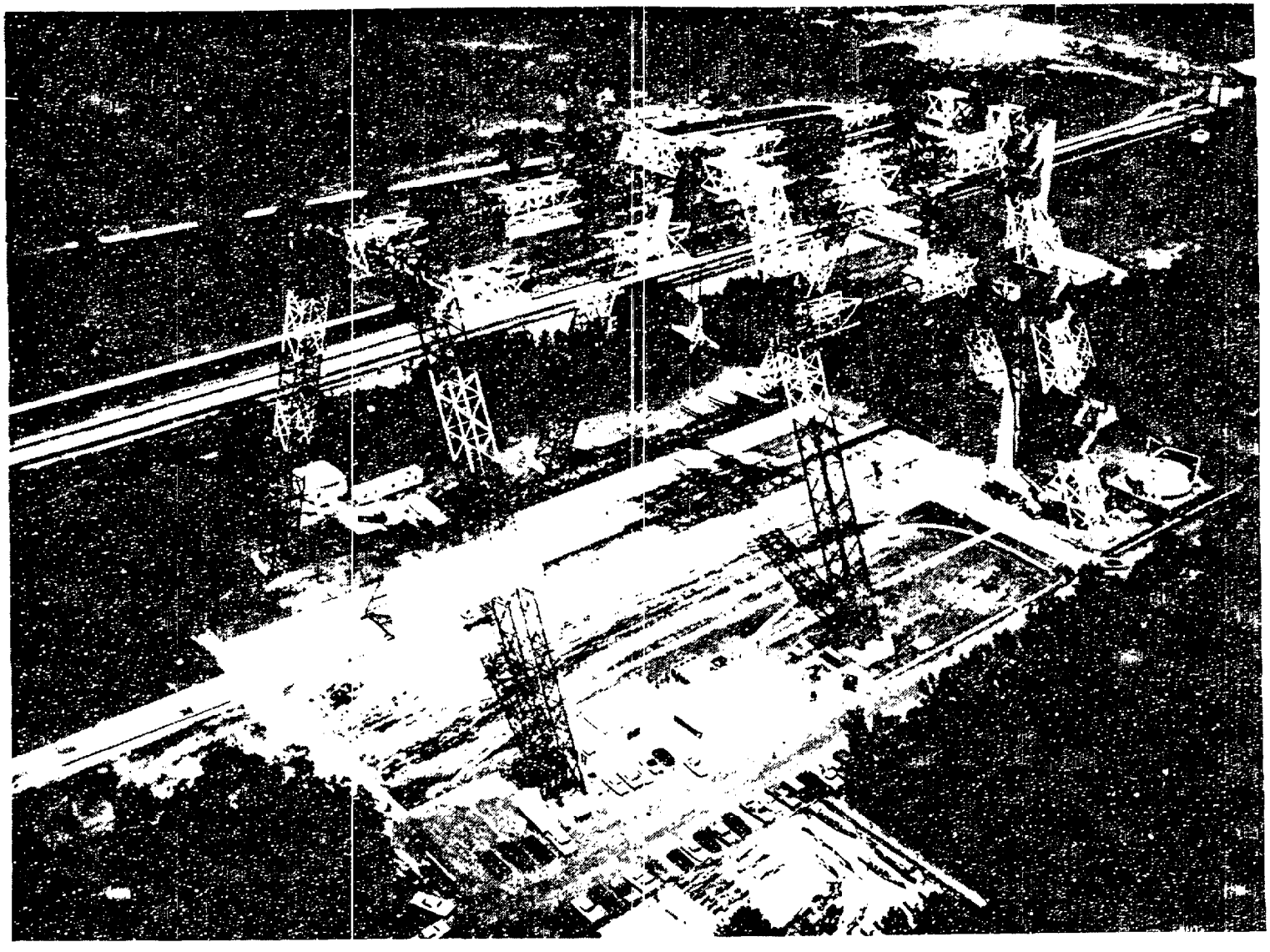

FIGURE 111. NASA LANGLEY IMPACT DYNAMIC FACILITY.

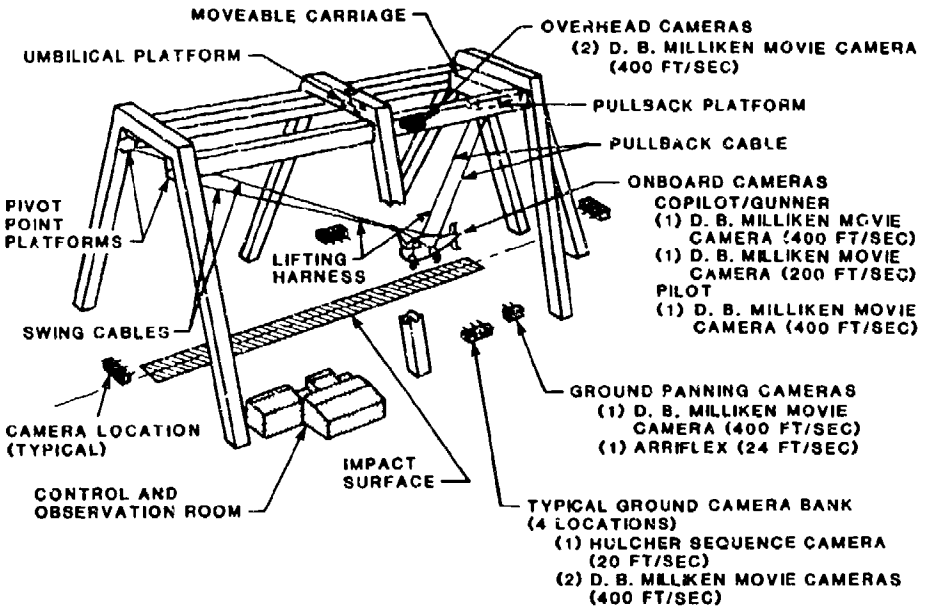

FIGURE 112. NASA LANGLEY CRASH FACILITY LAYOUT AND FIXED CAMERA POSITIONS. (FROM REFERENCE 137)

Scale modeling of major structural members may provide data that can be used for crash-resistance studies; however, when semimonocoque construction is considered, stringers and skin are often made from relatively thin sheet material, measuring from approximately 0.015 to 0.06 in. Depending on the structure being modeled, certain nondimensional parameters must be satisfied for both the model and the aircraft. Examples of these are:

$$\frac{X_i}{L}, \epsilon, \frac{\sigma}{E}, \dot{\epsilon}t, \frac{vt}{L} \tag{60}$$

where X_i = spatial coordinate

L = characteristic length

ϵ = strain

σ = stress

E = Young's Modulus

$\dot{\epsilon}$ = strain rate

t = time

v = velocity

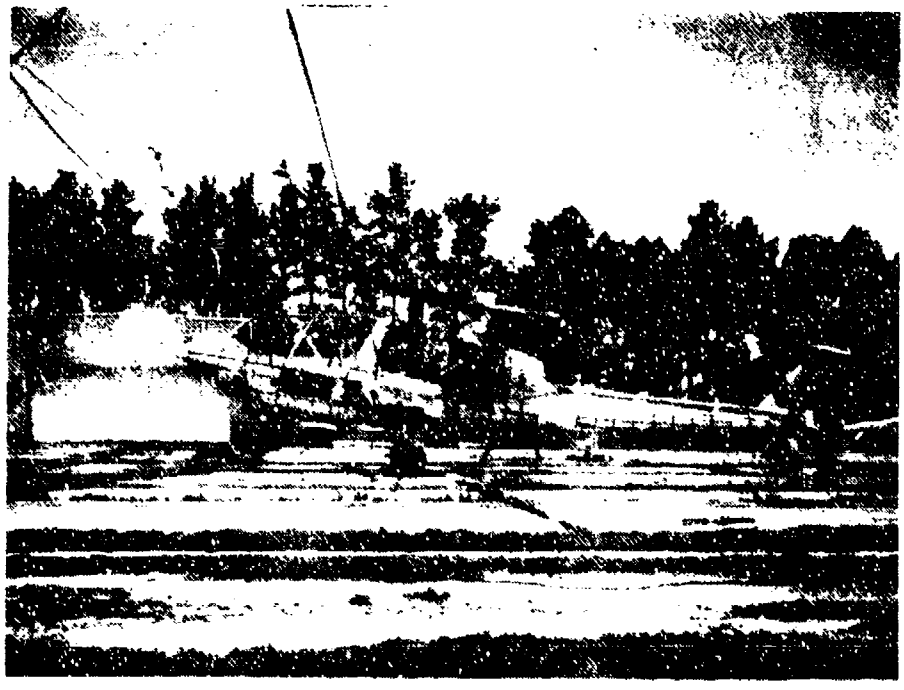

TAIL IMPACT

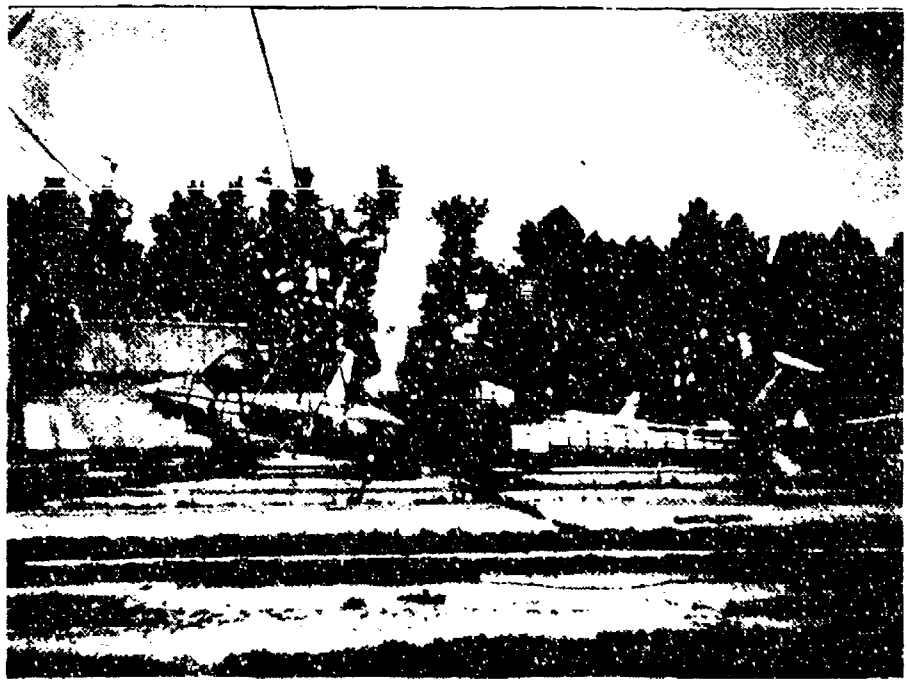

ENERGY-ABSORBING LANDING GEAR STROKING

FIGURE 113. FULL-SCALE CRASH TEST OF A YAH-63 HELICOPTER.

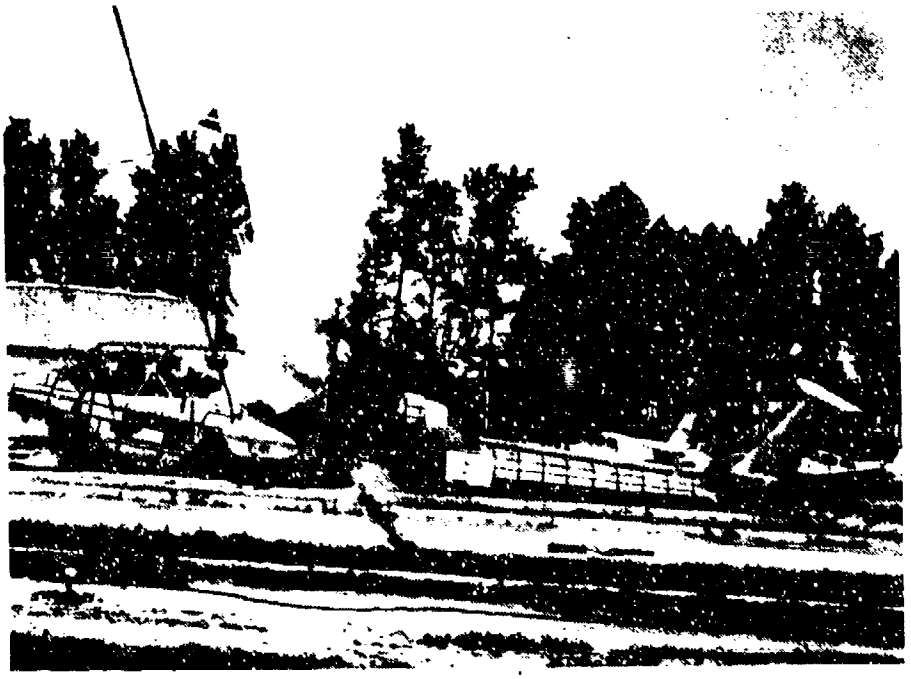

FUSELAGE IMPACT

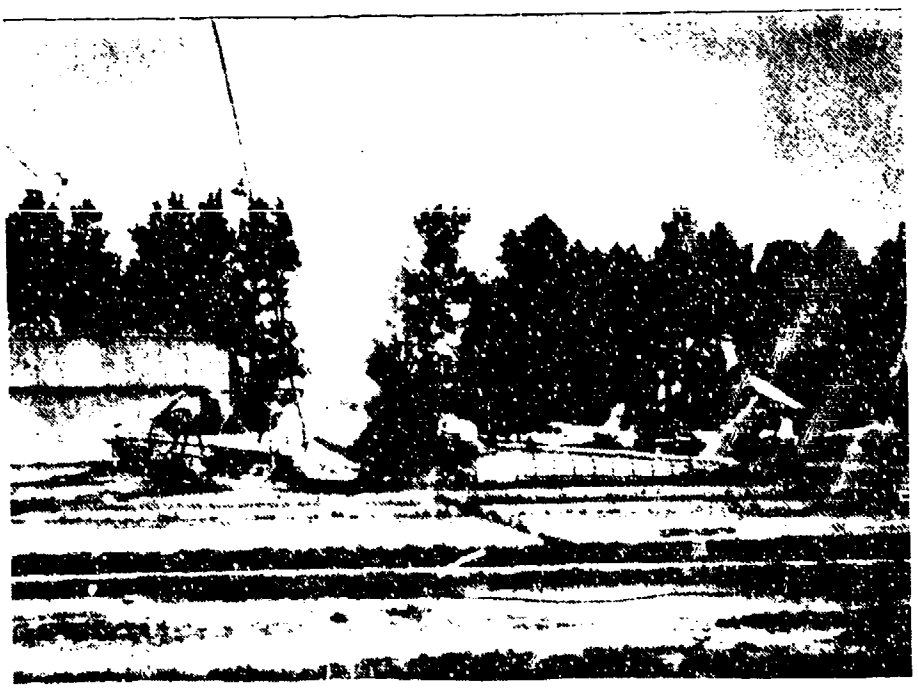

ENERGY-ABSORBING FUSELAGE DEFORMATION

FIGURE 113 (CONTD). FULL-SCALE CRASH TEST OF A YAH-63 HELICOPTER.

Some of these parameters involve the thickness of the material, and for example, scaling 0.015-in.-thick sheet metal for a one-tenth scale poses major problems in the manufacture, handling, and tolerance effects when using 0.0015-in. shim material.

Reference 143 presents a discussion of scale-modeling techniques applied to structural crash resistance. Practical considerations in geometric scaling are discussed and illustrated using barrier tests of two different automobile front-end structures and an impulsively loaded section of semimonocoque cylinder similar to an aircraft fuselage.

A conclusion of that study was that for prototype structures in the 1,000- to 10,000-lb weight range, and for scale factors of from 3 to 8, a model test can be performed at less than half the cost of a corresponding full-scale test, depending on the scale factor, as demonstrated by Figure 114. It was concluded that scale model tests can meet the same objectives and could therefore replace many full-scale tests in a crash-resistance research and development program. Model tests are particularly useful for screening new concepts, for performing parametric experimental studies, and for the initial optimization of a given concept. Full-scale tests are still required for proving the concept and for making detailed measurements such as those of occupant response.

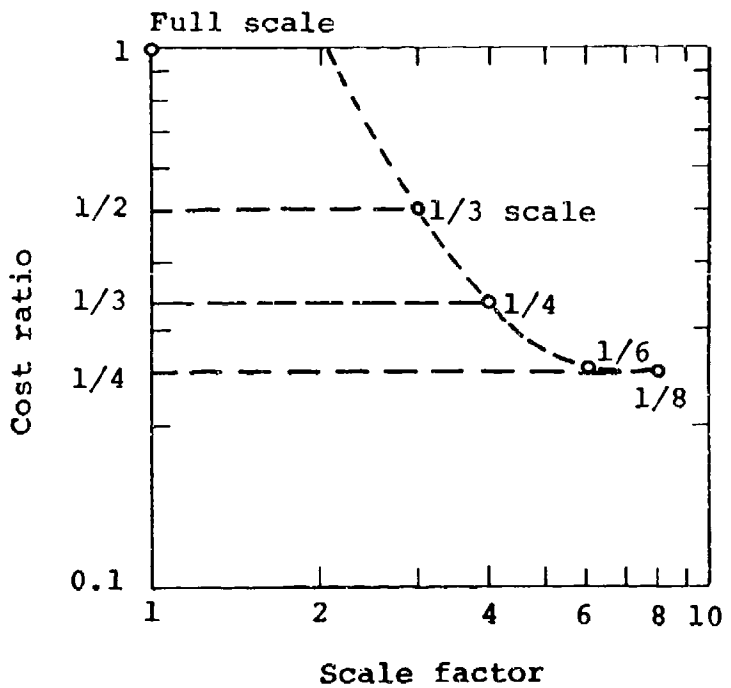

FIGURE 114. COST RATIO (SCALE MODEL TEST COST/FULL-SCALE TEST COST) VERSUS SCALE FACTOR FOR STRUCTURES WEIGHING LESS THAN 10,000 LB. (FROM REFERENCE 144)

Also, in another recent study 1/3-scale models of various configurations of stiffened sheet panels, like that shown in Figure 115 (Reference 144), were tested in order to determine the influence of the following parameters:

- Variation of the stiffener pitch (d) with respect to the height (h)
- Variation of the stiffener section (S) with respect to the panel sheet section
- Variation of the lightening hole diameters (ϕ) with respect to the stiffener pitch
- Type of stiffener (Z sections, angles, stiffening beads)
- Load influence (distributed load, load concentrated at the ends)
- Bottom shape influence (flat bottom, curved bottom).

Comparison of model-test results with those of full-scale tests showed that the models exhibited the same failure modes and predictable failure loads.

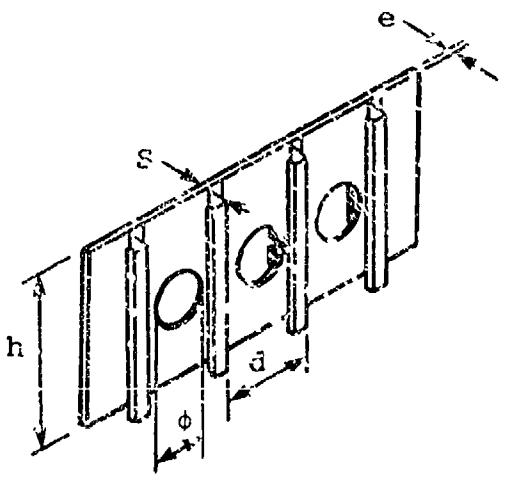

FIGURE 115. STIFFENED PANEL SPECIMEN. (FROM REFERENCE 132)

The techniques of dynamic testing become more involved as the required quantity of data increases. For instance, if the final deformation shape is the only result needed, the instrumentation and data handling requirements can be minimized. Since a test is of short duration, even for full-scale specimens, specialized equipment is required if data requirements are expanded to include time histories of structural response, acceleration, stress, etc. This equipment must have rapid response characteristics and maintain high-fidelity measuring capability when subjected to high-G levels.

REFERENCES

1. Military Standard, MIL-STD-1290A(AV), LIGHT FIXED AND ROTARY-WING AIRCRAFT CRASH RESISTANCE, Department of Defense, Washington, DC 20301, 26 September 1988.

2. ENGINEERING ANALYSIS OF CRASH INJURY IN ARMY OH-58 AIRCRAFT, USASC Technical Report, U.S. Army Safety Center, Fort Rucker, Alabama, to be published.

3. ENGINEERING ANALYSIS OF CRASH INJURY IN ARMY CH-47 AIRCRAFT, USAAAVS Technical Report 78-4, U.S. Army Agency for Aviation Safety, Fort Rucker, Alabama, June 1978.

4. ENGINEERING ANALYSIS OF CRASH INJURY IN ARMY AH-1 AIRCRAFT, USAAAVS Technical Report 78-3, U.S. Army Agency for Aviation Safety, Fort Rucker, Alabama, March 1978.

5. Carnell, B. L., CRASHWORTHINESS DESIGN FEATURES FOR ADVANCED UTILITY HELICOPTERS, in Aircraft Crashworthiness, K. Saczalski, et al,. eds., University Press of Virginia, Charlottesville, Virginia, 1975, pp. 51-64.

6. Bainbridge, M. E., Reilly, M. J., and Gonsalves, J. E., CRASHWORTHINESS OF THE BOEING VERTOL UTTAS, in Aircraft Crashworthiness, K. Saczalski, et al., eds., University Press of Virginia, Charlottesville, Virginia, 1975, pp. 65-82.

7. Rich, M. J., INVESTIGATION OF ADVANCED HELICOPTER STRUCTURAL DESIGNS, Volume I, ADVANCED STRUCTURAL COMPONENT DESIGN CONCEPT STUDY, Sikorsky Aircraft, Division of United Technology Corporation; USAAMRDL Technical Report 75-59A, Eustis Directorate, U.S. Army Air Mobility Research and Development Laboratory, Fort Eustis, Virginia, May 1976, AD A026246.

8. Hoffstedt, D. J., and Swatton, S., ADVANCED HELICOPTER STRUCTURAL DESIGN INVESTIGATION, Boeing Vertol Company; USAAMRDL Technical Report 75-56A, Eustis Directorate, U.S. Army Air Mobility Research and Development Laboratory, Fort Eustis, Virginia, March 1976, AD A024662.

9. Hicks, J., E., AN ANALYSIS OF LIFECYCLE ACCIDENT COSTS FOR THE ADVANCED SCOUT HELICOPTER, U.S. Army Agency for Aviation Safety, Fort Rucker, Alabama, January 1977.

10. McDermott, J. M., and Vega, E., THE EFFECTS OF LATEST MILITARY CRITERIA ON THE STRUCTURAL WEIGHT OF THE HUGHES ADVANCED ATTACK HELICOPTER YAH-64, Journal of the American Helicopter Society, Vol. 23, No. 4, October 1978, pp. 2-9.

11. Haley, J. L., Jr., CRASHWORTHINESS VERSUS COST: A STUDY OF ARMY ROTARY WING AIRCRAFT ACCIDENTS IN PERIOD JANUARY 1970 THROUGH DECEMBER 1971, paper presented at the Aircraft Crashworthiness Symposium, University of Cincinnati, Cincinnati, Ohio, October 1975.

REFERENCES (CONTD)

12. Hicks, J. E., ECONOMIC BENEFITS OF UTILITY AIRCRAFT CRASHWORTHINESS, USAAAVS Technical Report 76-2, U.S. Army Agency for Aviation Safety, Fort Rucker, Alabama, July 1976.

13. THE ECONOMIC BENEFITS OF CRASHWORTHINESS AND FLIGHT SAFETY DESIGN FEATURES IN ATTACK HELICOPTERS, USAAAVS Technical Report 77-2, U.S. Army Agency for Aviation Safety, Fort Rucker, Alabama, June 1977.

14. Cronkhite, J. D. DESIGN OF AIRFRAME STRUCTURES FOR CRASH IMPACT, Bell Helicopter Textron, Inc., presented at the American Helicopter Society National Specialist's Meeting on Crashworthy Design of Rotorcraft at Georgia Institute of Technology, Atlanta, GA, April 7-9, 1986.

15. Cook, R. L., and Goebel, D. E., EVALUATION OF THE UH-1D/H HELICOPTER CRASHWORTHY FUEL SYSTEM IN A CRASH ENVIRONMENT, Dynamic Science, Division of Marshall Industries; USAAMRDL Technical Report 71-47, U.S. Army Air Mobility Research and Development Laboratory, Fort Eustis, Virginia, November 1971, AD 739567.

16. Gell, C. F., TABLE OF EQUIVALENTS FOR ACCELERATION TERMINOLOGY, Aerospace Medicine, Vol. 32, No. 12, December 1961, pp. 1109-1111.

17. Haley, J. L., ANALYSIS OF EXISTING HELICOPTER STRUCTURES TO DETERMINE DIRECT IMPACT SURVIVAL PROBLEMS, U.S. Army Board for Aviation Accident Research, Fort Rucker, Alabama, 1971.

18. ENGINEERING DESIGN HANDBOOK, HELICOPTER ENGINEERING, Part One, PRELIMINARY DESIGN, AMC Pamphlet 706-201, U.S. Army Material Command, Alexandria, VA, August 1974.

19. Military Specification, MIL-S-8698, STRUCTURAL DESIGN REQUIREMENTS, HELICOPTERS (ASG), Department of Defense, Washington, DC, 28 February 1958.

20. Military Specification, MIL-A-21180D, ALUMINUM-ALLOY CASTINGS, HIGH STRENGTH, Department of Defense, Washington, DC, 05 November 1984.

21. Military Handbook, MIL-HDBK-17, PLASTICS FOR AEROSPACE VEHICLES, Part I, REINFORCED PLASTICS, Department of Defense, Washington, DC.

22. Military Handbook, MIL-HDBK-5, METALLIC MATERIALS AND ELEMENTS FOR AEROSPACE VEHICLE STRUCTURES, Department of Defense, Washington, DC.

23. Ezra, A. A., and Fay, R. J., AN ASSESSMENT OF ENERGY-ABSORBING DEVICES FOR PROSPECTIVE USE IN AIRCRAFT IMPACT SITUATIONS, Dynamic Response of Structures, Pergamon Press, New York, 1972, pp. 225-246.

REFERENCES (CONTD)

24. Kirsh, P. A. and Jahnle, H. A., ENERGY ABSORPTION OF GLASS POLYESTER STRUCTURES, The Budd Company Technical Center, SAE Technical Paper Series No. 810233, International Congress and Exposition, Cobo Hall, Detroit, MI, February 23-27, 1981.

25. Gustafson, A. J., Shek Ng, G., and Singley, G. T., IMPACT BEHAVIOR OF FIBROUS COMPOSITES AND METAL SUBSTRUCTURES, Report No. USAAVRADCOM TR-82-D-31, Applied Technology Laboratory, U.S. Army Research and Technology Laboratories (AVRADCOM), Fort Eustis, VA 23604, October 1982.

26. Cronkhite, J. D., and Hass, T. J.; Winter, R.; and Singley, G. T., III, INVESTIGATION OF THE CRASH IMPACT CHARACTERISTICS OF COMPOSITE AIRFRAME STRUCTURES, Bell Helicopter Textron, Inc., Fort Worth, TX; Grumman Aerospace Corporation, Bethpage, NY; and Applied Technology Laboratory, U.S. Army Research and Technology Laboratories (AVRADCOM), Fort Eustis, VA, presented at the 34th National Forum of the American Helicopter Society, Washington, DC, May 1987.

27. Sen, J. K., and Votaw, M. W., A SKIN-STRINGER DESIGN FOR A CRASHWORTHY COMPOSITE FUSELAGE FOR THE HUGHES 500E HELICOPTER, Hughes Helicopter, Inc., presented at the 41st Annual Forum, American Helicopter Society, Fort Worth, TX, May 15-17, 1985.

28. Carden, H. D., IMPACT DYNAMICS RESEARCH ON COMPOSITE TRANSPORT STRUCTURES, NASA Technical Memorandum 86391, National Aeronautics and Space Administration, Langley Research Center, Hampton, VA 23665, March 1985.

29. Farley, G. L., ENERGY ABSORPTION OF COMPOSITE MATERIAL AND structure, Aerostructures Directorate, U.S. Army Aviation Research and Technology Activity (AVSCOM), Hampton, VA 23665-5225, presented at the American Helicopter Society 43rd Annual Forum and Technology Display, St. Louis, MO, May 18-20, 1987.

30. Farley, G. L., EFFECT OF FIBER AND MATRIX STRAIN ON THE ENERGY ABSORPTION OF COMPOSITE MATERIALS, NASA Langley Research Center, Hampton, VA 23665, presented at the 41st Annual Forum of the American Helicopter Society, May 15-17, 1985.

31. Crorkhite, J. D., IMPACT OF MIL-STD-1290 CRASHWORTHINESS REQUIREMENTS ON DESIGN OF HELICOPTER COMPOSITE STRUCTURES, Bell Helicopter Textron, Inc., Fort Worth, Texas, Paper No. 1567 presented at the 42nd Annual Conference of Society of Weight Engineers, Inc., Anaheim, CA May 23-25, 1983.

32. McComb, H. G., Jr., SAFE STRUCTURES FOR FUTURE AIRCRAFT, NASA Langley Research Center, Astronautics & Aeronautics, September 1983.

REFERENCES (CONTD)

33. Gibbs, H. H., K-POLYMER COMPOSITE MATERIALS - A NEW APPROACH TO DAMAGE-TOLERANT AEROSPACE STRUCTURES, E. I. du Pont de Nemours & Co., Inc., Wilmington, DE, SAE Technical Paper Series 841518, presented at Aerospace Congress & Exposition, Long Beach, CA, October 15-18, 1984.

34. Alexander, J. V., and Messinger, R. H., ADVANCED CONCEPTS FOR COMPOSITE STRUCTURE JOINTS AND ATTACHMENT FITTINGS - VOLUME 1; DESIGN AND EVALUATION, Hughs Helicopter Division of Summa Corp., Culver City, CA, 90230, Report No. USAAVRADCOM-TR-81-D-21A, Applied Technology Laboratory, U.S. Army Research and Technology Laboratories (AVRADCOM), Fort Eustis, VA 23604, November 1981, AD A110212.

35. Cronkhite, J. D., and Berry, V. L.; and Winter, R., INVESTIGATION OF THE CRASH IMPACT CHARACTERISTICS OF HELICOPTER COMPOSITE STRUCTURES, Bell Helicopter Textron, Inc.; and Grumman Aerospace Corp., Report No. USAAVRADCOM TR-82-D-14, Applied Technology Laboratory, U.S. Army Research and Technology Laboratories (AVRADCOM), Fort Eustis, VA 23604, February 1983, AD B071763L.

36. Foye, R. L., and Hodges, W. T., SOME RESULTS FROM A CRASH ENERGY ABSORPTION TEST FOR EVALUATING COMPOSITE FUSELAGE CONSTRUCTION, U.S. Army Research and Technology Laboratories (AVRADCOM), Applied Technology Laboratory, Fort Eustis, VA 23604, and Structures Laboratory, NASA Langley Research Center, Hampton, VA 23605, presented at the 37th Annual Forum of the American Helicopter Society, New Orleans, LA, May 1981.

37. Sen, J. K., DESIGNING FOR A CRASHWORTHY ALL-COMPOSITE HELICOPTER FUSELAGE, Hugues Helicopters, Inc., Culver City, CA, presented at the 40th Annual Forum of the American Helicopter Society, Arlington, VA, May 16-18, 1984.

38. Rich, M. J., DESIGN, FABRICATION AND TEST OF A COMPLEX HELICOPTER AIRFRAME SECTION, Sikorsky Aircraft Division of United Technologies Corporation, Stratford, CT 06602, Paper No. 801213, Society of Automotive Engineers, Inc., 400 Commonwealth Drive, Warrendale, PA 15096, 1980.

39. Minecci, J. J., and Hess, T. E., COMPOSITE FUSELAGE DEVELOPMENT FOR NAVAL AIRCRAFT, Naval Air Development Center, Warminster, PA, presented at the 25th National SAMPE Symposium and Exhibition, May 6-8, 1980.

40. Kindervater, C. M., CRASH IMPACT BEHAVIOR AND ENERGY ABSORBING CAPABILITY OF COMPOSITE STRUCTURAL ELEMENTS, DFVLR, Stuttgart, FRG, Visiting Scientist at Air Force Materials Laboratory/MLBM, Wright Patterson Air Force Base, Ohio 45433, presented at the 30th National SAMPE Symposium, March 19-21, 1985.

REFERENCES (CONTD)

41. Thornton, P. M., Harwood, J. J., and Beardmore, P., FIBER-REINFORCED PLASTIC COMPOSITES FOR ENERGY ABSORPTION PURPOSES, Ford Motor Company, Dearborn, MI 48121, presented at the International Symposium on Composites: Materials and Engineering, University of Delaware, Newark, DE, September 24-28, 1984, published in Composites Science and Technology 24 (1985), 275-298, by Elsevier Applied Science Publishers Ltd. (England).

42. Torres, M., DEVELOPMENT OF COMPOSITE MATERIAL HELICOPTER STRUCTURES, Helicopter Division, Aerospatiale, presented at the 37th Annual Forum of the American Helicopter Society, New Orleans, LA, May 1981.

43. Kay, B. F., ACAP STRUCTURAL DESIGN, Sikorsky Aircraft Division, United Technologies Corporation, Stratford, CT, presented at the 39th Annual Forum of the American Helicopter Society, May 9-11, 1983.

44. Goldberg, J., and Camaratta, F. A., CRASHWORTHINESS OF THE ACAP DESIGN, Sikorsky Aircraft Division, United Technologies Corporation, Stratford, CT, presented at the 39th Annual Forum of the American Helicopter Society, May 9-11, 1983.

45. Mazza, L. T., and Foye, R. L., ADVANCED COMPOSITE AIRFRAME PROGRAM PRELIMINARY DESIGN PHASE, U.S. Army Research and Technology Laboratories (AVRADCOM), Fort Eustis, VA 23604, and Moffett Field, CA 94035, presented at the 36th Annual Forum of the American Helicopter Society, Washington, DC, May 1980.

46. Alsmiller, G. R., Jr., and Anderson, W. P., ADVANCED COMPOSITES AIRFRAME PROGRAM - PRELIMINARY DESIGN, Volume I - Basic Report (Part I), Bell Helicopter Textron, Inc., P. O. Box 482, Fort Worth, TX 76101, Report No. USAAVRADCOM TR-80-D-37A, Applied Technology Laboratory, U.S. Army Research and Technology Laboratories (AVRADCOM), Fort Eustis, VA 23604, February 1982, AD B063687L.

47. Chronkhite, J. D., and Mazza, L. T., BELL ACAP FULL-SCALE AIRCRAFT CRASH TEST AND KRASH CORRELATION, Bell Helicopter Textron, Inc., Fort Worth, TX, and Aviation Applied Technology Directorate, U.S. Army Aviation Research and Technology Activity (AVSCOM), Fort Eustis, VA, presented at the 44th Annual Forum & Technology Display of the American Helicopter Society, Washington, DC, June 16-18, 1988.

48. Clarke, C. W., EVOLUTION OF THE ACAP CRASH ENERGY MANAGEMENT SYSTEM, Engineering Structural Technologies - Loads and Criteria, United Technologies - Sikorsky Aircraft, Stratford, CT, presented at the 44th Annual Forum & Technology Display of the American Helicopter Society, Washington, DC, June 16-18, 1988.

49. Air Force Systems Command, ADVANCED COMPOSITE DESIGN GUIDE, Advanced Development Division, Air Force Materials Laboratory, Wright-Patterson Air Force Base, Ohio, January 1973.

REFERENCES (CONTD)

50. Cronkhite, J. D., et al., INVESTIGATION OF THE CRASH-IMPACT CHARACTERISTICS OF ADVANCED AIRFRAME STRUCTURES, Bell Helicopter Textron, Inc.; USARLT Technical Report 79-11, U.S. Army Research and Technology Laboratories (AVRADCOM), Fort Eustis, VA April 1979, AD A075163.

51. Pinkel, I. I., et al., MECHANISM OF START AND DEVELOPMENT OF AIRCRAFT CRASH FIRES, Lewis Flight Propulsion Laboratory; NACA Technical Note 2996, National Advisory Committee for Aeronautics, Cleveland, Ohio, 1953.

52. Campbell, J. A., APPRAISAL OF THE HAZARDS OF FRICTION-SPARK IGNITION OF AIRCRAFT CRASH FIRES, Lewis Flight Propulsion Laboratory; NACA Technical Note 4024, National Advisory Committee for Aeronautics, Cleveland, Ohio, May 1957.

53. Jones, N., and Wierzbicki, T., Editors, STRUCTURAL CRASHWORTHINESS, a book of 15 lectures presented at the First International Symposium on Structural Crashworthiness, Department of Mechanical Engineering at the University of Liverpool, September 14-16, 1983, published by Butterworths, London, England.

54. Sharman, P. W., ENERGY ABSORPTION OF CHANNEL BEAMS DURING GROSS DEFORMATION, Dept. of Transport Technology, Loughborough Univ. of Technology, Vehicle Structural Mechanics, Fourth International Conference Proceedings, Code 811303, SAE 1981 Proceedings.

55. Gannon, B. T., Maris, J. L., and Waldrop, P. S., CREW SURVIVABLE HELICOPTER UNDERCARRIAGE, LTV Vought Corporation, Report No. AMMRC TR 84-1, Army Materials and Mechanics Research Center, Watertown, MA, January 1984.

56. Cronkhite, J. D., and Berry, V. L., CRASHWORTHY AIRFRAME DESIGN CONCEPTS - FABRICATION AND TESTING, NASA Contractor Report 3603, September 1982.

57. Mahmood, H. F., and Paluszny, A., DESIGN OF THIN WALLED COLUMNS FOR CRASH ENERGY MANAGEMENT - THEIR STRENGTH AND MODE OF COLLAPSE, Ford Motor Company, Vehicles Structural Mechanics, Fourth International Conference Proceedings, Code 811302, SAE 1981 Proceedings.

58. Sen, J. K., and Dremann, C. C., DESIGN DEVELOPMENT TESTS FOR COMPOSITE CRASHWORTHY HELICOPTER FUSELAGE, Hughes Helicopters, Inc., Culver City, California, SAMPE Quarterly Volume 17, No. 1, October 1985, pp 29-39.

59. Farley, G. L., ENERGY ABSORPTION OF COMPOSITE MATERIALS, NASA Technical Memorandum 84638, AVRADCOM Technical Report TR-83-B-2, Structures Laboratory, U.S. Army Research & Technical Laboratories (AVRADCOM), Langley Research Center, Hampton, VA 23665, March 1983.

REFERENCES (CONTD)

60. Hanagud, S., Chen, H. P., and Sriram, P., A STUDY OF THE STATIC POST BUCKLING BEHAVIOR OF COMPOSITE SANDWICH PLATES, School of Aerospace Engineering, Georgia Institute of Technology, Atlanta, GA, presented at the International Conference on Rotorcraft Basic Research, Research Triangle Park, North Carolina, February 19-21, 1985.

61. Reddy, A. D., and Rehfield, L. W., POSTBUCKLING AND CRIPPLING BEHAVIOR OF GRAPHITE/EPOXY THIN-WALLED AIRFRAME MEMBERS, Center for Rotary Wing Aircraft Technology, School of Aerospace Engineering, Georgia Institute of Technology, Atlanta, GA 30332, Paper No. A-85-41-50-8000 presented at the 41st Annual Forum of the American Helicopter Society, May 15-17, 1985.

62. Cronkhite, J. D., HELICOPTER STRUCTURAL CRASHWORTHINESS, Bell Helicopter Textron, Inc., presented at the ASME Winter Meeting, Anaheim, CA December 7-12, 1986.

63. Cronkhite, J. D., CRASHWORTHY DESIGN CONCEPTS FOR AIRFRAME STRUCTURES OF LIGHT AIRCRAFT, Bell Helicopter Textron, Inc., Fort Worth, TX SAE Technical Paper Series 810613, Business Aircraft Meeting & Exposition, Wichita, KS, April 7-10, 1981.

64. Carden, H. D., and Hayduk, R. J., AIRCRAFT SUBFLOOR RESPONSE TO CRASH LOADINGS, NASA Langley Research Center, Hampton, VA, SAE Technical Paper Series No. 810614, Business Aircraft Meeting & Exposition, Wichita, KS, April 7-10, 1981.

65. Cronkhite, J. D., and Tanner, A. E., TILT ROTOR CRASHWORTHINESS, Bell Helicopter Textron, Inc., Fort Worth, TX, and Boeing Vertol Company, Philadelphia, PA, presented at the 41st Annual Forum of the American Helicopter Society, Fort Worth, TX, May 15-17, 1985.

66. Bark, L. W., Burrows, L. T., and Cronkhite, J. D., et al., "Crash Testing of Advanced Composite Energy-Absorbing Repairable Cabin Subfloor Structures," paper presented at American Helicopter Society National Technical Specialists' Meeting on Advanced Rotorcraft Structures, Williamsburg, Virginia, October 25-27, 1988.

67. Smith, H. G., DESIGNING HELICOPTERS FOR IMPROVED CRASH SURVIVABILITY, paper presented at NATO/AGARD Aerospace Medical Panel Specialist Meeting, Oporto, Portugal, 23, 24, and 26 June 1971.

68. Fox, R. G., LATERAL ROLLOVER PROTECTION CONCEPTS, Bell Helicopter Textron; USARTL Technical Report 80-D-1, U.S. Army Research and Technology Laboratories (AVRADCOM), Fort Eustis, VA, August 1979, ADA081420.

69. Military Specification, MIL-T-27422, TANK, FUEL, CRASH RESISTANT, AIRCRAFT, Department of Defense, Washington, DC, 13 April 1971.

REFERENCES (CONTD)

70. Mens, J., and Bianchini, J. C., COMPUTING CODES FOR DEVELOPMENT OF HELICOPTER CRASHWORTHINESS STRUCTURES AND TEST SUBSTANTIATION, presented at the American Helicopter Society National Specialist's Meeting on Crashworthy Design of Rotorcraft, Georgia Institute of Technology, Atlanta, GA, April 7-9, 1986.

71. Military Specification, MIL-S-58095A(AV), GENERAL SPECIFICATION FOR CRASH-RESISTANT, NON-EJECTION, AIRCREW SEAT SYSTEM, Department of Defense, Washington, DC, 31 January 1986.

72. Military Specification MIL-S-85510(AS), SEATS, HELICOPTER CABIN, CRASHWORTHY, GENERAL SPECIFICATION FOR, Naval Air Systems Command, Naval Air Engineering Center, Lakehurst, NJ 98733, 19 November 1981.

73. Military Specification, MIL-P-27443, PALLET, CARGO, AIRCRAFT, TYPE HCU-6/e, HCU-12/e, AND HCU-10/C, Department of Defense, Washington, DC, 24 February 1967.

74. Military Specification, MIL-N-27444, NET, CARGO TIEDOWN, PALLETS, HCU-7/E, HCU-15C, HCU-11C, AND HCU-16/C, Department of Defense, Washington, DC, 8 May 1969.

75. Military Specification, MIL-A-8421, AIR TRANSPORTABILITY REQUIREMENTS, GENERAL SPECIFICATION FOR, Department of Defense, Washington, DC.

76. CARGO AIRCRAFT AND SPACECRAFT FORWARD RESTRAINT CRITERIA, USAF Technical Report 76-30, Aeronautical Systems Division, Wright-Patterson Air Force Base, Ohio, December 1977.

77. Shefrin, J., et al., INTEGRAL HELICOPTER CARGO RESTRAINT SYSTEMS, Boeing Vertol Company; USAAVLABS Technical Report 69-68, U.S. Army Aviation Material Laboratories, Fort Eustis, VA, October 1969, AD 864899.

78. Shefrin, J., DEMONSTRATION OF ADVANCED CARGO RESTRAINT HARDWARE FOR COD AIRCRAFT, Boeing Vertol Company; NADC Technical Report 77154-60, Naval Air Development Center, Warminster, PA, December 1978.

79. Shefrin, Joseph, INVESTIGATION OF ADVANCED CARGO RESTRAINT SYSTEM FOR COD AIRCRAFT, NADC 77085-60, December 1981.

80. Burrows, L. , Lane, R., and McElhenney, J., et al., CH-47 CRASH TEST (T-40) STRUCTURAL, CARGO RESTRAINT, AND AIR CREW INFLATABLE RESTRAINT EXPERIM NTS, USARTL Technical Report 78-22, U.S. Army Research and Technology Laboratories (AVRADCOM), Fort Eustis, VA, April 1978, AD A055804.

REFERENCES (CONTD)

81. Shefrin, J., and Campbell, R. F, Hate, R. L., and George, H. L., STATE-OF-THE-ART CRASHWORTHY CARGO RESTRAINT SYSTEMS FOR MILITARY AIRCRAFT, Boeing Vertol Company, Philadelphia, PA; NADC, Warminster, PA; and NAVAIRSYSCOM, Washington, DC, presented at the American Helicopter Society National Specialist's Meeting on Crashworthy Design of Rotorcraft, Georgia Institute of Technology, Atlanta, GA, April 7-9, 1986.

82. Russo, A., Jr., CARGO RESTRAINT SYSTEM PHASE I REPORT, All American Engineering Company, Wilmington, DE, January 1964.

83. Hate, R. L., NAVY CARGO RESTRAINT CRITICAL REVIEW, NADC Technical Report 74082-30, Naval Air Development Center, Warminster, PA, May 1974.

84. Coltman, J. W., et al., ANALYSIS OF ROTORCRAFT CRASH DYNAMICS FOR DEVELOPMENT OF IMPROVED CRASHWORTHINESS DESIGN CRITERIA, DOT/FAA/CT-85/11, Simula Inc., U.S. Department of Transportation, Federal Aviation Administration, Technical Center, Atlantic City Airport, NJ, June 1985.

85. Coltman, J. W., THE NAVAL AIRCRAFT CRASH ENVIRONMENT, PHASE I - HELICOPTER AIRCREW SURVIVABILITY AND STRUCTURAL RESPONSE, TR-84006, Simula Inc., Naval Air Development Center, Warminister PA, March 1984.

86. Warrick, J. C., ACTIVE CONTROL LANDING GEAR, (Phase I Final Report), Simula Inc., TR-86402, Aviation Applied Technology Directorate, Fort Eustis, VA, August 1986.

87. Crist, D. and Symes, L. H., HELICOPTER LANDING GEAR DESIGN AND TEST CRITERIA INVESTIGATIONS, Bell Helicopter Textron, Inc., Fort Worth, Texas; USAAVRADCOM-TR-81-D-15, Applied Technology Laboratory, U.S. Army Research and Technology Laboratories (AVRADCOM), Fort Eustis, VA 23604, August 1981, AD A105512.

88. Sen, J. K., Votaw, M. W., and Downer, G. R., INFLUENCES OF TWO LANDING GEAR DESIGNS ON HELICOPTER CRASHWORTHINESS AND WEIGHT, presented at the 41st Annual Forum, American Helicopter Society, Ft. Worth, TX, May 1985.

89. Lee, B. L., and Garbo, S. P., EFFECTS OF VARIATIONS IN CRASHWORTHINESS CRITERIA ON SIKORSKY S-75 ACAP LANDING GEAR WEIGHTS, presented at the 41st Annual Forum, American Helicopter Society, Ft. Worth, TX, May 1985.

90. Smith, K. F., ARMY HELICOPTER CRASHWORTHINESS: LOADING THE BATTLEFIELD DICE IN OUR FAVOR, presented at the 41st Annual Forum, American Helicopter Society, Ft. Worth, TX, May 1985.

REFERENCES (CONTD)

91. Logan, A. H., ANALYTICAL INVESTIGATION OF AN IMPROVED HELICOPTER LANDING GEAR CONCEPT, Hughs Helicopters; USAAMRDL Technical Report 76-19, Eustis Directorate, U.S. Army Air Mobility Research and Development Laboratory, Fort Eustis, VA, August 1976, AD A029372.

92. Military Specification, MIL-H-83282C, HYDRAULIC FLUID, FIRE RESISTANT, SYNTHETIC HYDROCARBON BASE, AIRCRAFT, METRIC, NATO CODE NUMBER H-537, Department of Defense, Washington DC, 25 March 1986.

93. Darlington, R. F., LANDING GEAR - A COMPLETE SYSTEMS APPROACH, Vertiflight, March/April 1987.

94. Gupta, B. P., HELICOPTER OBSTACLE STRIKE ANALYSIS, Bell Helicopter Textron, Inc., USARTL Technical Report 78-46, U.S. Army Research and Technology Laboratories (AVRADCOM), Fort Eustis, VA, April 1979, AD A069877.

95. Greer, D. L., CRASHWORTHY DESIGN PRINCIPLES, Convair, Division of General Dynamics Corporation, San Diego, CA, September 1964.

96. Phillips, N. S., Carr, R. W., and Scranton, R. S., CRASHWORTHY LANDING GEAR STUDY, Beta Industries, Inc.; USAAMRDL Technical Report 72-61, U.S. Army Air Mobility Research and Development Laboratory, Fort Eustis, VA, 1973, AD 765489.

97. Wittlin, G., and Park, K. C., DEVELOPMENT AND EXPERIMENTAL VERIFICATION OF PROCEDURES TO DETERMINE NONLINEAR LOAD DEFLECTION CHARACTERISTICS OF HELICOPTER SUBSTRUCTURES SUBJECTED TO CRASH FORCES, Volumes I and II, Lockheed-California Company; USAAMRDL Technical Reports 74-12A, 74-12B, U.S. Army Air Mobility Research and Development Laboratory, Fort Eustis, VA, 1974, AD 784191 and 784192.

98. Needham, R. S., THE ULTIMATE STRENGTH OF ALUMINUM ALLOY FORMED STRUCTURAL SHAPES IN COMPRESSION, Journal of Aerospace Science, Vol. 21, No. 4, 1954, pp. 217-229.

99. Gerard, G., HANDBOOK OF STRUCTURAL STABILITY, NACA Technical Note 3781-3785, National Advisory Committee for Aeronautics, Cleveland, Ohio, 1957.

100. D'Amato, R., STATIC POSTFAILURE STRUCTURE CHARACTERISTICS, WADC Technical Report 59-112, Wright Air Development Center, Wright-Patterson Air Force Base, Ohio, 1959.

101. Chitner, A. H., THIN WALLED STRUCTURES, John Wiley, New York, 1967.

102. Sechler, E. E., and Dunn, L. G., AIRPLANE STRUCTURAL ANALYSIS AND DESIGN, Dover, New York, 1963.

REFERENCES (CONTD)

103. Singley, G. T., III, FULL SCALE CRASH TESTING OF A CH-47C HELICOPTER, paper presented at 32nd Annual National V/STOL Forum, American Helicopter Society, Washington, DC, May 1976.

104. Greer, D. L., Heid, T. L., and Weber, J. D., DESIGN STUDY AND MODEL STRUCTURES TEST PROGRAM TO IMPROVE FUSELAGE CRASHWORTHINESS, Convair, Division of General Dynamics Corporation; FAA DS-67-20, Federal Aviation Administration, Washington, DC, October 1967, AD 666816.

105. Saczalski, K. J., STRUCTURAL PROBLEMS ASSOCIATED WITH THE PREDICTION OF VEHICLE CRASHWORTHINESS, in Surveys of Research in Transportation Technology, AMD-Vol 5, presented at ASME Winter Annual Meeting, American Society of Mechanical Engineers, 11-15 November 1973.

106. Hayduk, R. J., et al., NONLINEAR STRUCTURAL CRASH DYNAMICS ANALYSES, SAE Paper No. 790588, presented at Business Aircraft Meeting, Society of Automotive Engineers, Inc., Wichita, KS, 1979.

107. McIvor, I. K., MODELING, SIMULATION, AND VERIFICATION OF IMPACT DYNAMICS, VOLUME I, EXECUTIVE REPORT, Highway Safety Research Institute and Department of Applied Mechanics, University of Michigan, Ann Arbor, MI, October 1973.

108. Kamat, M. P., SURVEY OF COMPUTER PROGRAMS FOR PREDICTION OF CRASH RESPONSE AND OF ITS EXPERIMENTAL VALIDATION, in Measurement and Prediction of Structural and Biodynamic Crash-Impact Response, Winter Meeting, American Society of Mechanical Engineers, New York, 5-10 December 1976, pp. 33-48.

109. Gatlin, C. I., Goebel, D. E., and Larsen, S. E., ANALYSIS OF HELICOPTER STRUCTURAL CRASHWORTHINESS, VOLUME I, MATHEMATICAL SIMULATION AND EXPERIMENTAL VERIFICATION OF HELICOPTER CRASHWORTHINESS, Dynamic Science, Division of Marshall Industries; USAAVLABS Technical Report 70-71A, Eustis Directorate, U.S. Army Air Mobility Research and Development Laboratory, Fort Eustis, VA, January 1971, AD 880680.

110. Wittlin, G., and Gamon, M. A., EXPERIMENTAL PROGRAM FOR THE DEVELOPMENT OF IMPROVED HELICOPTER STRUCTURAL CRASHWORTHINESS ANALYTICAL AND DESIGN TECHNIQUES, VOLUMES I and II, Lockheed-California Company; USAAMRDL Technical Report 72-72A and 72-72B, Eustis Directorate, U.S. Army Air Mobility Research and Development Laboratory, Fort Eustis, VA, May 1973, AD 764985 and AD 764986.

111. Shieh, R. C., BASIC RESEARCH IN CRASHWORTHINESS II - LARGE DEFLECTION DYNAMIC ANALYSIS OF PLANE ELASTOPLASTIC FRAME STRUCTURES, Calspan Corporation; Report No. DOT-HS-800-781, U.S. Department of Transportation, Washington, DC, December 1972.

REFERENCES (CONTD)

112. Young, J. W., "CRASH": A COMPUTER SIMULATION OF NONLINEAR TRANSIENT RESPONSE OF STRUCTURES, Philco-Ford, Subsidiary of the Ford Motor Company; Report No. DOT-HS-091-125B, U.S. Department of Transportation, Washington, DC, March 1972.

113. Yeung, K. S. and Welch, R. E., REFINEMENT OF FINITE ELEMENT ANALYSIS OF AUTOMOBILE STRUCTURES UNDER CRASH LOADING, Volume II, IIT Research Institute; Report No. DOT-HS-803-466, U.S. Department of Transportation, Washington, DC, October 1977, PB 287589.

114. Melosh, R. J., and Kamat, M. P., COMPUTER SIMULATION OF A LIGHT AIRCRAFT CRASH, Journal of Aircraft, 14, 10, 1009, 1977.

115. Pifko, A. B., Winter, R. E., and Ogivie, P. L., DYCAST - A FINITE ELEMENT PROGRAM FOR CRASH ANALYSIS OF STRUCTURES. National Aeronautics and Space Administration, NAS-13148, 1982.

116. Wittlin, G., and Gamon, M. A., FULL-SCALE CRASH TEST EXPERIMENTAL VERIFICATION OF A METHOD OF ANALYSIS FOR GENERAL AVIATION AIRPLANE STRUCTURAL CRASHWORTHINESS, Lockheed-California Company, Report No. FAA RD 77-188, Federal Aviation Administration, Washington DC, February 1978.

117. Gamon, M. A., Wittlin, G., and LaBarge, W. L., KRASH85 USER'S GUIDE - INPUT/OUTPUT FORMAT, Lockheed-California Company, Report No. DOT/FAA/CT/-85/10, Federal Aviation Administration, Washington, DC May, 1985.

118. Gamon, M. A., GENERAL AVIATION AIRPLANE STRUCTURAL CRASHWORTHINESS USER'S MANUAL, Volume I, PROGRAM "KRASH" THEORY, Lockheed-California Company; FAA-RD-77-189-I, Federal Aviation Administration, Washington, DC, February 1978.

119. Gamon, M. A., Wittlin, G., and LaBarge, W. L., GENERAL AVIATION AIRPLANE STRUCTURAL CRASHWORTHINESS USER'S MANUAL, VOLUME II, INPUT-OUTPUT, TECHNIQUES AND APPLICATIONS (REVISED), Lockheed-California Company; FAA-RD-77-189-II, Federal Aviation Administration, Washington, DC, September 1979.

120. Wittlin, G., GENERAL AVIATION AIRPLANE STRUCTURAL CRASHWORTHINESS USER'S MANUAL, VOLUME III, RELATED DESIGN INFORMATION, Lockheed-California Company; FAA-RD-77-189-III, Federal Aviation Administration, Washington, DC, February 1978.

121. LaBarge, W. L., GENERAL AVIATION AIRPLANE STRUCTURAL CRASHWORTHINESS PROGRAMMER'S MANUAL, (REVISED), Lockheed-California Company; Report No. FAA-RD-78-120, Systems Research and Development Service, Federal Aviation Administration, Washington, DC, June 1979.

REFERENCES (CONTD)

122. Wittlin, G., PROGRAM KRASH: THE EVOLUTION OF AN ANALYTICAL TOOL TO EVALUATE AIRCRAFT STRUCTURAL CRASH DYNAMICS RESPONSE, presented at the American Helicopter Society National Specialist's Meeting on Crashworthy Design of Rotorcraft, Georgia Institute of Technology, Atlanta, GA, April 7-9, 1986.

123. Carnell, B. L., and Pramanik, M. B., ACAP CRASHWORTHINESS ANALYSIS BY KRASH, presented at the National Specialist's Meeting on Composite Structures, American Helicopter Society, Philadelphia, Pennsylvania, March 23-25, 1983.

124. BadriNath, Y. V., SIMULATION, CORRELATION, AND ANALYSIS OF THE STRUCTURAL RESPONSE OF A CH-47A TO CRASH IMPACT, Boeing Vertol Company, USARTL Technical Report 78-24, U.S. Army Research and Technology Laboratories, Fort Eustis, VA, August 1978, AD A062643.

125. Berry, V. L., and Cronkhite, J. D., KRASH ANALYSIS CORRELATION WITH FULL SCALE YAH-63 HELICOPTER CRASH TEST, presented at the American Helicopter Society National Specialist's Meeting on the Crashworthy Design of Rotorcraft, Georgia Institute of Technology, Atlanta, GA, April 7-9, 1986.

126. Bolukbasi, A. O., and Sen, J. K., MODELING STRATEGIES FOR CRASHWORTHINESS ANALYSIS OF LANDING GEARS, presented at the American Helicopter Society 45th Annual Forum and Technology Display, Boston, MA, May 22-24, 1989.

127. Wittlin, G., and LaBarge, B., KRASH DYNAMICS ANALYSIS MODELING - TRANSPORT AIRPLANE CONTROLLED IMPACT DEMONSTRATION TEST, Lockheed-California Company, Report No. DOT/FAA/CT-85/9, Federal Aviation Administration, Washington DC, May 1985.

128. Cronkhite, J. D., and Mazza, L. T., "Bell ACAP Full-Scale Aircraft Crash Test and KRASH Correlation," American Helicopter Society, 44th Annual Forum and Technology Display, Washington, DC, June 16-18, 1988.

129. Pifko, A. B., Levine, H. S., and Armen, H., Jr., PLANES - A FINITE ELEMENT PROGRAM FOR NONLINEAR ANALYSIS OF STRUCTURES, VOLUME I, THEORETICAL MANUAL, NASA CR-2568, National Aeronautics and Space Administration, Washington, DC, November 1975.

130. Winter, R., Pifko, A. B., and Armen, H., Jr., CRASH SIMULATION OF SKIN-FRAME STRUCTURES USING A FINITE ELEMENT CODE, SAE Paper No. 770484, presented at Business Aircraft Meeting, Society of Automotive Engineers, Inc., New York, March 29 - April 1, 1977.

REFERENCES (CONTD)

131. Winter, R., and Pifko, A. B., MODELING STRATEGIES FOR FINITE ELEMENT CRASH SIMULATION OF COMPLETE VEHICLES, presented at the American Helicopter Society National Specialist's Meeting on Crashworthy Design of Rotorcraft, Georgia Institute of Technology, Atlanta, GA, April 7-9, 1986.

132. Fasanella, E. L., Hayduk, R. J., Robinson, M. P., and Widmayer, E., ANALYSIS OF A TRANSPORT SECTION DROP TEST, NASA Report N85-10400, 1985.

133. Mens, J., "Computing Codes for Development of Helicopter Crashworthy Structures and Test Substantiation," paper presented at AHS/NAI International Seminar, Nanjing, China, November 6-8, 1985.

134. Snyder, R. G. CRASHWORTHINESS INVESTIGATION OF GENERAL AVIATION ACCIDENTS, SAE Paper No. 750537, presented at Business Aircraft Meeting, Society of Automotive Engineers, Inc., Wichita, KS, April 8-11, 1975.

135. Snyder, R. G., GENERAL AVIATION CRASH SURVIVABILITY, University of Michigan; SAE Paper No. 780017, presented at Congress and Exposition, Society of Automotive Engineers, Inc., Detroit, MI, February 27-March 3, 1978.

136. ENGINEERING DESIGN HANDBOOK, HELICOPTER ENGINEERING, Part Three, QUALIFICATION ASSURANCE, AMC Pamphlet 706-203, U.S. Army Materiel Command, Alexandria, VA, April 1972.

137. Smith, Kent F., FULL-SCALE CRASH TEST (T-41) OF THE YAH-63 ATTACK HELICOPTER, Report No. USAAVSCOM TR-86-D-2, Aviation Applied Technology Directorate, U.S. Army Aviation Research and Technology Activity (AVSCOM), Fort Eustis, VA 23604-5577, April 1986, AD A167813.

138. Alfaro-Bou, E., and Vaughan, V. L., Jr., LIGHT AIRPLANE CRASH TEST AT IMPACT VELOCITIES OF 13 AND 27 M/SEC, NASA Technical Paper 1042, NASA Langley Research Center, National Aeronautics and Space Administration, Washington, DC, November 1977.

139. Castle, C. B., and Alfaro-Bou, E., LIGHT AIRPLANE CRASH TESTS AT THREE ROLL ANGLES, NASA Technical Paper 1477, National Aeronautics and Space Administration, Washington, DC, October 1979.

140. Haley, J. C., Turnbow, J. W., and Walhout, G. J., FLOOR ACCELERATIONS AND PASSENGER INJURIES IN TRANSPORT AIRCRAFT ACCIDENTS, Aviation Safety Engineering and Research (AVSER), Division of Flight Safety Foundation, Inc.; USAAVLABS Technical Report 67-16, U.S. Army Aviation Materiel Laboratories, Fort Eustis, VA, May 1967, AD 815877L.

141. Vaughan, V. L., and Alfaro-Bou, E., IMPACT DYNAMICS RESEARCH FACILITY FOR FULL-SCALE AIRCRAFT CRASH TESTING, NASA Technical Note D-8179, National Aeronautics and Space Administration, Washington DC, April 1976.

REFERENCES (CONTD)

142. Holmes, B. S., and Colton, J. D., APPLICATION OF SCALE MODELING TECHNIQUES TO CRASHWORTHINESS RESEARCH, in Aircraft Crashworthiness, K. Saczalski, et al., eds., University Press of Virginia, Charlottesville, VA, 1975, pp. 561-582.

143. Mens, J., HELICOPTER BEHAVIOR IN CRASH CONDITIONS, Aerospatiale, Helicopter Divison; Paper 66 presented at Fourth European Rotorcraft and Powered Lift Aircraft Forum, Stressa, Italy, September 13-15, 1978.

BIBLIOGRAPHY

Alfaro-bou, E., et al., SIMULATIONS OF AIRCRAFT CRASH AND ITS VALIDATION, in Aircraft Crashworthiness, K. Saczalski, et al., eds., University Press of Virginia, Charlottesville, Virginia, 1975, pp. 485-498.

Armen, H., Jr., Pifko, A., and Levine, H., NONLINEAR FINITE ELEMENT TECHNIQUES FOR AIRCRAFT CRASH ANALYSIS, in Aircraft Crashworthiness, K. Saczalski, et al., eds., University Press of Virginia, Charlottesville, Virginia, 1975, pp. 517-548.

Avery, J. P., Ph.D., CARGO RESTRAINT CONCEPTS FOR CRASH RESISTANCE, Aviation Safety Engineering and Research (AvSER), Division of Flight Safety Foundation, Inc.; USAAMRDL Technical Report 65-30, U. S. Army Aviation Materiel Laboratories, Fort Eustis, Virginia, June 1965, AD 618493.

Belytschko, T. B., Welch, R. E., and Bruce, R. W., NUMERICAL ANALYSIS OF SHEET METAL IN CRASH LOADING, in Aircraft Crashworthiness, K. Saczalski, et al., eds., University Press of Virginia, Charlottesville, Virginia, 1975, pp. 549-560.

Brownfield, H. A., and Rogers, D. O., ANALYSIS OF 30 MPH FRONTAL BARRIER UTILIZING HALF-SCALE METAL MODELS, SAE Paper No. 780366, presented at 1978 Congress and Exposition, Society of Automotive Engineers, Inc., Detroit, Michigan, 27 February-3 March 1978.

Carnell, B. L., REVIEW OF NAVY HELICOPTER CRASHWORTHINESS. Document Number SER-50941, Sikorsky Aircraft, Division of United Technology Corporation, Stratford, Connecticut, September 1976.

Chernoff, M., ANALYSIS AND DESIGN OF SKID GEARS FOR LEVEL LANDING, Journal of the American Helicopter Society, Vol. 7, No. 1, January 1961, pp. 33-39.

Davies, R. G., and Magee, C. L., THE EFFECT OF STRAIN RATE UPON THE BENDING BEHAVIOR OF MATERIALS, Ford Motor Company; Paper No. 76-Mat-FF, Journal of Engineering Materials and Technology, Vol. 99, No. 1, January 1977, pp. 47-51.

Gamon, M. A., and Wittlin, G., ANALYTICAL TECHNIQUES FOR PREDICTING VEHICLE CRASH RESPONSE, in Aircraft Crashworthiness, K. Saczalski, et al., eds., University Press of Virginia, Charlottesville, Virginia, 1975, pp. 605-622.

Hone, H. T., Huebner, W. E., and Baxter, D. J., DEVELOPMENT OF CARGO SLINGS WITH NONDESTRUCTIVE CHECKOUT SYSTEMS, Sikorsky Aircraft, Division of United Technology Corporation; USAAMRDL Technical Report 73-106, Eustis Directorate, U. S. Army Air Mobility Research and Development Laboratory, Fort Eustis, Virginia, February 1974.

Heubner, W. E., DESIGN GUIDE FOR LOAD SUSPENSION POINTS, SLINGS, AND AIRCRAFT HARD POINTS, Sikorsky Aircraft, Division of United Technology Corporation; USAAMRDL Technical Report 72-36, Eustis Directorate, U. S. Army Air Mobility Research and Development Laboratory, Fort Eustis, Virginia, July 1972.

BIBLIOGRAPHY (CONTD)

Kruse, G. S., AN AUTOMATED PROCEDURE FOR PRELIMINARY DESIGN OF PRIMARY STRUCTURE FOR TRANSPORT AIRCRAFT, Convair, Division of General Dynamics Corporation; Paper No. 76-WA/Aero-9, American Society of Mechanical Engineers, New York, December 1976.

McIvor, I. K., A SIMULATION PROGRAM FOR LARGE DYNAMIC DEFORMATION OF VEHICLES, SAE Paper No. 770054, presented at 1977 International Automotive Engineering Congress and Exposition, Society of Automotive Engineers, Inc., Detroit, Michigan, 28 February-4 March 1977.

Melosh, R. J., CRASHWORTHINESS ENGINEERING OF AUTOMOBILES AND AIRCRAFT: PROGRESS AND PROMISE, Journal of Aircraft, Vol. 14, No. 7, July 1977, pp 693-698.

Melosh, R. J., and Kamat, M. P., COMPUTER SIMULATION OF LIGHT AIRCRAFT CRASH, Journal of Aircraft, Vol. 14, No. 10, October 1977, pp 1009-1014.

Ni, C-M., and Fine, D. S., PREDICTING CRUSH RESPONSE OF AUTOMOTIVE STRUCTURAL COMPONENTS, SAE Paper No. 780671, presented at Passenger Car Meeting, Society of Automotive Engineers, Inc., Troy, Michigan, 5-9 June 1978.

Park, K. C., MODELING AND ANALYSIS TECHNIQUES FOR VEHICLE CRASH SIMULATION, in Aircraft Crashworthiness, K. Saczalski, et al., eds., University Press of Virginia, Charlottesville, Virginia, 1975, pp 499-516.

Pifko, A., et al., PLANS - A FINITE ELEMENT PROGRAM FOR NONLINEAR ANALYSIS OF STRUCTURES, Paper No. 74-WA/PVP-6, American Society of Mechanical Engineers, New York, November 1974.

Robinson, D. C., CRUSH CHARACTERISTICS OF AUTOMOBILE STRUCTURAL COMPONENTS, National Bureau of Standards; Report No. COM-75-10464, National Highway Traffic Safety Administration, U. S. Department of Transportation, Washington, D. C., January 1975.

Saczalski, K. J., and Pilkey, W. D., eds., MEASUREMENT AND PREDICTION OF STRUCTURAL AND BIODYNAMIC CRASH-IMPACT RESPONSE, The American Society of Mechanical Engineers, New York, 1976.

Saczalski, K. J., and Pilkey, W. D., TECHNIQUES FOR PREDICTING VEHICLE STRUCTURE CRASH-IMPACT RESPONSE, in Aircraft Crashworthiness, K. Saczalski, et al., eds., University Press of Virginia, Charlottesville, Virginia, 1975, pp. 467-484.

Simonian, S., and Hart, G. C., IDENTIFICATION OF STRUCTURAL COMPONENT FAILURES UNDER DYNAMIC LOADING, SAE Paper No. 770950, presented at Aerospace Meeting, Society of Automotive Engineers, Inc., Los Angeles, California, November 1977.

Skogh, J., and Stern, P., POSTBUCKLING BEHAVIOR OF A SECTION REPRESENTATIVE OF THE B-1 AFT INTERMEDIATE FUSELAGE, Lockheed-California Company; AFFDL Technical Report 73-63, Air Force Flight Dynamics Laboratory, Wright-Patterson Air Force Base, Ohio, May 1973.

BIBLIOGRAPHY (CONTD)

Smith, H. G., and McDermott, J. M., DESIGNING FOR CRASHWORTHINESS AND SURVIVABILITY, Paper presented at 24th Annual National Forum Proceedings, National Helicopter Society, Inc., Washington, D. C., May 1968.

Tani, M., and Funahashi, A., ENERGY ABSORPTION BY THE PLASTIC DEFORMATION OF BODY STRUCTURAL MEMBERS, SAE Paper No. 780368, presented at 1978 Congress and Exposition, Society of Automotive Engineers, Inc., Detroit, Michigan, 27 February 3 March 1978.

Townley, G. E., and Krahs, J. W., DYNAMIC SIMULATION OF AN AUTOMOBILE BODY UTILIZING FINITE ELEMENT AND MODAL SYNTHESIS TECHNIQUES, SAE Paper No. 780364, presented at 1978 Congress and Exposition, Society of Automotive Engineers, Inc., Detroit, Michigan, 27 February-3 March 1978.

Weingarten, J. L., Mayrand, C. V., and Muller, G. E., AIR CARGO RESTRAINT CRITERIA, ASD-Technical Report 73-17, Aeronautical Systems Division, Wright-Patterson Air Force Base, Ohio, April 1973.

Widmayer, E., APPLICATION OF KRASH TO THE SOAC ACCIDENT, in Aircraft Crashworthiness, K. Saczalski, et al., eds., University Press of Virginia, Charlottesville, Virginia, 1975, pp. 583-604.

Yeung, K. S., and Hollowell, T., LARGE DISPLACEMENT, NONLINEAR STATIC AND DYNAMIC ANALYSIS OF AUTOMOBILE SHEET METAL STRUCTURE, SAE Paper No. 780367, presented at 1978 Congress and Exposition, Society of Automotive Engineers, Inc., Detroit, Michigan, March 1978.

U.S. GOVERNMENT PRINTING OFFICE: 1990, 727-075/00618, Region 3.